Total Synthesis of (−)-Himalensine A and Development of Novel C(sp^3)-H Functionalisation Reactions



Heyao Shi
Lady Margaret Hall
University of Oxford

A thesis submitted in partial fulfilment of the requirement for the degree of Doctor of Philosophy (DPhil)

Michaelmas Term 2018

Supervisor: Professor Darren J. Dixon

Contents

Abstract 7

Declarations and copyright 9

Acknowledgements 11

Abbreviations 13

Chapter 1: The Calyciphylline A-type *Daphniphyllum* Alkaloids 17

1.1 The *Daphniphyllum* Alkaloids 1 17

1.2 Biosynthetic Studies 17

1.3 The Calicyphylline A-Type Alkaloids 20

1.4 Synthetic Efforts Towards the Calyciphylline A-type Alkaloids 22

1.5 Previous Work in the Dixon Group 33

Chapter 2: The ABCD Tetracyclic Core 37

2.1 Introduction to the Synthetic Challenge 37

2.2 Access to IMDAF Cascade Precursor 87 38

2.3 Enantioselective IMDAF Cascade 39

2.4 Computational Calculations on the IMDAF Cascade 41

2.5 Approach to the ABCD Tetracyclic Core 45

2.6 Metal-Catalysed Cycloisomerisation 49

2.6.1 Conia-ene Type Cycloisomerisation 49

2.6.2 Metal-Catalysed Cycloisomerisation 53

2.7 Reductive Radical Cyclisation Cascade 59

2.7.1 Overview of the Thiol-Ene Reaction 59

2.7.2 Thiol-Mediated Reductive Radical Cascade 62

2.7.3 Reductive Desulfurisation 63

2.7.4 Tin-Mediated Radical Cyclisation Cascade 67

2.8 Diastereoselective Alkene Hydrogenation 68

2.9 Conclusions 73

Chapter 3: The Total Synthesis of (−)-Himalensine A 75

3.1 Endgame Strategy 75

3.3 Synthesis of the E ring 80

3.3.1 Sp^3-sp^2 Negishi Cross Coupling 80

3.3.2 Stetter Reaction to Furnish Cyclopentenone E ring 81

3.4 Late-Stage Chemoselective Lactam Reduction 85

3.5 Comparison of Synthetic and Natural Samples 89

Chapter 4: Introduction to Cp^*Rh^{III} C-H Functionalisation 95
4.1 Development of the Direct C-H Amination Reaction 95
4.2 Rh^{III} Catalysed C-H Amination 102
4.3 Introduction to Rh^{III} catalysed C(sp^3)-H Functionalisation 107
4.4 Directing Group-Enabled Functionalisation of Unactivated C(sp^3)-H Bonds 109
4.5 Concluding Remarks 113
Chapter 5: Dithiane Directed Rh^{III} Catalysed Amidation of Unactivated C(sp^3)-H Bonds 114
5.1 Introduction to Dithianes: Corey-Seebach Reaction 114
5.2 New Synthetic Applications of Dithianes 117
5.3 Dithiane-directed C-H Functionalisation 119
5.4 Development of Optimised C(sp^3)-H Amidation Conditions 121
5.5 Substrate Scope 125
5.6 Substrate Control Experiments 129
5.7 Reaction Scale-up and Derivatisation 130
5.8 Proposed Mechanism 131
5.9 Conclusions 133
Chapter 6: Rh^{III} Catalysed Amidation of Unactivated C(sp^3)-H Bonds *via* a Transient Imine Directing Group 134
6.1 Introduction to Transient Directing Groups 134
6.2 Imines as Transient Directing Groups 136
6.3 C-H Activation of Aldehydic C-H Bonds 137
6.4 C(sp^2)-H Functionalisation *via* a Transient Imine Directing Group 138
6.5 C(sp^3)-H Functionalisation *via* a Transient Imine Directing Group 140
6.6 Development of Rh^{III} Catalysed Amidation of unactivated C(sp^3)-H Bonds *via* a Transient Imine Directing Group 142
6.7 Conclusions and Future Work 148
References 150
Experimental 156
General Methods and Materials 156
Compound 85 158
Compound 86. 159
Compound 86a 160
Compound 82 161
Compound 93 162
Compound 87 163

Compound 88 164
Compound 104 165
Compound 105 166
Compound 108 170
Compound 106 174
Compound 108 177
Compound 123 178
Compound 124 and 125 179
Compound 137 180
Compound 145 181
Compound 156 182
Compound 146 185
Compound 158 189
Compound 159 190
Compound 62 191
Compound 167 192
Compound 170 193
Compound 171 194
Compound 191 195
Himlensine A (1). 199
General Procedure A: Synthesis of Dioxazolones from Acid Chlorides 201
Compound 288a 201
Compound 288b 201
Compound 288c 202
Compound 288d 202
Compound 288e 203
Compound 288f 203
Compound 288g 204
Compound 288h 204
Compound 288i 205
Compound 288j 205
Compound 288k 205
Compound 288l 206
Compound 288m 206

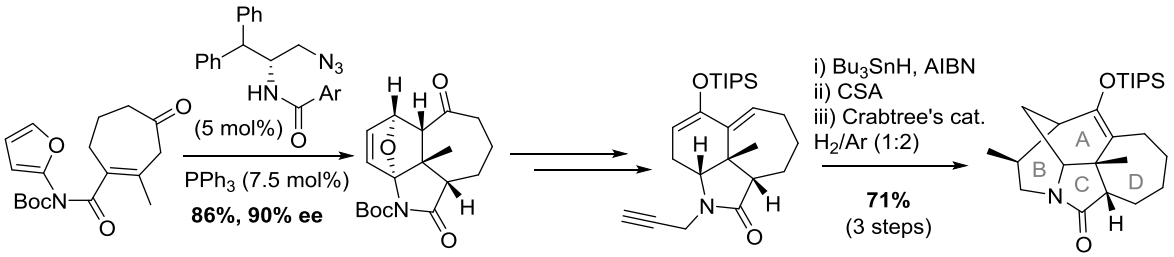
Compound 288n 207
Compound 288o 207
General Procedure B: Synthesis of Dithianes 207
Compound 290a 208
Compound 290b 208
Compound 290c 209
Compound 290d 209
Compound 290e 210
Compound 290f 210
Compound 290g 211
Compound 290h 211
Compound 290i 213
Compound 290j 213
General Procedure C: Synthesis of Amidated dithianes 293. 214
Compound 293a 214
Compound 293b 214
Compound 293c 215
Compound 293d 216
Compound 293e 216
Compound 293f 217
Compound 293g 218
Compound 293h 218
Compound 293i 219
Compound 293j 219
Compound 293k 220
Compound 293l 221
Compound 293m 221
Compound 293n 222
Compound 293o 222
Compound 293p 223
Compound 293q 224
Compound 293r 224
Compound 293s 225
Compound 293t 226

Compound 293u 226
Compound 293v 227
Compound 293w 228
Compound 293x 228
Product Derivatisation 229
Compound 304 229
Compound 305 230
Compound 306 231
Compound 339 232

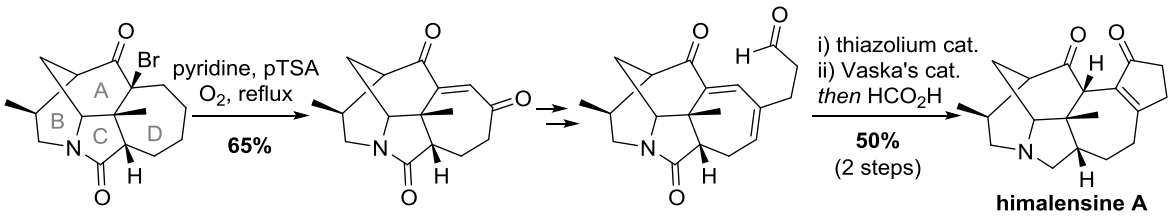
Abstract

This thesis describes the 22-step enantioselective total synthesis of (−)-himalensine A, and the Cp*Rh^{III} catalysed amidation of unactivated C(sp^3)-H bonds utilising dithianes or imines as directing groups.

Chapter 1 introduces the calyciphylline A-type *Daphniphyllum* alkaloids, their biosynthetic origin and himalensine A as one family member. Current published syntheses of these alkaloids are also highlighted as well as previous work conducted on this project.



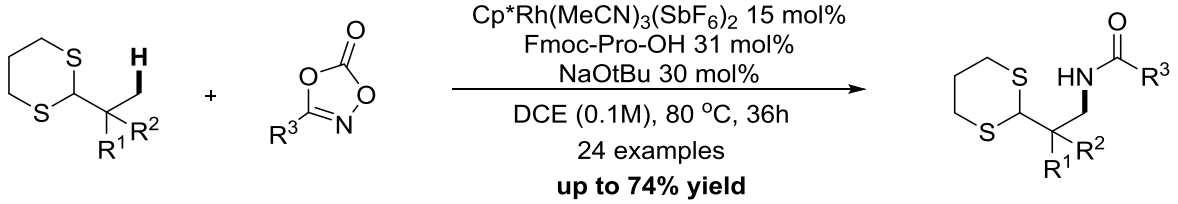
Chapter 2 focuses on the route development towards the ABCD tetracyclic core. Optimisation of the key enantioselective organocatalytic IMDAF cascade enabled the synthesis of large quantities of the tricyclic core. After elaboration to a key cycloisomerisation precursor, a reductive radical cascade was developed to close the B ring. Finally, a highly diastereoselective low-pressure hydrogenation delivered the completed tetracyclic core.



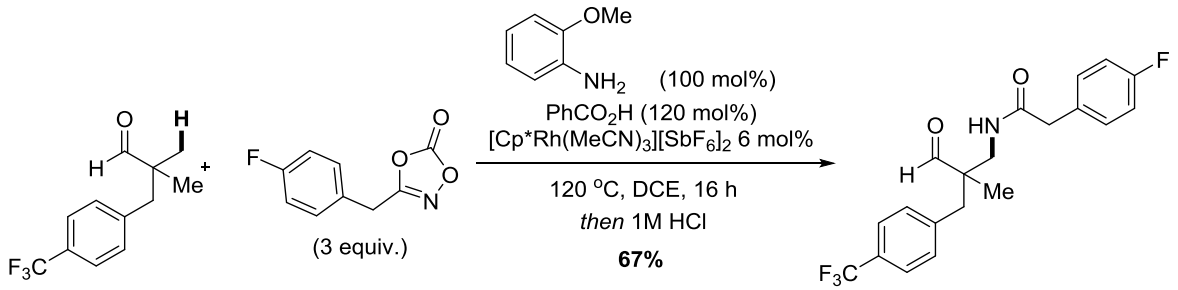
Chapter 3 describes the route from the tetracyclic core through the end-game to access himalensine A. A pyridine and molecular oxygen mediated elimination/C-H oxidation was developed to access an enedione intermediate with the correct oxidation level and

chemical handle required to complete the final ring. The E ring was furnished *via* a Stetter cyclisation and final chemoselective lactam reduction delivered the natural product.

Chapter 4 summarises C-H functionalisation within the context of C-N bond forming reactions. A focus is placed on rhodium, it's ability for directed C-H amination/amidation chemistry and previous work in the field. The challenge of Rh^{III} catalysed C(sp^3)-H functionalisation is introduced.



Chapter 5 features the development of a novel Cp*Rh^{III} catalysed dithiane-directed amidation of unactivated C(sp^3)-H bonds utilising dioxazolone amidating reagents. With the optimised method, a wide range of dioxazolone reagents as well as dithiane partners are well-tolerated. Downstream derivatisation of the amidated products is also demonstrated, including the Corey-Seebach *umpolung* reaction.



Chapter 6 highlights use of a transient imine directing group strategy for metal catalysed C-H functionalisation, and development of this strategy for a Cp*Rh^{III}-catalysed transient imine-directed amidation of unactivated C(sp^3)-H bonds using dioxazolone reagents. Completed optimisation studies enable amidation of a sterically hindered aldehyde in good yield, delivering a synthetically useful 1,3 amidoaldehyde derivative.

Declarations and copyright

I declare that thesis has been written by me, that it is the record of work carried out by me and that it has not been submitted in any previous application for a higher degree at this or any other university or institute of learning. Any work done in collaboration with a research colleague has been fully acknowledged and referenced within the text. All compounds in the experimental chapter were synthesised and characterised by myself unless otherwise stated.

I was admitted as a probationary research student in October 2014 and as a candidate for the degree of Doctor of Philosophy in October 2016; the higher study for which this is a record was carried out in the University of Oxford between 2015 and 2018.

Heyao Shi

Date Signature of candidate:

In submitting this thesis to the University of Oxford, I understand that I am giving permission for it to be made available for use in accordance with the regulations of the University Library for the time being in force, subject to any copyright vested in the work not being affected thereby. I also understand that the title and the abstract will be published, and that a copy of the work may be made and supplied to any *bona fide* library or research worker, that this thesis will be electronically accessible for personal or research use, and that the library has the right to migrate this thesis into new electronic forms as required to ensure continued access to the thesis. I have

obtained any third-party copyright permissions that may be required in order to allow such access and migration.

Acknowledgements

There are many people whom I owe my most sincere gratitude for making these past 4 years in the Dixon group the most interesting, character-building, rewarding, fulfilling and enjoyable time of my life.

I would like to thank Darren for the experience of working in his research group and for supporting me through the DPhil. His enthusiasm for chemistry is infectious and his constant support and desire to overcome the next hurdle has taught me much. I am truly grateful for his supervision and guidance.

To all the members of the Dixon group, thank you for making this truly the most 'interesting' and unique 'work' environment I have ever experienced. A big thank you to Sam for being here from the start till the end, and for always being there to help me and chat (chemistry or not!). Alistair, thanks for your friendship and constant willingness to sacrifice your time to help me with anything in the lab. Thanks Tao for your friendship and humour! Gerard, you are the greatest brother and friend, thank you. Well done and don't give up. Pablo, it has been amazing learning life's important skills with you. From chess to hearthstone, it's never a boring day with you as a fumehood neighbour. Pete, thank you for amusing me every time I've starting a sentence with the words 'Surely….' The Mix, without you, G6 would never have become the Boom Boom lab, so thank you sincerely. Hope you really go big in Japan one day.

A massive thanks to those who helped to proof-read. Pete, Alistair, Mix, Jamie, Pablo and Gerard. Your comments have helped me to see my strongly colloquial writing style. Thank you for setting aside your time for me.

Scoopwatch, you are truly the reason the Dixon group is so unique. Thank you all of you for making the group so great and a less miserable place. Particular mentions must go to SkuPing, Don Dadder and Big Bert.

To my mother and father, you have always supported me and I owe you my deepest gratitude for getting me here. Thanks for your unconditional love and always supporting me.

Finally, none of the works of this thesis would be possible without His wisdom. Great are the works of the LORD; they are pondered by all who delight in them. It is the glory of God to conceal things, but the glory of kings is to search things out. The simple believes everything, but the prudent gives thought to his steps.

Abbreviations

°C	Degrees Celsius
Å	Ångström
Ac	Acetyl
AcOH	Acetic acid
AIBN	2,2’-Azobis(2-methylpropionitrile)
Aq	Aqueous
App	Apparent
Ar	Aryl
atm	atmosphere
9-BBN	9-Borabicyclo[3.3.1]nonane
BINAP	2,2'-Bis(diphenylphosphino)-1,1’-binaphthyl
BINOL	1,1´-binaphtalene-2,2´-diol
Bn	Benzyl
Boc	*tert*-butoxycarbonyl
Bp	Boiling point
br	Broad
brsm	Based on recovered starting material
n-Bu	*n*-Butyl
CAN	Ceric ammonium nitrate
Cbz	carboxybenzyl
Cod	1,5-cyclooctadiene
Conc	Concentration
COSY	Correlation spectroscopy
Cp	Cyclopentadienyl
Cy	Cyclohexyl
d	Doublet
DA	Diels–Alder
DABCO	1,4-diazabicyclo[2.2.2]octane
DBU	1,8-Diazabicyclo[5.4.0]undec-7-ene
DCE	1,2-dichloroethane
DCM	Dichloromethane
dd	Doublet of doublets
DEPT	Distortionless enhancement by polarisation transfer
DIBAL	Diisobutylaluminium hydride
DIPEA	*N*,*N*-diisopropylethylamine
DMAP	4-Dimethylaminopyridine
DMF	Dimethylformamide
DMP	Dess-Martin periodinane
DMSO	Dimethyl sulfoxide
DPP	Diphenylphosphate
dppe	1,2-Bis(diphenylphosphino)ethane
dq	Doublet of quartets
dr	Diastereoisomeric ratio
dt	Doublet of triplets

ee	Enantiomeric excess
EI	Electron impact
equiv	equivalents
ES	ElectroSpray Ionisation
Et	Ethyl
EDG	Electron donating group
EWG	Electron withdrawing group
Et_2O	Diethyl ether
EtOAc	Ethyl acetate
fcc	Flash column chromatography
FI	Field ionisation
G	Gram
H	Hour(s)
HOMO	Highest occupied molecular orbital
HMBC	Heteronuclear multiple-bond correlation experiment
HPLC	High performance liquid chromatography
HRMS	High Resolution Mass Spectrometry
HSQC	Heteronuclear single-quantum coherence experiment
Hz	Hertz
IR	Infrared
IUPAC	International Union of Pure and Applied Chemistry
IMDAF	Intramolecular Diels–Alder of furan
IMPKR	Intramolecular Pauson–Khand reaction
IPA	*Iso*-propylalcohol
IPr	1,3-Bis(2,6-diisopropylphenyl)-1,3-dihydro-2*H*-imidazol-2-ylidene
J	Coupling constant
JohnPhos	Au[P(*t*-Bu)$_2$(*o*-biphenyl)]
KHMDS	Potassium bis(trimethylsilyl)amide
LDA	Lithium diisopropylamide
LUMO	Lowest unoccupied molecular orbital
[M]	Metal complex
M	Molar concentration
m	Multiplet
Me	Methyl
MeOH	Methanol
mg	Milligram
MHz	Mega hertz
Min	Minute(s)
mL	Millilitre
µL	Microlitre
mmol	Millimole
mM	millimolar
Mol	mole
MOM	methoxymethyl
mp	Melting point
MS	Molecular sieves
MS	Low resolution mass spectrometry

Ms	Methanesulfonyl
m/z	Mass to charge ratio
NMR	Nuclear Magnetic Resonance
NMO	4-Methylmorpholine *N*-oxide
Ns	*Para*-nitrobenzenesulfonyl
nOe	Nuclear Overhauser Effect
Nu	nucleophile
o	Ortho
OH	Hydroxy
OTf	Trifluoromethanesulfonate
p	*para*
PCC	Pyridinium chlorochromate
PE	Petroleum ether bp 30-40 °C
PG	Protecting group
Ph	Phenyl
PMB	*Para*-methoxybenzyl
PMP	*Para*-methoxyphenyl
ppm	Parts per million
Pr	propyl
q	Quartet
R	Generic substituent
rac	Racemic
R_f	Retardation factor
r.r.	Regioisomeric ratio
quint	Quintet
RCM	Ring-closing metathesis
rt	Room temperature
s	Singlet
sxt	Sextet
t	Triplet
TBAF	Tetrabutylammonium fluoride
TBAI	Tetrabutylammonium iodide
TBAB	Tetrabutylammonium bromide
TBS	*tert*-butyldimethylsilyl
t-Bu	*tert*-butyl
Temp	temperature
t/*tert*	*tertiary*
Tf	triflate
TFA	trifluoroacetic acid
THF	Tetrahydrofuran
TLC	Thin layer chromatography
TMS	Trimethylsilyl
TMSOTf	Trimethylsilyl trifluoromethanesulfonate
t_R	Retention time (HPLC)
Ts	*Para*-toluenesulfonyl
TS	Transition state
p-TsCl	*Para*-toluenesulfonyl chloride

p-TsOH	*Para*-toluenesulfonic acid
UV	ultraviolet

Chapter 1: The Calyciphylline A-type *Daphniphyllum* Alkaloids

1.1 The *Daphniphyllum* Alkaloids

The *Daphniphyllum* alkaloids are a diverse family of natural products isolated from 15 species of the genus *Daphniphyllum*. [1][2] Since the first isolation report by Yagi in 1909[3], hundreds of *Daphniphyllum* alkaloids displaying unique, diverse, and structurally complex skeletons have been isolated and characterised. To this day, work towards discovering new *Daphniphyllum* alkaloids is still continuing, with new molecules being found up to and including 2016.[4,5] Within this large family, 14 structural types have been classified based on the carbon skeleton they possess, with representative examples shown in figure 1.[1] Many natural products within this large family also display diverse biological properties[2], ranging from anti-tumour and anti-HIV[6] to pesticidal and insecticidal activity.

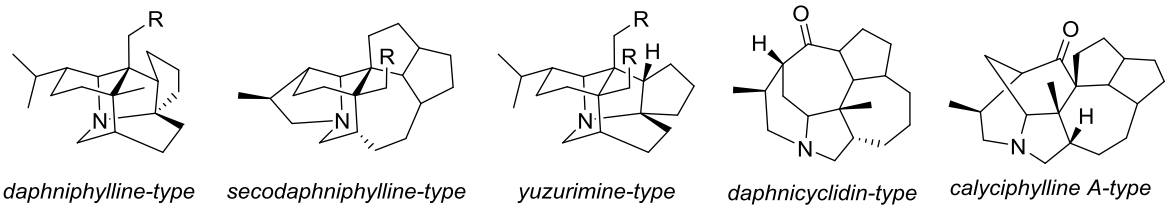


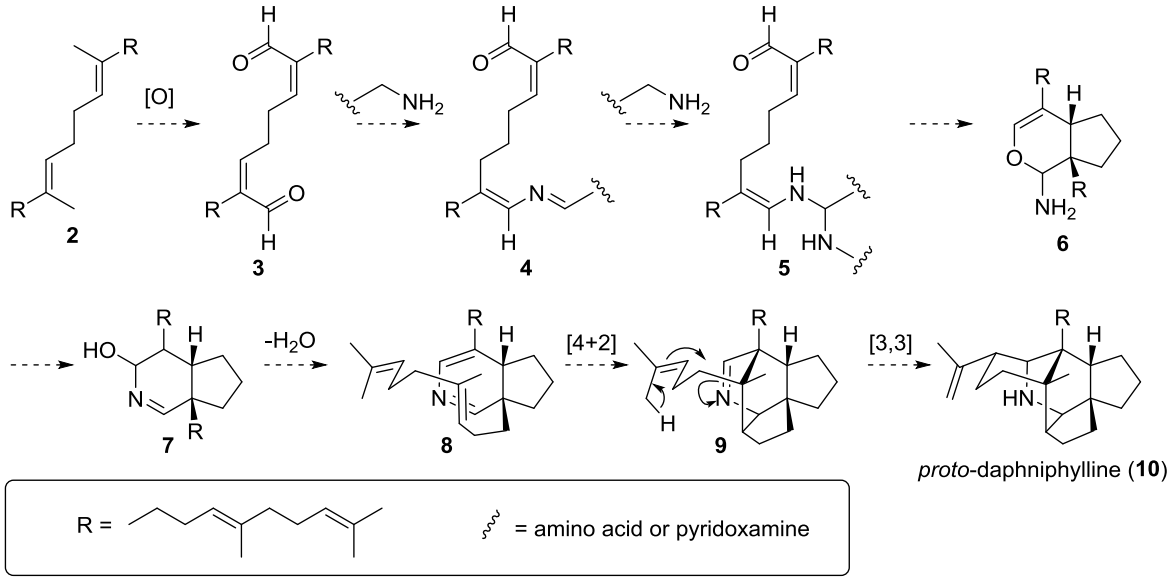
Figure 1: 5 representative structural classes of *Daphniphyllum* alkaloids**.**

1.2 Biosynthetic Studies

Unlike 'pure alkaloids', where both the carbon skeleton and the basic nitrogen atom are introduced from natural amino acids, the *Daphniphyllum* alkaloids can be described as pseudo-, crypto-[7] or terpenoid-alkaloids[8] where the carbon skeleton is constructed from prenyl units. The nitrogen source in this case is thought to be derived from primary amines such as β-aminoethanol or methylamine. In 1973, Suzuki and Yamamura

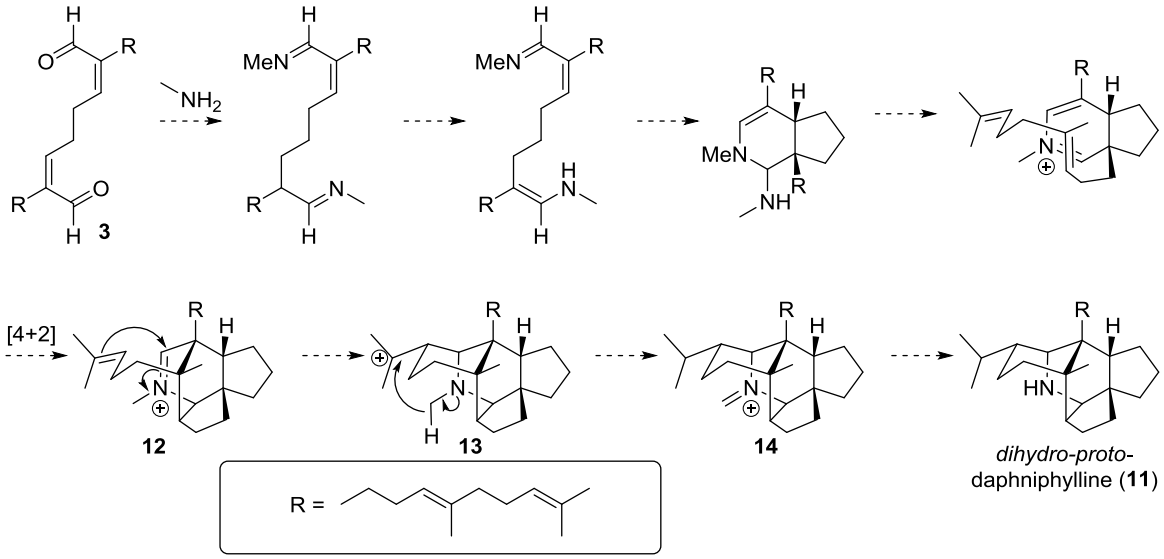
conducted feeding experiments on the leaves of *D. Macropodum* and the fruits of *D. Teijsmanni* using ^{14}C labelled mevalonic acid and ^{14}C labelled squalene.[9,10] From degradation studies, they concluded that the natural products daphniphylline, codaphniphylline and daphnilactone B were biosynthesised from squalene-like intermediates thus proving the terpene provenance of the *Daphniphyllum* alkaloids.

Following on from this important work, Heathcock conducted further extensive studies into the biosynthetic pathway including proposing a mechanism to describe how the nitrogen atom is introduced (scheme 1)[11,12]. From squalene **2**, allylic oxidation to reach a dialdehyde **3** occurs, from which imine formation with an amino acid or pyridoxamine and prototropic shift gives rise to enimine **4**. This enimine is poorly nucleophilic, and so initial trapping with another amine to give enamine **5** occurs, which subsequently undergoes intramolecular Michael addition to form bicycle **6**. Following on, isomerisation to iminal **7** occurs, and subsequent loss of water generates diene **8** posed for an *aza*-Diels-Alder reaction with the geranyl side arm to give **9**. Finally, an ene reaction is proposed to occur, leading to the natural product *proto*-daphniphylline **10**.



Scheme 1: Heathcock's proposed biosynthesis of *proto*-daphniphylline.

Through skeletal rearrangements and oxidations, *proto*-daphniphylline is the natural product and common intermediate from which all 250+ *Daphniphyllum* alkaloids are derived from.[1] Taking knowledge from their biosynthetic studies, Heathcock and co-workers were able to accomplish the diastereoselective synthesis of *proto*-daphniphylline **10** in a single step through pentacyclisation of dihydrosqualene dialdehyde **3**. When treated with ammonia, followed by warming with acetic acid, *proto*-daphniphylline **10** can be isolated in 15% yield. Additionally, when methylamine is employed as the nitrogen source, the reduced natural product *dihydro-proto*-daphniphylline **11** is furnished in a single step with an impressive 65% yield (scheme 2). The mechanism is postulated to follow a similar route to the biosynthetic pathway of *proto*-daphniphylline, however given that in intermediate **12** the nitrogen is methylated to give the iminium, no ene-type reaction can occur. Instead, the pendant prenyl alkene attacks the electrophilic iminium, giving a tertiary carbocation **13**, which is trapped by a hydride shift from the methylamine moiety to give **14**. Finally, after hydrolysis, *dihydro-proto*-daphniphylline **11** is afforded, completing the pentacyclisation sequence.



Scheme 2: Heathcock's 1 step synthesis of *dihydro-proto*-daphniphylline **11.**

1.3 The Calicyphylline A-Type Alkaloids

Named after the first molecule in the family to be isolated[13], the calyciphylline A-type *Daphniphyllum* alkaloids possess a unique and structurally complex architecture (figure 2). They all share a common ABCD tetracyclic core and most members of the family contain a hexacyclic framework (exceptions include himalensine A (**1**) and daphniyunnine B (**15**)). The congested fused skeleton of these natural products makes them attractive as a stage for total synthesis and method development; given no total synthesis of any family member had been completed prior to 2017, and envisaging strategic disconnections towards these molecules, the Dixon group were interested in this synthetic challenge.

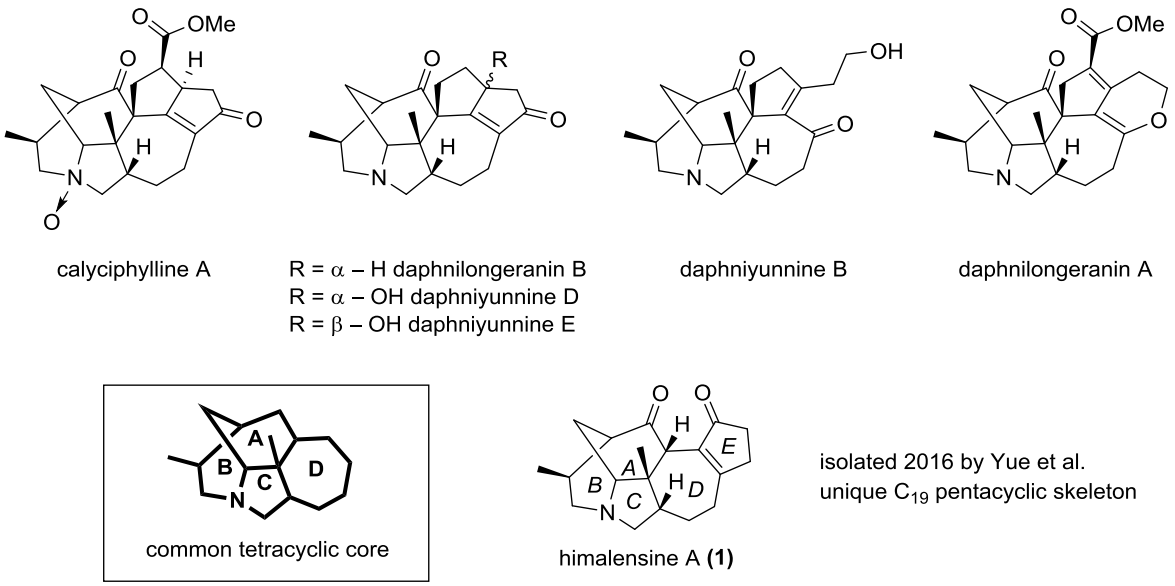
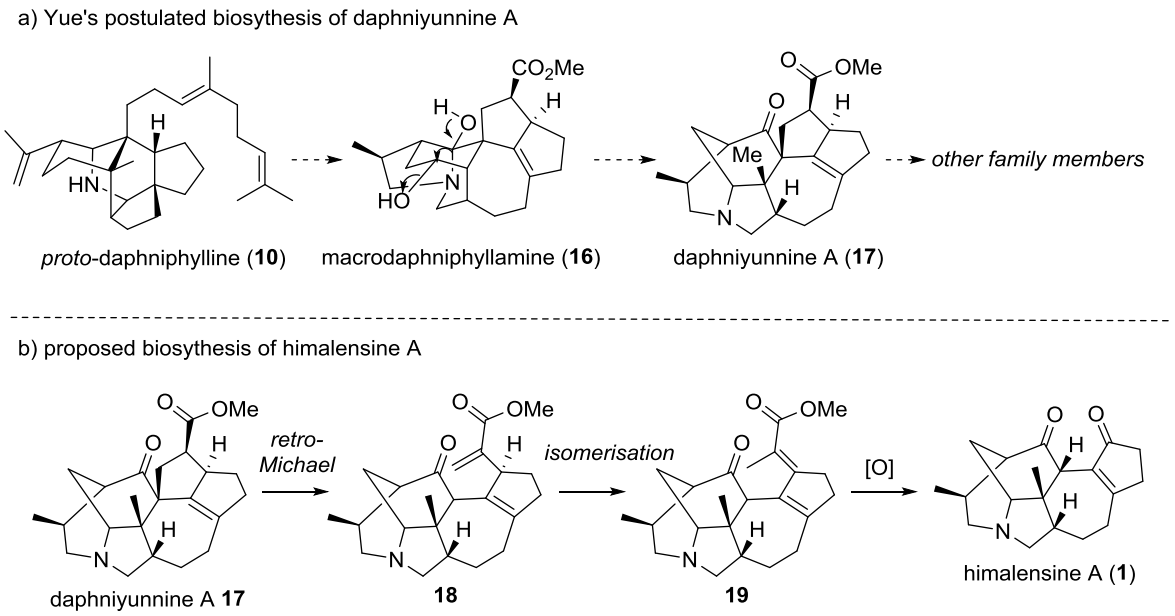


Figure 2: Representative calyciphylline A-type *Daphniphyllum* alkaloids

In 2006, Yue and co-workers isolated 5 calyciphylline A-type alkaloids accordingly named daphniyunnine A-E.[14] In his paper, Yue's provides a plausible biosynthetic pathway where a structural rearrangement from macrodaphniphyllamine **16** (which is formed from skeletal rearrangement of *proto*-daphniphylline **10**) occurs to give daphniyunnine A **17** (scheme 3). This plausible pathway from the macrodaphniphyllamine-type skeleton is

postulated to be the route to access all other members of the calyciphylline A-type family.

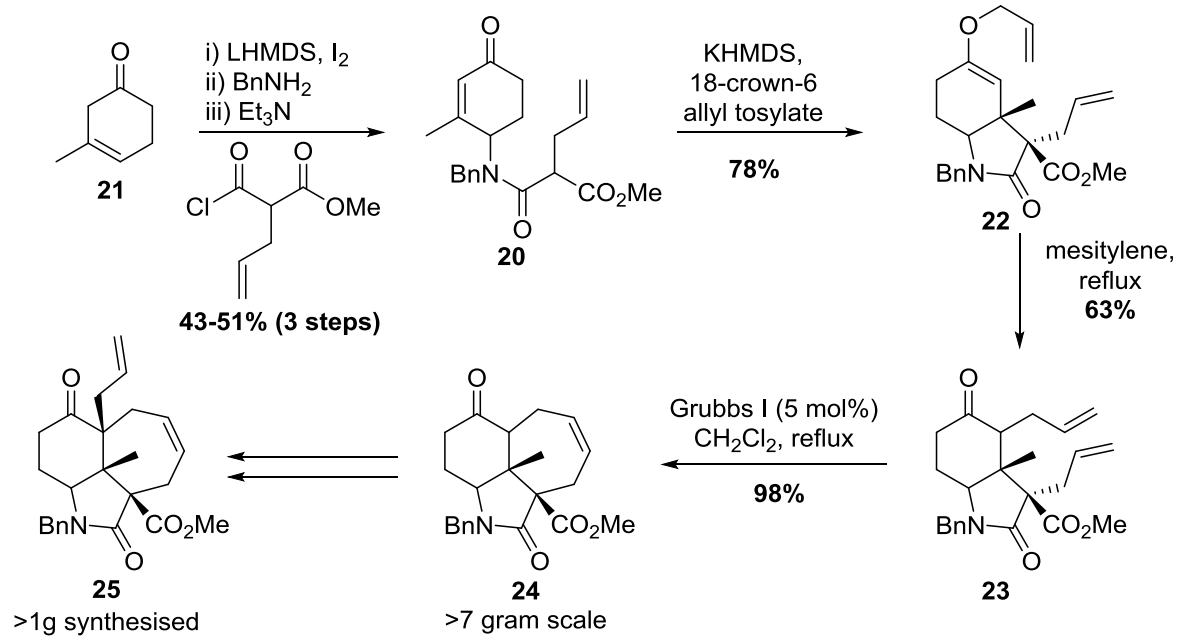


Scheme 3: a) Yue's proposed biosynthesis of macrodaphniphyllamine (**16**) and daphniyunnine A (**17**) from *proto*-daphniphylline (**10**). b) Proposed biosynthesis of himalensine A (**1**).

Himalensine A (**1**), isolated and characterised in 2016 by Yue, possesses a unique pentacyclic carbon skeleton with the cyclopentane ring adjacent to the ketone moiety missing. To date, it is the only natural C_{19} *Daphniphyllum* alkaloid isolated.[4] The biosynthesis of this molecule is still unknown, however it can postulated that from daphniyunnine A, a retro-Michael addition to give **18**, followed by bond isomerisation to afford **19** and final oxidative cleavage could generate the natural product.

1.4 Synthetic Efforts Towards the Calyciphylline A-type Alkaloids

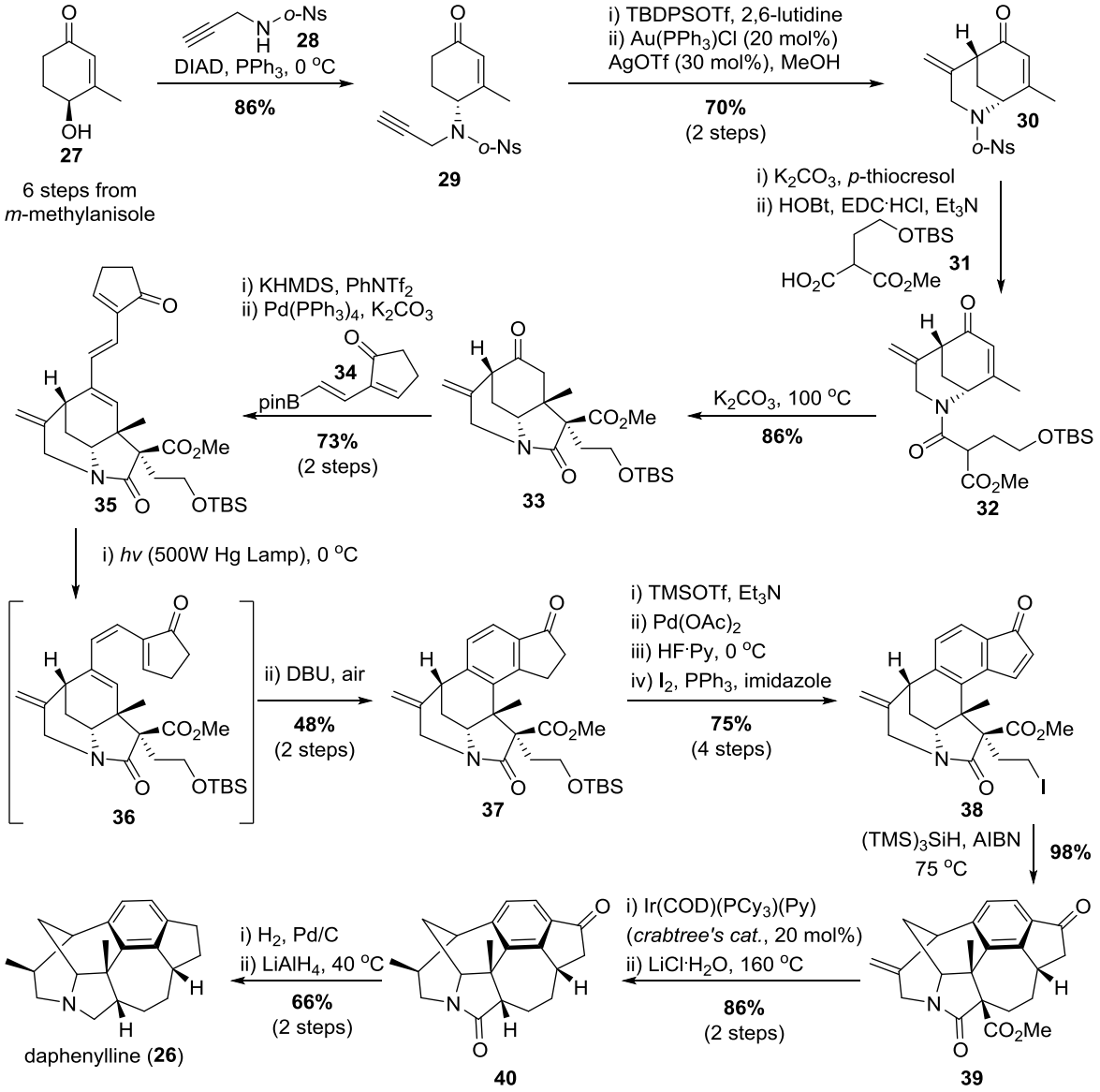
In their seminal publication of 2011, Dixon and co-workers reported an expedient synthesis of the tricycle core of the calyciphylline A-type alkaloids (scheme 4).[17] The key step featured an intramolecular Michael addition of intermediate **20** (synthesised in 3 steps from **21**) followed by *O*-allylation to deliver bicycle **22**. A thermal Claisen rearrangement then afforded **23** which was treated with Grubbs I catalyst to facilitate a ring closing metathesis reaction and close the 7-membered ring, delivering tricycle **24**. Using this approach, >1 g of an advanced intermediate **25** was synthesised.



Scheme 4: Dixon's expedient synthesis of the calyciphylline A tricyclic core.

In his 2013 report, Li and co-workers published the landmark synthesis of daphenylline **26**,[15] a related member of the calyciphylline A-type alkaloids (scheme 5).[16] This alkaloid shares a common tetracyclic core with calyciphylline A, however features an unusual tetra-substituted arene ring moiety. Taking inspiration from Dixon's 2012 publication, Li and co-workers were able to quickly access the tetracyclic core of daphenylline **26** from known hydroxyenone **27** (which was synthesised in 6 steps and then enantioenriched

through enzymatic resolution to 97% ee). Mitsunobu substitution with nosyl-protected propargylamine **28** gave **29**, which after formation of the TBDPS enol ether using TBDPSOTf, was treated with 0.2 equivalents of $Au(PPh_3)Cl$ and 0.3 equivalents of AgOTf (standard cationic gold complex formation conditions), giving rise to bicycle **30** in 70% over 2 steps. Subsequent nosyl deprotection with *para*-thiocresol as a suitable thiol followed by amide coupling with substituted malonic acid **31** gave **32** which was subjected to modified Dixon cyclisation conditions to deliver tricyclic core **33** in 62% yield over 3 steps.

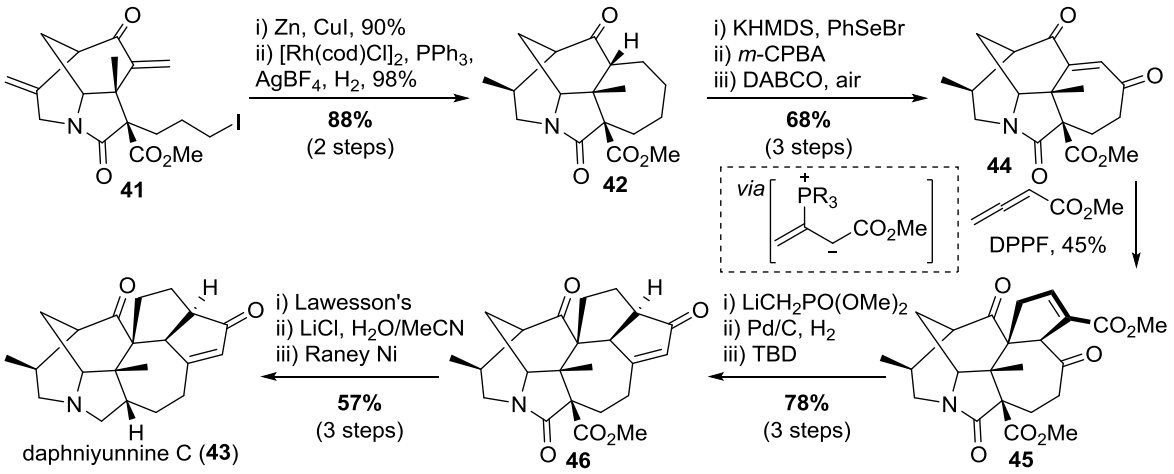


Scheme 5: Li's landmark total synthesis of daphenylline **26**.

The pendant cyclopentane moiety was next introduced through conversion of **33** to the enol triflate followed by cross coupling with pinacolboronic ester **34**, giving **35** which possesses all necessary carbon atoms required to complete the total synthesis. This triene precursor then enabled Li to employ his `signature' reaction strategy. When irradiated with a mercury lamp, the triene moeity was found to isomerise to **36** and undergo a 6π electrocyclisation, closing the central 6 membered ring. Subsequent mild oxidation with air in the presence of DBU then generated the arene moiety, leading to pentacycle **37**. To close the final ring and complete the synthesis, a 2-step Saegusa-Ito oxidation[18] was performed followed by TBS deprotection and an Appel reaction, affording iodoenone **38**. The final ring was then furnished with a reductive radical cyclisation mediated by tristrimethylsilylsilane as a tin hydride equivalent to give **39**, with the completed daphenylline carbon skeleton. A key diastereoselective hydrogenation with Crabtree's catalyst was then performed, delivering hydrogen from within the concave face of the alkene to set the key stereocentre of the methyl group (**40**). Finally, Krapcho dealkoxycarbonylation for removal of the methyl ester group and reduction of both carbonyl groups *via* hydrogenation for the benzylic ketone and hot lithium aluminium hydride for the lactam carbonyl was performed, delivering daphenylline **26** and completing this landmark total synthesis.

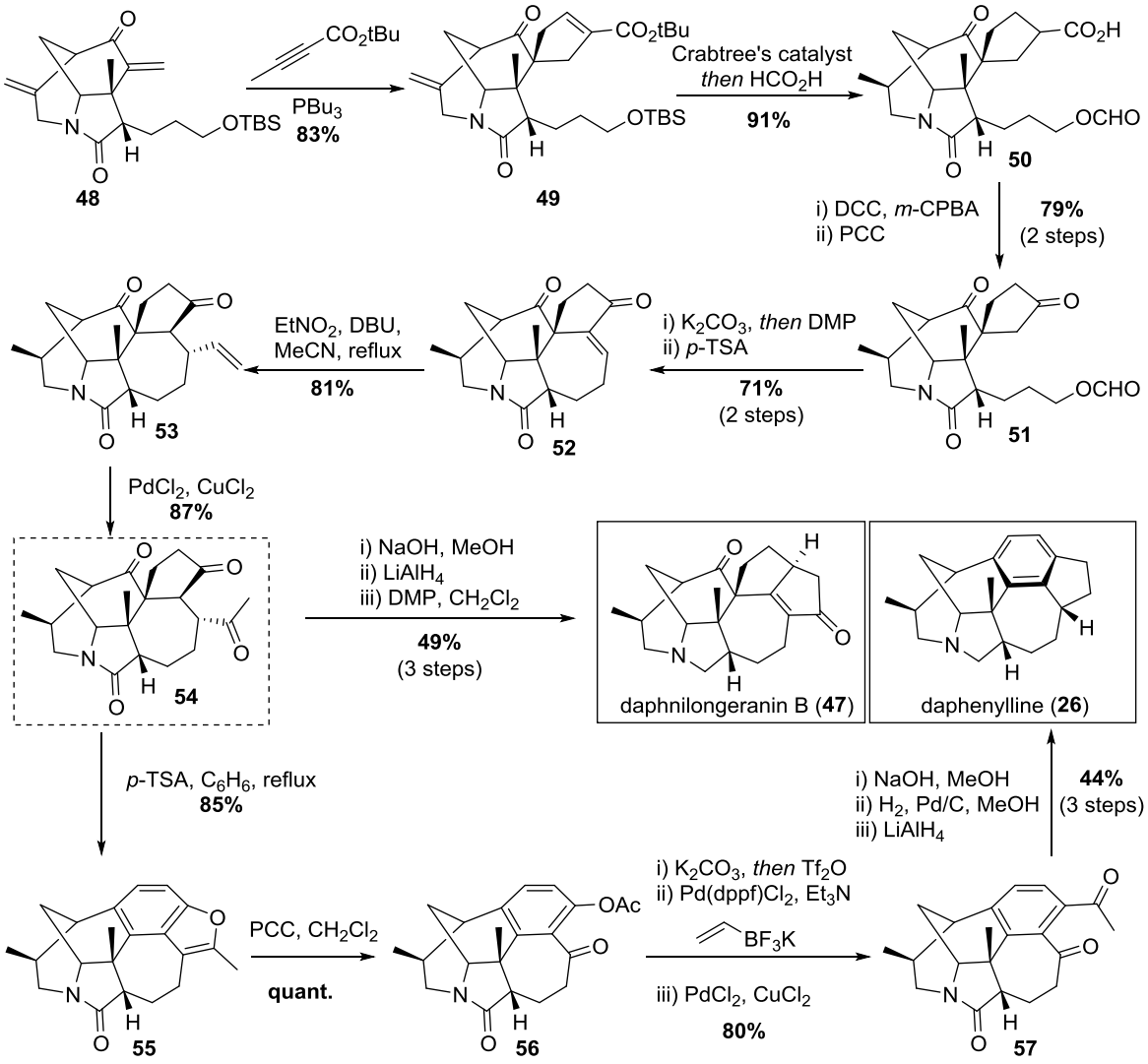
Following on from this report in 2013**,** Fukuyama was also able to complete the total synthesis of daphenylline in 2016 publication[19], however it was not until 2017 that another alkaloid within this family, daphniyunnine C (**43** (also known as longeracinphyllin A),[14] succumbed to total synthesis, once again by the hands of the Li group (scheme 6).[20] Utilising a similar strategy to that established in his previous synthesis of

daphenylline, the tricyclic core of **41** was constructed as the platform to continue the synthesis. This time, instead of ring closing metathesis, an intramolecular cuprate Michael addition was used to close the 7 membered D ring. This was followed by a diastereoselective hydrogenation catalysed by a cationic rhodium complex to deliver **42** in 88% yield over 2 steps.



Scheme 6: Li's total synthesis of daphniyunnine C (**43**).

Subsequently, α-selenation and selenoxide-elimination was performed to give an enone intermediate which was subjected to DABCO in air to effect a molecular oxygen ϒ-CH oxidation, affording dienone **44**. The key step of the synthesis next featured, where the cyclopentane ring fragment was constructed by a phosphine-mediated [3+2] formal cycloaddition with methyl allenoate to give pentacycle **45**. The final ring was then closed through substitution with a suitable phosphonate equivalent, hydrogenation of the cyclopentenone alkene and triazabicyclodecene (TBD) mediated intramolecular Horner-Wadsworth-Emmons olefination to give **46**. Final end-game manipulations involved reduction of the lactam through initial conversion to the thioamide, Krapcho decarboxylation and final Raney nickel desulfurisation, giving daphniyunnine C (**43** in 57% over the previous 3 steps and completing this milestone synthesis.



Scheme 7: Zhai's divergent synthesis of daphnilongeranin B **47** and daphenylline **26**.

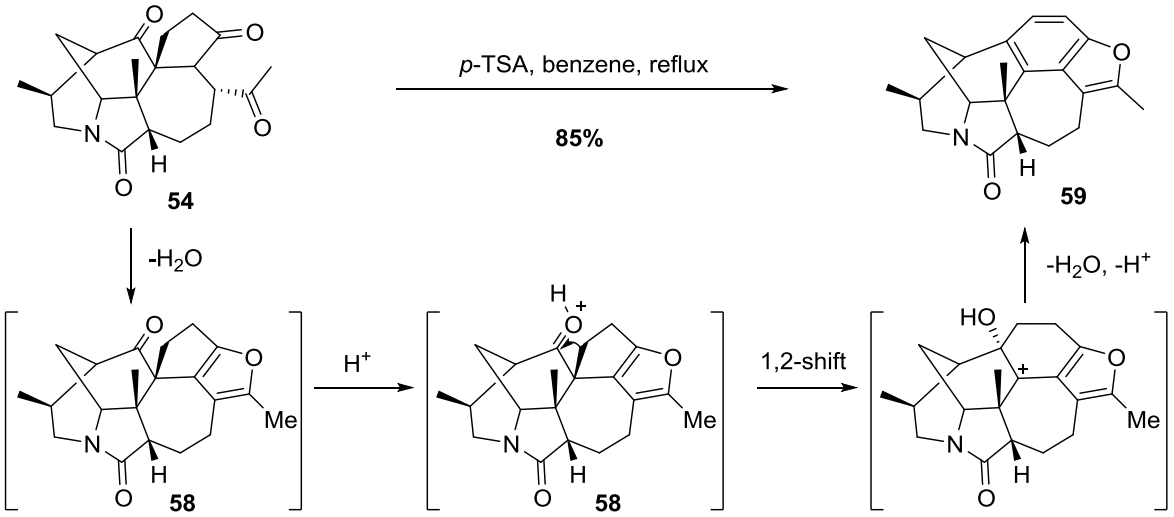
With the fall of daphniyunnine C (**43**), the total synthesis floodgates were truly opened, and in the following months, multiple other family members were conquered. This began with Zhai's publication describing the total synthesis of daphnilongeranin B **47** and daphenylline **26** through a divergent synthetic strategy (Scheme 7). [21][22] Due to the very short timing between the publications, Zhai unknowingly intercepted a very similar intermediate published in Li's synthesis of daphniyunnine C. From this tricyclic core **48**, a related tributylphosphine-mediated [3+2] cycloaddition with *tert*-butyl butynoate gave an excellent yield of **49**. Similarly, Crabtree's catalyst was utilised to effect the diastereoselective hydrogenation of the terminal alkene followed by formic acid

treatment to give acid **50** in 91% yield. DCC/m-CPBA mediated oxidative cleavage of this acid to the secondary alcohol followed by PCC-mediated oxidation to the ketone converted the acid to ketone **51**, which was then able to participate in a key intramolecular aldol reaction after unmasking the pendant aldehyde moiety through formate deprotecting and DMP oxidation. This sequence delivered pentacycle **52** in 71% yield over two steps. Zhai next employed an elegant strategy to introduce the final two carbon atoms required to complete the synthesis. Nitroethane was selected as a suitable nucleophile to perform a nitro-Michael addition to enone **52**, and under the reaction conditions, unexpected elimination of nitrous acid occurred to give terminal alkene **53**. A Wacker oxidation then transformed this alkene to ketone **54** in 87% yield; this key intermediate is the branch point enabling access to the two different natural products. To complete daphnilongeranin B **47**, Zhai performed a base mediated intramolecular condensation followed by lithium aluminium hydride reduction and DMP reoxidation of the secondary alcohols, delivering the natural product in 49% yield over these 3 steps.

Daphenylline was accessed through a different synthetic pathway. Taking inspiration from nature and the biosynthesis of daphenylline, pentacycle **54** was treated with *para*-toluenesulfonic acid in refluxing benzene to afford **55** *via* a key 1,2 Wagner-Meerwein rearrangement. Oxidative cleavage of the benzofuran with PCC afforded **56** in good yield.[23] Following on, methanolysis, sulfonylation and Suzuki cross coupling yielded a styrene, which was subjected to a Wacker oxidation to give ketone **57** in 80% combined yield over 3 steps. Finally, an intramolecular aldol condensation followed by exhaustive reduction of the carbonyls completed the synthesis of daphenylline **26**.

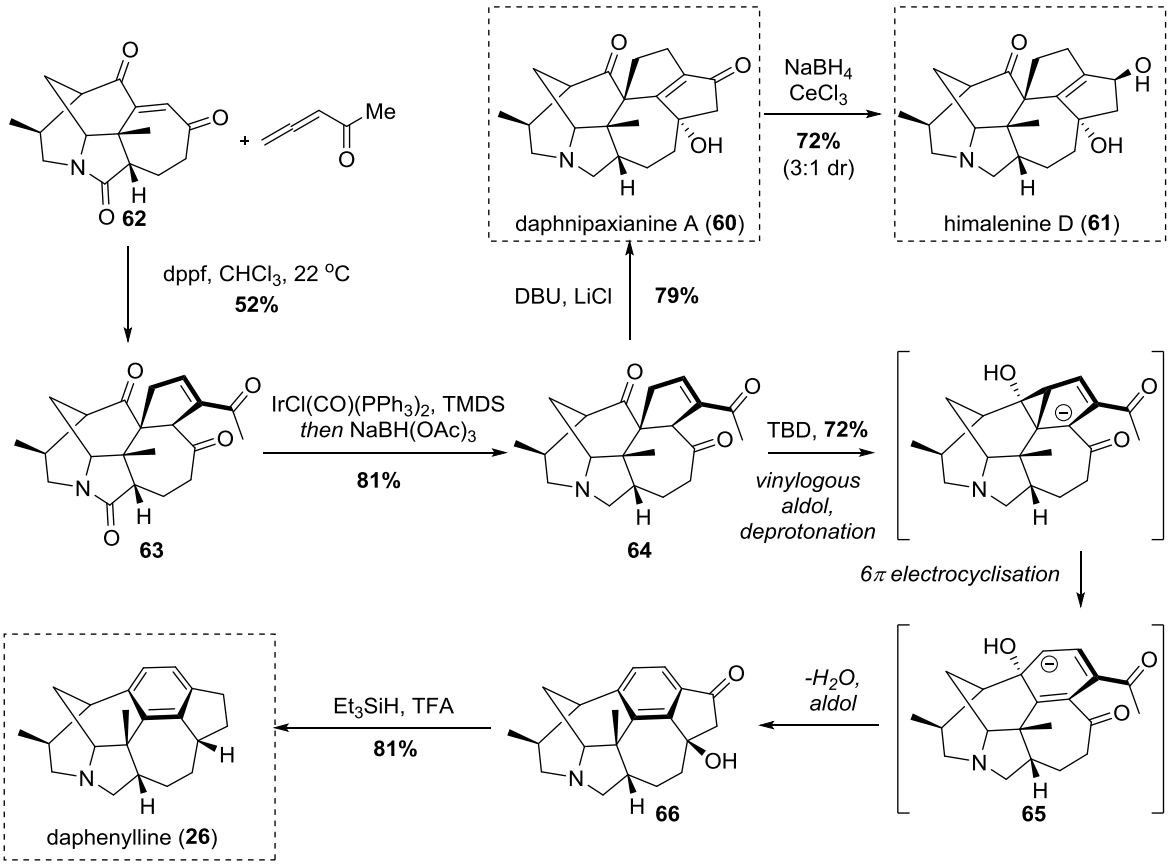
The proposed mechanism for the Wagner-Meerwein step is shown in scheme 8. After initial intramolecular condensation of the two ketone moieties, furan **58** was formed. The

ketone carbonyl is protonated enabling a biomimetic Wagner-Meerwein 1,2-shift, expanding the 5 membered cyclopentane ring. Subsequent loss of a proton and water formed the aromatic ring and furnished benzofuran **59** to complete the cascade sequence.[23]



Scheme 8: Proposed mechanism for Zhai's rearrangement of **52** to **59**.

It can be noted that Li's seminal paper on daphniyunnine C (**43**) was published during the preparation of Zhai's manuscript, therefore even though Zhai utilises many similar strategic disconnections such as the phosphine promoted [3+2] cycloaddition, there can be no doubt that the two works were conducted independently. However in a strange twist of fate, Zhai's elegant realisation of the biomimetic Wagner-Meerwein rearrangement of intermediate **52** very similarly featured in Li's publication just 21 days later, where he was able to conquer daphnipaxianine A **60** and himalenine D **61** as well as complete his second synthesis of daphenylline **26** (scheme 9).[24] From enedione **62** (constructed from similar methods as mentioned previously and also featuring in this thesis), a phosphine-promoted [3+2] cycloaddition gave enone **63**. This structure, bearing



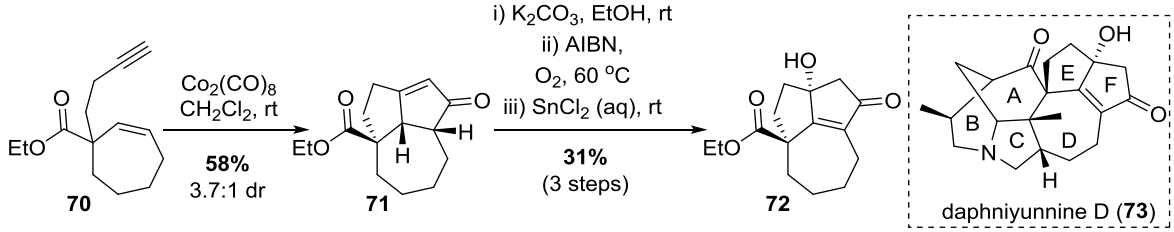
Scheme 9: Li's synthesis of daphnipaxianine A **60**, himalenine D **61** and daphenylline **26**.

two ketones and an enone in the presence of a lactam carbonyl, presents the perfect platform to demonstrate the impressive chemoselectivity of Vaska's catalyst ($IrCl(CO)(PPh_3)_2$), which Li, taking inspiration from published work performed in this thesis, utilised in conjunction with tetramethyldisilane (TMDS) as a reductant to selectively reduce the lactam carbonyl down to the hemiaminal. Subsequent treatment with a secondary mild reductant in the form of sodium triacetoxyborohydride completed the lactam reduction and delivered amine **64** in 81% yield. The discovery of this protocol was pioneered by Nagashima and its adoption in natural product synthesis and demonstration of its chemoselectivity and effectiveness was pioneered by Dixon and Chida.[25–28] It is noteworthy that the lactam precursor differs from Zhai's intermediate, *en* route to daphnilongeranin B, by only the alkene on the 5 membered ring, however this subtle difference allows two different natural products possessing a higher oxidation state to be

obtained. Pentacyclic ketone **64** was then the platform to which the three reported natural products were accessed. Treatment with DBU and lithium chloride effected an intramolecular Aldol reaction to deliver daphnipaxianine A **60** in 79% yield, from which himalenine D **61** was also obtained *via* Luche reduction. When pentacyclic ketone **64** was treated with TBD as a base, it was postulated to undergo an initial vinylogous aldol reaction, followed by electrocyclisation to open the cyclopropane ring[29], giving rise to intermediate **65** from which loss of water furnishes the benzene moiety. Final reduction of **66** with triethylsilane in TFA effected deoxygenation and provided daphenylline in 81% yield.

By the start of 2018, many of the calyciphylline A-type *Daphniphyllum* alkaloids had been completed by the groups of Li, Fukuyama, Zhai and Dixon and elegantly described in their seminal publications. However, the greatest natural product champion, perhaps thought of as undefeatable, was soon after to fall. Testament to the efficiency of Li's route to access the tetracyclic core of these alkaloids and his expertise and understanding of these molecules, he was able to complete the total synthesis of hybridaphniphylline B **67**[30], featuring 11 rings and 19 stereocentres, with daphnilongeranin B **47** and daphniyunnine E **68** also obtained (scheme 11).[31]

This large complex natural product was formed from the late stage Diels-Alder cycloaddition of a cyclopentadiene-bearing calyciphylline A-type alkaloid and an asperulide-based dienophile. Using chemistry now well established, Li was quickly able to access large quantities of enone **69** and create a platform to launch his synthetic efforts and discoveries.

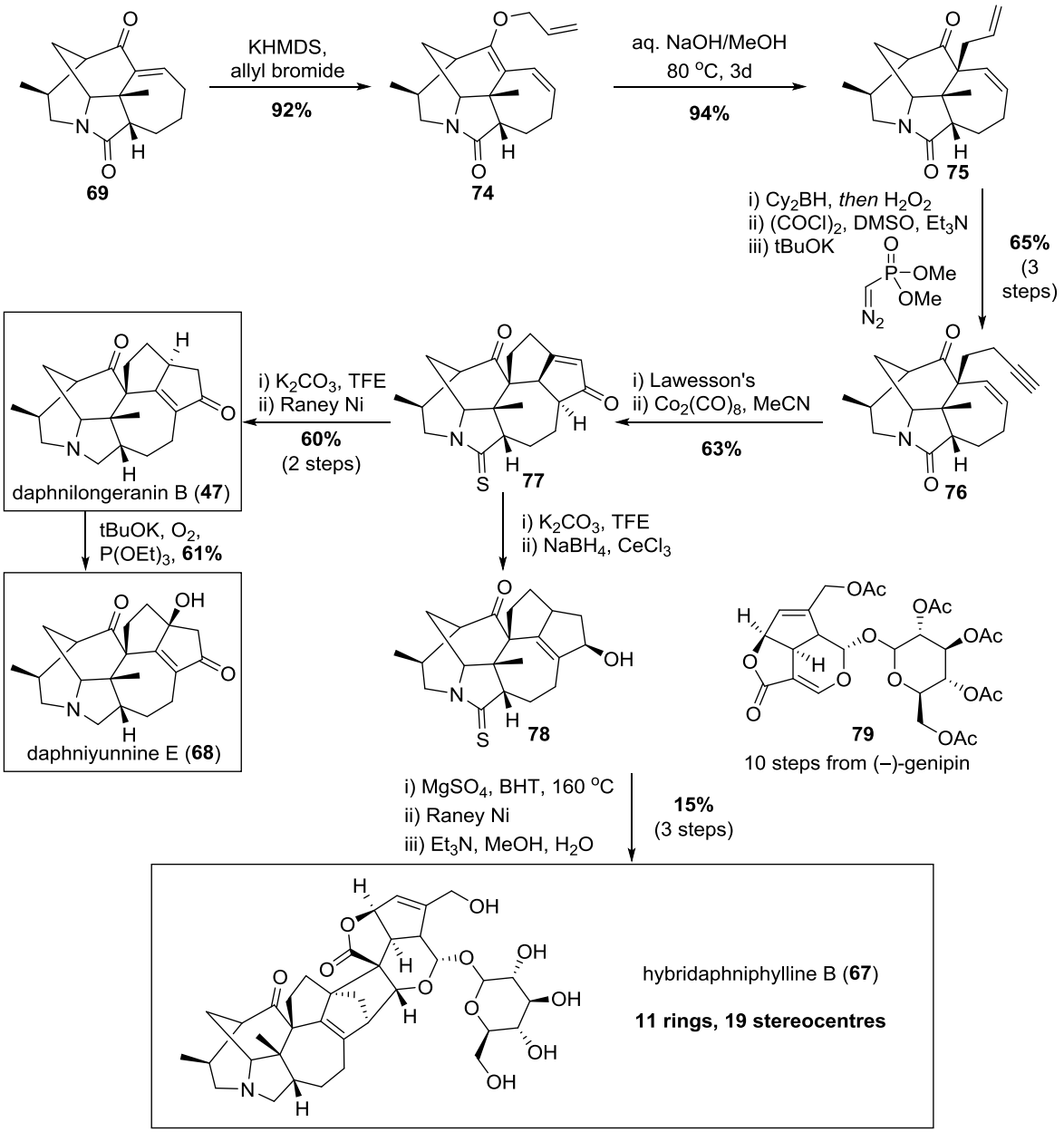


Scheme 10: Dixon's synthesis of the tricyclic core of daphnilongeranin B **47** and daphniyunnine D **73**.

In 2012, Dixon and co-workers published a seminal paper describing a unique strategy to access the core of daphnilongeranin B and related daphniyunnine alkaloids (scheme 10).[32] The key step of this work featured an intramolecular Pauson-Khand reaction of eneyne **70** to give **71**, simultaneously constructing the E and F rings. The enone alkene **71** was then isomerised to the position required for the natural product with potassium carbonate in ethanol followed by subsequent allylic oxidation to install the tertially allylic acohol in **72** required for daphniyunnine D **73**.

Taking inspiration from this publication, as well as Dixon's previously established Claisen rearrangement method for installing the quaternary allyl group[17], Li applied these synthetic strategies to his system (scheme 11). Deprotonation of enone **69** followed by trapping of the enolate with allyl bromide delivered *O*-allyl enol ether **74** in excellent yield. Next, Li was able to find protic solvent conditions to transform enol-ether **74**, via a Claisen rearrangement, to C-allylated ketone **75**. Importantly, the solvent and condition choice were crucial in order to suppress any subsequent Cope rearrangement which would have placed the allyl group at the ϒ position. With his carefully optimised conditions, a remarkable 94% yield for the rearrangement was achieved. Following on, hydroboration with dicyclohexylborane and oxidation to the primary alcohol was performed, followed by a Swern oxidation and subsequent Seyforth-Gilbert homologation to give alkyne **76**. Exposure to Lawesson's reagent converted the amide moiety to a thioamide, after which

the intramolecular Pauson-Khand reaction was performed with dicobalt octacarbonyl and acetonitrile as a promoter, giving hexacycle **77** in 63% yield over the last 2 steps. From here, double bond isomerisation followed by Raney Ni desulfurisation delivered daphnilongeranin B **47** in 60% yield. Allylic oxidation of daphnilongeranin B then afforded daphniyunnine E **68**.



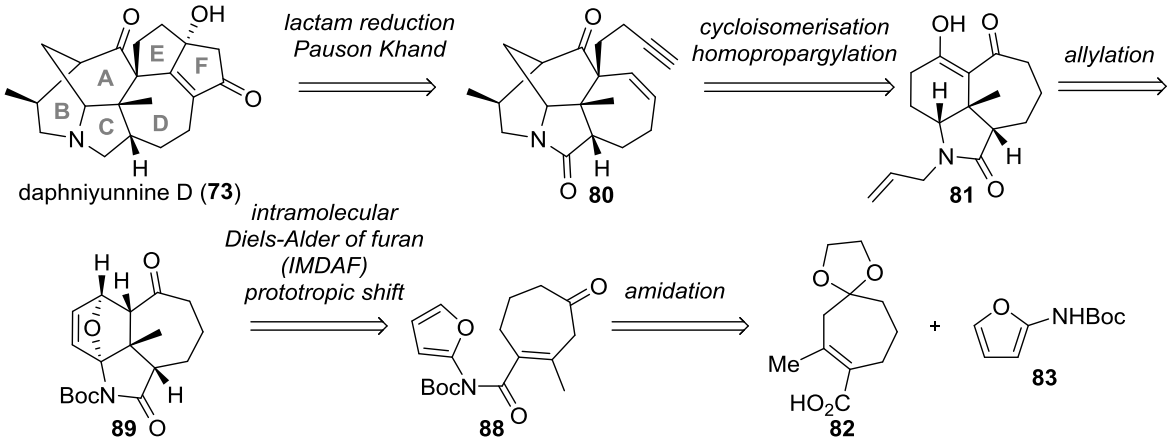
Scheme 11: Li's synthesis of daphnilongeranin B **47**, daphniyunnine E **68** and hybridaphniphylline B **67**.

In order to obtain hybridaphniphylline B **67**, intermediate **77** was isomerised and reduced *via* Luche reduction to give allylic alcohol **78**. This alcohol, upon treatment with magnesium sulfate as a dessicant, eliminated water to unmask a cyclopentadiene Diels-Alder partner, poised to react with a suitably chosen dienophile **79** synthesised in 10 steps from (-)-genipen. Remarkably, when heated to 160 ^{o}C, the desired late stage Diels-Alder cycloaddition of these two highly functionalised substrates was successful in 24% yield, and after Raney nickel mediated desulfurisation and global deacetylation, the landmark total synthesis of hybridaphniphylline B **67** was completed.

1.5 Previous Work in the Dixon Group

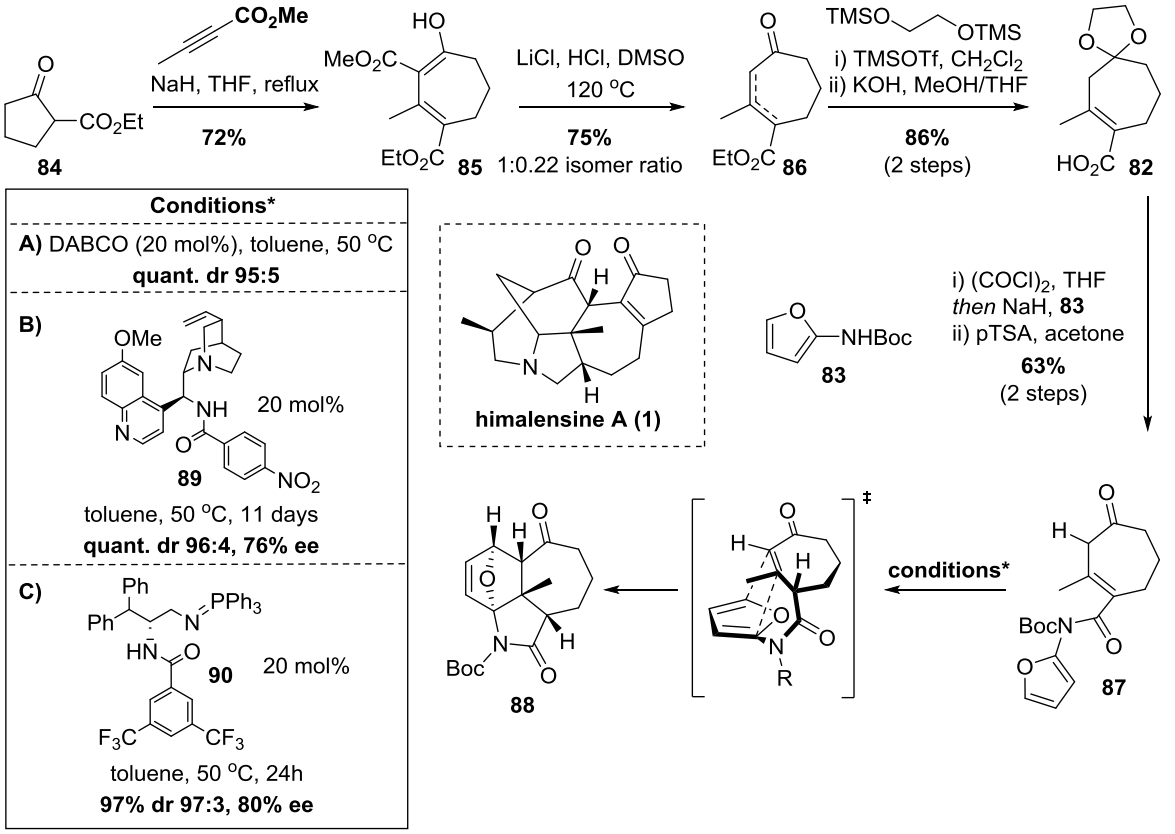
Prior to work conducted in this thesis, many synthetic studies towards the synthesis of calyciphylline A-type *Daphniphyllum* alkaloids had already been performed within the Dixon group. On this project, the vast amount of knowledge and understanding generated by Iacovos Neal Michalides, Benjamin Darses and Pavol Jakubec created a platform for the advancements described here within. Originally, daphniyunnine D[14,33] **73** was selected as the target. This natural product has not previously succumbed to total synthesis, however its sister compound daphniyunnine E **68**, which differs only by epimerisation of the allylic alcohol stereocentre, was recently completed by Li in his report of the synthesis of hybridaphniphylline .[31]

In an early stage retrosynthetic analysis (scheme 12), the E and F rings could initially be disconnected through a Pauson Khand reaction, and the bridgehead amine could be strategically protected as a lactam amide, leading to **80**. This can then be brought back through a metal catalysed cycloisomerisation to close the B ring and a suitable homopropargylation reaction/sequence of reactions to give **81**.



Scheme 12: Retrosynthetic analysis of daphniyunnine D **73**.

Allylation and suitable FGI would allow **81** to be synthesised from **88** which leads to the key disconnection pivotal to this synthetic proposal. **88** can be disconnected through an intramolecular Diels-Alder/prototropic shift cascade, enabling the ACD tricyclic core and multiple stereocentres to be constructed in a single step. Final disconnection takes **87** back to two simple precursors, a 7-membered ring acid **82** and amidofuran **83**.



Scheme 13: Proof of concept for the IMDAF cascade.

In order to test this proposal, Darses and Michaelides within the Dixon group were able to develop a route to obtain the Diels-Alder precursor (scheme 13). Starting from ketoester **84**, deprotonation and trapping with methyl butynoate afforded diester **85** *via* a Grob fragmentation cascade. The methyl ester was then removed through a selective Krapcho dealkoxycarbonylation, giving rise to ketoester **86**, existing as a 1:0.22 mixture of double bond isomers with conjugation to the ester dominant. In order to eliminate these regioisomers, the ketone was acetal protected followed by hydrolysis of the ester to obtain acid **82**. Next, a challenging amide coupling reaction was performed by initially converting the acid to the acid chloride, and then reacting this *in situ* with the sodium salt of amidofuran **83** to form the required amide bond. Acid deprotection of the acetal protecting group then yielded Diels-Alder precursor **87** in 63% yield over the previous two steps. Importantly, the alkene in this molecule remained exclusively conjugated to the amide; this is critical to the synthetic strategy since an enantioselective prototropic shift is envisaged to create a chiral intermediate able to perform the intramolecular Diels-Alder cycloaddition. The key disconnection (termed the IMDAF cascade) was then tested.

Pleasingly, when treated with 20 mol% DABCO as a base in toluene at 50 ^{o}C (scheme 13 Conditions A), the desired IMDAF cascade proceeded smoothly, leading to Diels-Alder adduct **88** in quantitative yield and 95:5 dr. The initial plan was to screen bifunctional cinchona-based catalysts to effect an enantioselective IMDAF cascade reaction, and therefore DABCO was chosen accordingly to mimic the quinuclidine basic moiety of the cinchona alkaloids. Extensive studies into these catalysts identified catalyst **89** as proficient in this reaction (conditions B), smoothly catalysing the IMDAF cascade to deliver Diels-Alder adduct in quantitative yield, 96:4 dr and 76% ee. However, due to the poor Brønsted basicity of this cinchona-based catalyst, a prolonged reaction time of 11

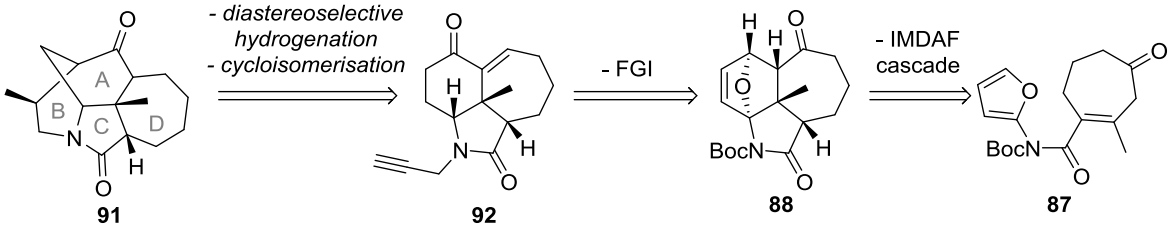
days was required to achieve full conversion as well as a high catalyst loading of 20 mol%. Both these factors severely limited scalability of the reaction and so a different approach had to be identified. Accordingly, the bifunctional iminophosphorane (BIMP) class of catalysts was tested in this reaction.[34–38] These catalysts utilise a highly basic iminophosphorane moiety mounted on a chiral scaffold containing hydrogen-bond donors. This way, the catalyst can both activate electrophiles *via* hydrogen bonding as well as deprotonate pronucleophiles, thus orientating both reaction partners within a chiral framework and imparting enantioselectivity. After extensive screening, catalyst **90** was identified as having the best performance, and with 20 mol% catalyst loading, the Diels-Alder adduct **88** could be obtained in 97% yield, 97:3 dr and 80% ee after only slight optimisation of reaction conditions. Importantly, the reaction time was drastically reduced from 11 days to 24 hours, improving the scalability of the synthesis.

Although Darses, Michaelides and Jakubec were not able to complete the total synthesis of daphniyunnine D, their tremendous efforts and the passing on of their vast wealth of knowledge was crucial to the work within this thesis, which culminated in the first total synthesis of himalensine A (**1**).

Chapter 2: The ABCD Tetracyclic Core

2.1 Introduction to the Synthetic Challenge

As highlighted in chapter 1, an approach to the tricyclic core of the calyciphylline A-type alkaloids had been validated, featuring a key IMDAF cascade reaction. This reaction could be catalysed by chiral bases, enabling quick access to enantioenriched material, creating a platform from which a major push to the final target could be launched.



Scheme 14: Retrosynthetic analysis for the tetracyclic core of the Calyciphylline A-type alkaloids.

With this key method established, a retrosynthetic analysis of the ABCD tetracyclic core **91** of the calyciphylline A-type *Daphniphyllum* alkaloids was envisaged (scheme 14). We planned to set the B-ring methyl group stereochemistry via a diastereoselective hydrogenation reaction and close the LHS B ring by a cycloisomerisation/Conia-ene type reaction. Several functional group interconversions and transformations from **92** would lead to tricycle **88**, the product of the key IMDAF method from amidofuran precursor **87.**

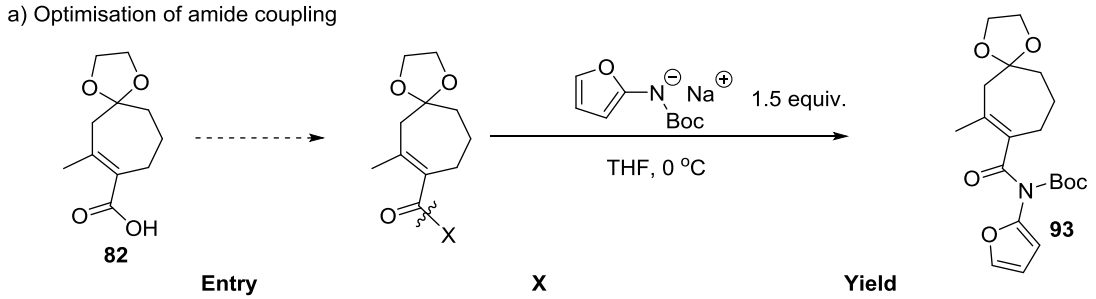
In order to realise this synthetic plan, three major challenges had to be overcome.

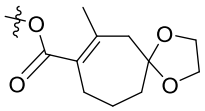
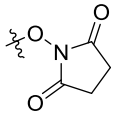
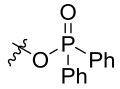
- Development of a scalable route to access IMDAF precursor **87**.
- Optimisation of the enantioselective IMDAF reaction.
- Development of a method to access the LHS B ring, enabling progression to the tetracyclic core.

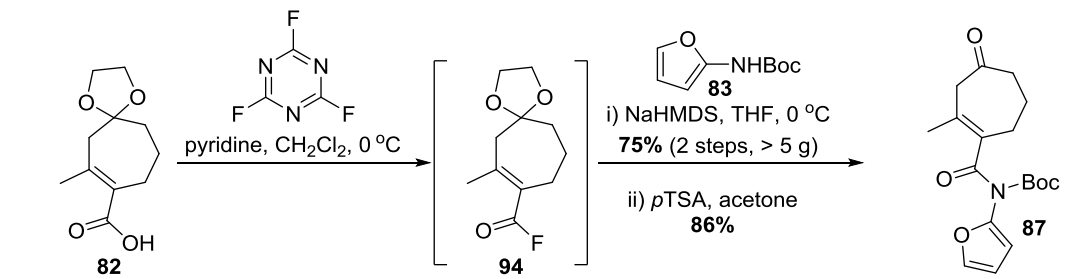
Solutions to these three challenges have been found during the course of this thesis and are presented in this chapter.

2.2 Access to IMDAF Cascade Precursor 87

In order to study the enantioselective IMDAF cascade reaction, the key reaction for our planned synthesis, significant quantities of the Diels-Alder precursor **87** had to be obtained. A previous route to this compound was developed by Michaelides featuring an acid chloride mediated imide coupling of acid **82** with amidofuran **83**, however this method was poorly reproducible. Therefore another scalable and reproducible approach was sought to form this challenging C-N bond (scheme 15).



Entry	X	Yield
1		0%
2		0%
3		67%
4		92%



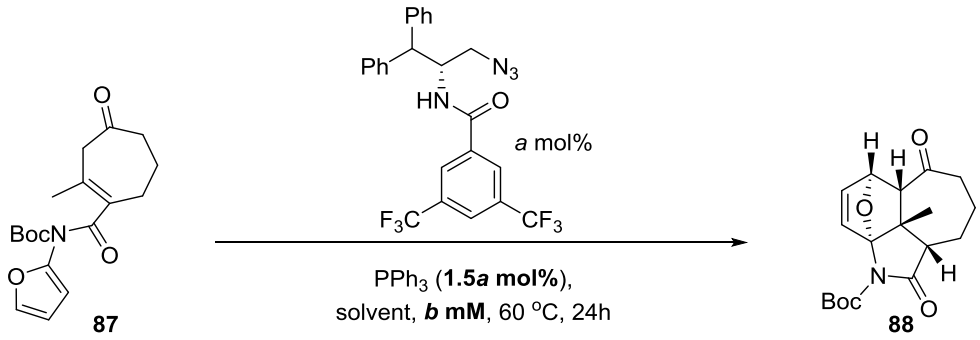
Scheme 15: a) Optimisation of amide coupling to access amide **93**. b) Acid fluoride **94** scale up procedure.

Four different activated acid equivalents of **82** were synthesised and tested in the imide coupling reaction (scheme 15). Both the symmetrical anhydride and the *N*-hydroxysuccinimide ester did not display any reactivity despite being commonly used as active ester equivalents; this result highlights the poor nucleophilicity of amidofuran salt **95** given its direct conjugation with the aromatic ring as well as the *N*-Boc protecting group. When the more active phosphinic anhydride (entry 3) was employed, the desired amide could be isolated in 67% yield. Upon closer examination, the major by-product of this reaction was a phosphinylated amidofuran, pointing to attack of the amidofuran anion at the electrophilic phosphorus centre as well as the carbonyl. Finally, trial of the acid fluoride, which was stable to column chromatography, displayed an excellent yield for the desired amide product.[39] Acid fluorides are unique amongst the acyl halides as they are the most stable to hydrolysis and epimerisation of the α-stereocentre, however they are more reactive towards anionic nucleophiles due to high δ-positive character of the acyl carbon centre. With this discovery, scale-up from acid **82** was conducted, enabling synthesis of multigram quantities of Diels-Alder precursor **87**.

2.3 Enantioselective IMDAF Cascade

With large quantities of Diels-Alder precursor **87** in hand, studies to improve the key IMDAF cascade reaction began. Taking Jakubec's previously developed conditions as a starting point (table 1, entry 1), catalyst loading was the first variable to consider. The catalytically inactive precatalyst components, azide **96** and triphenylphosphine **97**, could be introduced directly into the reaction without prior premixing. An *in situ* Staudinger reaction forms an iminophosphorane superbase which is the catalyst for the reaction.

When the catalyst loading was gradually lowered from 20 mol% down to 5 mol% (table 1, entries 1-4), the excellent yield was maintained, accompanied by an increase in ee from 79% with 20 mol% loading to 89% with 5 mol%. One possible explanation for this phenomenon is supramolecular dimerization of the catalyst at high concentrations, leading to a less stereoselective catalyst for the system.



87 88

Entry	cat. loading (*a* mol%)	solvent	concentration / *b* mM	Yield / %	ee / %
1	20	toluene	0.06	90	79
2	10	toluene	0.06	82	85
3	7.5	toluene	0.06	91	88
4	5	toluene	0.06	86	89
5	5	toluene	0.03	<50%	n.d.
6	5	toluene	0.09	92	87
7	5	toluene	0.12	84	84
8	5	toluene	0.30	74	79
9	5	benzene	0.06	88	87
10	5	$PhCF_3$	0.06	46	85

Table 1: Optimisation of the BIMP catalysed IMDAF cascade reaction.

Next, the effect of concentration was investigated, and the reaction concentration was both decreased from 0.06 M to 0.03 M as well as increased to 0.09 M and 0.12 M. At 0.03 M (entry 5), the yield dropped below 50% and the ee was not measured in light of the poor yield. When the concentration was increased to 0.09 M, the yield was excellent,

though the ee dropped slightly from 89% to 87%. Further increasing the concentration to 0.12M led to continued lowering of ee to 84% (entry 7). These concentration effects reflect the same trends as catalyst loading, where higher catalyst concentration leads to a lower ee of IMDAF product **88**. Finally, solvent effects were screened, with toluene, benzene (entry 9) displaying similar results, and trifluorobenzene leading to a large drop in yield to 46% (entry 10). Thus, entry 4 was selected for scale-up. Utilising these conditions, the reaction was scaled up to 4 grams of starting material **87**. Pleasingly, the reaction maintained the excellent yield and enantioselectivity, and 3.4 g of Diels-Alder adduct **88** was isolated in 84% yield and 90% ee with a 92:8 mixture of diastereomers. The configuration of the major diastereomer had previously been assigned by nOe experiments as an *exo*-cycloaddition product, however the structure of the minor diastereomer remained unclear and was tentatively assigned as the *endo*-diastereomer. After computational modelling, this assignment was later revised and described in section 2.4.

2.4 Computational Calculations on the IMDAF Cascade

In order to further understand the reaction, rationalise the origin of enantioselectivity and determine the identity of the minor diastereomer, computational calculations were performed on this IMDAF cascade reaction in collaboration with Professor Robert Paton and Dr Quynh Nguyen.

Initially, the racemic reaction catalysed by DABCO was modelled in order to understand the stereoselectivity of the reaction (figure 3). When the Diels-Alder reaction was modelled, the *endo*-IMDA reaction was found to be substantially disfavoured with a barrier greater than 10 kcal/mol than the *exo* cycloaddition mode. The *endo*-cycloaddition

product **98** was also thermodynamically unstable with respect to the starting material. This result casts heavy doubt on the minor diastereomer being the *endo*-cycloaddition product.

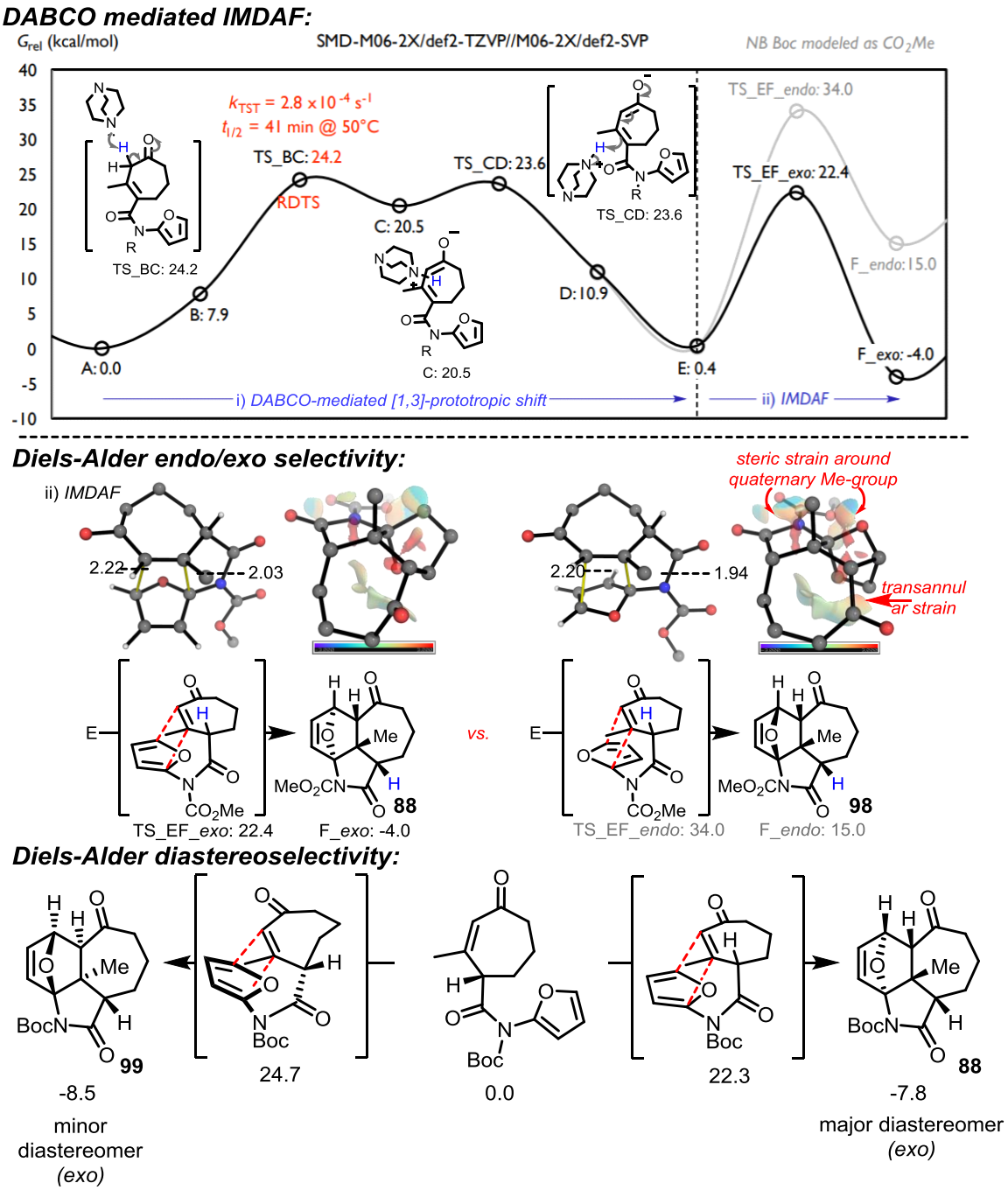


Figure 3: Computational studies on the DABCO catalysed IMDAF cascade reaction.

Two possible *exo*-cycloaddition modes were found corresponding to approach of the furan to both diastereotopic faces of the dienophile leading to the experimentally

confirmed major diasteromer **88** and a proposed minor diastereomer **99**. Both of these modes were computed to occur irreversibly, with the cycloaddition product ~8 kcal/mol lower in energy than the starting material. Under kinetic control, a diastereomeric ratio of 97:3 at 60 ^{o}C is predicted, which matches well with the experimental value of 94:6 with DABCO as a catalyst.

In order to further confirm this hypothesised structure for the minor diastereomer, the computed and experimental ^{13}C NMR shifts were compared and good agreement was observed for the corresponding chemical shifts. This agreement between computed and experimental ^{13}C NMR shifts for the major and minor products as well as agreement between computed and experimental diastereoselectivity provides strong evidence for the minor diastereomer being *exo*-epimer **99**, rather than *endo*-adduct **98**. **99**

BIMP catalyzed enantioselective IMDAF:

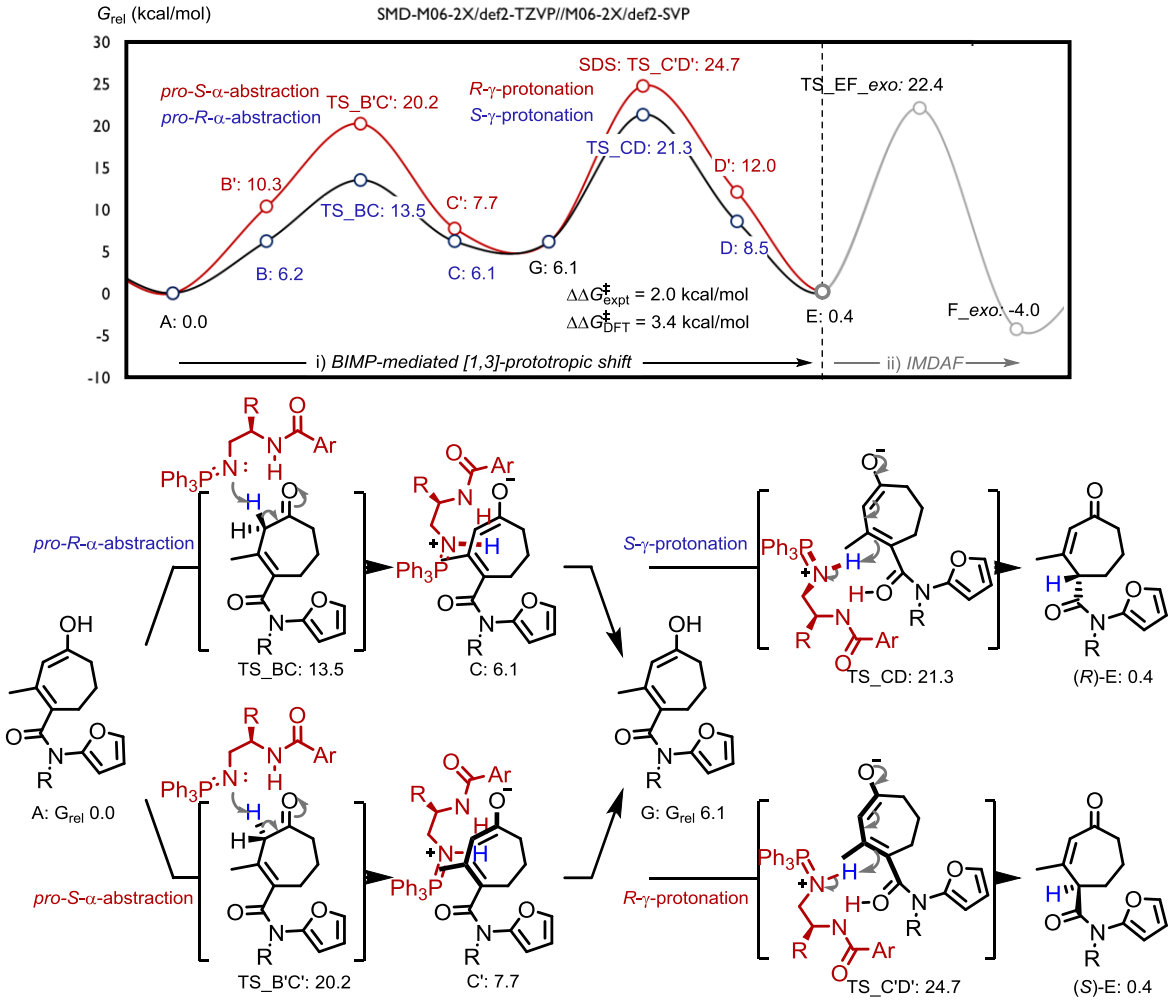


Figure 4: Computational studies on the BIMP catalysed enantioselective IMDAF reaction.

Next, in order to understand the origin of enantioselectivity, the BIMP catalysed reaction was also modelled with DFT calculations. A methyl carbamate protecting group was used instead of the *N*-Boc group to simplify the calculation (figure 4). The model shows catalyst **90** selectively deprotonates the pro-*R* proton via transition state **BC**, leading to intermediate ion pair **C** where the BIMP catalyst is situated above the substrate. The transition state going via this pathway is favoured over deprotonation of the pro-*S* proton by 6.7 kcal/mol, and intermediate **C** lies 1.6 kcal/mol lower in energy than **C'**. Both these intermediate enolates can reprotonate on oxygen, leading to intermediate **G**, or the catalyst can progress directly toward the next step, where ϒ-reprotonation creates the chiral enone product **E**. This is the turnover-determining and enantiodetermining step

and the catalyst mediates this through hydrogen bonding of the catalyst amide N-H with the carbonyl of the amide bond on the substrate.

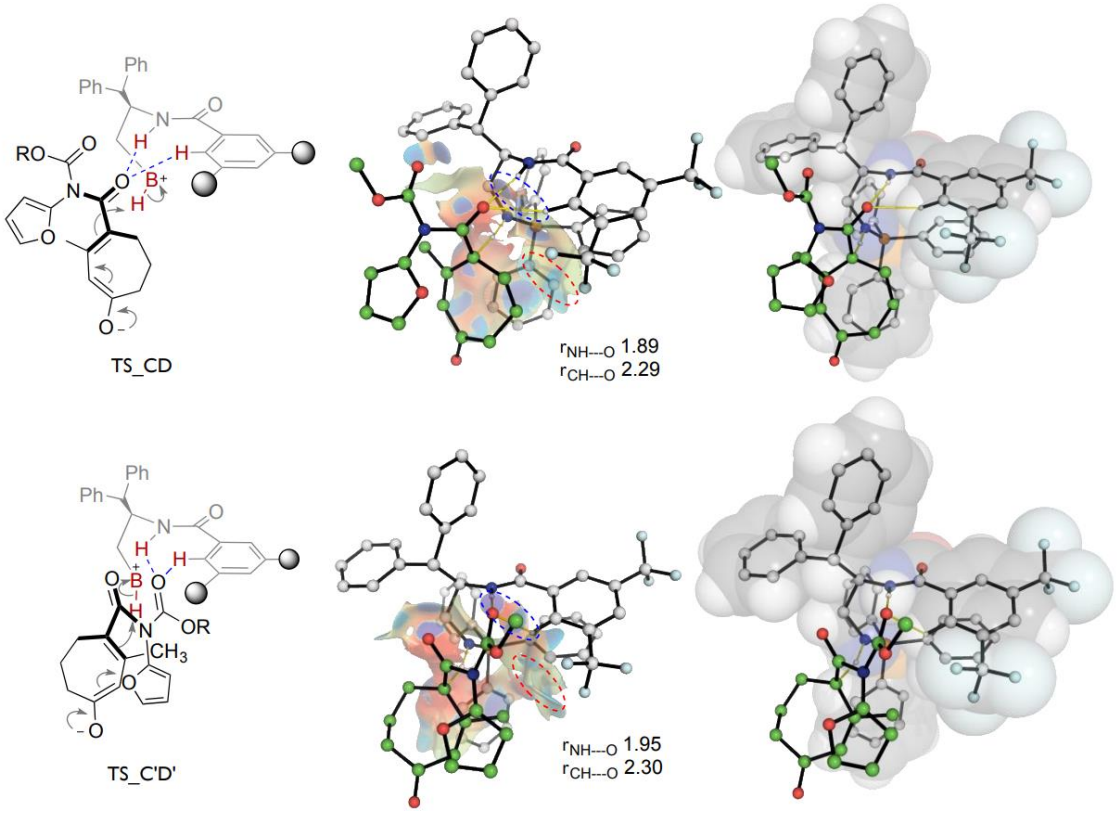
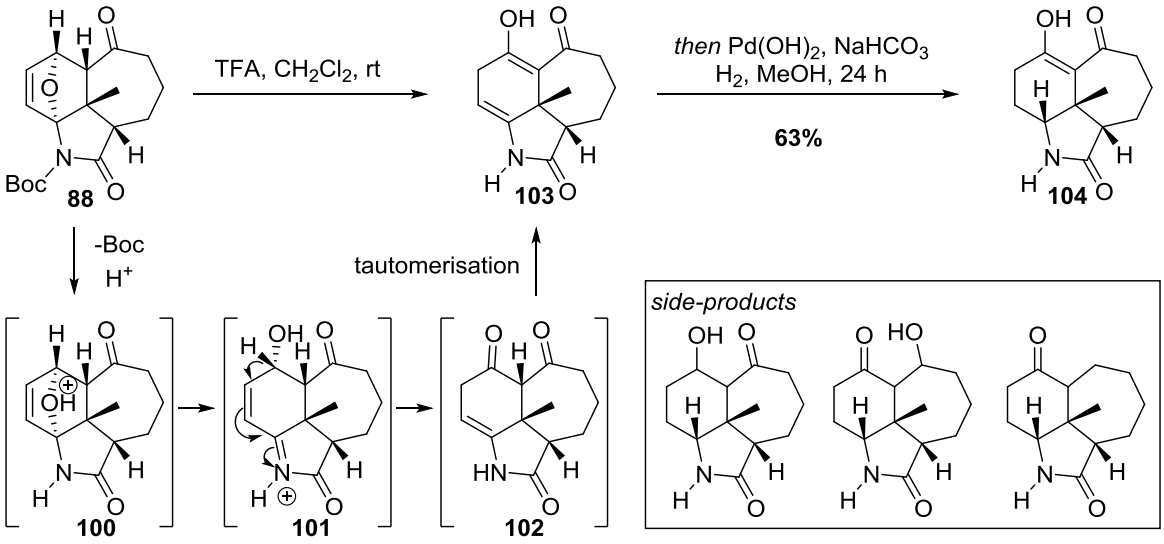


Figure 5: Detailed modelling of the enantiodetermining protonation step.

Detailed modelling of this step (figure 5) shows participation of the *ortho* C-H bond on the arene group of the catalyst providing a hydrogen bond to the substrate amide carbonyl. This additional weak interaction allows the catalyst to exhibit two-point binding, increasing enantio-induction. In transition state **C'D',** leading to the undesired enantiomer, the two-point binding is still present, however the carbamate group on the amidofuran moiety directly clashes with the CF_3 group on the catalyst, creating an unfavourable interaction. These calculations help to rationalise why this particular BIMP catalyst is able to impart high enantioselectivity for this transformation.

2.5 Approach to the ABCD Tetracyclic Core

With the key IMDAF cascade reaction realised and the ability to access large quantities of the enantioenriched tricyclic core established, the synthesis of the LHS B ring was next explored (scheme 16).

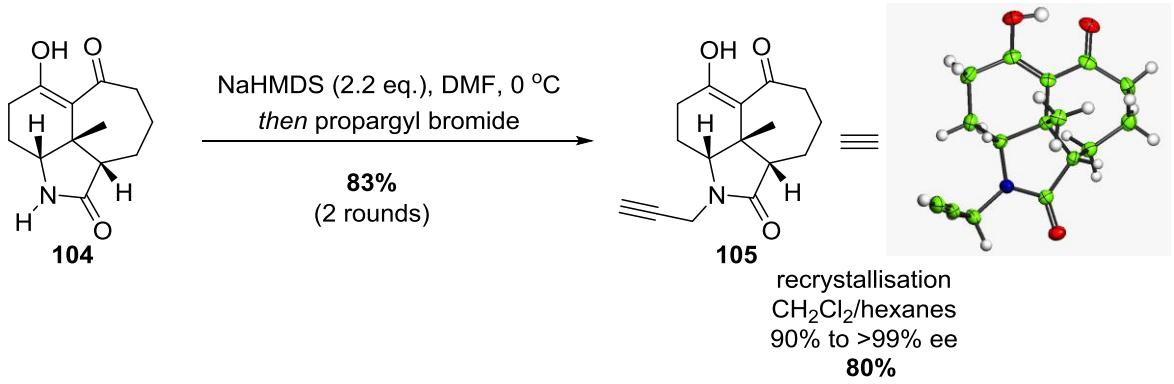


Scheme 16: Acid mediated ring-opening and hydrogenation of Diels-Alder adduct **88**.

Utilising a procedure previously developed by Michaelides within the Dixon group, Diels-Alder adduct **88** was treated with TFA in dichloromethane to initiate a reaction cascade. Initial *N*-Boc-deprotection gave aminal **100**, which then opened through the action of acid catalysis to *N*-acyliminium **101**. This intermediate undergoes two tautomerisation processes, initially to diketone **102**, then finally to the thermodynamically stable enamide **103**. Surprisingly, this enamide was found to be light sensitive, and was therefore taken directly on without purification. Hydrogenation with Pearlman's catalyst in methanol with the addition of a small amount of sodium hydrogencarbonate then selectively reduced the enamide alkene to give ketoenol **104** as a single isomer in 63% yield over the whole process. This excellent diastereoselectivity arises from the bowl-shaped architecture of enamide **103**, allowing the hetereogeneous $Pd(OH)_2$ to only access the alkene from the outer convex face and leading to the desired diastereomer **104**. Crucially, addition of a small amount of sodium hydrogencarbonate to neutralise any remaining trifluoroacetic

acid prevents formation of over-reduced side products in this reaction (3 identified side products shown in scheme 16). These side products likely appear due to acid catalysed activation of the ketoenol moiety, allowing the enol alkene to be susceptible to hydrogenation. Subsequent E1cb elimination of the resultant hydroxyketone reveals an enone which is further reduced by the Pd catalyst, leading to further reduced side products. Without acid activation, the ketoenol is inert with the reaction conditions employed, and remains untouched.

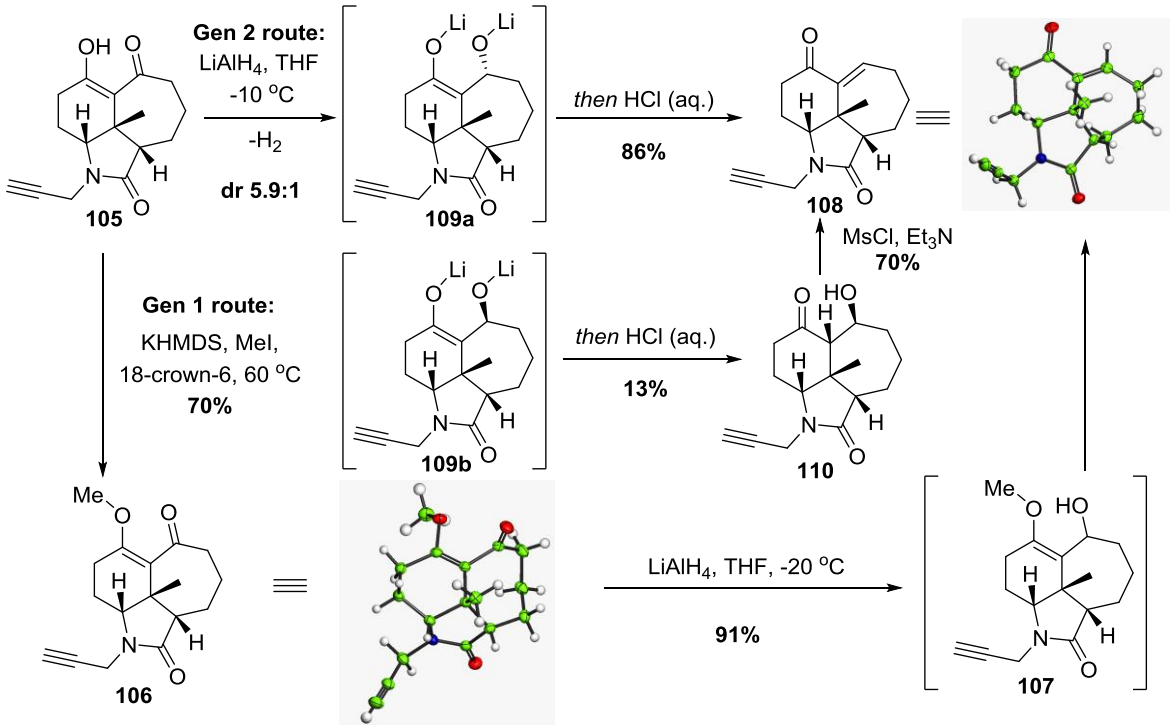
The synthesis up to ketoenol **104** had previously been explored within the group, and this knowledge and understanding greatly aided to progress this thesis toward the current point. Progressing on, ketoenol **104** was treated with 2.2 equivalents of NaHMDS, deprotonating both the ketoenol and amide moieties, followed by propargyl bromide to deliver propargylamide **105**. Pleasingly, this material was highly crystalline, and recrystallisation by slow evaporation of minimal dichloromethane in hexanes afforded an 80% yield of a single enantiomer from a 90% ee starting material. Both the connectivity and absolute configuration of **105** was confirmed by single crystal X-ray diffraction.



Scheme 17: Synthesis of propargylamide **105** and recrystallisation.

From the crystal structure of propargylamide **105** as well as the ^{1}H NMR spectrum (scheme 17), this molecule exists exclusively in the keto-enol form at room temperature with the LHS ketone adopting the enol tautomer. We proposed to exploit this

phenomenon to selectively reduce the cycloheptanone carbonyl without affecting the LHS cyclohexanone. In a first-generation route, the ketoenol was treated with potassium hexamethyldisilazane and methyl iodide to give selectively methyl enol ether **106** in 70% yield (the structure was confirmed by single crystal X-ray diffraction). With the LHS ketone now suitably protected, subsequent reduction with lithium aluminium hydride at -20 °C exposed cycloheptanone to give alcohol **107** and upon acidic work up, the enol ether collapsed to eliminate water, providing enone **108** in excellent 91% yield.



Scheme 18: Reduction of ketoenol **105** to enone **108**.

Although this provided proof of concept, an alternative method that alleviated the need for a protecting group was attractive. Given that in **105** the LHS cyclohexanone exclusively adopts the enol form, we postulated that a direct protection of this group as the enolate could be used to effect the selective reduction of the RHS cycloheptanone carbonyl in a single step. Protection of a carbonyl *via* its corresponding enolate was pioneered by Frazier in his 1980 publication[40] and this strategy has been widely used since[41]. Initially, ketoenol **105** was treated with one equivalent of LiHMDS or NaHMDS to generate the

enolate, before addition of lithium aluminium hydride, giving smooth conversion to enolate alkoxide intermediate **109** (scheme 18). Subsequent acidic work up effected an elimination of water to deliver enone **108** in good yield. We then decided to treat ketoenol **105** directly with $LiAlH_4$ in the hope that the LHS ketone could be transformed into the lithium enolate before reduction. Pleasingly, after acidic workup to eliminate water, enone **108** could be isolated in 86% yield. Interestingly, 13% of hydroxyketone **110** was also isolated as a single diastereomer. Although the relative configuration of this structure was not confirmed, it is postulated that the initial lithium aluminium hydride reduction results in a diastereomeric mixture of β-ketoalcohols, with only one diastereomer progressing through the acid catalysed elimination to give enone **108**, with the second diastereomer surviving as the hydroxyketone. This hydroxyketone side product **110** could be converted smoothly to the desired enone **108** in 70% yield *via* mesylation and E1cb elimination in the presence of triethylamine as base. Overall, enone **108** was delivered in 95% total yield from ketoenol **105** via this 2-step protocol, and its structure was confirmed by single crystal X-ray diffraction analysis.

2.6 Metal-Catalysed Cycloisomerisation

2.6.1 Conia-ene Type Cycloisomerisation

With significant quantities of enone **108** in hand, the next challenge was to form the crucial C-C bond needed to close the LHS B ring of the molecule. We envisaged utilising a metal catalysed Conia-ene type cycloisomerisation reaction and this proposal was initially tested on enone **108**. Conceptually, if a suitable π-acid was used to activate the alkyne moiety, then the ketone (reacting through an enol or enol equivalent) could capture this intermediate to form a key C-C bond (scheme 19) and close the B ring. Examination of the

literature finds that many metals are able to catalyse similar cycloisomerisation reactions between ketones and alkynes and selected examples are shown in figure 6. In 2004, Toste published his seminal work describing the intramolecular gold-catalysed Conia-ene reaction between 1,3-ketoesters and a pendant alkyne (**111**), leading to highly substituted cyclopentane derivatives **112** in excellent yield and diastereoselectivity (figure 6a).[42] The reaction requires just 1 mol% of a cationic gold catalyst and is complete in under an hour at room temperature, highlighting the ability for Au(I) catalysts to activate alkynes. In the subsequent year, Toste also demonstrated a highly enantioselective variant of this reaction using a chiral SEGPHOS based bisphosphine ligand and Pd(II) catalyst system (figure 6b)[43]. An additional Lewis acid (ytterbium triflate) was required to activate the ketoester moiety **113** for nucleophilic attack. This reaction demonstrates Pd(II) complexes as a competent catalyst for activating alkynes for cycloisomerisation reactions. In 2009, Dixon published his landmark paper describing the use of a cinchona-derived urea precatalyst **114** in conjuction with Cu(I) salts to enable a highly enantioselective Conia-ene reaction (figure 6c).[44] In this case, the urea catalyst acts both as a Brønsted base to deprotonate the ketoester, and also as a ligand for the resulting copper enolate, thus imparting enantioselectivity to the subsequent carbocupration enantiodetermining step. The presence of the N-H bonds in the urea group were found to be required for acceleration of the turnover-limiting step, though their precise function is unknown. One possible explanation is that these strong hydrogen bond donors increase the strength of the precatalyst as a ligand for copper, thus accelerating the carbocupration step. Finally, silver(I) can also be used as a suitable π-acid for Conia-ene type reactions, as exemplified in Dixon's 2016 publication (figure 6d)[45]. In this transformation, a chiral secondary amine **115** is chosen to activate the ketone by enamine catalysis and this is used in conjunction

with a chiral aminophosphine ligated Ag(I) species to activate the alkyne. Under the action of both co-catalysts, a cycloisomerisation reaction occurs on substrate **116**, leading to formation of the morphan **117** in remarkable 99% yield and 95% ee. This transformation is particularly notable as the connectivity of the reacting partners in the material and product closely resembles that of the desired transformation for this synthesis.

Encouraged by these literature findings, different metal catalysed cycloisomerisation conditions were applied to enone **108** and representative reaction conditions with different metal catalysts are shown in scheme 19.

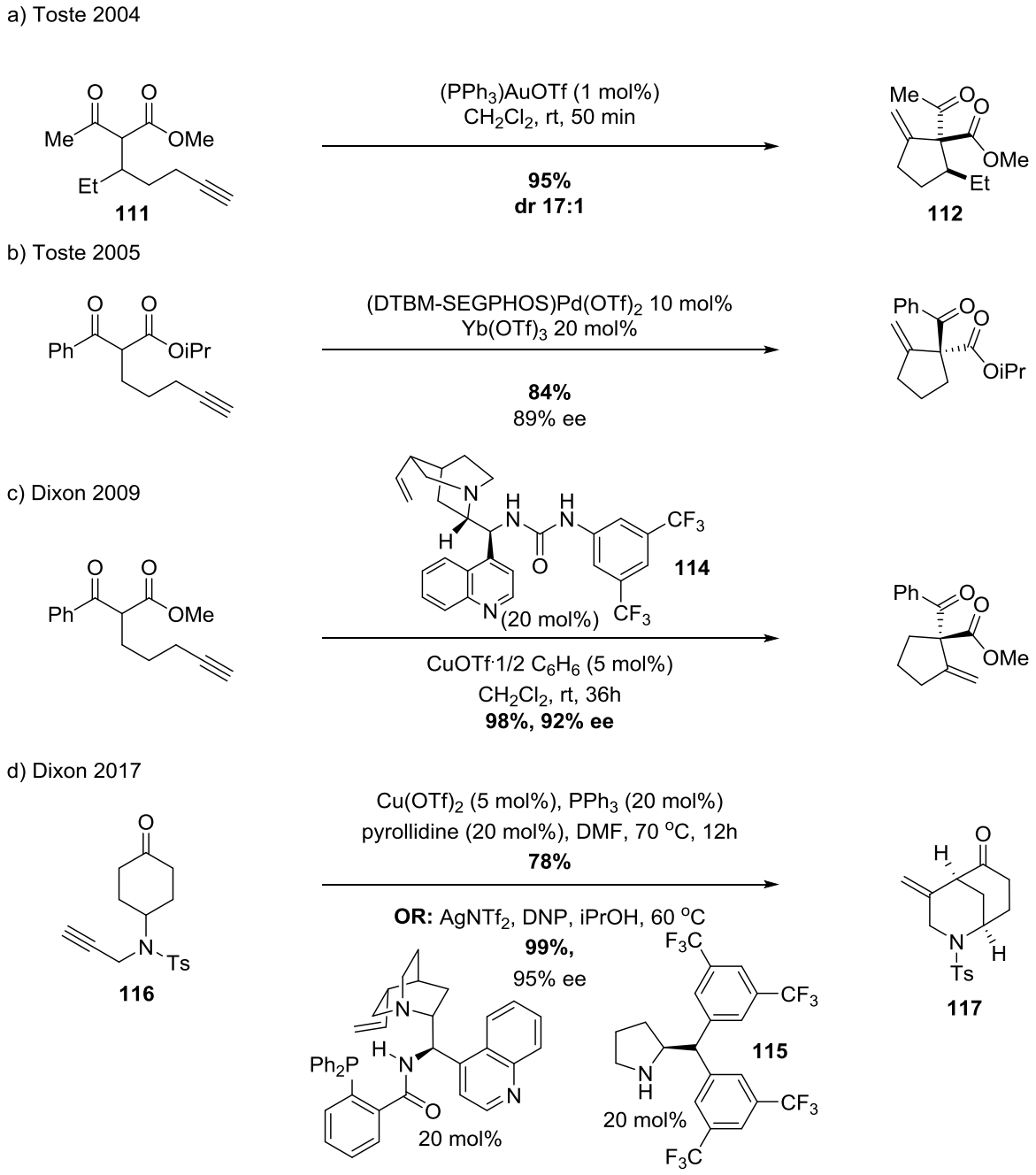
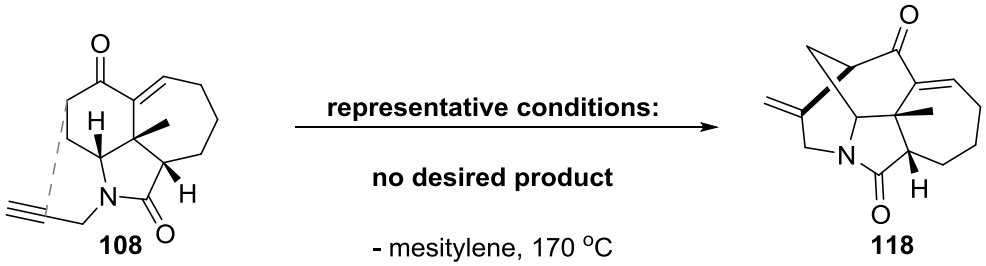


Figure 6: Selected metal catalysed Conia-ene type cycloisomerisation reactions.

Disappointingly in all cases, with the use of Au(I), Cu(I), Ag(I) and Pd(II), no desired product **118** was detected. When pyrrolidine was employed, hydrolysis of the alkyne moiety to the ketone was detected as a side product, showing successful activation of the alkyne moiety by the π-acid employed. Therefore, we concluded that the enone functionality was too unreactive and required stoichiometric conversion to an enol equivalent. Although there was good literature precedent for the Conia-ene reaction of

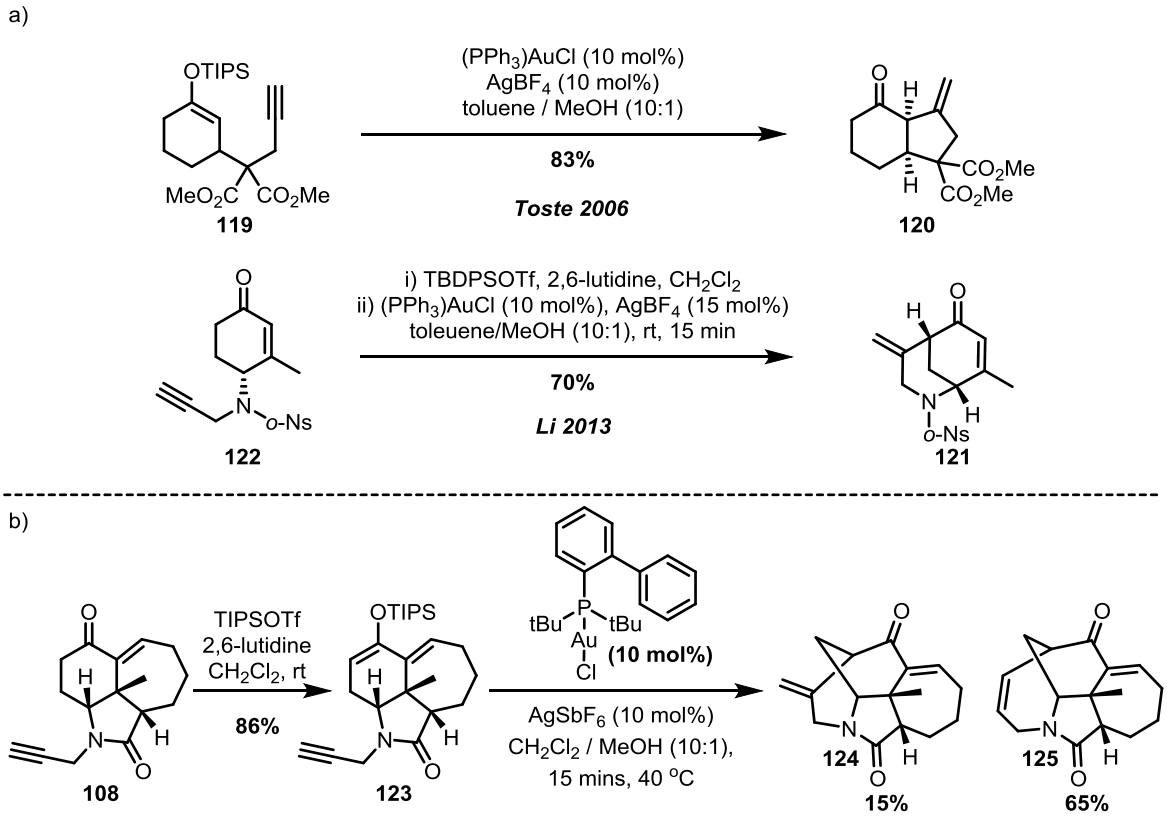
ketones, the deactivated enone functionality of **108** and high ring strain of the congested system appears to make forming this C-C bond a significant challenge.



Scheme 19: Representative conditions trialled for the Conia-ene reaction of **108**.

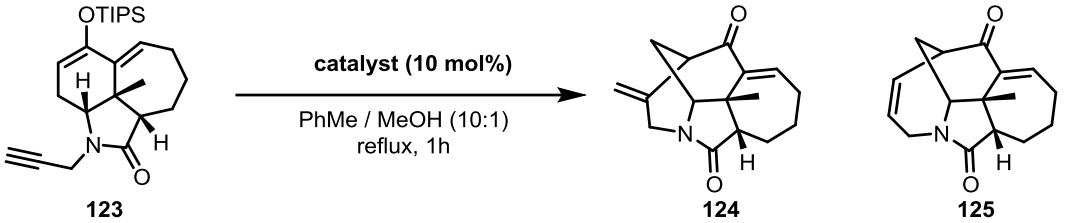
2.6.2 Metal-Catalysed Cycloisomerisation

With the enone **108** unsuccessfully performing the desired Conia-ene reaction, a new approach was sought. Noticing alkyne hydrolysis as evidence for successful metal activation of the alkyne moiety, we decided to preactivate the ketone moiety as the silyl-enol-ether and boost its nucleophilicity, creating a system poised for an intramolecular cationic Au(I) catalyst cycloisomerisation reaction as championed by Toste (scheme 20a)[46,47] and demonstrated by Li[16] (scheme 20b). Toste found triphenylphosphine bound gold(I) chloride as a powerful precatalyst for this transformation. When combined with a silver salt as a chloride scavenger, a cationic Au(I) catalyst is generated which could efficiently catalyse the cycloisomerisation of **119** to **120**. Li was then able to apply this reaction type to generate morphan **121** from ketone **122** proceeding through the TBDPS-protected enol ether.



Scheme 20: a) Toste and Li's silylenolether cyclisations. b) Silylenolether cyclisation applied to enone **108**.

Li's example is especially notable when considering our desired cyclisation reaction, as similarly, the reaction occurs between an enone-silylenolether and alkyne creates a morphan core. In line with this strategy, enone **108** was transformed into TIPS-silylenolether **123** in good yield, and this was subjected to standard cationic Au(I) cyclisation conditions (scheme 20b). Pleasingly, the desired tetracyclic product **124** was formed and isolated in 15% yield, with a major 65% yield of the undesired 7-*endo* cyclisation product **125** also isolated. This landmark result for this project, though still with poor selectivity for the desired product, is significant for being the first formation of the B ring in isolable yield.



123 124 125

Entry	Catalyst	Ratio 124:125	Notes
1	Au(JohnPhos)Cl $AgSbF_6$	1:4.3	CH_2Cl_2/MeOH, rt
2	$Cu(MeCN)_4PF_6$	1:20	-
3	$Cu(PPh_3)_3Br$	1:15	-
4	$Pd(PPh_3)_3Br$	-	enolether hydrolysis
5	$PdCl_2$	-	enolether hydrolysis
6	$HgCl_2$	-	enolether hydrolysis
7	$Hg(OTf)_2$	-	decomposition
8	AgOTf	-	enolether hydrolysis
9	Vaska's catalyst	-	enolether hydrolysis
10	Wilkinson's catalyst	-	enolether hydrolysis

Table 2: Cycloisomerisation reaction metal catalyst screen.

To begin our investigation, different metal catalysts were evaluated in the cycloisomerisation reaction (table 2). Refluxing enol-ether **123** and 10 mol% catalyst in a 10:1 toluene/methanol mixture was selected as sufficiently forcing conditions to screen for selectivity between the desired *exo* and undesired *endo* isomers. Of all the metals evaluated which are known to catalyse addition reactions to alkynes[48–50], only gold and copper displayed reactivity. Interestingly, the two copper catalysts evaluated, $Cu(MeCN)_4PF_6$ and $Cu(PPh_3)_3Br$, displayed high selectivity for the undesired 7-*endo*-isomer **125** (entries 2 and 3). From this screen, Au(I) catalysis was selected as the most promising, and subsequent investigation into the ligand effects proceeded.

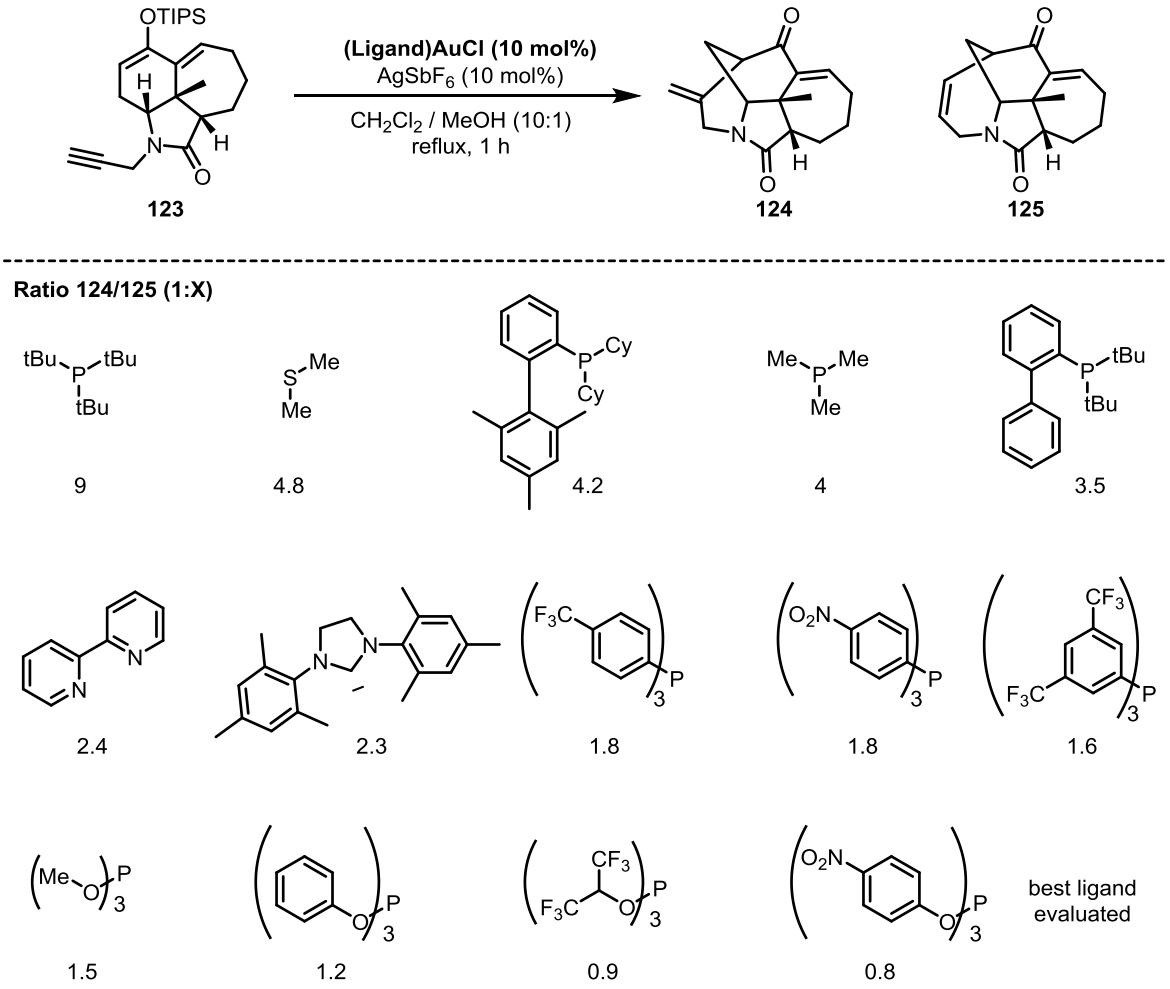
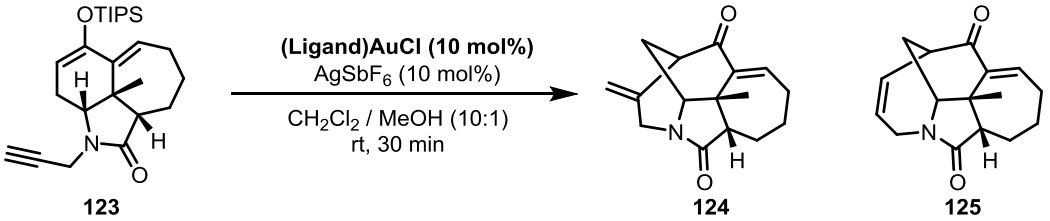


Table 3: Representative ligand screen for the Au(I) catalysed cycloisomerisation of **123**.

Only the selectivity between the two isomers was determined (by NMR) as this was the primary problem with the reaction. Taking JohnPhos as a starting point with a product/isomer ratio of 1:3.5, a range of differently substituted phosphines were screened (table 3). Initial results suggested that use of electron rich phosphine ligands such as $P(tBu)_3$, JohnPhos or CyJohnPhos favoured production of the undesired isomer **125** and use of more electron deficient phosphines such as $(pCF_3\text{-}Ph)_3P$ and $(pNO_2\text{-}Ph)_3P$ could improve selectivity for the desired 6-*exo* isomer **124** to 1:1.8, albeit still in favour of undesired **125**. This general trend between the electronics of the ligand and the selectivity observed in the cycloisomerisation reaction was reaffirmed with all of the

ligands evaluated, and accordingly when the strongly electron-deficient phosphite ligands were evaluated, further improved selectivities were obtained.

In Suresh and Koga's 2001 report, the molecular electrostatic potential minimum (V_{min}) of a range of phosphine ligands was calculated using DFT.[51] The molecular electrostatic potential (MEP) is the force at a given point acting upon a positive charge,[52] and therefore by calculating the MEP in the phosphine lone pair region, the electronic contribution of the phosphine ligand can be quantified. When comparing the experimental selectivity for the desired isomer product with Koga's computed value for the electronic effect of the phosphine, a general positive correlation was observed (table 4). In several cases, ligands which feature in Koga's calculation tables were also evaluated in the cycloisomerisation reaction, and fit the general trend of improved selectivity with increasing V_{min} (decreasing electronic contribution). JohnPhos ((biphenyl)$(Cy)_2Ph$), entry 4) can be well-approximated by $PhEt_2P$ (entry 5), and also fits in with the general trend. The same comparison can be made between (p-$C_6H_4F)_3P$, (p-$C_6H_4CF_3)_3P$ and ((3,5-$CF_3)C_6H_4F)_3P$ (entries 5-7). Although still only preliminary evidence, this correlation could be used in the future to predict selectivities in other cycloisomerisation reactions.



Entry	Ligand	V_{min} (kcal/mol)	Ratio 1:X (124:125)
1	$(tBu)_3P$	-45.48	9.0
2	Me_3P	-43.02	4.0
3	$Ph(Et_2)P$	-40.76	-
4	JohnPhos	-	3.5
5	$(p\text{-}C_6H_5F)_3P$	-32.88	-
6	$(p\text{-}C_6H_5CF_3)_3P$	-	1.8
7	$((3,5\text{-}CF_3)C_6H_3))_3P$	-	1.6
8	$(MeO)_3P$	-26.12	1.5
9	$(PhO)_3P$	-15.88	1.2
10	$(Cl_3CCH_2O)_3P$	-6.30	-
11	$((CF_3)_2CHCH_2O)_3P$	-	0.9
12	$(p\text{-}C_6H_4NO_2O)_3P$	-	0.8

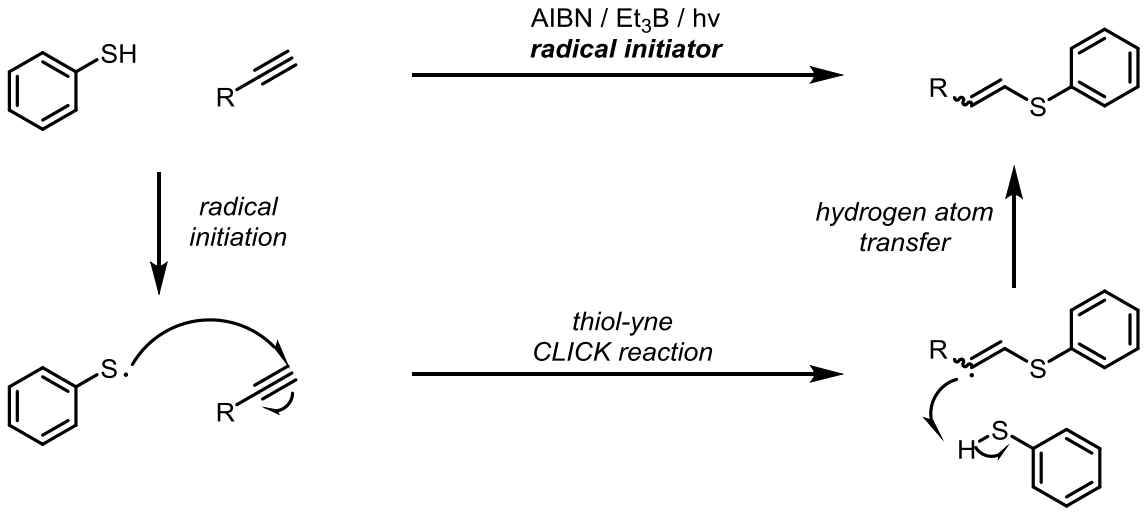
Table 4: Comparison of computed phosphine electronic effect and experimental selectivity.

To date, the best selectivity of 1:0.8 favouring the desired isomer **124** was achieved with use of the hyper-electron-deficient $(pNO_2\text{-}C_6H_4O)_3P$ ligand. This highly electron withdrawn phosphite ligand represents the extreme of hyper-electron deficiency and yet the selectivity displayed for the desired isomer of 1:0.8 was still at an impractical level. Thus, we ceased our exploration into ever more electron-deficient ligands and sought a new approach towards the B ring.

2.7 Reductive Radical Cyclisation Cascade

2.7.1 Overview of the Thiol-Ene Reaction

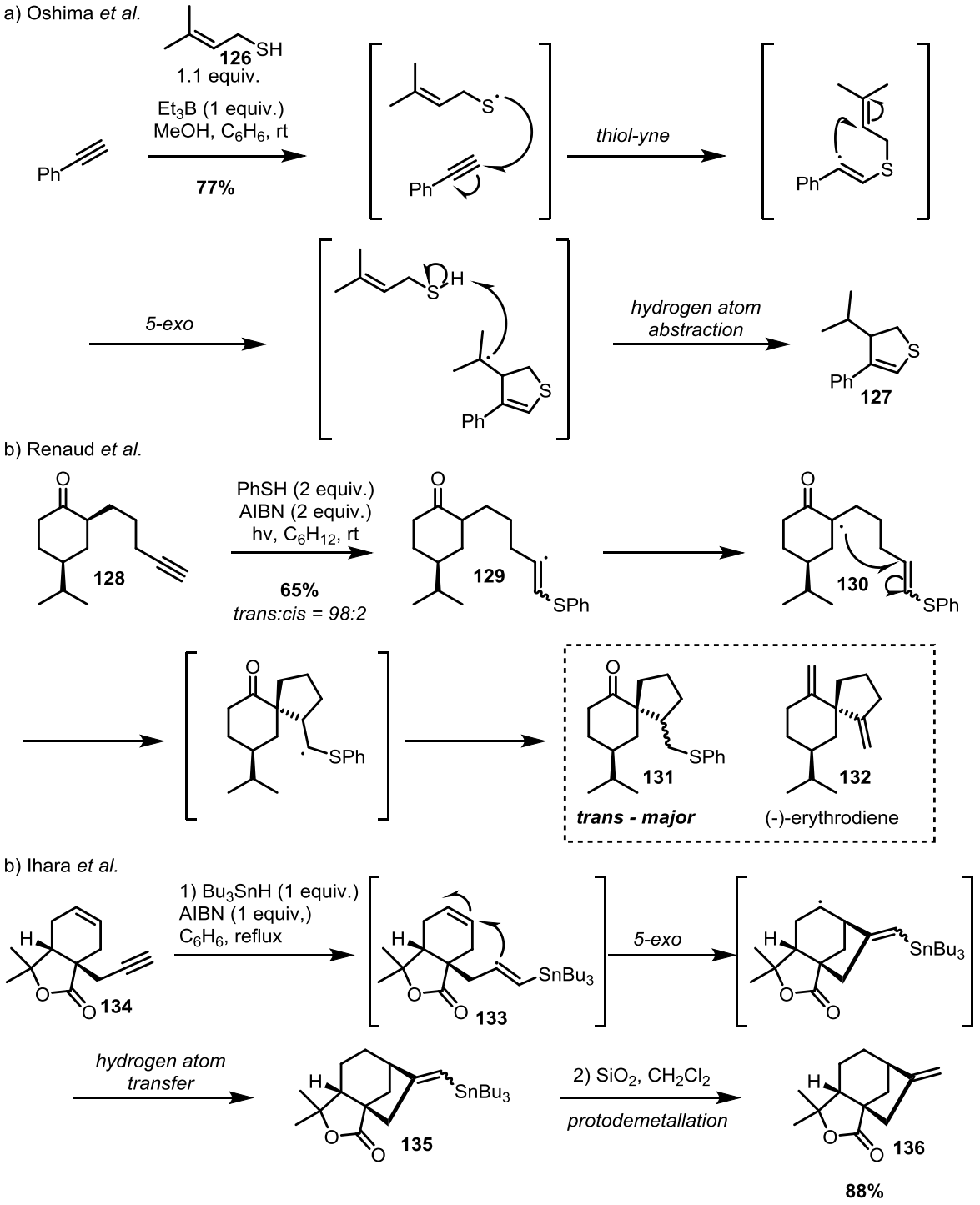
The thiol-ene reaction is a radical addition reaction between a thiol and an appropriate alkene or alkyne, leading to a corresponding alkyl or vinyl sulfide product. First reported in 1905[53], this reaction has found a wide range of applications within the past couple of decades.[54–56] The reaction is accepted as click chemistry, given its generally high yields, selectivity and efficiency.[57]



Scheme 21: Thiol-yne reaction general mechanism.

Typically, a radical initiator or UV radiation facilitates the reaction by generating a sulfanyl radical species. This radical adds onto the π-bond, and the resulting carbon-centred radical can abstract a hydrogen atom from another thiol species, thus propagating the reaction. When applied to alkynes (scheme 21), an anti-Markovnikov addition mode proceeds, and the resultant vinylsulfide product usually exists as a mixture of E/Z isomers.[58] Importantly, the intermediate vinyl radical generated from initial addition can engage in secondary intramolecular reactions before intermolecular hydrogen atom transfer ends the cascade process.[59,60] This strategy of initiating radical cascade

cyclisations *via* radical addition reactions to alkynes has been widely explored in the past decade and applied to a range of synthetic challenges. Other than thiols, a large range of radical addition precursors have been shown to be compatible, ranging from carbon centred radicals to stannyl and germanyl radicals.[61] Representative examples are shown in scheme 22.



Scheme 22: Representative radical cascade reactions initiated by addition to terminal alkynes.

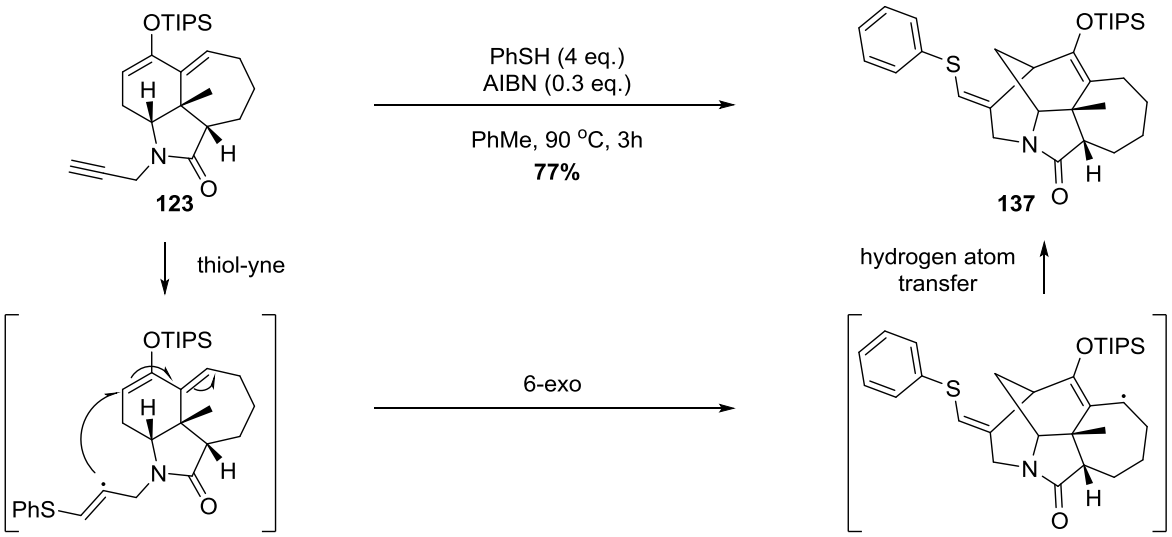
Oshima utilised an alkene-bearing thiol **126** as a radical precursor to add to phenylacetylene (scheme 22a).[62] The resultant vinyl radical intermediate underwent an intramolecular 5-exo-trig cyclisation to give tetrahydrothiophene **127** in 77% yield. This reaction notably demonstrates the much faster reaction of the thiyl radical with the

acetylene moiety over the isoprenyl alkene, thus avoiding polymerisation of the thiol. Renaud and co-workers also demonstrated a radical cascade initiated by a thiol-yne reaction on substrate **128**.[63] In this case, the resultant intermediate vinyl sulfide **129** underwent a 1-5 hydrogen atom transfer to generate a stable α-keto radical **130**. This radical subsequently underwent an intramolecular 5-exo cyclisation to afford spiroketone **131** after radical termination through hydrogen atom transfer. Using this reaction, Renaud was able to quickly construct a skeletal core of erythrodiene **132** and related natural products. Finally to exemplify the use of non-sulfur based radicals in this strategy, Ihara utilised a stannyl radical cascade to construct the tricyclic core of the kaurenoic acid natural product family.[64] The intermediate vinyl radical **133** formed through addition of the tributylstannyl radical to acetylene **134** then underwent a 5-*exo*-trig cyclisation process to form a strained bridged bicyclic ring system **135**. This example also demonstrates the utility of the accessory stannane group. This can be used for downstream cross coupling reactions, or in Ihara's case, can be easily removed via protodemetallation with silica gel or mild acid to give a terminal alkene product **136.**

2.7.2 Thiol-Mediated Reductive Radical Cascade

Encouraged by the literature precedents of such a reaction strategy, the thiol-yne reaction was applied to enolether **123**. Remarkably in the first attempt, using ten equivalents of thiophenol with 30 mol% AIBN in refluxing toluene, tetracycle **137** was formed in 38% yield as a single isomer. The major side product in this reaction was the standard thiol-yne reaction, where the intermediate vinyl radical did not undergo the intermolecular cyclisation process. By lowering the equivalents and concentration of

thiophenol (the terminal reductant in the reaction) to 4 equivalents, the yield was improved to 77% (scheme 23).



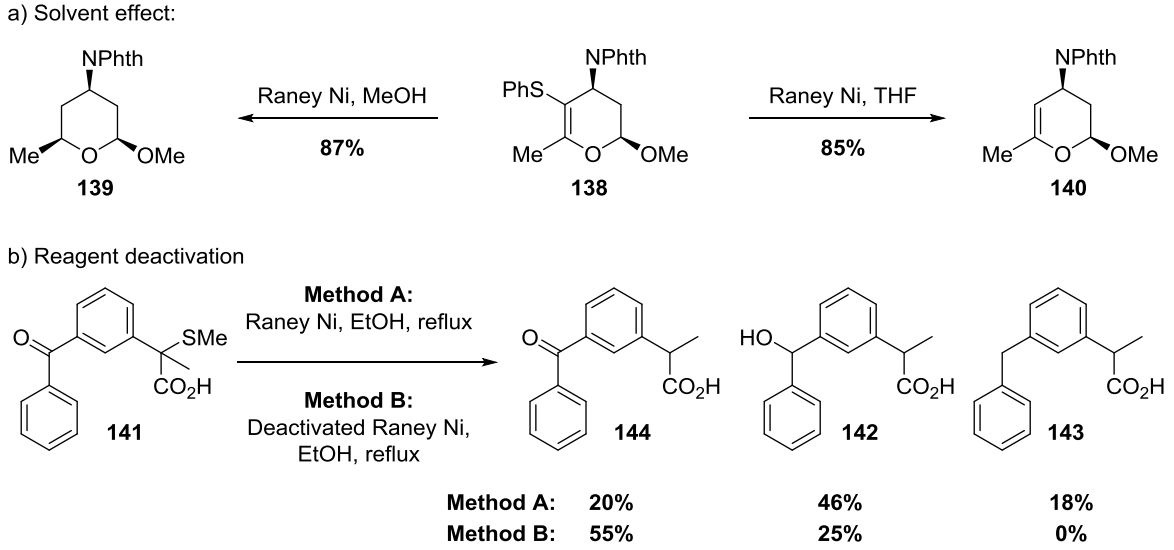
Scheme 23: Reductive radical cascade to construct B ring.

Notably, only a single geometric isomer of vinyl sulfide **137** was observed and the stereochemistry was assigned by analogy to the major isomer in similar radical cyclisation reactions.[65–67] In the context of this synthesis however, the geometry of the vinyl sulfide product is inconsequential, as the accessory sulfide functional group was to be removed through reductive desulfurisation in the following step.

2.7.3 Reductive Desulfurisation

In order to effect the desulfurisation of vinyl sulfide **137**, Raney nickel was employed.[68,69] This reagent is commonly used to desulfurize a range of sulfur containing compounds, and is generally tolerant of a wide range of sensitive functional groups. However, a common side reaction when applied to desulfurisation is the hydrogenation of other alkene functionality within the molecule. It is difficult to predict which alkenes are susceptible to reduction by Raney nickel and so this problem must be evaluated on a case by case basis. Additionally, Raney nickel is known to lose activity over time and so the

quality of individual batches of this reagent differ greatly between suppliers and bottle storage conditions.

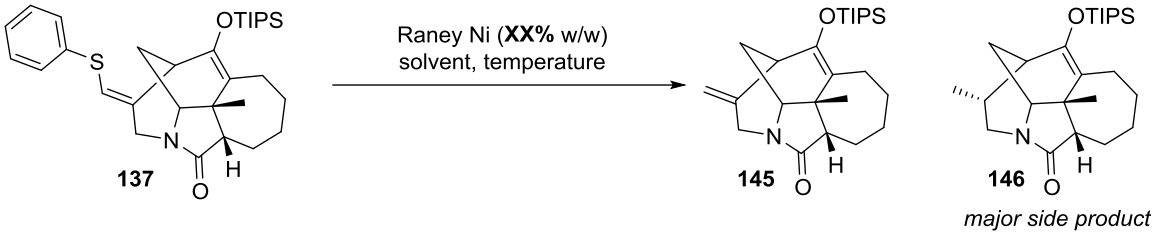


Scheme 24: a) Wichmann's selective vinyl sulfide desulfurisation controlled by solvent effects. b) Hannoun's selective desulfurisation using deactivated Raney nickel.

The reactivity of Raney nickel can be modified by choice of solvent. Wichmann demonstrated this where solvent effects can control selectivity for different reduction product (scheme 24a).[70] Raney nickel is known to be more active in highly polar protic solvents, and when vinyl sulfide **138** is treated with Raney nickel in methanol, both desulfurisation and alkene hydrogenation occurs to give tetrahydropyran **139**. However, the same reduction when performed in tetrahydrofuran as solvent retains the alkene and dihydropyran **140** is afforded in 85% yield.

The hydrogen gas adsorbed to the high surface area of Raney nickel can also be partially removed by refluxing the catalyst in acetone for several hours.[71–73] Hannoun demonstrated this is the reductive dethiomethylation of **141** (scheme 24b).[73] When commercial grade Raney nickel was employed, significant amounts of over-reduced side products (**142** and **143**) due to ketone hydrogenation are formed. However, when the Raney nickel is partially deactivated by refluxing in acetone for 4 hours, improved

selectivity for the desired product was observed and the selective desulfurisation product **144** could be isolated in 55% yield.



Entry	XX	Solvent	Temperature / °C	Yield / %
1	10	EtOH	23	40
2	35	EtOH	23	68
3	50	EtOH	23	55
4	35	MeOH	23	28
5	35	THF	23	trace
6	35	EtOH	-78	0
7	35	EtOH	-10	0
8	35	EtOH	0	81

Table 5: Raney nickel desulfurisation optimisation.

Initially, following commonly employed literature conditions for similar desulfurisation reactions, **137** was treated with a 10 times weight equivalence of Raney nickel (approximated by weighing Raney nickel moistened with ethanol) in ethanol at room temperature (Table 5). Pleasingly, a 40% yield of desulfurised tetracycle **145** was isolated, with the remaining material still existing as the starting material vinyl sulfide. Accordingly, the mass loading of Raney nickel was increased to 35 times with an increase of yield to 68% for the desired product. Formation of over-reduced side product **146** was observed, explaining the rest of the yield. The hydrogenation in the over-reduced product occurs exclusively from the convex face of the bowl-shaped architecture, leading to the undesired diastereomer **146**. Further increase to 50 times weight loading led to a

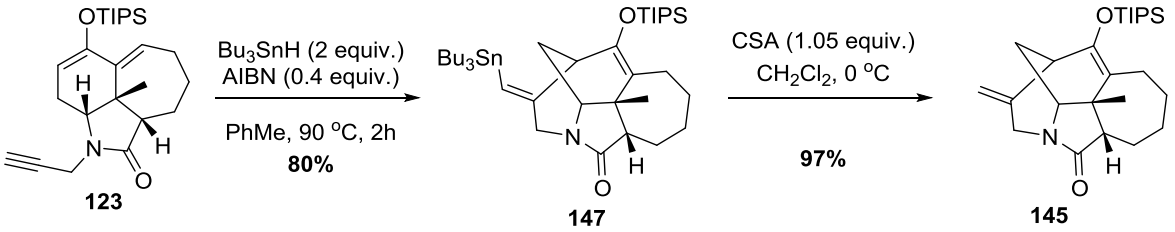
decreased yield of desired **145** due increased hydrogenation of the terminal alkene and formation of over-reduction product **146**.

To avoid this over-reduction problem, different solvents were examined. In methanol, over-reduction prevailed, leading to only a 23% yield of desired **145**. This result is understandable since methanol is more polar than ethanol and the activity of Raney nickel is therefore enhanced. Disappointingly, when the less polar tetrahydrofuran solvent was employed in the reaction, only trace reactivity was observed and the starting material was recovered. Finally, the reactivity of the Raney nickel was tempered by reducing the reaction temperature. At -78 ^{o}C and -10 ^{o}C (entry 6 and 7), no reaction was observed, but pleasingly when the temperature was set to 0 ^{o}C, an 81% isolated yield for the desired alkene **145** was obtained.

Despite the encouraging result, it was noted that the loading of Raney nickel required to effect this transformation was extremely high. For example a reaction on a 500 mg scale of substrate would require 17.5 grams of Raney nickel to desulfurise. This high mass loading of Raney nickel would make scale-up an extremely difficult and impractical process, given the large quantity of pyrophoric Raney nickel required. The batch of Raney nickel used for optimisation in this reaction was over 10 years old and had lost much of its activity. Therefore, a new commercial batch of reagent was purchased and evaluated. With the active fresh reagent, selectivity for the desired desufurisation product **145** was extremely poor, with over-reduction to the undesired diastereomer **146** prevailing in all cases and conditions tested. Even when the reaction was run to only partial completion, the major product was still the over-reduced product which indicated the desired product **145** underwent hydrogenation faster than the desulfurisation of vinyl sulfide starting material **137**. Attempts to partially deactivate the fresh Raney nickel were also

unsuccessful in improving selectivity. Although very disappointing, extensive efforts to reproduce the decade old bottle of Raney nickel were unsuccessful and a new non-desulfurisation approach to alkene **145** was pursued.

2.7.4 Tin-Mediated Radical Cyclisation Cascade



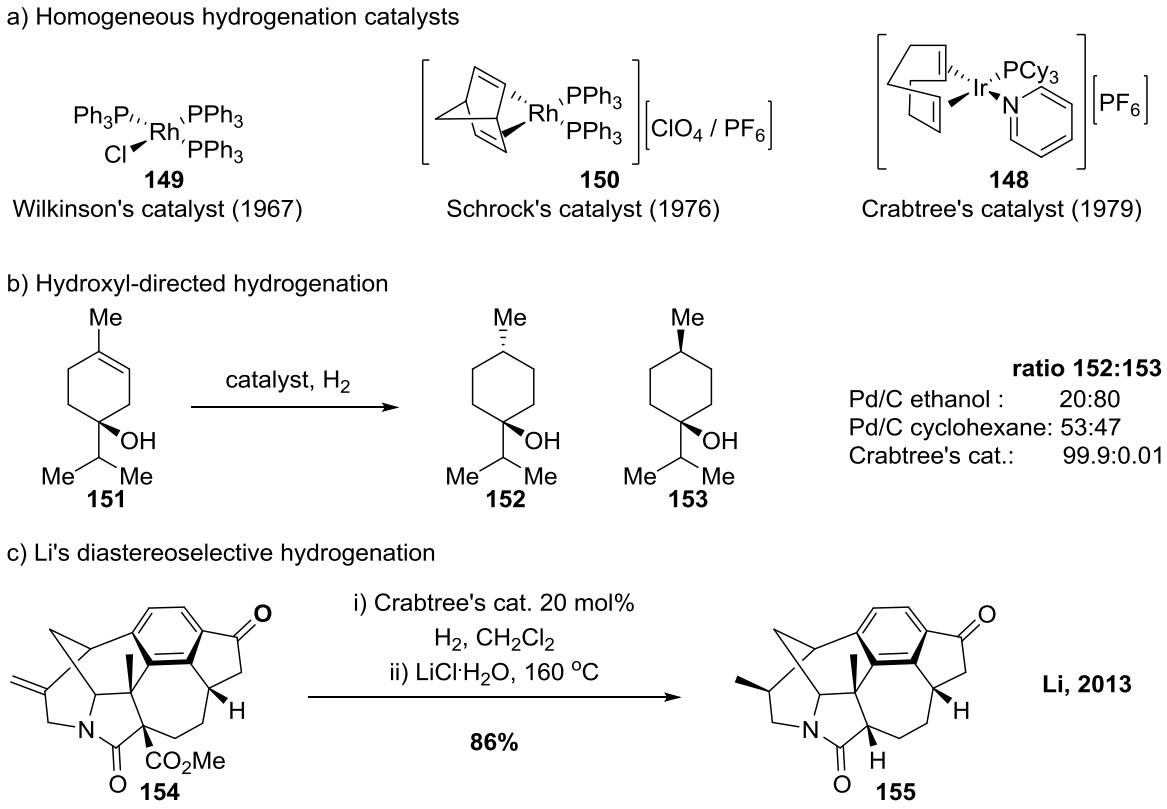
Scheme 25: Tributyltin hydride mediated radical cyclisation and protodestannylation.

As removal of the vinylsulfide proved to be a difficult and irreproducible, a non-thiol based radical mediator was investigated and tributyltin hydride was tested for compatibility as Ihara and co-workers have shown (scheme 22c). Use of tin is complementary to thiol approaches and the accessory tributyltin group in the vinyl tin product can easily be removed using acid. When tributyltin hydride was utilised in the radical cyclisation of **123**, vinyl stannane **147** could be isolated in a remarkable 80% yield as a single isomer, matching the efficiency displayed with the thiophenol based method. Importantly, protodestannylation of the vinyl stannane product **147** was easily achieved using camphor sulfonic acid in dichloromethane and this enabled the formation of desired alkene **145** in 97% yield with no overreduction observed. Despite the toxic nature of tributyltin hydride, the efficiency of the radical cyclisation along with ease of protodestannylation of the accessory tributyltin group made this strategy a viable and efficient method to continue the synthesis. With a reproducible and robust method for

the construction of the B-ring complete, investigations into fixing the stereochemical configuration of the B-ring methyl group could then begin.

2.8 Diastereoselective Alkene Hydrogenation

A diastereoselective hydrogenation reaction was envisaged to set the key LHS methyl group stereochemical configuration. Due to the highly curved bowl-like architecture of the molecule, the hydrogen must be delivered from within the highly congested concave face, posing a difficult synthetic challenge.



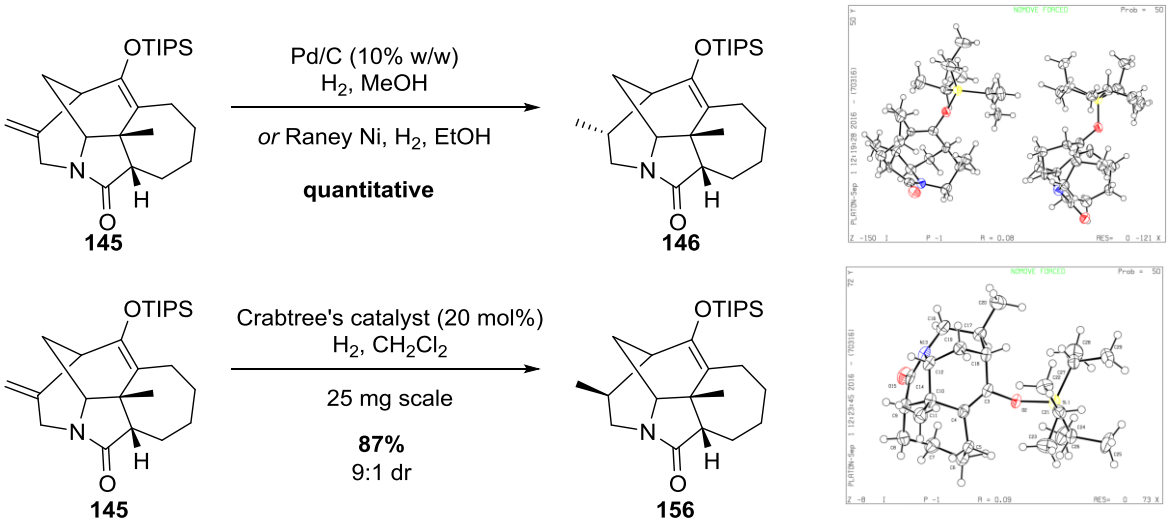
Scheme 26: a) Homogeneous hydrogenation catalysts. b) Hydroxyl-directed hydrogenation c) Li's use of Crabtree's catalyst in his synthesis of daphenylline.

Crabtree's catalyst **148** is a square planar Ir(I) complex with the formula $[CODIrPCy_3Py][PF_6]$. It was discovered by Robert Crabtree in 1979 during his investigation into iridium-based analogues of Wilkinson's catalyst **149** and similar rhodium based complexes (scheme 26a).[74] At the time of its discovery, a cationic Rh(I) bisphosphine

catalyst **150** had been developed by Osborn and Shrock. [75] Unlike Wilkinson's catalyst, the norbordiene ligand on this complex is irreversibly hydrogenated during the reaction, leading to a coordinationally unsaturated cationic Rh(I) complex. By performing the reaction in strongly coordinating solvents such as acetonitrile, alcohols or acetone, the bis-solvent adduct of the catalyst is formed and can be isolated as a stable complex; this is the active catalyst and dissociation of a solvent molecule or phosphine allows binding to the substrate and subsequent hydrogenation to occur. Crabtree noticed that the turnover-limiting step in homogeneous hydrogenation reactions was this ligand dissociation step which is especially slow for iridium when compared with analogous rhodium complexes. In order to combat this problem, Crabtree came up with an elegant solution. By performing the hydrogenation reaction in dichloromethane, a non-coordinating solvent, this ligand dissociation step is bypassed as after hydrogenation of the cyclooctadiene (COD) ligand, two coordination sites are vacated which can accommodate binding of the substrate. The presence of these two coordination sites is also an important property of Crabtree's catalyst, as binding of a directing group as well as the olefin reaction site can occur, allowing directed diastereoselective hydrogenation to take place.

Since this seminal work, Crabtree's catalyst has been utilised in many different applications. [76,77] One example of its ability to coordinate directing groups is shown in scheme 26b.[78] When terpene alcohol **151** is reduced under heterogeneous hydrogenation conditions using palladium on charcoal, a poor diastereoselectivity is obtained leading to a mixture of **152** and **153**. However, use of Crabtree's catalyst **148** exhibits near perfect diastereoselectivity for the hydrogenation with hydrogen delivered from the same face as the neighbouring hydroxyl directing group.

Li and co-workers encountered a similar challenge in their synthesis of daphenylline,[16] and by using Crabtree's catalyst they were able to direct hydrogenation from within the concave face of a related molecule (scheme 26c). In his case, the lactam carbonyl group in **154** acts as the directing group to enable the diastereoselective synthesis of hydrogenation product **155**.

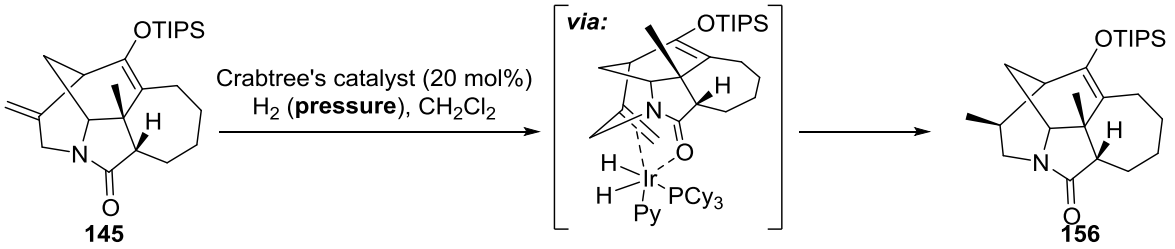


Scheme 27: Comparison of heterogeneous catalysts with Crabtree's catalyst.

In order to establish whether a homogeneous catalyst such as Crabtree's catalyst was required, heterogeneous hydrogenation conditions were employed with palladium on charcoal and Raney nickel as hydrogenation catalysts (scheme 27). Both of these catalysts led to exclusive formation of the undesired diastereomer **146** in quantitative yield. When Crabtree's catalyst was employed in an initial test reaction, the reaction exhibited a 9:1 diastereoselectivity for the desired diastereomer **156** and an 87% isolated yield could be obtained. The stereochemical configuration of both the undesired and desired diastereomers were confirmed unambiguously by single crystal X-ray analysis.

Despite this pleasing initial result, an unforeseen problem, as often occurs in chemistry, arose when attempting to repeat the reaction. Much lower diastereoselectivities were

observed, and the values were observed to change dramatically without a perceived change in the experimental set-up (range of 63:37 to 85:15). After continued attempted optimisation, it was noticed that the actual balloon (from the balloon stash) used to deliver the hydrogen gas had a significant effect on the reaction. Repeated use of the same balloon for the hydrogenation reaction led to improved diastereoselectivity, and once the balloon was too old to use and was replaced with a fresh new balloon, the diastereoselectivity would drop dramatically. Thus, we concluded the reaction must be highly pressure sensitive and conducted control experiments to probe this hypothesis.



Entry	H_2 Pressure (mbar)	dr
1	1086 (quad-skin balloon)	2.2:1
2	1055 (double-skin balloon)	2.8:1
3	1029 (single-skin balloon)	3.4:1
4	1029 (Ar/H_2 1:1)	6.8:1
5	1029 (Ar/H_2 2:1)	>20:1

Optimised Conditions: Crabtree's catalyst 20 mol%, H_2 (1029 mbar, Ar/H_2 (2:1), CH_2Cl_2, rt
300 mg scale: 92%, >20:1 dr

Table 6: Hydrogen pressure optimisation for hydrogenation of **145** to **156**.

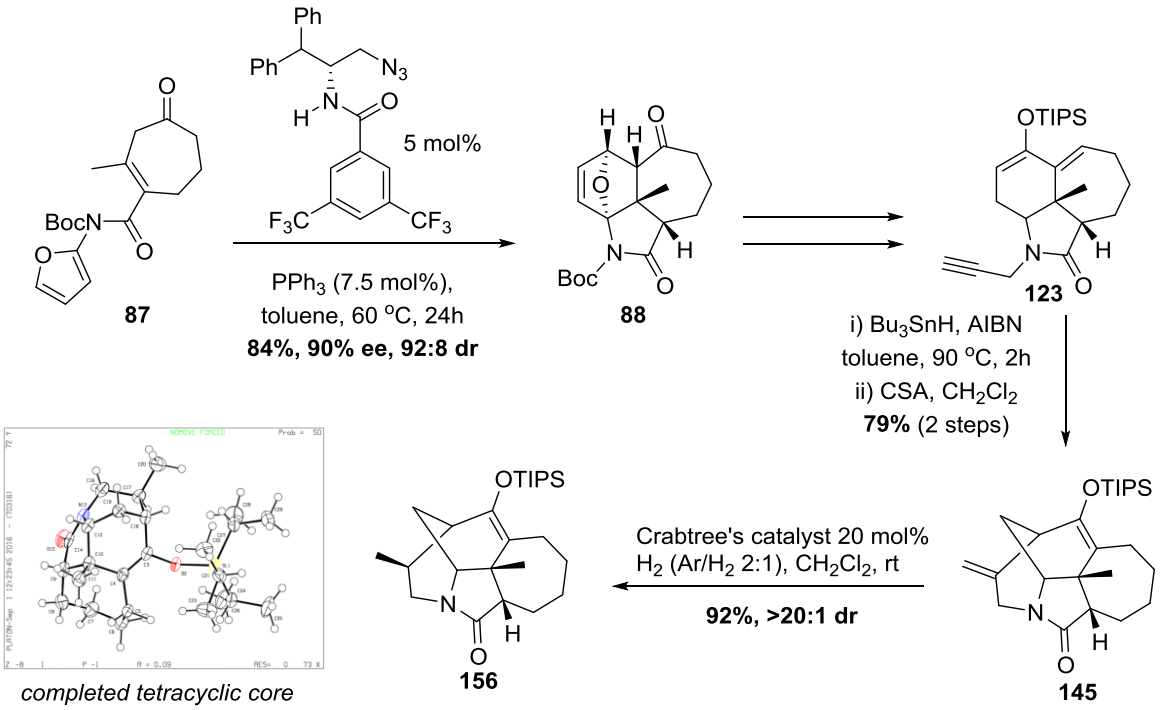
Initially, the standard experimental set up was tested using a fresh double-skinned balloon of hydrogen and the diastereoselectivity was measured as 2.8:1 by NMR integration. When the hydrogen pressure was increased to 1086 mbar by using a quad-

skinned balloon, the diastereoselectivity decreased to 2.2:1. The balloon pressure was therefore reduced by using a single-skinned balloon (1029 mbar pressure) and a corresponding increase of dr to 3.4:1 was seen. With these results indicating a reduced partial pressure of hydrogen leads to increased diastereoselectivity, the pressure of hydrogen was further reduced by adding argon to generate a gas mixture. Experimentally, this was achieved by filling an evacuated flask simultaneously with quad-skin balloons of hydrogen and argon, and then using this chamber to fill a single-skinned balloon used for the reaction. With this method, 1:1 hydrogen and 1:2 hydrogen in argon gas mixtures were created and tested. Pleasingly, the diastereoselectivity further increased with use of a 1:1 Ar/H_2 gas mixture to 6.8:1 and with a 2:1 Ar/H_2 ratio, a greater than 20:1 selectivity for the desired diastereomer was obtained. The optimised hydrogenation reaction was subsequently performed a 300mg scale, affording **156** as a single diastereomer in 92% yield.

In order to rationalise the observed selectivity and high sensitivity to hydrogen pressure, we postulated that the lactam carbonyl is acting as the directing group, bringing the iridium catalyst and hydrogen into the concave bowl of the molecule. The substrate acts as a weakly binding bidentate ligand, and under high pressures of hydrogen gas, binding of dihydrogen can outcompeting binding of the lactam carbonyl directing group; this outcome results in hydrogenation from the more accessible convex face, leading to undesired diastereomer **146**. In low pressures of hydrogen, catalyst binding to the substrate via the lactam carbonyl occurs before association of dihydrogen, allowing delivery from the concave face leading to the desired diastereomer **156**. The phenomenon of hydrogen pressure affecting stereoselectivity is well known in the field of asymmetric hydrogenation,[79] however the term ‘low pressure’ hydrogenation is often

characterised as below 2 bar pressure. To the best of our knowledge, no example of a highly pressure sensitive directed hydrogenation reaction exists in the literature where a lower than atmospheric pressure of hydrogen gas is required for high selectivity, though interestingly, Li makes a comment of Crabtree's catalyst displaying 'inconsistent results' during a similar hydrogenation reaction in his synthesis of Daphniyunnine C.[20] This may be in relation to a similar problem encountered during this thesis.

2.9 Conclusions



Scheme 28: Chapter 2 overview; synthesis of tetracyclic core **156**.

The ABCD tetracyclic core of the calyciphylline A-type *Daphniphyllum* alkaloids has been completed. The skeletal core **88** was constructed through a key organocatalysed enantioselective prototropic shift / Diels-Alder cascade reaction from **87**. Further elaborations gave **123**, the substrate for a cycloisomerisation reaction in order to furnish the B ring. Although attempts to find scalable conditions for a cationic Au(I) catalysed Toste-type cycloisomerisation reaction were unsuccessful, an alternative reductive radical

cyclisation cascade protocol mediated by tributyltin hydride was discovered which enabled access to alkene **145**. Finally, a highly diastereoselective hydrogenation reaction using Crabtree's catalyst under a low partial pressure of hydrogen gas was developed, affording **156**. With this result, an efficient and scalable synthesis of the enantiopure tetracycle core correct with all desired stereochemistry was completed, which hereby provided a platform for us to launch end-game investigations.

Chapter 3: The Total Synthesis of (−)-Himalensine A

3.1 Endgame Strategy

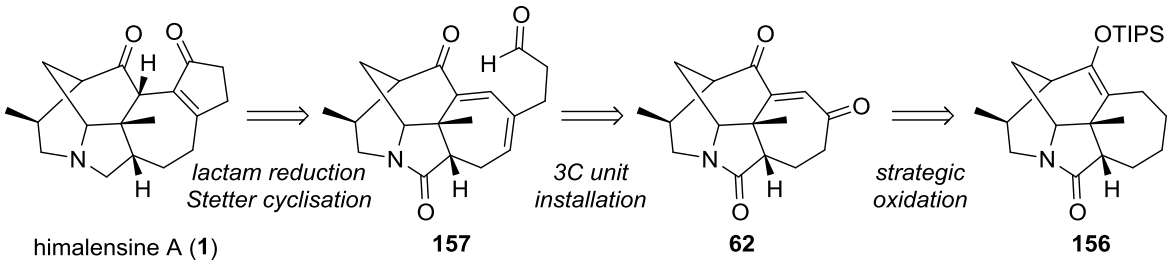


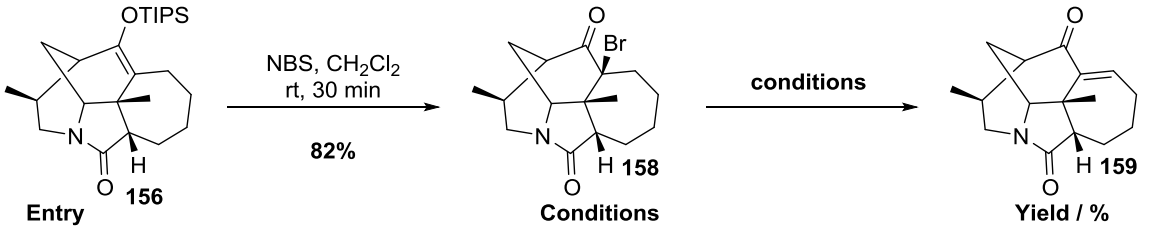
Figure 7: Endgame disconnection strategy towards himalensine A **1**.

With enantiopure tetracycle **156** in hand, a strategy to access himalensine A (**1**) was devised. We envisaged the bridgehead amine of himalensine A could be unmasked at a late-stage via a chemoselective lactam carbonyl reduction, and the E ring constructed through a Stetter cyclisation onto an appropriate extended enone present in **157**. We envisaged that the three-carbon aldehyde containing unit could be attached through a suitable coupling reaction from enedione **62**. This could then be synthesised from tetracycle **156** through a series of strategic oxidation reactions. This synthetic proposal was subsequently realised and is presented in this chapter.

3.2 Synthesis of Enedione 62

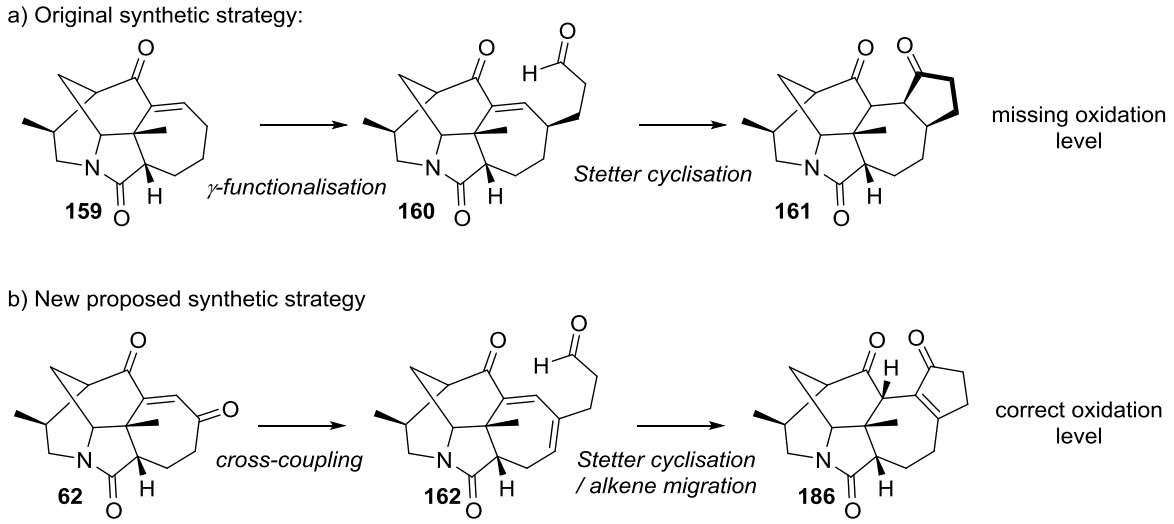
In order to progress, a method to convert tetracycle **156** to the corresponding enone was required. This investigation began with treatment of tetracycle **156** with *N*-bromosuccinimide to afford bromoketone **158** in 82% yield. A range of literature reported conditions to effect an E2 elimination of this bromide were then evaluated in order to obtain enone **159**. When treated with DBU in refluxing toluene, full decomposition of the starting material was observed (table 7, entry 1).[80] Pleasingly, the desired enone was

isolated, albeit in moderate yield of 38%, when bromoketone **158** was treated with Li_2CO_3 and LiBr in hot 125 °C DMF. This combination of lithium bromide and lithium carbonate has been proven as a powerful reagent for the dehydrohalogenation of a wide range of α-haloketones.[81] Though the role of the LiBr additive in the reaction mechanism is unclear, its omission led to complete decomposition, highlighting its necessity in the reaction (table 7, entry 3). A reduction in temperature to 80 °C led to a cleaner reaction profile, but the yield of desired enone remained moderate at 40%. Gratifyingly, a good yield in the elimination reaction was achieved in neat pyridine at 85 °C, affording enone **159** in 71% yield. Li later matched this enone intermediate in his published synthesis of hybridaphniphylline B, and thus we intercepted a formal synthesis of this complex natural product.[31] Interestingly, a side product was also isolated in this elimination reaction whose molecular mass matched that of an oxidized oxo-derivative of enone **159**. After extensive analysis, this product was characterised as enedione **62**, formed from the γ-oxidation of enone **159** (scheme 29). This γ-oxidation also featured in Li's later published synthesis of himalenine D, daphnipaxianine A and daphenylline, creating a second matched intermediate between his work and this synthesis.[24]



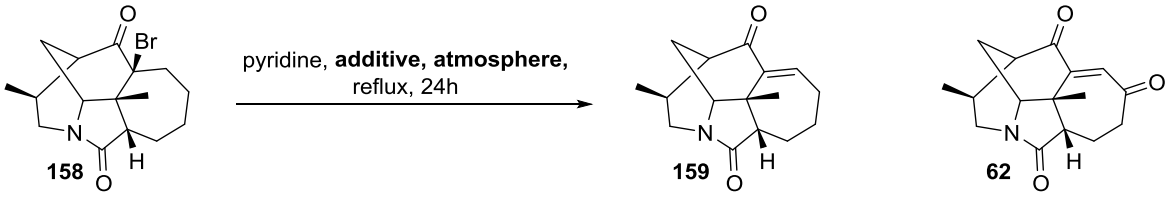
Entry	Conditions	Yield / %
1	DBU, toluene, reflux	0
2	Li_2CO_3, LiBr, DMF, 125 °C	38
3	Li_2CO_3, DMF, 125 °C	0
4	Li_2CO_3, LiBr, DMF, 80 °C	40
5	pyridine, 85 °C	71 ***(4% side product)***

Table 7: Transformation of tetracycle **156** to enone **159**.



Scheme 27: New synthetic strategy based on manipulation of the oxidation side product enedione **62**.

With the identification of this new side product, albeit formed in trace quantities, a new synthetic plan which enabled a more streamline and efficient strategy was devised, exploiting this increased oxidation state of the molecule. According to the original synthetic strategy (scheme 27a), a γ-functionalisation of enone **159** would allow synthesis of aldehyde **160**, poised to undergo an intramolecular Stetter cyclisation to close the B ring, leading to pentacycle **161**. Although this strategy allows construction of the carbon skeleton of himalensine A, a further oxidation is required to install the tetra-substituted double bond present in the natural product. We therefore decided to design a new strategy based around enedione **62** with the higher oxidation level (scheme 27b). A suitable cross-coupling reaction could be used to synthesise aldehyde **162**, which could undergo a similar Stetter cyclisation to close the final E ring. Importantly, the alkene moiety required in the final natural product is already present, and after alkene migration following the Stetter cyclisation, the correct oxidation state for the cyclopentenone moiety would be achieved **186**. **191**

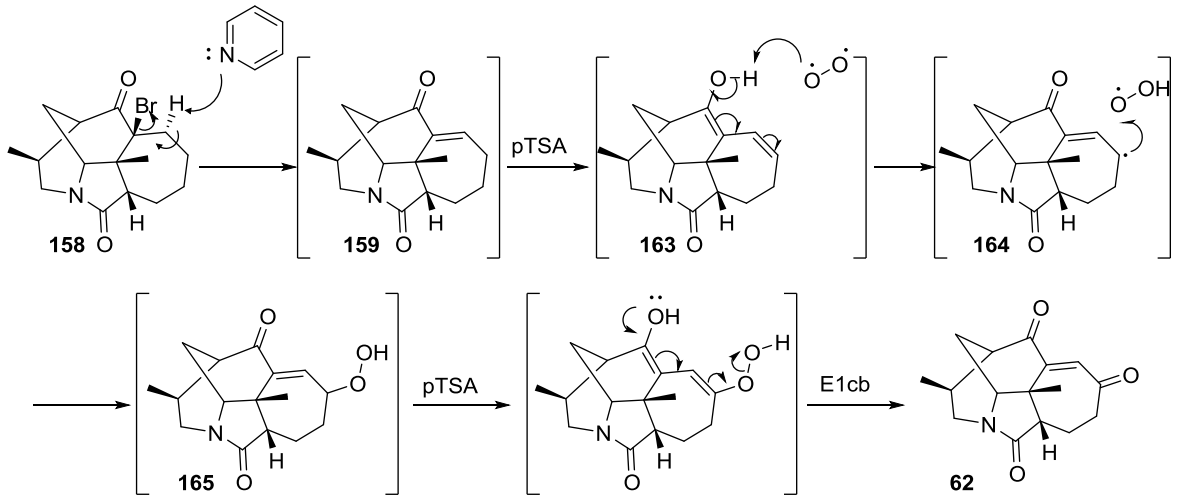


Entry	Additive	Atmosphere	159:62 ratio	isolated yield 62 / %
1	none	N_2	93:7	4
2	none	O_2	74:26	n.d
3	NMO (2 eq.)	N_2	-	0
4	CSA (2 eq.)	O_2	75:25	n.d
5	pTSA (2 eq.)	O_2	60:40	28
6	pTSA (6 eq.)	O_2	0:100	65

Table 8: Elimination/oxidation tandem reaction optimisation.

In order to realise this proposal, optimisation of the elimination reaction for the synthesis of enedione **62** was performed (table 8).[82] Analysis of the crude ^{1}H NMR post reaction showed only a trace quantity of enedione **62**, however after exposure to air during the work-up and concentration procedure, a 93:7 ratio between enone **159** and enedione **62** was obtained leading to a 4% isolated yield for enedione **62**. As oxygen can be the only oxidant mediating this transformation, ketobromide **158** was refluxed in pyridine under an atmosphere of oxygen for 24h (table 8, entry 2). Despite these harsh oxidative reaction conditions, only a 74:26 ratio of enone to enedione was observed. An attempt to use N-methylmorpholine oxide as an oxidant was unsuccessful, leading to material decomposition. Accordingly, we turned to the use of acidic additives to improve the reaction yield. The addition of 2 equivalents of camphor sulfonic acid led to significant decomposition of material and no improvement in the ratio between enone and enedione. Pleasingly, the addition of two equivalents of pTSA monohydrate could improve the ratio towards enedione and a 28% isolated yield was obtained (table 8, entry

5). Finally, the equivalents of acid was increased to 6, and with this large excess, complete conversion of enone was achieved with a 65% isolated yield of enedione **62** was obtained.



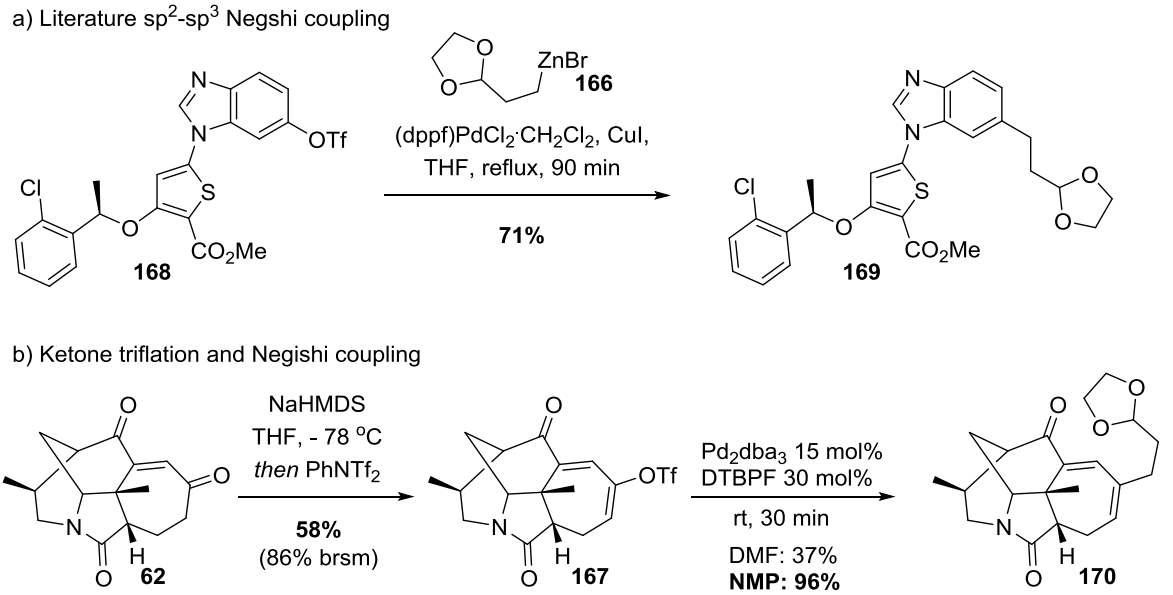
Scheme 28: Proposed mechanism for formation of enedione **62.**

A proposed mechanism for this transformation is shown in scheme 28. Initially, pyridine effects a standard E2 elimination of bromoketone **158** to give enone **159** as an intermediate. As an acid additive is required to effect smooth oxidation of this intermediate, we propose that enol **163** is the key intermediate from which hydrogen atom abstraction by oxygen can occur. Recombination of the resultant radical cation **164** with the generated superoxide radical gives peroxide **165**. This subsequently undergoes a Kornblum-DeLaMare rearrangement to deliver enedione **62** and complete the sequence.[83] With enedione **62** in hand, methods to introduce the final three carbon atoms required to form the E ring were then investigated.

3.3 Synthesis of the E ring

3.3.1 Sp^3-sp^2 Negishi Cross Coupling

As previously described previously (see chapter 3.2), we envisaged use of a Stetter reaction to generate the pendant cyclopentenone E ring. In order to obtain the substrate for this ring closing step, the final 3 carbon atoms required for himalensine A had to be attached through a cross coupling strategy.



Scheme 28: a) Literature precedent for Negishi coupling with **166**. b) Attachment of the three-carbon aldehyde side chain.

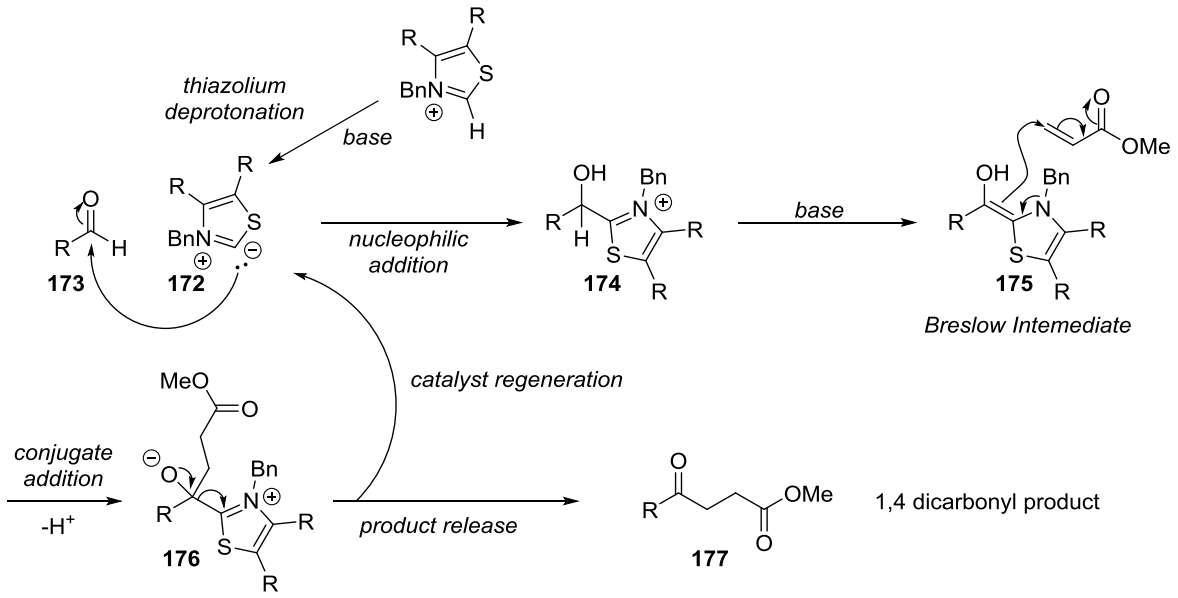
The sequence began with selective triflation of **62** to give vinyl triflate **167**. Only a single equivalent of NaHMDS was required to generate a reactive enolate as the amide α-proton is at a bridgehead position and thus difficult to deprotonate. Quenching the enolate with phenyltriflimide afforded the vinyl triflate product in 58% yield alongside a 28% recovery of starting material enedione **62**. Efforts to improve this yield by varying the reaction temperature and triflating reagent were unsuccessful, and this first attempt proved to be the best of the conditions evaluated to date.

Vinyl triflate **167** was perfectly poised for an sp^2-sp^3 cross coupling reaction to bring in a masked aldehyde three carbon subunit. To effect this transformation, we turned to the Negishi coupling due to the superior reactivity of zinc organometallic reagents over organoboronates, yet high functional group tolerance compared with organomagnesium or organolithium reagents.[84] In the literature, only a single example exists for use of organozinc **166** in a Negishi cross coupling reaction with sp^2-triflates (scheme 28a).[85] A dppf ligated palladium complex was used to catalyse the reaction, transforming aryl triflate **168** into the cross-coupled product **169**. Taking inspiration from this literature precedent, DTBPF, a bulky ferrocene based ligand, was selected (scheme 28b).[86] From word of mouth, this sterically-hindered bidentate phosphine ligand is often used within the pharmaceutical industry for challenging palladium catalysed reactions where other phosphine ligands are unable to succeed. When DMF was evaluated as a solvent in the reaction, the starting material was completely consumed within 30 min at room temperature and a 37% isolated yield of acetal **170** was obtained. A major unknown side product was found in this reaction with a molecular mass of 328, indicating an adduct with solvent DMF. Due to very limited quantity of material, this side product was not fully characterised, and instead the solvent was replaced with N-methylpyrrolidinone, a more inert replacement to DMF. Remarkably, on this second attempt a 96% isolated yield of coupled product **170** was afforded.

3.3.2 Stetter Reaction to Furnish Cyclopentenone E ring

Continuing on, acetal **170** was deprotected with aqueous HCl in wet THF to unmask aldehyde **171** ready for intramolecular Stetter cyclisation. The Stetter reaction is a powerful method for the synthesis of 1,4 dicarbonyl compounds through an *umpolung*

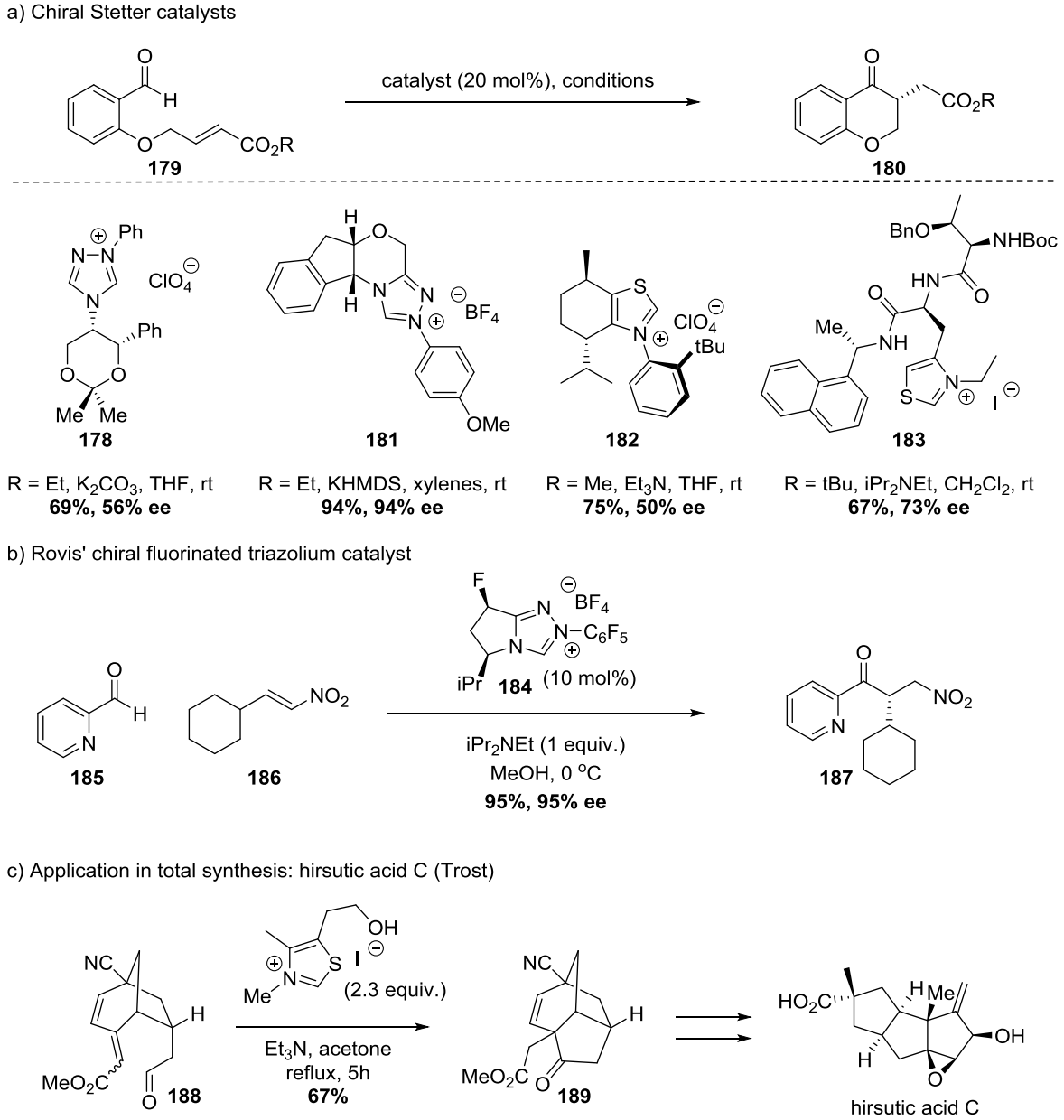
disconnection between aldehydes and Michael acceptors.[87] First discovered and published in 1973 by Stetter and Shreckenberg, the reaction allows use of aldehydes, usually electrophilic a^1 synthons, as nucleophilic d^1 synthons.



Scheme 29: Mechanism for the Stetter reaction.

The reaction is analogous to the benzoin condensation and can be catalysed by cyanide, thiazolium salts or other suitable carbene precursors, with perhaps the most famous example being thiamine used in biological enzymes to catalyse benzoin condensations.[88] In the first step of the reaction mechanism, the active carbene catalyst **172** must be generated by deprotonation of the thiazolium salt with an appropriate base (scheme 29). This can then attack the electrophilic aldehyde substrate **173** to give **174**, which can subsequently tautomerise to give intermediate **175**, the Breslow intermediate. Proposed in 1958 by Ronald Breslow, this key intermediate is now nucleophilic through the aldehyde carbonyl carbon and allows for *umpolung* reactivity.[89] Conjugate addition into methyl acrylate or any suitable Michael acceptor next occurs, giving rise to tetrahedral

intermediate **176** which collapses to deliver both the 1,4 dicarbonyl product **177** and the active catalyst.



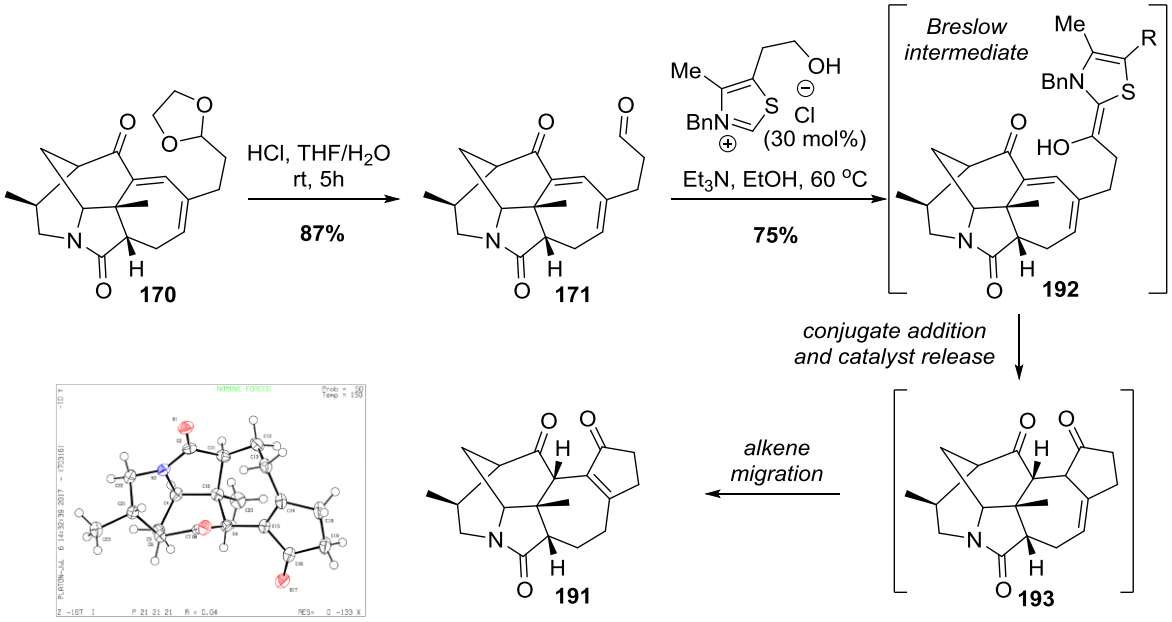
Scheme 30: Development and applications of the Stetter reaction.

Since Stetter's seminal publication, his namesake reaction has been widely utilised in a range of different applications. Perhaps one great testament to the power of this transformation is Ender's pioneering work into chiral carbene catalysts to enable synthesis of enantioenriched 1,4 dicarbonyl products (scheme 30a). Utilising catalyst **178**,

he was able realise the first enantioselective Stetter cyclisation of aldehyde **179** to deliver dihydrochromone **180** in a moderate 56% ee.[90] This exact transformation became the platform for other groups to develop more efficient and selective catalysts, and the groups of Rovis[91], Bach[92] and Miller[93] also report novel chiral catalysts **181**, **182** and **183** respectively to effect this transformation. Later, Rovis also reported the use of a highly fluorinated triazolium catalyst **184** to effect the enantioselective Stetter reaction of heteroaromatic aldehydes (**185**) onto nitroolefins (**186**) to give heteroarene-bearing β-nitroketone derivatives (**187**) (scheme 30b).[94] Stereoelectronic effects of fluorination on the LHS pyrrolidine ring was found to be crucial for enantioselectivity as this strongly favoured one specific conformation of the catalyst giving rise to higher enantioselectivity in the Stetter reaction. This advancement to the field shows how the Stetter reaction can be tolerant of Lewis basic functionality which metal-catalysed alternatives would be unable to accommodate. One final example to highlight is Trost's use of an intramolecular Stetter cyclisation from aldehyde **188** to create a new quaternary stereocentre within a densely functionalised congested fused tricycle **189**, leading to the total synthesis of racemic hirsutic acid C (scheme 30c).[95] Although an excess of a thiazolium catalyst is employed, the reaction is a testament to the utility of the Stetter reaction in total synthesis and represents a powerful and general method for constructing cyclopentanones through an intramolecular cyclisation process.

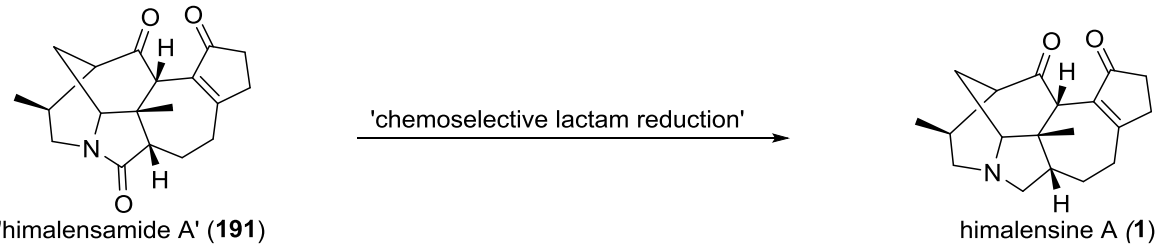
Accordingly, the Stetter reaction was applied to the real system. Initially, deprotection of acetal **170** with HCl in tetrahydrofuran unmasked aldehyde **171** poised for the key ring forming step. Pleasingly on the first attempt, treatment of this precursor with thiazolium catalyst **190** at 60 ^{o}C in the presence of triethylamine and ethanol delivered pentacycle **191** in 75% yield. This remarkable result, which was confirmed by single crystal X-ray

analysis, highlights several key features designed into substrate **171** which enable the desired product to be formed in high yield. As described previously, γ,δ-unsaturation of the enone adds an extra oxidation level to the structure which is required in the final molecule. This alkene is an observer to the Stetter cyclisation reaction as the *in situ* formed Breslow intermediate **192** can only attack the β-position of the extended enone due to Baldwin's rules. After the Stetter reaction was completed, this alkene in **193** migrates into the thermodynamic position and completing the synthesis of the pendant cyclopentenone E ring.



Scheme 31: Formation of the E ring *via* an intramolecular Stetter reaction.

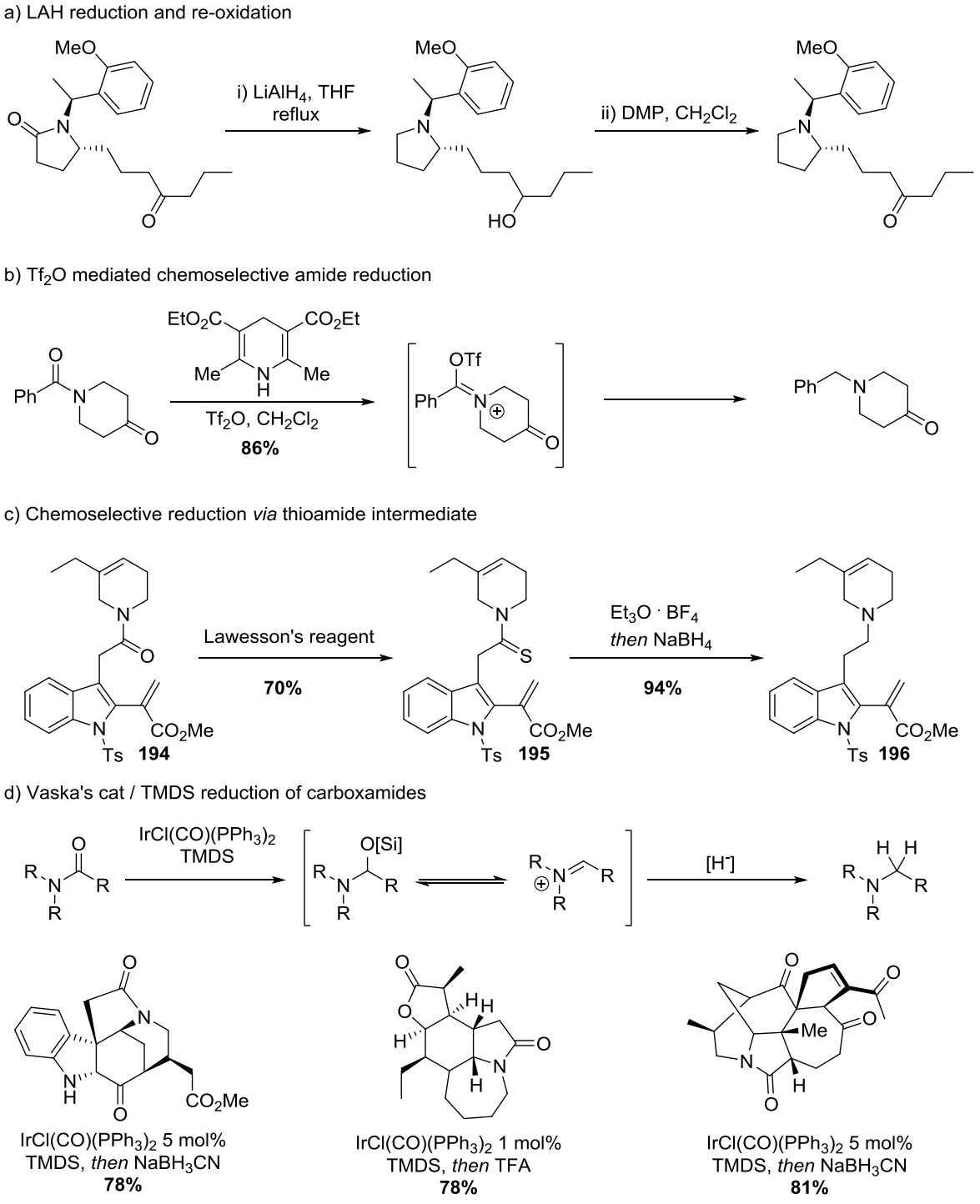
3.4 Late-Stage Chemoselective Lactam Reduction



'himalensamide A' (**191**) himalensine A (**1**)

Scheme 32: Final synthetic challenge: chemoselective lactam reduction.

191, termed 'himalensamide A' from hereon due to the additional lactam carbonyl group, has the completed pentacyclic skeletal core with all but one required functional group decorations and stereocentres correctly set. Only the chemoselective reduction of the lactam carbonyl group remained as a final synthetic challenge (scheme 32).



Scheme 33: Representative strategies and examples for amide reduction.

The lactam carbonyl has been strategically utilised throughout the entire synthesis as a protecting group for the otherwise reactive amine functionality, and with its purpose now served, the success of the entire synthesis project now rested with its successful chemoselective reduction.

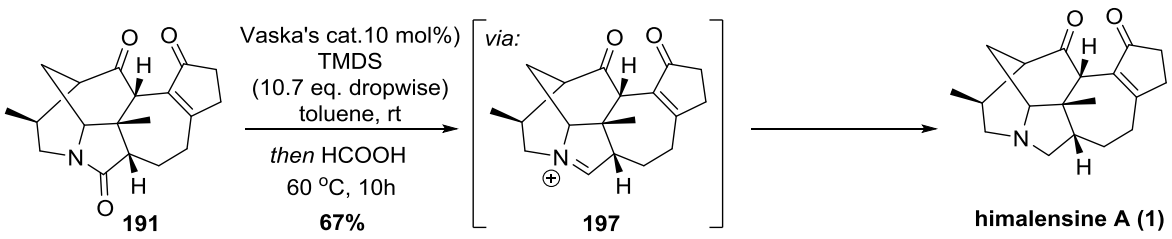
Traditionally, lactams are reduced to the corresponding amine with strong hydridic reductants such a lithium aluminium hydride. If other sensitive functional groups such as ketones or aldehydes are present in the molecule, then typically a 2-step procedure with complete full reduction followed by re-oxidation of the resultant alcohols back to the parent carbonyl moieties is employed (scheme 33a).[96] In the past decade, much work has been focused on developing chemoselective methods for amide and lactam reduction which exploit the stronger Lewis basicity of the amide carbonyl group.[97] In 2008, Charette and co-workers reported a method for the chemoselective reduction of lactams using triflic anhydride as an electrophilic activating reagent.[98] This incredibly reactive electrophile reacts selectively with the amide functional group over other less Lewis basic carbonyls, giving rise to a reactive cationic intermediate which can be reduced with a weak hydride source such as Hantzsch ester or silanes (scheme 33b). Using this method, a wide range of amides could be reduced in the presence of sensitive functional groups such as ketones, esters, epoxides and nitriles. Alternatively, chemoselective amide reduction can be conducted by initial conversion to the corresponding thioamide using a suitable thionylation reagent such Lawesson's reagent; this strategy was initially reported by Raucher and Klein in their seminal 1980 paper.[99] Amide **194** is initially converted to thioamide **195** using Lawesson's reagent in hot toluene. Subsequent activation of the thioamide with Meerwein's salt and reduction with sodium borohydride delivers the reduced amine **196** in 66% yield over two steps.

These two powerful advancements in the field allowed for the selective reduction of amides in the presence of other sensitive functional groups, however the use of stoichiometric activating reagents is required. Therefore, the development of suitable catalytic protocols would create an attractive alternative to the well-established stoichiometric approaches. This proposition has been very well explored in recent years and although many different methods have been developed[100–103], one system in particular has been much more widely applied in the context of total synthesis. Developed by the group of Nagashima, the combination of Vaska's catalyst $IrCl(CO)(PPh_3)_2$ and tetramethyldisiloxane (TMDS) is a potent and selective catalytic system for the highly chemoselective reduction of amides and lactams to the corresponding hemiaminal species (scheme 33d).[25] Functionalisation of this intermediate hemiaminal is possible through generation of a reactive enamine/iminium intermediate[104–106] though if further reduction is required, addition of an external hydride source can deliver the fully reduced amine. Modified variants of Nagashima's original protocol has been applied to several total syntheses (scheme 33d) often at a late stage and on highly functionalised substrates, thus highlighting the power of this method.[24,27,107,108]

At the time of the work described in this thesis, this protocol was being investigated within our group and the only example of Vaska's catalyst applied to total synthesis was in 2016[27]. Therefore, if Vaska's catalyst could be used to complete the total synthesis of himalensine A, then it would establish this method as a powerful strategy for late stage amide reduction.

When lactam **191** was treated with Vaska's catalyst (10 mol%) in the presence of TMDS (2 equiv.), conversion of the starting material to the reduced hemiaminal was observed by

mass spectrometry. Although a significant amount of starting material was still present, formic acid was added to the reaction mixture and after heating overnight at 60 ^{o}C, a highly impure sample of himalensine A was isolated in ~15% yield. Since 2 equivalents of TMDS failed to convert most of the starting material, the equivalents of were increased in order to improve conversion. Given the Vaska's-mediated reduction of a lactam carbonyl group to a hemiaminal is an extremely fast reaction, the TMDS reductant was added dropwise and analysis of the reaction mixture by TLC was taken after the addition of each drop. By this method, 6 drops of TMDS (approximately 0.025 mL per drop, 10.7 equivalents) was added until no starting material was present. Excess formic acid was then immediately added in order to quench the catalyst and any unreacted silane. If the reaction was left longer without formic acid quench, or if additional TMDS was added, over-reduction of the ketone and enone moieties was observed by mass spectrometry analysis.



Scheme 34: Lactam reduction delivering himalensine A.

After addition of formic acid, the reaction mixture was heated to 60 ^{o}C overnight in order to deliver hydride to the *in situ* generated iminium ion **197**, and after work-up and purification, himalensine A was delivered in 67% yield, thus completing the 22 step synthetic sequence and fulfilling the efforts of multiple hands through many years of hard work (scheme 34).

3.5 Comparison of Synthetic and Natural Samples

With a synthetic sample himalensine A in hand, comparison between its spectral properties and those reported in the literature were made.[4] Throughout the project, the final Vaska's reduction was carried out multiple times, leading to multiple batches of synthetic himalensine A. We found that although the all the relevant peaks were present, the chemical shifts would differ each time with a significant shift in ppm. This behaviour of bridgehead amines to display drifting of signals in ^{1}H NMR analysis has been observed previously in our group and was attributed to protonation or capture of CO_2 from the air. In order to investigate if the shifting was due to amine protonation in solution, the ^{1}H spectrum in chloroform of a freshly synthesised batch of himalensine A (purified by flash column chromatography using basified silica with Et_3N containing eluent) was taken (figure 8). This same sample was then concentrated *in vacuo* and re-dissolved in chloroform and the ^{1}H spectrum re-measured, resulting in all the peaks shifting downfield to higher ppm levels. The procedure was repeated and the ^{1}H NMR signals were found to further shift upfield. Finally, the same sample was passed through a solid potassium carbonate filter to generate the fully free-base form of the natural product and the spectrum re-measured. The ^{1}H signals in the fully free-base form were more shifted upfield than reported in the literature for the natural isolated material; therefore, we believe the reported spectrum of the natural product is of a partially protonated form of himalensine A.

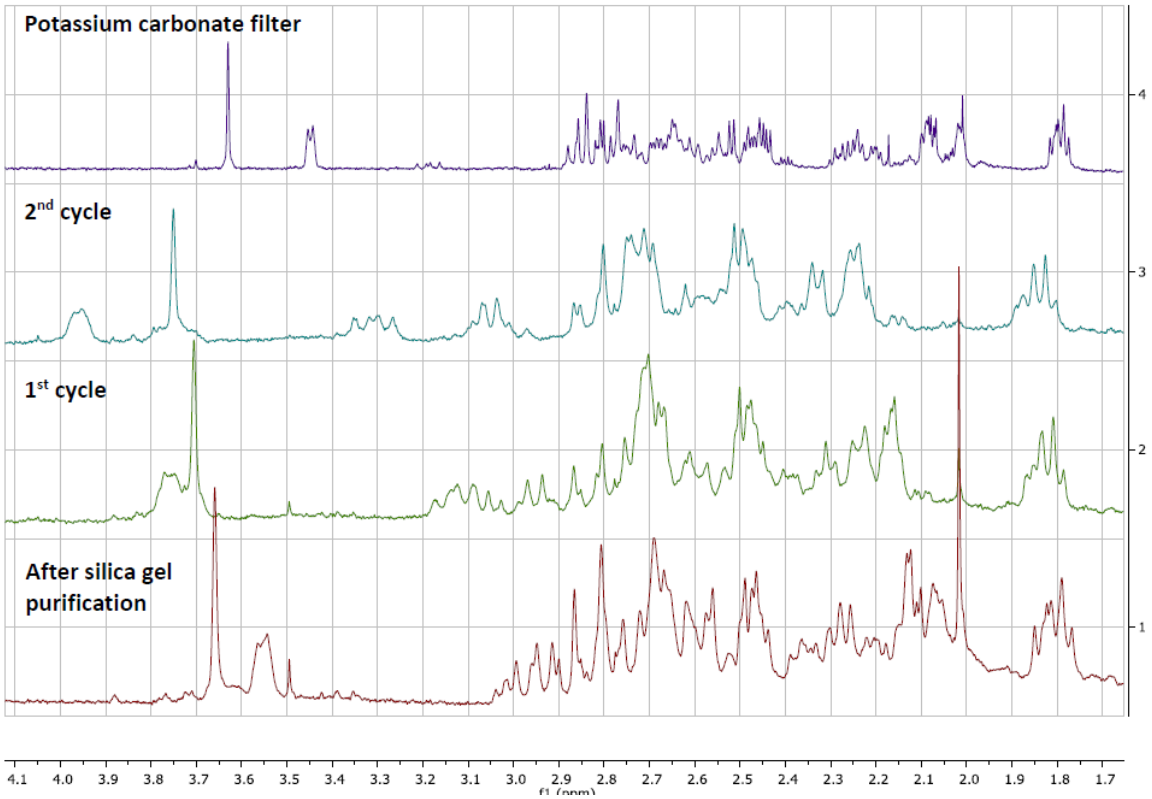
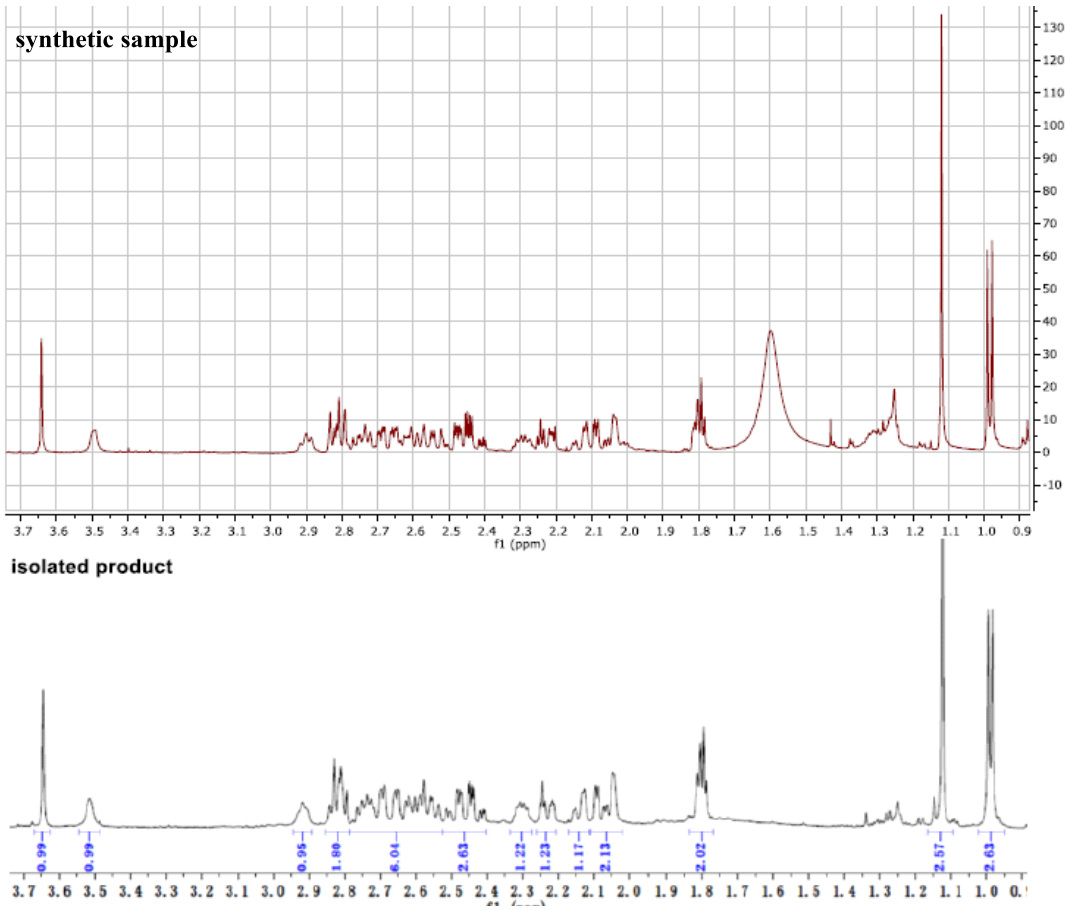


Figure 8 Shifting of the ^{1}H spectrum with successive solvent removal.

a) Comparison of ^{1}H spectra



b) Comparison of ^{13}C spectra

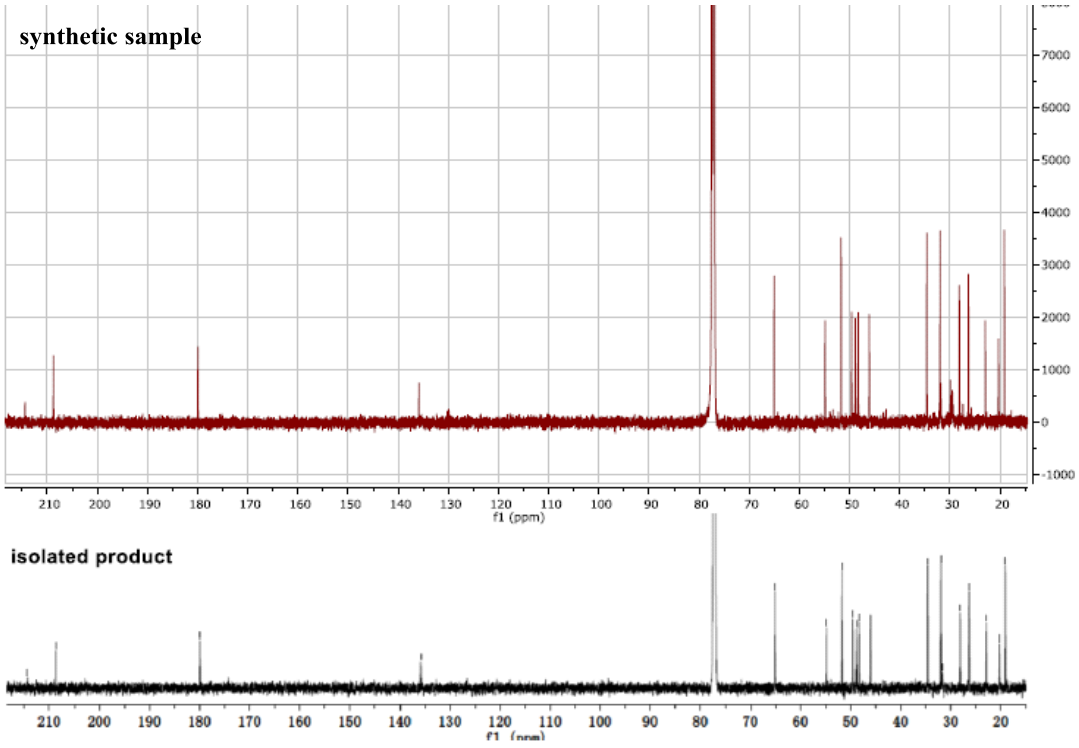


Figure 9: Comparison of synthetic and natural himalensine A ^{1}H and ^{13}C NMR spectra.

no.	reported ^{1}H/δ	synthetic ^{1}H/δ	Δ/δ	reported ^{13}C/δ	synthetic ^{13}C/δ	Δ/δ
1	-	-	-	214.4	214.4	0.0
2	2.04, brs	2.04, brs	0.00	46.1	46.1	0.0
3	a 2.14, dd (14.8, 3.5)	2.13, dd, (14.8, 4.3)	0.01	20.3	20.3	0.0
.	b 2.08, brdd (14.8, 4.9)	2.07, ddd, (14.8, 4.9, 1.8)	0.01	-	-	-
4	3.52, brs	3.50, brs	0.02	65.1	65.1	0.0
5	-	-	-	48.3	48.3	0.0
6	2.30, m	2.30, dt (11.8, 5.8)	0.00	48.8	48.9	0.1
7	β 2.92, m	2.90, t (8.0)	0.02	54.9	54.9	0.0
.	α 2.80, m	2.80, m	0.00	-	-	-
8	3.65, s	3.64, s	0.01	51.7	51.7	0.0
9	-	-	-	135.8	135.9	0.1
10	-	-	-	179.9	179.9	0.0
11	a 2.60, m	2.59, m	0.01	28.1	28.1	0.0
.	b 2.23, m	2.22, m	0.01	-	-	-
12	1.80, m, 2H	1.80, m, 2H	0.00	22.9	22.9	0.0
13	-	-	-	208.7	208.7	0.0
14	a 2.49, ddd (18.9, 6.5, 2.5)	2.49, m	0.00	34.6	34.6	0.0
.	b 2.43, ddd (18.9, 6.5, 2.5)	2.43, ddd (18.8, 6.4, 2.8)	-	-	-	-
15	a 2.71, m	2.70, m	0.01	32.0	32.0	0.0
.	b 2.64, m	2.65, m	0.01	-	-	-
16	2.74, m	2.73, m	0.01	31.8	31.8	0.0
17	α 2.82, dd (14.1, 7.1)	2.81, dd (13.6, 7.2)	0.01	49.6	49.6	0.0
.	β 2.56, dd (14.1, 10.3)	2.55, dd (14.1, 10.1)	0.01	-	-	-
18	0.99, d (6.8)	0.98, d (6.7)	0.01	19.2	19.1	0.1
19	1.12, s	1.12, s	0.00	26.3	26.3	0.0

Table 9: Numerical comparison of ^{1}H and ^{13}C chemical shifts.

With this knowledge in hand, we were able to confirm the structure of the isolated sample of himalensine A by obtaining a sample in strong agreement with the reported ^{1}H and ^{13}C NMR spectra (Figure 9, table 9) displaying a maximum disagreement of 0.02ppm in the proton spectrum and 0.1ppm in the carbon. Though there was little doubt on the assignment of the absolute configuration of the isolated natural himalensine A, it was confirmed by matching of specific rotation to our synthetic sample whose configuration was confirmed by single crystal X-ray diffraction analysis. Finally, in order to obtain a high purity and resolution NMR spectrum, a small amount of material was re-purified by C-18 HPLC and the ^{1}H and ^{13}C NMR spectra measured using a 700 MHz and 175 MHz probe respectively (figure 10). This high resolution ^{1}H spectrum of himalensine A allowed fine

coupling constants to be measured and acts as a reference for future work relating to this natural product.

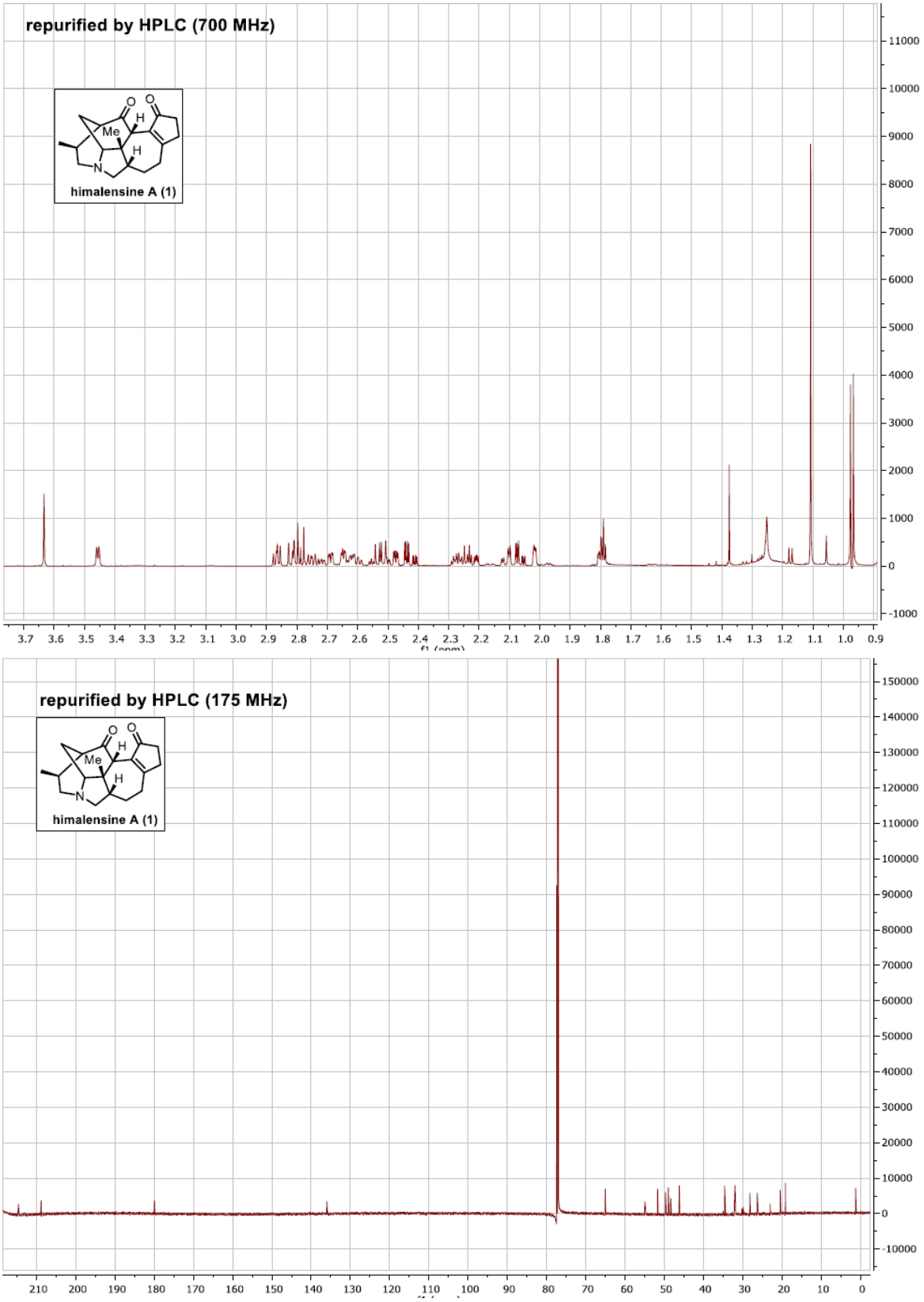
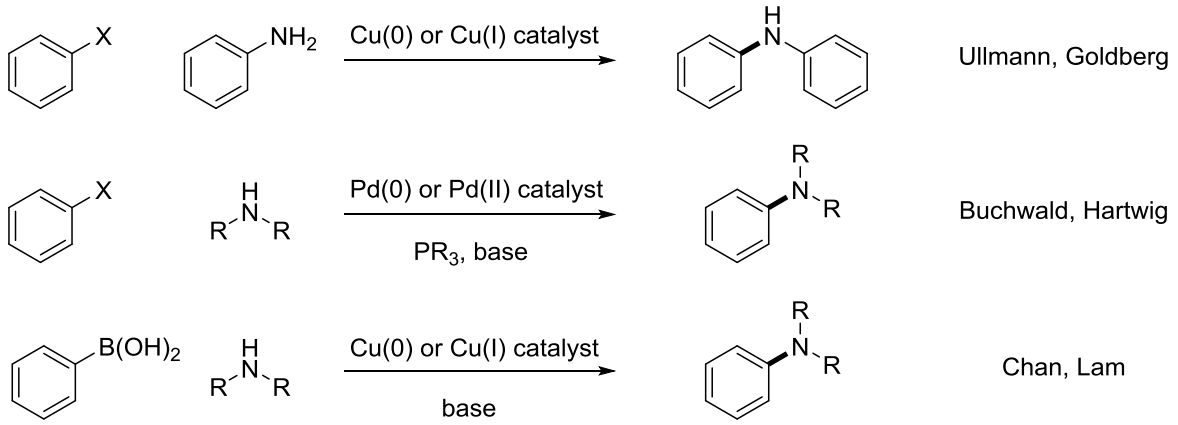


Figure 10: High resolution ^{1}H and ^{13}C NMR spectra of himalensine A.

Chapter 4: Introduction to Cp^*Rh^{III} C-H Functionalisation

4.1 Development of the Direct C-H Amination Reaction

Transition metal catalysed C-H functionalisation is a powerful strategy for atom-economical and efficient synthesis.[109] By eliminating the need for pre-functionalised substrates required in traditional cross coupling methods, direct transition metal C-H functionalisation has been an attractive and well explored field of study in the past decade.[110,111] Amongst these reactions, Pd(II) catalysed C-H functionalisation dominates and notably the groups of Yu, Blackmond, Gaunt, Itami, Sanford and Daugulis amongst others have made great advancements to the field.[109,112]



Scheme 35: Traditional C-N cross coupling strategies.

Of the many different transformations possible, C-N bond formation is especially important for streamlining the synthesis of medicinally relevant nitrogen containing molecules.[113] Amines and nitrogen containing heterocycles are ubiquitously found in pharmaceutically relevant molecules and new ways of directly introducing these functionalities would be attractive alternatives to the well-established cross-coupling methods such as those developed by Ullmann/Goldberg, Buchwald/Hartwig and Chan/Lam. (scheme 35).[114–120] These cross coupling reactions, especially the methods

developed by Buchwald and Hartwig, are the standard 'go-to' methods for C-N bond introduction within the chemical and pharmaceutical industries.[121]

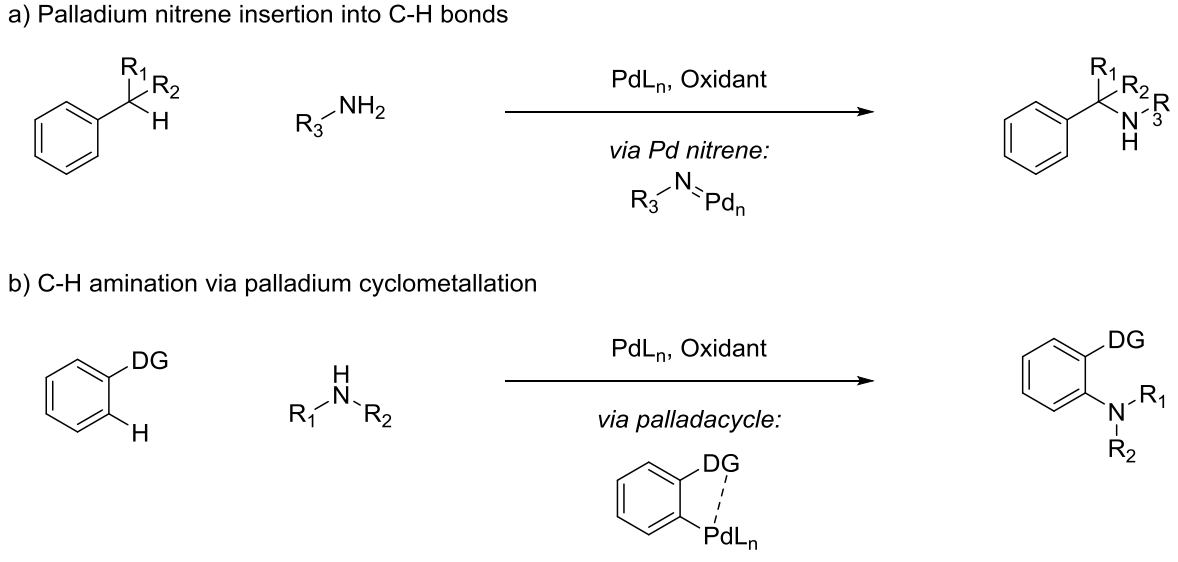
Concerning the direct transformation of C-H bonds, many challenges must be overcome in order to develop a successful method. These include:

a) The inert C-H bond with high bond strength (85-105 kcal/mol) creates a strong kinetic barrier to activation.

b) Achieving energetically demanding C-N bond formation by finding suitable high energy amine sources.

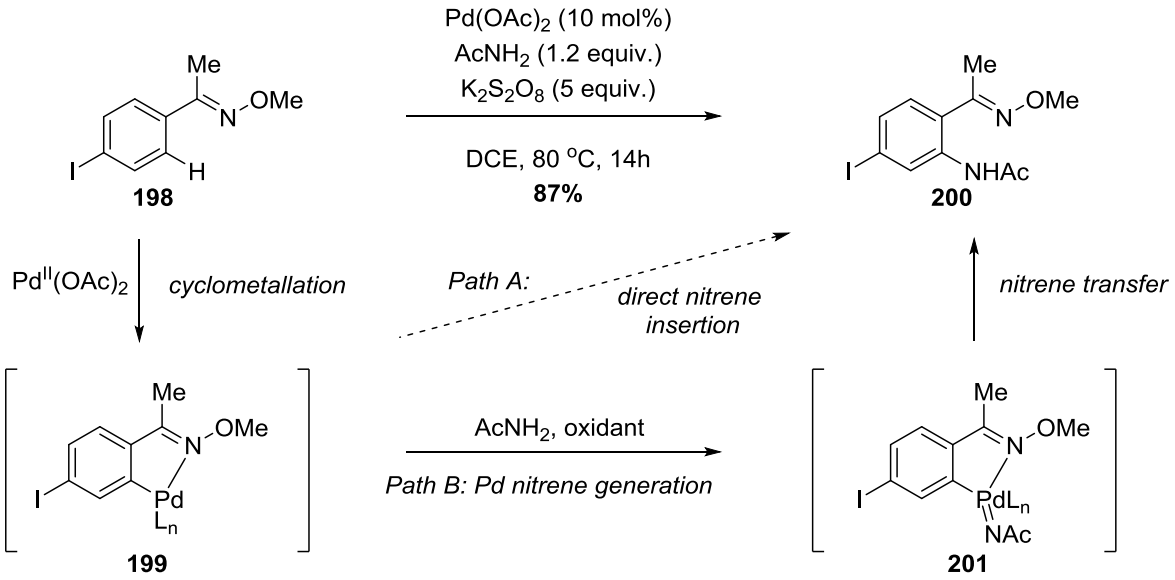
c) Ligand or directing group controlled site selectivity in the presence of multiple C-H bonds.[122]

Two main practical solutions to these challenges have been developed within the literature (scheme 36). The first is an outer sphere pathway through generation of a palladium nitrene species able to transfer to reactive C-H bond (scheme 36a). This strategy with palladium, first demonstrated by Breslow and Gellman[123,124], is relatively less explored when compared with rhodium or ruthenium based counterparts.[125,126]



Scheme 36: Strategies for palladium catalysed C-H amination.

The second strategy is to utilise a suitable Lewis basic directing group to form an intermediate palladacycle intermediate through C-H bond metallation (scheme 36b). Oxidative amination of this reactive C-Pd bond then delivers the aminated product. This has become the more widely utilised strategy and allows for site selective and predictable functionalisation of a wide range of directing group bearing molecules.



Scheme 37: Che's direct C-H amidation of aromatic oximes.

One representative example of this field is Che's palladium catalysed C-H amidation reaction utilising oximes as a directing group (scheme 37).[127] Treatment of a wide range of oximes with 10 mol% palladium acetate, a primary amide and potassium persulfate as oxidant led to smooth conversion to the amidated product in high yield. Using ketoxime **198** as an example, the postulated mechanism is illustrated in scheme 37. Initial Pd(II) cyclometallation occurs through a concerted metallation deprotonation (CMD) pathway to give palladacycle intermediate **199**. Next, the corresponding nitrene of acetamide is generated by oxidation with potassium persulfate. This nitrene either directly inserts into the carbon-palladium bond through path A to give amidated product **200**, or proceeds through nitrene-palladacycle intermediate **201** and nitrene transfer to the carbon-

palladium bond. Since palladium remains as Pd(II) throughout the whole cycle, sensitive functionality such as aryl halides are well tolerated in this transformation. In addition to aromatic oximes, a range of sp^3 C-H bonds were also activated demonstrating the wide applicability of the method.

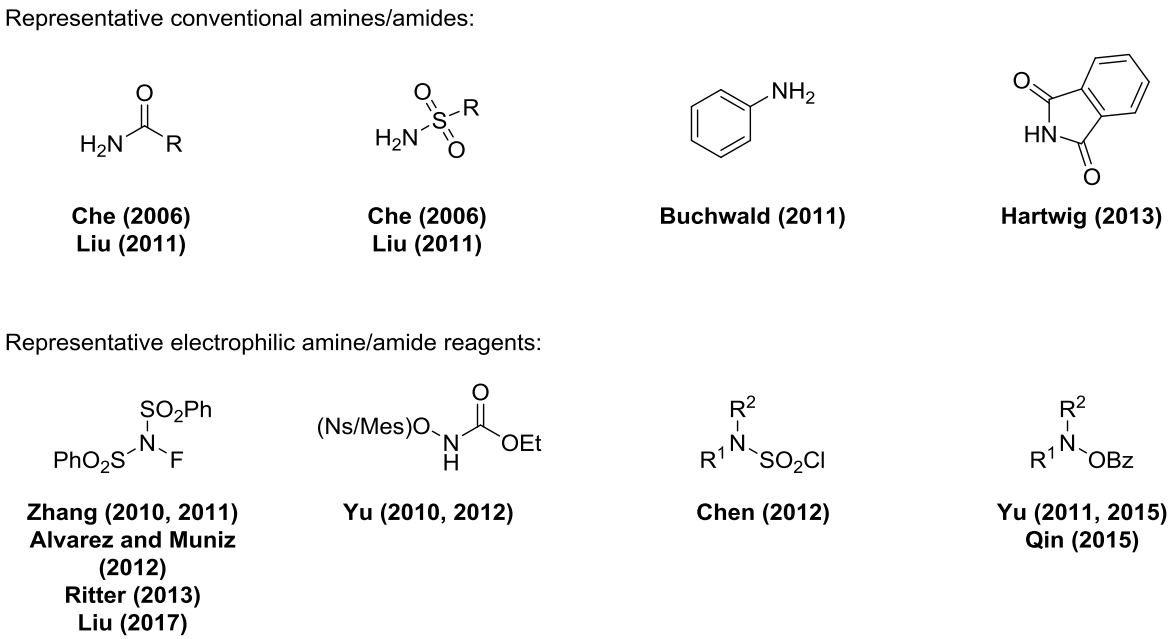
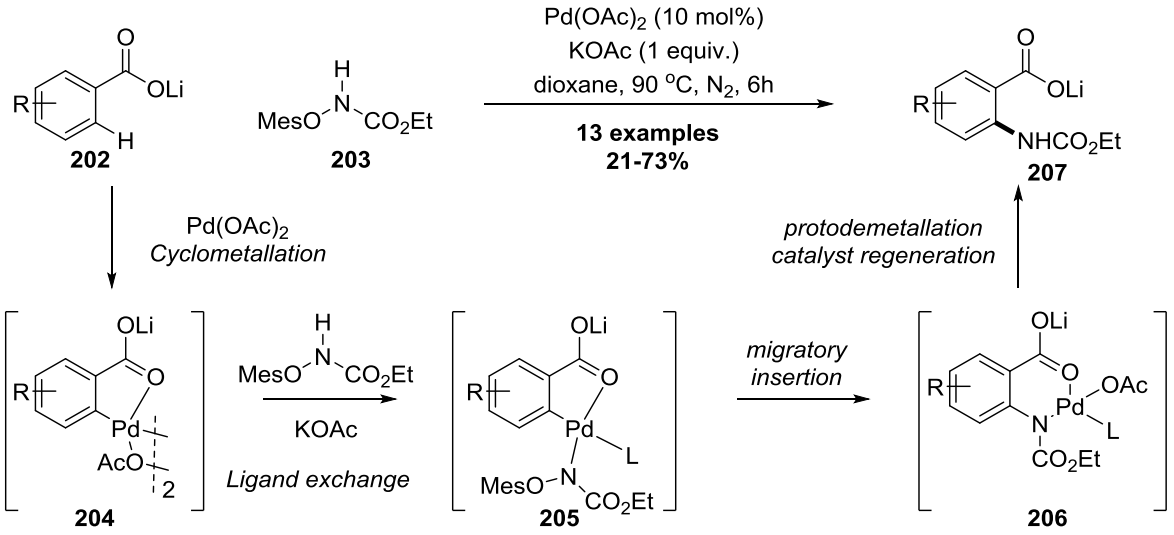


Figure 11: Representative amines/amides and electrophilic amination/amidation reagents used in Pd catalysed C-H bond functionalisation reactions.

A wide range of amine/amide partners are possible in this reaction (figure 11). Ideally, the optimal nitrogen source would be common commercially available amines and amides. Since amines are inherently nucleophilic, addition of an external oxidant is required to convert these into electrophilic partners for reaction with the nucleophilic cyclometallated carbon-palladium bond. Alternatively, electrophilic amine reagents, such as N-halides and hydroxylamine/hydroxamic acid derivatives, can also be employed which mitigates the need for addition of an external oxidant and avoid the use of unstable or unattractive organic azides.[128]

A representative example of the use of electrophilic amination reagents is Yu's Pd(II) catalysed *ortho* amidation of benzoic acids **202** using ethyl mesitylsulfonyloxycarbamate **203** as a nitrogen source (scheme 38).[129] This electrophilic hydroxylamine derivative is able to bind to the *in situ* generated palladacycle **204** to give **205**, which undergoes migratory insertion of the aryl-palladium bond onto the electrophilic nitrogen centre, displacing mesitylalcohol as a leaving group. Final protodemetallation of intermediate **206** affords the anthranilic acid product **207**.

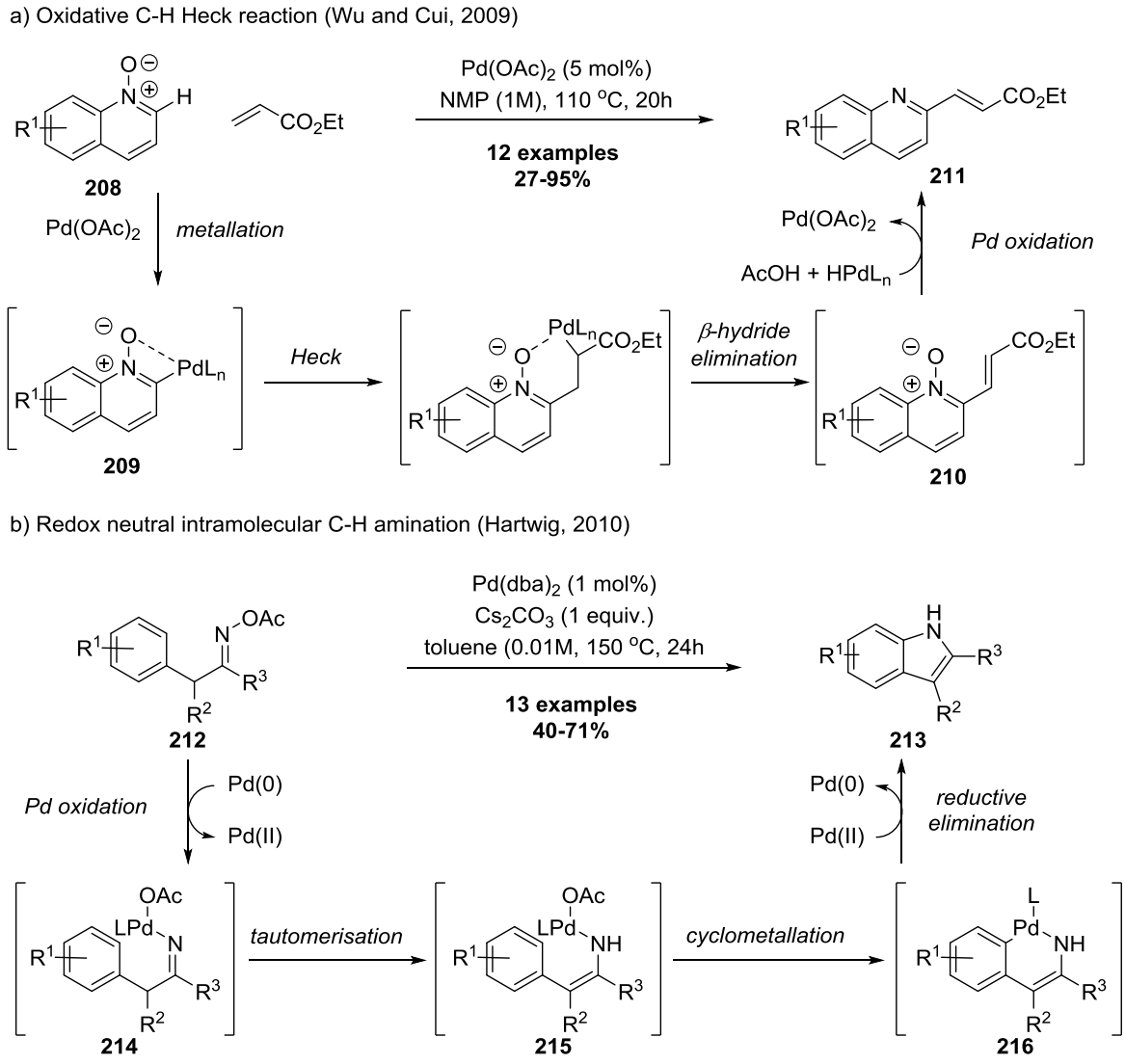


Scheme 38: Yu's ortho C-H amidation to access anthranilic acid derivatives.

One additional application of utilising electrophilic amine equivalents is their ability to act as internal oxidants when employed as part of the substrate molecule. The discovery of this concept has made a significant impact on the field of C-H activation and led to the discovery of many new transformations.[130–132] In their 2009 seminal report, Wu and Cui reported the first use of a cleavable N-O bond to effect the oxidative C-H Heck reaction of quinoline N-oxides under oxidant free conditions.[133] The N-oxide functionality **208** can direct *ortho* metallation to give cyclopalladated intermediate **209**, poised to perform an intermolecular Heck reaction with ethyl acrylate. After β-hydride elimination, the reduced

palladium-hydride species was oxidized by the resultant product **210** to regenerate palladium acetate and deliver quinoline **211**.

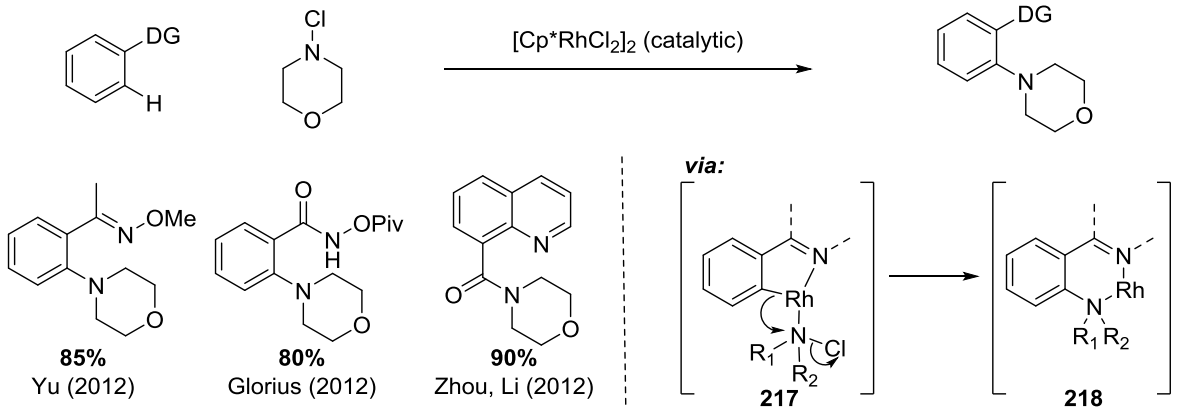
Within the context of C-N bond formation, Hartwig demonstrated use of ketoximes **212** as an internal oxidant to mediate and direct intramolecular C-H amination, leading to diverse indole derivatives **213.**[134] Under the reaction conditions, Pd(0) is able to insert into the weak N-O bond of the oxime functionality leading to a ligated Pd(II) intermediate **214**. After tautomerization to **215**, an intramolecular C-H metallation occurs, giving palladacycle **216**. Finally, reductive elimination affords the final indole product and regenerates Pd(0) to continue the catalytic cycle.



Scheme 39: Use of N-oxo internal oxidants in C-H functionalisation.

4.2 Rh^{III} Catalysed C-H Amination

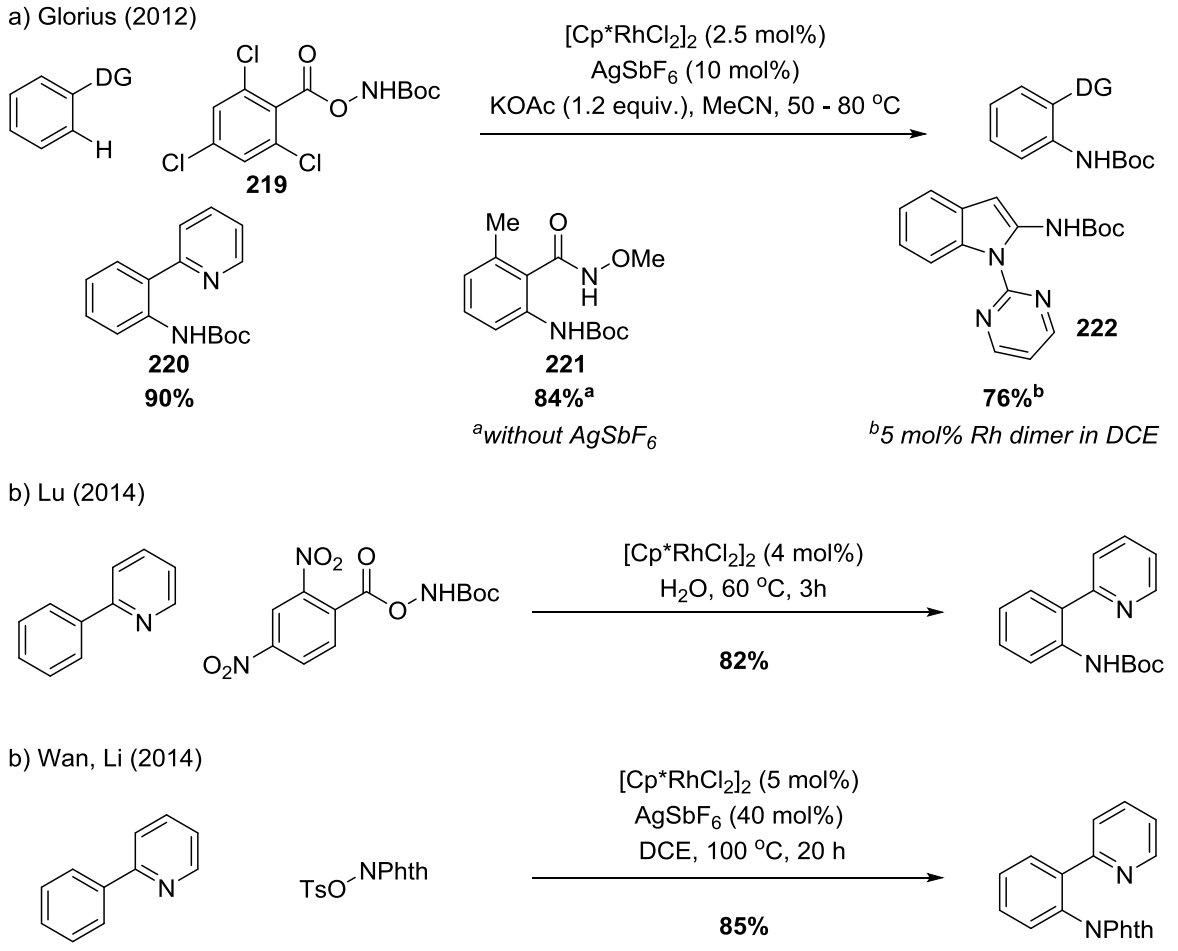
In recent years, remarkable advancements in Rh^{III}-catalysed C-H functionalisation has led to numerous C-C bond forming methodologies being discovered. In particular, $[Cp^*RhCl_2]_2$ is prominently utilised as a competent catalyst for such reactions.[135][136] Following on from these successes, attempts to further functionalise the intermediate rhodacycle generated from initial cyclometallation with various amino precursors was explored. The first breakthroughs was reported independently in 2012 by Yu[137,138] and Glorius[139] then later by Zhou and Li[140] in 2013, who used chloramines as aminating reagents for C(sp^2)-H bonds. From rhodacycle intermediate **217**, C-Rh bond migration onto the electrophilic nitrogen centre with loss of a chloride leaving group is postulated to form the C-N bond in **218**. These three elegant methodologies demonstrate the generality of this strategy towards different directing group classes, however there remains need to replace the highly reactive and unstable chloramine partner with a more practical solution.



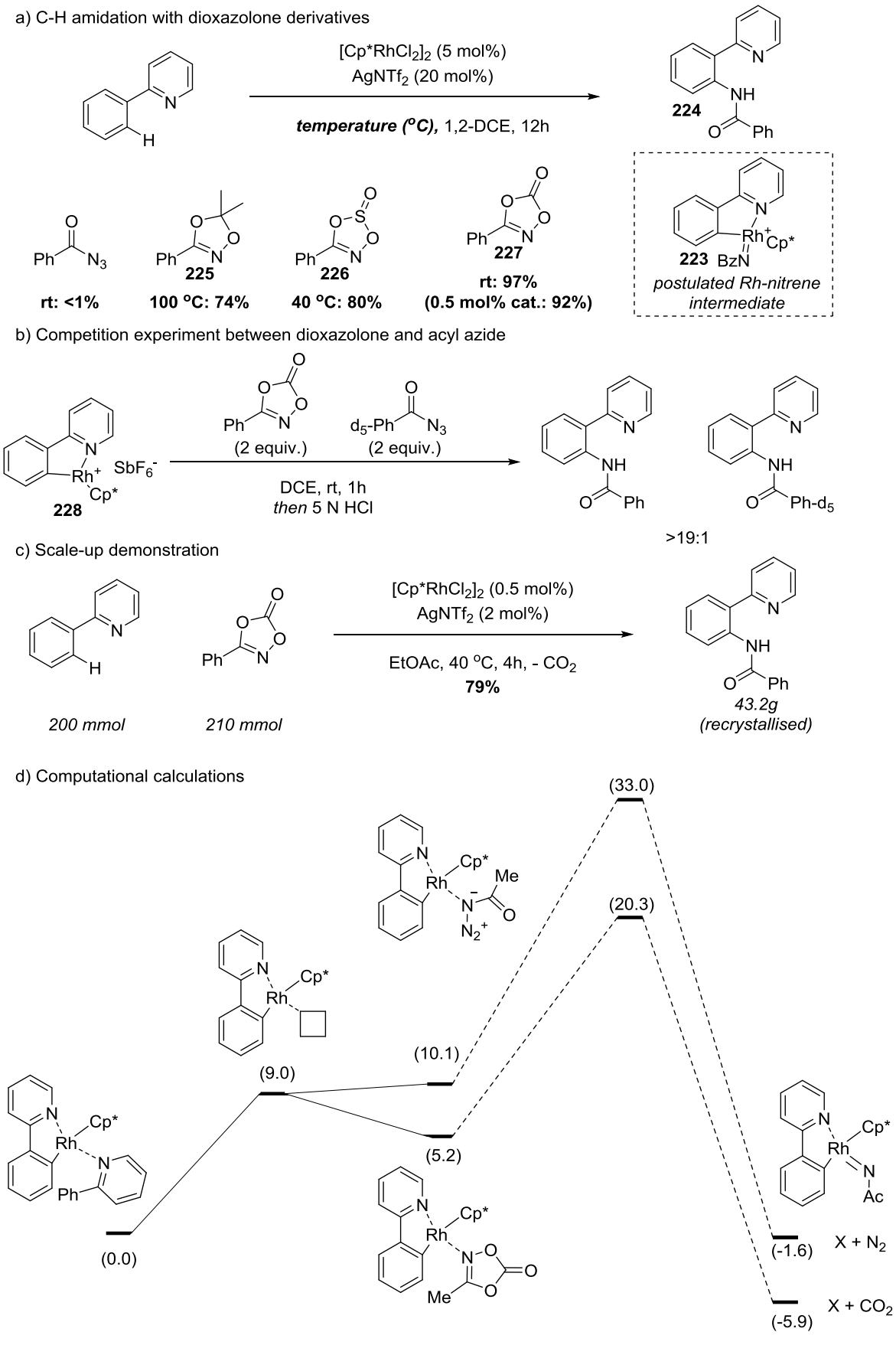
Scheme 40: Directed C-H amination using chloramine reagents.

Hydroxylamine derivatives present an alternative to chloramine electrophiles. Glorius first envisioned this and demonstrated *O*-(2,4,6-trichlorobenzoyl) hydroxylamine **219** as suitable for C-H amidation reactions (scheme 41a).[139] Using this reagent, a range of

different aromatic systems were activated to produce usefully protected aniline products (**220** and **221**). Xu and Yi later showed this electrophile was competent for the synthesis of a range of 2-aminoindole derivatives **222**.[141] Lu further demonstrated the robustness of this protocol by conducting the reaction in water (scheme 41b).[142] Interestingly, no carboxylate additive, usually needed to mediate initial CMD, was required for this reaction, and the authors postulate hydroxyl groups present in the water served as the base in this case. Wan and Li demonstrated sulfonylated hydroxylamines were also amenable to this C-H amidation protocol (scheme 41c).[143] Using *O*-tosyl protected *N*-phthalamidohydroxylamine, synthetically usefully protected aminopyridines were obtained in good yield.



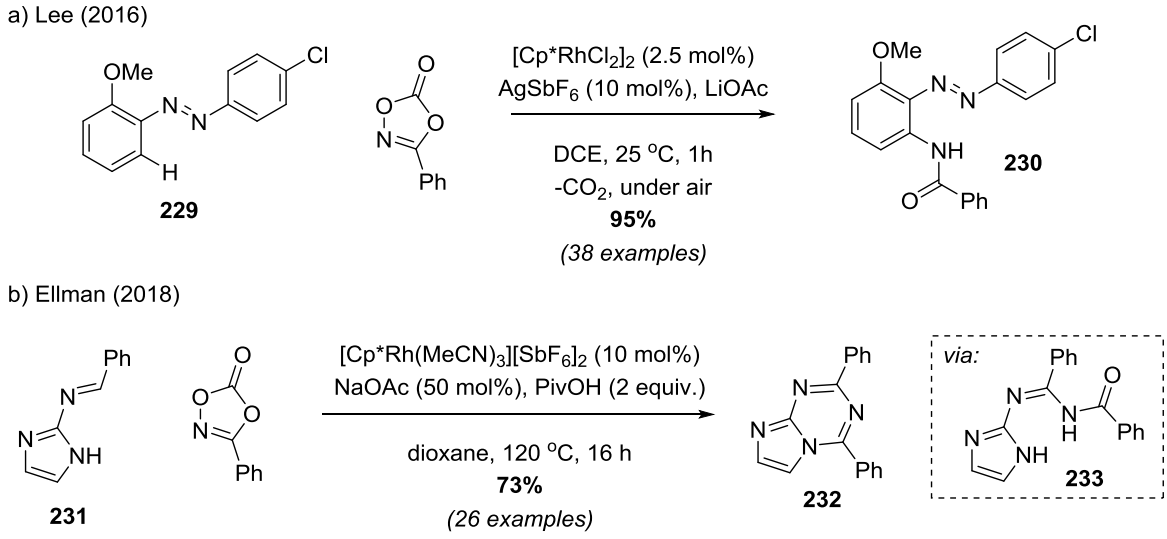
Scheme 41: Use of hydroxylamine derivatives as amidating reagents.



Scheme 42: Chang's seminal work on dioxazolone reagents for direct C-H amidation.

The practicality of *N*-oxo electrophilic amino reagents was further compounded with Chang's 2015 report of 1,2,5-dioxazolone reagents as suitable for C-H amidation reactions.[144] This class of cyclic amidating reagent has been known since 1968 to act as precursors to acyl nitrenes upon heating[145], thus acting as stable equivalents to previously employed acyl azides.[146] If the nitrene intermediate is not intercepted, then rearrangement to isocyanate occurs. However, Chang and co-workers were able to utilise the nitrene intermediate with the Cp*Rh catalyst system, leading to proposed intermediate **223** *en* route to amidated product **224**. A range of reagents **225, 226** and **227** were developed possessing different thermal stability and thus different reactivity profiles (scheme 42a). Chang compared them alongside benzoylazide for performance in the ortho-amidation reaction of 2-phenylpyridine and found phenyldioxazolone to be most efficient, affording a 92% isolated at room temperature with just 0.5 mol% rhodium catalyst loading. By preforming and isolating rhodacycle **228**, a competition experiment between phenyldioxazlone and perdeuterobenzoylazide was also performed, demonstrating reaction with the dioxazolone electrophile occurs more than 19 times faster (scheme 42b). Computational calculations on the two reactions was performed to try to rationalise the remarkable reaction rate displayed by the dioxazolone electrophile. These calculations showed that not only is binding of dioxazolone to the rhodacycle intermediate energetically preferred, but the transition state for nitrene formation is also significantly lower in energy. Furthermore, the formation of CO_2 compared with N_2 with regards to the two leaving groups is also more thermodynamically favoured. All these factors allow dioxazolones to be a powerful amidating tool in the context of C-H functionalisation, and Chang later demonstrated this with a 200 mmol scale up of the reaction (scheme 42c).[147] Utilising the dioxazolone reagent, the catalyst loading could be

lowered to 0.5 mol%, ethyl acetate could be used as solvent and with the reaction performed at a mild temperature of 40 °C with only a small excess of amidating reagent, this reaction demonstrates notably high sustainability, scalability and efficiency for metal catalysed C-H functionalisation reaction.



Scheme 43: Use of dioxazolone reagents in Rh^{III} catalysed C-H amidation reactions.

Since this discovery, dioxazolones have emerged as a champion for C-H amidation, with numerous literature reports of its use in combination with Rh, Ir and Co catalysis for C-H bond functionalisation. Shortly after Chang's seminal publication using dioxazolones for the C-H amidation of 2-phenylpyridine, Lee was able to apply this reaction only azobenzene substrates (scheme 43a).[148] Using precatalyst $[Cp^*RhCl_2]_2$ at 2.5 mol% loading, azobenzene **229** was selectively mono-amidated to give **230** in remarkable yield at room temperature in just one hour. A combination of steric and electronic factors was found to be important for governing which phenyl ring is transformed. Prescence of the electron withdrawing chloro-group was found to supress reactivity and so selective amidation of the other phenyl ring occurs. Recently, Ellman reported a C(sp^2)-H amidation / condensation cascade of imine **231** with dioxazolone reagents to give azolotriazine **232** proceeding through amidated intermediate **233** (scheme 43b).[149]

4.3 Introduction to Rh^{III} catalysed $C(sp^3)$-H Functionalisation

With the area of Rh catalysed $C(sp^2)$-H functionalisation well-explored over the past decade, extension to the more challenging $C(sp^3)$-H is an attractive but difficult synthetic proposition which remains still largely unrealised. Three major challenges exist for $C(sp^3)$-H bonds which are not present with sp^2 cases[150]:

a) High C-H bond strength creates large kinetic barrier to reactivity

b) Increased steric crowding around $C(sp^3)$-H bonds

c) Low reactivity/high stability of the resultant rhodacycle C(alkyl)-Rh species.

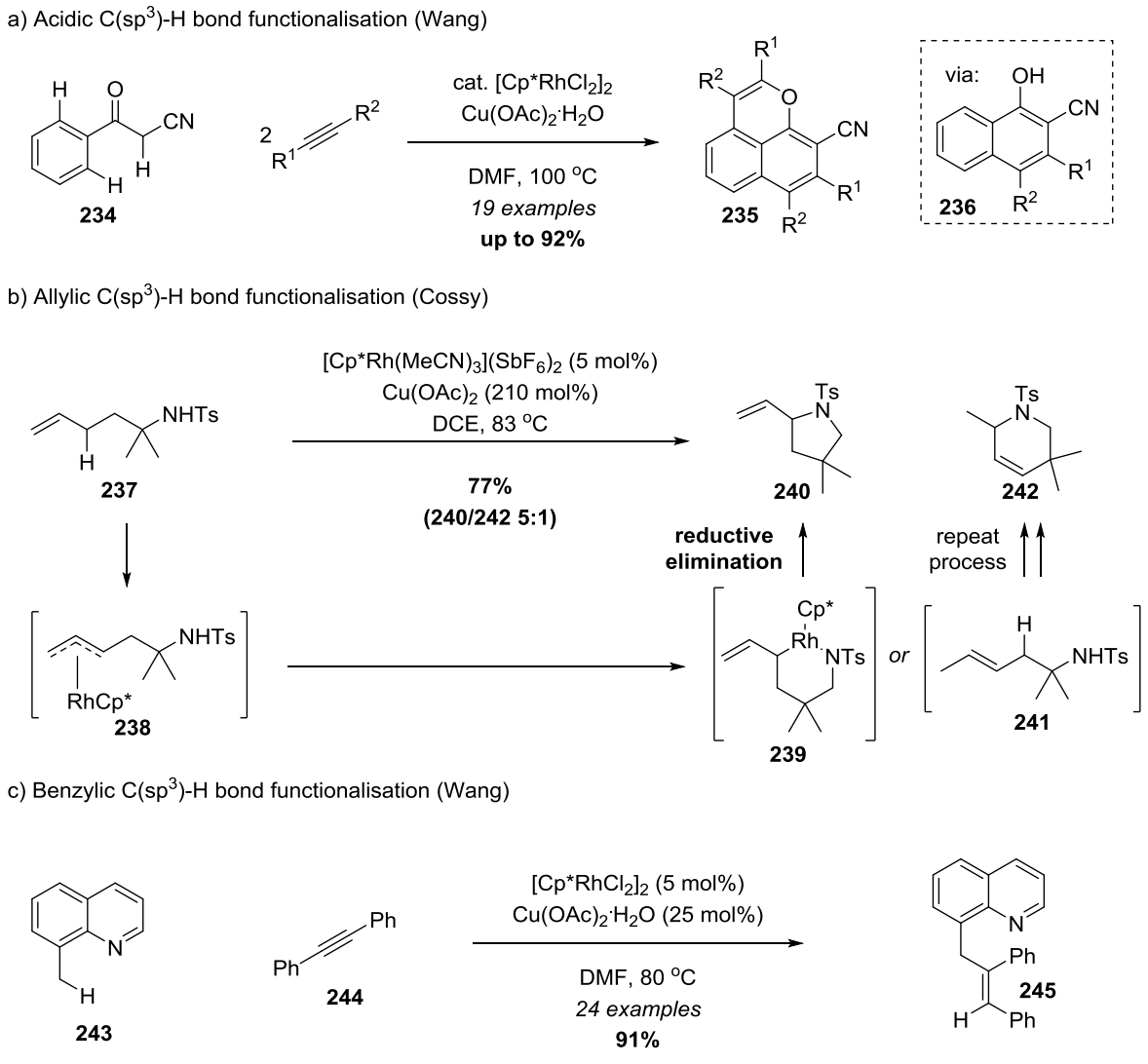
In order to overcome these challenges, researchers have used lessons learnt from palladium catalysis to develop novel transformations. One such strategy is to target activated, allylic or benzylic C-H bonds which are more acidic in comparison to unactivated alkyl C-H bonds. Higher acidity of the C-H bond translates to easier metallation by a suitable Rh^{III} catalyst, and comparing acidity values helps to rationalise the reactivity trends within bonds of a similar type (table 10).[151,152]

C-H Bond	pKa (H_2O)	Bond type
$(CH_3)_3CH$	53	t-butyl
H_3C-H	48	methyl
C_3H_5-H	46	cyclopropyl
CH_2CHCH_2-H	43	allylic
$C_6H_5CH_2$-H	41	benzylic
$EtC(=O)(CH_2$-H$)CH_3$	19	α-ketone

Table 10: pK_a values for a range of alkyl carbon-acids.

Benzylic, allylic and cyclopropyl C-H bonds are significantly more reactive than their unactivated alkyl counterparts. Wang and co-workers report activation of low pK_a β-ketonitrile C-H bonds in a double oxidative annulation of **234** with acetylenes to give

substituted napthopyran derivatives **235** through a triple C-H bond activation cascade (scheme 44a).[153] The reaction proceeds through initial metallation of the most acidic α-nitrile C-H bond and subsequent oxidative annulation to give intermediate **236**. A second



Scheme 44: Functionalisation of activated C(sp^3)-H bonds.

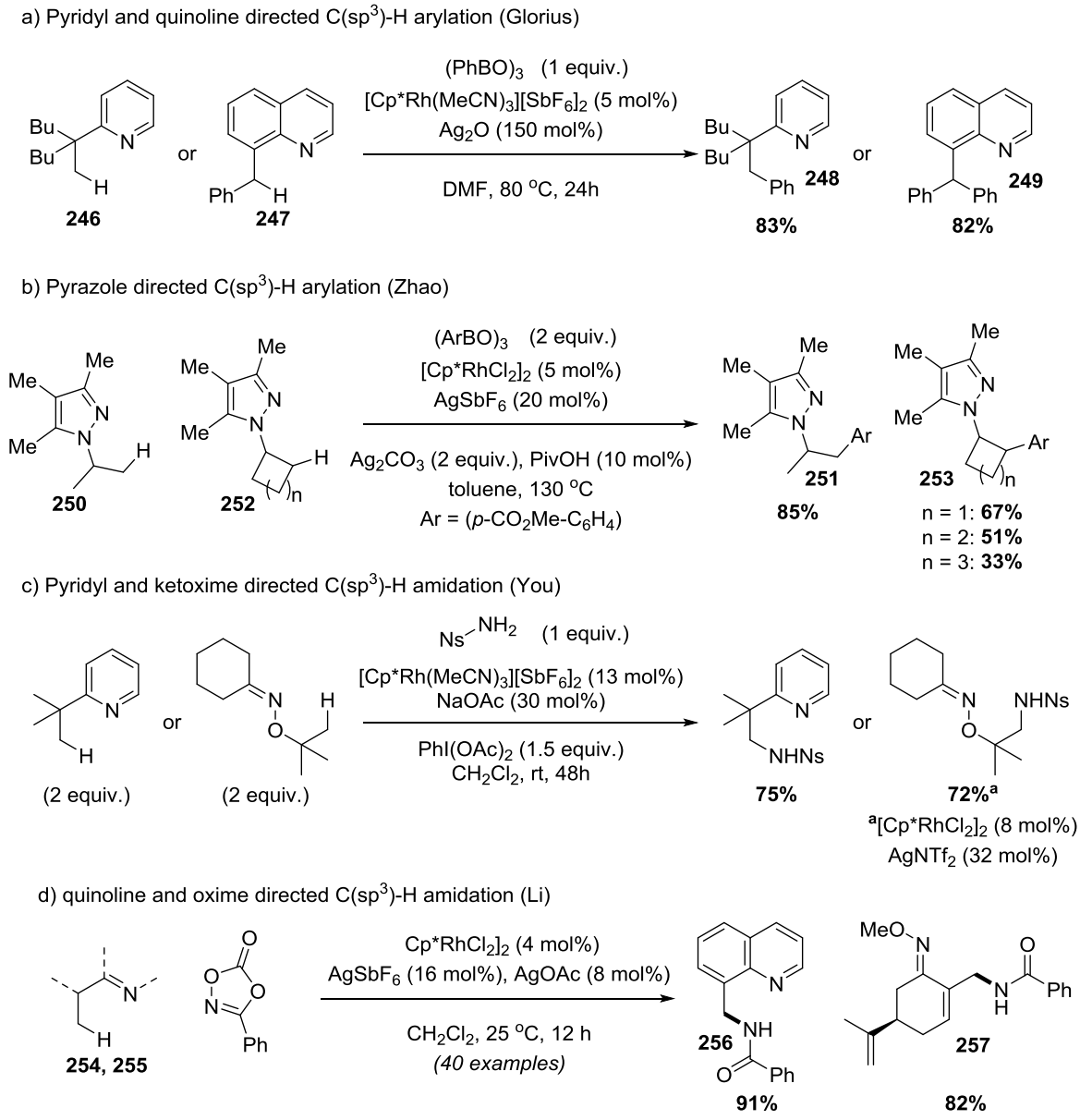
C-H metallation and oxidative annulation then delivered the final product in up to 92% yield. Allylic C(sp^3)-H bonds can also be functionalised as demonstrated by Cossy and co-workers.[154] When olefin bearing tosylamide **237** was treated with $[Cp^*Rh(MeCN)_3](SbF_6)_2$ and, metallation of the allylic C-H bond occurred to give allyl-rhodium intermediate **238**. Following this, *N*-metallation and reductive elimination from

239 afforded pyrrolidine **240**, the major product of the reaction. An alternative pathway could also occur where Rh-catalysed migration of the terminal olefin to the more thermodynamically favoured internal olefin **241** occurred, followed by a repeat of the same reaction mechanism to deliver piperidine **242**. Benzylic C-H bond functionalisation is exemplified by Wang and co-workers' 2014 report (scheme 44c).[155] The benzylic C-H bond of 8-methylquinoline **243**, a privileged substrate for C(sp^3)-H functionalisation[156], was functionalised with acetylene electrophiles such a diphenylacetylene **244** leading to a olefinated product **245**.

4.4 Directing Group-Enabled Functionalisation of Unactivated C(sp^3)-H Bonds

Extension to unactivated C(sp^3)-H bonds is a largely underexplored area of study with only limited examples present within the context of Rh^{III} catalysis. In order to activate a largely unreactive C-H bond, a suitable directing group must be selected. Traditionally, a strongly binding directing group is utilised, leading to a thermodynamically more favourable substrate-catalyst complex and subsequently a more stabilised cyclometallated intermediate. This strategy ensures the C-H functionalisation step can occur, however due to high stability of the cyclometallated intermediate, a larger kinetic barrier must be overcome in the subsequent C-metal bond functionalisation step.[150] Therefore, systems containing a suitably strong-binding directing group must be selected to enable activation of the unreactive C-H bond and allow functionalisation of the intermediate cyclometallated species. Following on from successes in C(sp^2)-H functionalisation, Glorius in his seminal 2015 paper reported the first example of Rh^{III} catalysed functionalisation of unactivated C(sp^3)-H bonds(scheme 45a).[157] Enabled by traditionally used strong-binding pyridyl and quinolyl functionality as directing groups (**246** and **247**), a range of methyl and

methylene C-H bonds were arylated to give the corresponding products (**248** and **249**) in good yield. In order to avoid double arylation, substrates were selected that possessed just one reactive methyl group or methylene C-H bond. Although this choice of substrate naturally limits the scope of the reaction and reduces the practicality of the method, this seminal report provides and important proof of concept for Rh^{III} catalysis applied to unreactive C(sp^3)-H bonds.



Scheme 45: Rh^{III} catalysed functionalisation of unactivated C(sp^3)-H bonds

Later, Zhao and co-workers reported a method to selectively deliver mono-arylated products in the presence of multiple reactive methyl C(sp^3)-H bonds (scheme 45b).[158] Utilising a trimethylpyrazole directing group, a range of β and γ methyl C(sp^3)-H bonds (**250**) were functionalised to give arylated products (**251**) in high yields. The use of this novel directing group also enabled the functionalisation of cyclic methylene C(sp^3)-H bonds and cyclobutyl, propyl and hexyl bearing substrates **252** were successfully transformed to afford arylated products **253** in good yields.

Within the context of C-N bond formation, You reported in his 2015 seminal paper the first Rh^{III} catalysed amidation of unactivated C(sp^3)-H bonds using pyridyl and oxime functionality as a directing group.[159] The combination of nosylamide and iodobenzene diacetate likely generates a nitrene precursor which is able to amidate the *in situ* generated cyclometallated C(sp^3)-Rh bond. Since nosylamide is utilised as the limiting reagent, the reaction yield with respect to the pyridyl starting material is relatively low and high catalyst loadings of >10 mol% are generally required. Despite these issues, this seminal report demonstrated the feasibility for Rh^{III} as a potential alternative to palladium in the activation of unreactive C-H bonds.

Soon afterward, Li reported the second example of Rh^{III} amidation of such unactivated C(sp^3)-H bonds.[160] Although both You and Li report C-H amidation of similar substrates, You was able demonstrate proof of concept for a difficult transformation whereas Li solved many of the practical problems with this reaction, enabling the highly efficient C(sp^3)-H amidation of both 8-methylquinoline **254** and a variety of ketoximes such as **255** with dioxazolone reagents, delivering amidated products **256** and **257** in high yield. The practicality of the dioxazolone reagents as described in section 4.3 is strongly evident

through the high yields, low catalyst loadings, extremely mild reaction conditions and absence of an external oxidant traditionally required for this transformation.

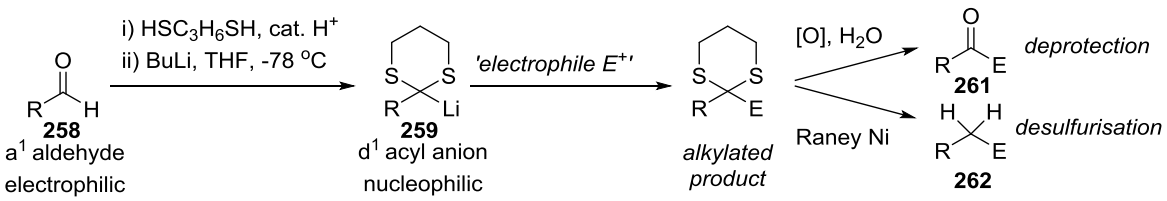
4.5 Concluding Remarks

Work in the past decade has established Rh^{III} catalysis within the field of C-H functionalisation alongside well known palladium and ruthenium catalyst systems. With emphasis on Cp*Rh catalysts, this privileged catalyst class has led to numerous discoveries within the context of $C(sp^2)$-H functionalisation, enabling a plethora of different transformations including arylation, amidation, halogenation and alkenylation amongst others. Recent work has also greatly advanced the field of $C(sp^3)$-H bond activation and chemists are now able to manipulate unreactive remote $C(sp^3)$-H bonds to effect C-C and C-N bond forming reactions. To enable these transformations, traditional directing groups such as pyridyl or oxime derivatives are employed, however these groups are typically integral structural elements of the molecule and are difficult to install/cleave or do not enable any useful downstream synthetic transformations. Therefore, an unsolved challenge is the development of new directing groups which can be easily installed/cleaved and enable new useful synthetic downstream functionalisation of the resultant products. To this end, work in this thesis focuses on this synthetic challenge and proposes dithianes as a solution to the problem.

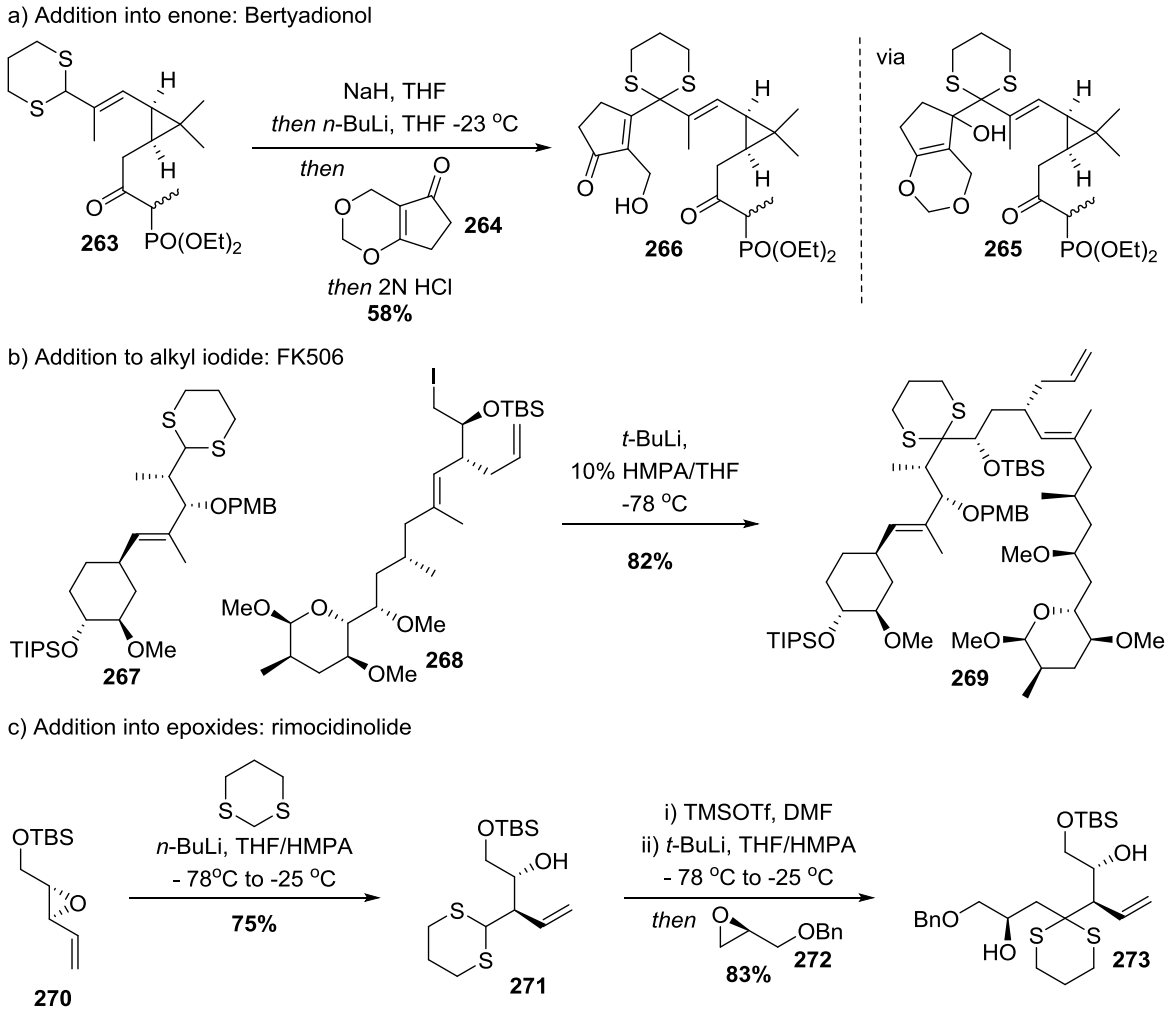
Chapter 5: Dithiane Directed Rh^{III} Catalysed Amidation of Unactivated C(sp^3)-H Bonds

5.1 Introduction to Dithianes: Corey-Seebach Reaction

Dithianes are highly versatile and common building blocks in synthesis. Not only are they able to act as masked carbonyl or methylene surrogates,[161] but their unique reactivity as *umpolung* C1 acyl anion synthons has led to their widespread use in complex target synthesis.[162,163] Pioneered by Corey and Seebach, the lithium anion *umpolung* reactivity of dithianes enables the transformation of a^1 aldehyde synthons into d^1 acyl nucleophiles able to react with a wide range of different electrophiles.[164–166] Aldehydes **258** can be converted to the corresponding dithiane by heating in the presence of propane dithiol under acid or Lewis acid catalysis. This protection is generally extremely efficient and clean, affording dithiane products in high yields and often without the need for further purification. Deprotonation of the resultant dithiane gives lithium anion **259**, poised for reaction with diverse electrophiles to give alkylated product **260**. With the dithiane having served its purpose, two common downstream cleavage reactions are deprotection to the corresponding ketone **261** (which can be mediated through metal catalysis or oxidative conditions), or reductive desulfurisation, often with Raney nickel, to reveal a methylene unit **262**.[161] Since the discovery of this reaction, numerous research groups have incorporated it as an enabling disconnection towards synthesis of complex molecules.



Scheme 46: The Corey-Seebach *umpolung* reaction of dithianes.



Scheme 47: Smith's application of dithianes in total synthesis.

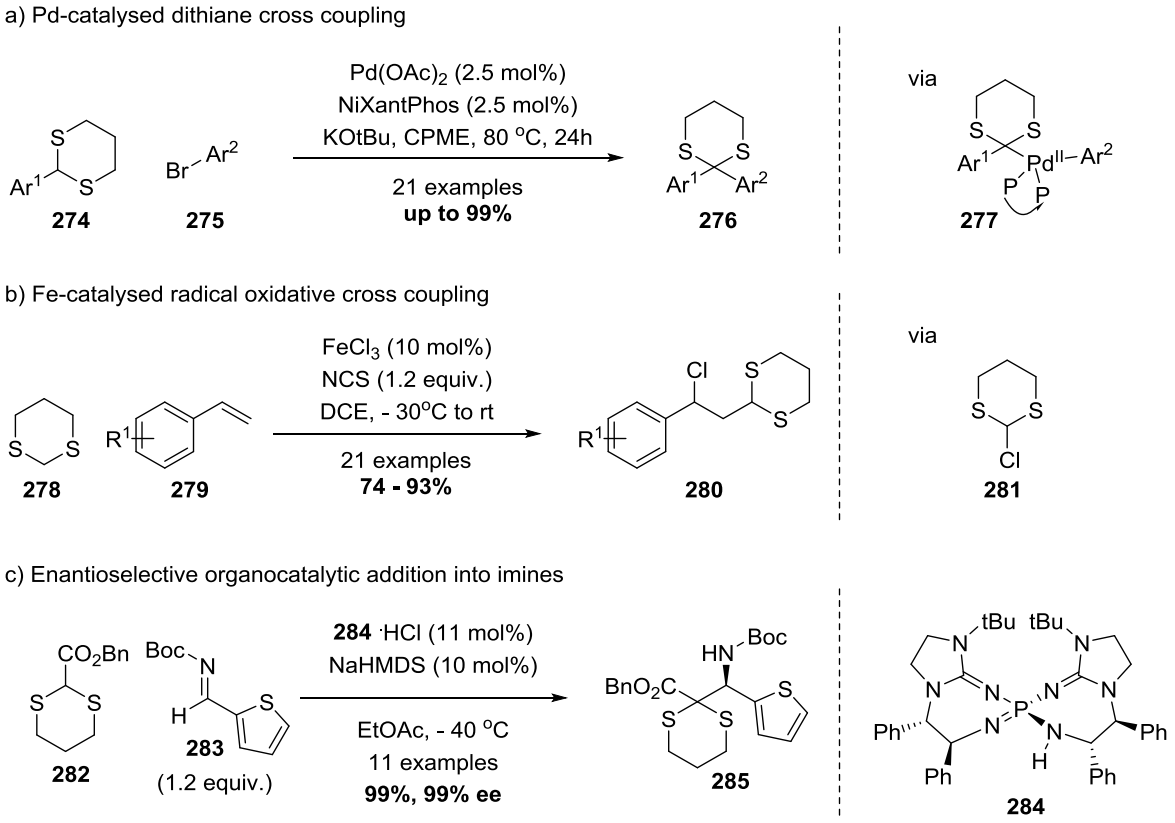
Though many chemists have utilised dithianes, Smith in particular has championed the Corey-Seebach *umpolung* reaction and has found numerous applications within the stage of total synthesis. He has commonly used complex dithiane fragments and added the lithium anion into different electrophile partners as a key C-C bond forming step in his syntheses. In his synthesis of bertyadionol (scheme 47a), initial generation of the sodium enolate of β-ketophosphonate bearing dithiane **263** was followed by deprotonation with *n*-BuLi to give the reactive dianion intermediate.[167] Selective addition of this mixed anion into enone **264** gave *umpolung* addition product **265**, which after subsequent acidic work up rearranged to the final product **266** in 58% yield.

In his synthesis of FK506**,** Smith also demonstrated alkyl iodides were suitable electrophiles for the alkylation of dithianes (scheme 47b).[168] Generation of the lithium anion of complex dithiane fragment **267** followed by quenching with iodide fragment **268** led to the alkylated product **269** in high yield. Utilising this remarkably efficient method, Smith was able to unite two complex fragments in a key C-C bond forming step whilst maintaining a carbonyl unit required in the final natural product.

One final demonstration and testament to the power of the Corey-Seebach reaction in polyketide synthesis is Smith's construction of a late stage fragment towards rimocidinolide.[169] In fact, the dithiane *umpolung* addition into an epoxide functionality is used a total of 6 times throughout the synthesis and a sample of this strategy is shown in scheme 47c. Epoxide **270** was opened at the allylic position by the lithium anion of dithiane to **271** in high yield. TBS protection of the resultant secondary alcohol, generation of the dithiane lithium anion followed by trapping with epoxide **272** afforded alcohol **273** in 83% yield. This addition into epoxides led to suitably protected β-hydroxyketone derivatives and provided a useful alternative to the aldol reaction.

5.2 New Synthetic Applications of Dithianes

Given the prevalence of dithianes and their unique reactivity in the Corey-Seebach reaction, discovery of new applications for this versatile functional group has been the focus of much interest in the past decade. Most examples involve functionalisation of the acidic dithiane C-H bond and metal catalysed cross coupling using dithianes as the nucleophilic partner is one such alternative to classic lithium anion chemistry.



Scheme 48: Alternative applications of dithianes.

The first cross coupling reaction of dithianes was reduced to practice in Schmink's seminal 2014 paper (scheme 48a),[170] although the group of Walsh independently reported a similar reaction shortly afterward.[171] In Schmink's work, a range of benzylic dithianes **274** were coupled with aromatic bromides **275** to give a range of benzophenone products **276** in excellent yield. The authors proposed deprotonation/metallation of the acidic dithiane C-H bond by Pd^{II} led to **277**, a key intermediate in the catalytic cycle. With a pK_a of around 30 in DMSO,[172] use of potassium tert-butoxide alone is insufficient to deprotonate the dithiane substrate. The authors propose strong binding of Pd to the sulfur centre activates the C-H bond and enables deprotonation/metallation to occur.

Dithianes are also compatible in radical cross coupling processes. Tang demonstrated this by coupling dithiane **278** with a range of terminal styrenes **279** to deliver β-

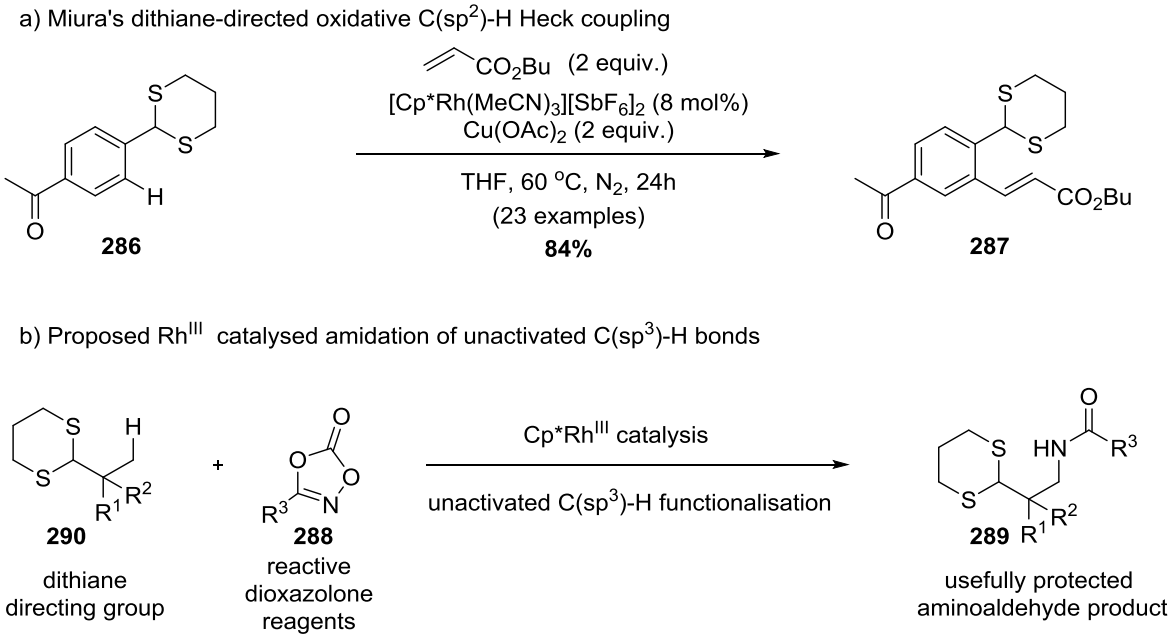
chlorodithianes **280** as the final product (scheme 48b).[173] The mechanism was proposed to proceed through initial *N*-chlorosuccinimide mediated chlorination of dithiane to give chlorodithiane **281**. Subsequent iron catalysed atom transfer radical addition to the styrene double bond led to the final product.

A final example of new methodology developed around the dithiane functional group is Terada's elegant and highly enantioselective organocatalysed addition of dithianeester **282** into aromatic Boc-imines (scheme 48c).[174] With thiophene-derived imine **283** as an example, deprotonation by chiral phosphazene-superbase organocatalyst **284** and subsequent Mannich reaction delivers the product **285** in near perfect yield and enantioselectivity. Not only does the dithiane help to acidify the reacting C-H bond for deprotonation, but the postulated confined steric bulk of the 6-membered ring is believed to help in the creation of an organised transition state allowing for exquisite enantioselectivities over a range of substrates.

5.3 Dithiane-directed C-H Functionalisation

Given the strong Lewis basicity of sulfur, the synthetic versatility of dithianes and the unique reactivity they possess, along with the ease of installation and downstream cleavage/functionalisation, dithianes possess all the properties desirable for a directing group in metal-catalysed direct C-H functionalisation reactions. Therefore, we decided to investigate dithiane functionality as a potential directing group for C-H activation of unreactive C(sp^3)-H bonds. Dithianes have only been used once in catalytic C-H bond activation by Miura, enabling *ortho* oxidative C-H alkenylation with electron deficient olefins.[175] Catalysed by $[Cp^*Rh(MeCN)_3][SbF_6]_2$ with copper acetate as oxidant, a range of benzylic dithianes could be coupled with butylacrylate to deliver the alkenylated

products (scheme 49). As an example substrate, ketone bearing dithiane **286** was well-tolerated in the reaction and could be converted to alkenylated product **287** in 84% yield.

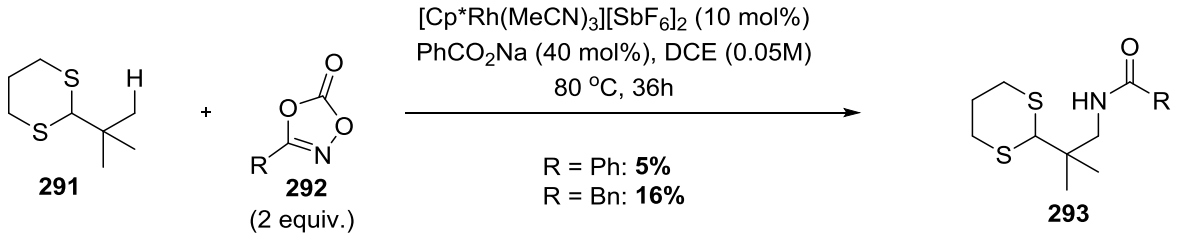


Scheme 49: a) Dithiane directed oxidative *ortho*-C(sp^2)-H alkenylation. b) Proposed functionalisation of unactivated C(sp^3)-H bonds.

Dithiane directed activation of remote C(sp^3)-H would be an attractive method for the synthesis of β-substituted aldehyde derivatives and therefore represent a powerful advancement, expanding the utility of this useful functional group and enabling access of sp^3-rich scaffolds and building blocks bearing a useful *umpolung* acyl anion equivalent. We propose to utilise the bench stable yet highly reactive dioxazolone reagents **288** to mediate amidation of C(sp^3)-H bonds and enable access to usefully protected 1,3 aminoaldehyde derivatives **289** from simple dithiane starting materials (**290**, scheme 49b). To this end, the extensive investigations into this proposal are described subsequently in this thesis, leading to the development of a novel amidation methodology.

5.4 Development of Optimised C(sp^3)-H Amidation Conditions

We began our investigations by evaluating Cp*Rh^{III} catalysis applied to pivaldehyde derived dithiane **291** and phenyl dioxazolone **292** as model substrates. Pleasingly, in the very first reaction, with the use of 10 mol% $[Cp^*Rh(MeCN)_3][SbF_6]$ with sodium benzoate as additive in dichloroethane at 80 °C led to the formation of amidodithiane **293** in ~5% yield. After evaluation of several dioxazolone reagents, substitution for benzyl derived dioxazolone **294** improved this result to 16%. Remarkably, the reaction profile was extremely clean with starting material conversion reflecting product yield and no bis-amidation was observed despite the presence of 3 potentially reactive methyl groups. Encouraged by these lead results establishing proof of concept, extensive optimisation studies were then performed.



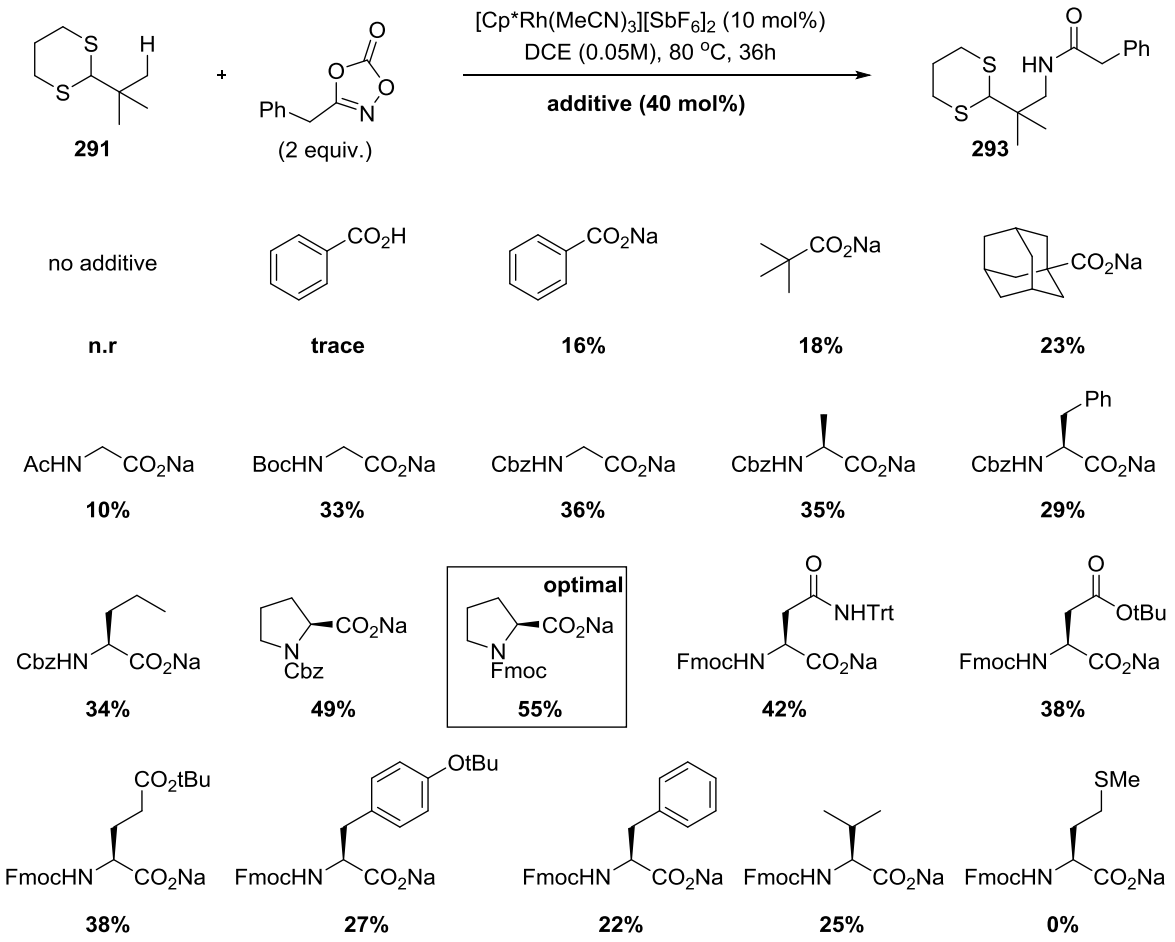
Scheme 50: Lead results establishing proof of concept.

Initially, evaluation of different solvents was performed, with dichloroethane being critical for this reaction. Toluene, dioxane, tetrahydrofuran and surprisingly chloroform led to complete suppression of reactivity. DCE is a popular solvent choice for C-H activation reactions, and often it is difficult to find a replacement with similar performance.[176]

Next, attention turned to the carboxylic acid salt additive in the reaction. This salt has the critical function of acting as a base during the concerted metallation deprotonation C-H

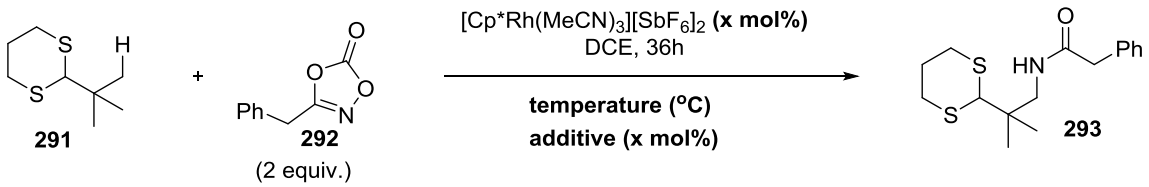
activation step, as well as acting as a ligand for rhodium after dissociation of the three acetonitrile ligands in the precatalyst (scheme 51). In the absence of a carboxylate additive, no reaction was observed and use benzoic acid led to trace conversion to the amidated product. For ease of handling, the carboxylic acid salts were generated *in situ* by addition 40 mol% of the corresponding acid with equimolar sodium *tert*-butoxide to generate the sodium anion. Initially, sterically bulky sodium pivalate and adamantylcarboxylate, which are commonly employed in C-H activation, were evaluated leading to slight improvement of yield to 18% and 23% respectively. Accordingly, we turned to amino acid derived additives as potential additives for this reaction. Amino acids have been used previously in C-H activation methodology, and often have the dual purpose of acting as a ligand for the metal centre in conjunction with acting as a base to

mediate CMD.[177–179]



Scheme 51: Identification of Fmoc-Pro-ONa as the optimal carboxylic acid salt additive.

Initial evaluation of differentially N-protected sodium glycinates identified carbamate protecting groups as the best. Continued screening around Cbz protected amino acids identified Cbz protected cyclic prolinate which delivered an improved yield of 49%. Pleasingly after alterations to the N-protecting group, Fmoc-Pro-ONa was identified as the best additive to date, delivering amidodithiane product **293** in 55% yield. Further extensive screening of varied structures around the Fmoc-amino acid family was unable to identify a more effective additive; accordingly, Fmoc-Pro-ONa was selected as the optimal additive and taken forward for further optimisation studies.



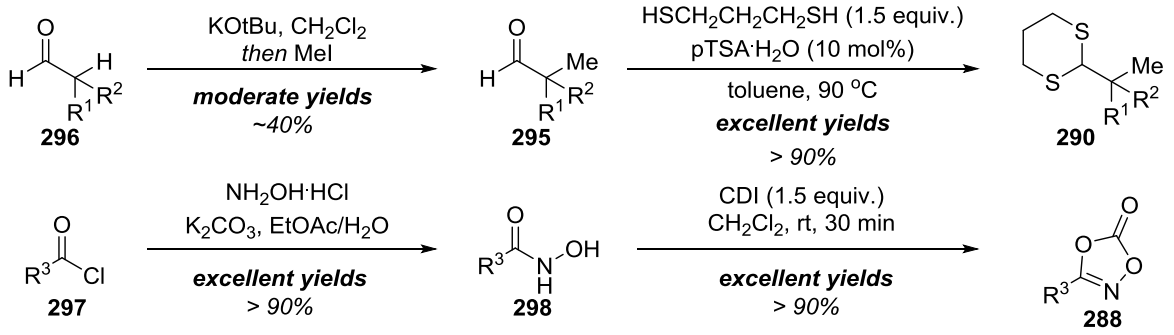
Entry	additive (x mol%)	temperature (°C)	cat. loading (x mol%)	yield (%)
1	Fmoc-Pro-ONa (40)	80	10	55
2	Fmoc-Pro-ONa (30)	80	10	62
3	Fmoc-Pro-ONa (20)	80	10	57
4	Fmoc-Pro-OLi (30)	80	10	0
5	Fmoc-Pro-OK (30)	80	10	0
6	Fmoc-Pro-OAg (30)	80	10	0
7	$(Fmoc\text{-}Pro\text{-}O)_2Zn$ (30)	80	10	0
8	Fmoc-Pro-ONa (30)	90	10	47
9	Fmoc-Pro-ONa (30)	70	10	45
10	Fmoc-Pro-ONa (30)	80	15	73 (71)

Table 11: Development and identification of optimised reaction conditions.

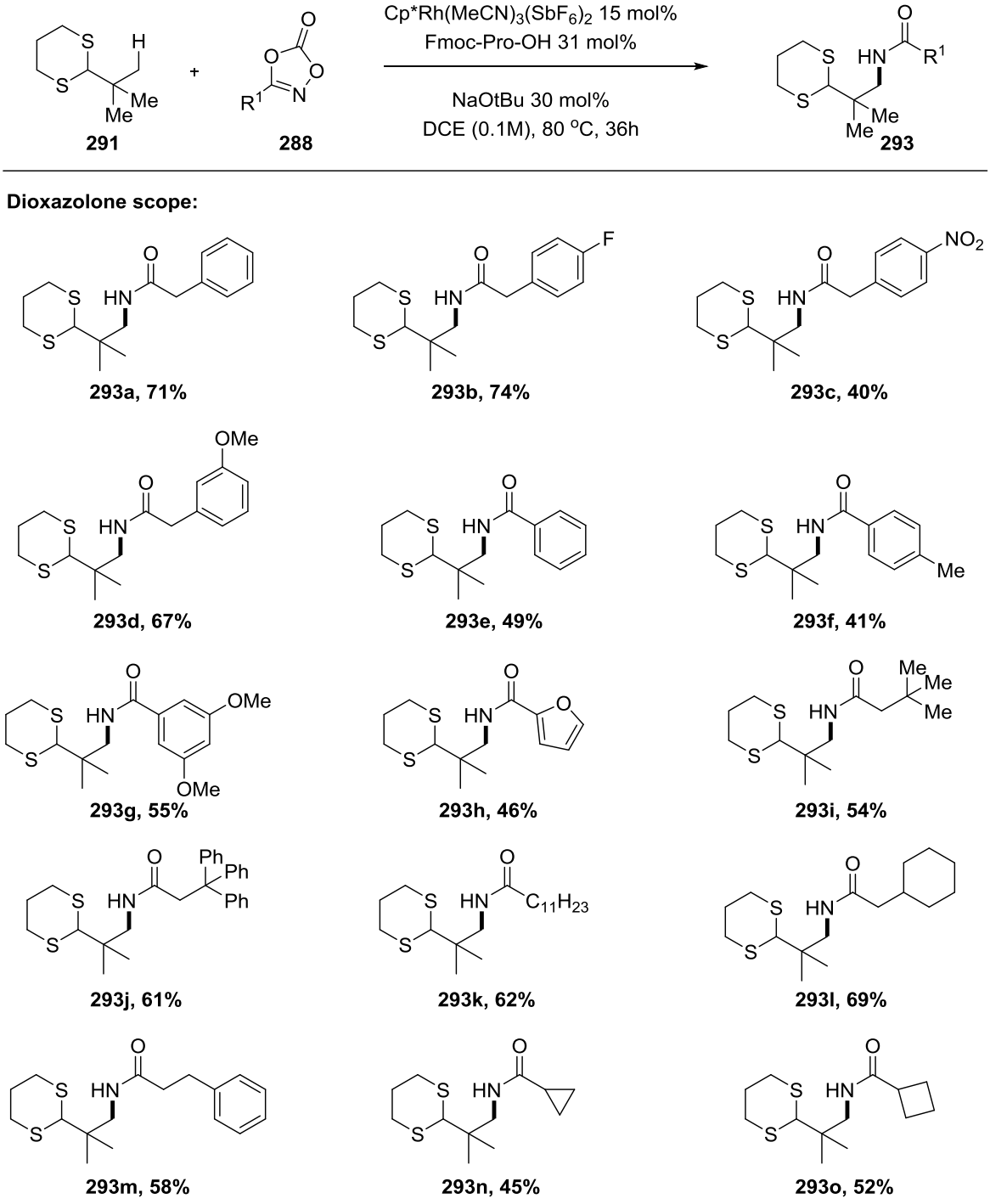
Studies found 30 mol% additive to be optimal, the yield decreasing slightly when 20 or 40 mol% Fmoc-Pro-ONa was used (table 11, entries 1-3). Interestingly, sodium as the cationic counterion to the carboxylate additive was critical for reactivity in this reaction (table 11, entries 4-7). Exchange for potassium, lithium, silver and zinc salts resulted in no reactivity whatsoever. Although in other C-H activation methodologies alternative metal counterions are well tolerated, in this case the highly Lewis basic sulfur atoms may easily chelate strongly binding metal counterions such as zinc, silver and lithium and hinder reactivity. Temperature variations of 10 degrees either side of 80 °C were also made, with decrease to the yield observed in each case. Finally, after extensive optimisation studies, the catalyst loading was increased from 10 to 15 mol%, and using these optimised conditions, an isolated yield of 71% for amidated dithiane **293** was delivered.

5.5 Substrate Scope

With optimised reaction conditions in hand, the scope of the reaction was investigated. To achieve this, a range of differentially substituted dithiane starting materials and dioxazolone reagents were synthesized. For dithianes where the corresponding α-methyl aldehyde **295** was commercially unavailable, it was synthesized from **296** via α-deprotonation with potassium tert-butoxide and quench with methyl iodide. Subsequent treatment with propanedithiol under acid catalysis in hot toluene delivered the dithianes **290** in excellent yield. To access dioxazolone reagents, the corresponding acyl chloride **297** was amidated with hydroxylamine under Schotten-Baumann conditions to give hydroxamic acid **298**. Subsequent treatment with carbonyldiimidazole delivered the dioxazolone reagent **288** in excellent yields over the two-step process.



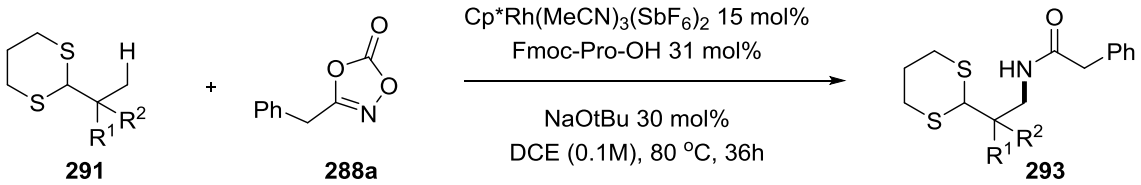
Scheme 52: Synthesis of starting materials.



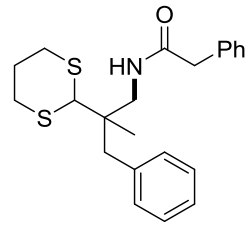
Scheme 53: Substrate scope with respect to dioxazolone amidating partner.

Pleasingly, the reaction was tolerant of a range of dioxazolone reagents **288**. Fluoro, nitro and methoxy substitution on aryl ring of benzyl substituted dioxazolones (**293b-d**) was well tolerated, delivering amidated products in 74, 40 and 67% yield respectively. Aromatic dioxazolones were also compatible, although provided only moderate to good

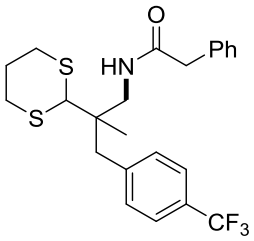
yields, of phenyl, tolyl, bis-*meta*-methoxyphenyl and furyl bearing amidodithianes **293e-h**. This reduced yield of product is likely due to increased steric bulk around the reaction centre compared with benzyl substituted dioxazolones. Alkyl-substituted dioxazolones were also evaluated and found to be well tolerated (**293i-m**). Finally, strained cyclopropyl and cyclobutyl rings could be introduced in 45% and 52% yield respectively without further activation of the reactive methylene C-H bonds (**293n**, **o**). Cyclopropanes and cyclobutanes are medicinal chemistry relevant, and their introduction is attractive for building block synthesis within this industry.[180]



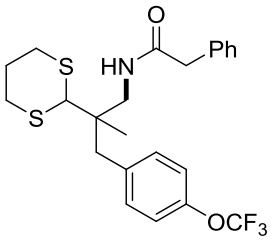
Dithiane scope:



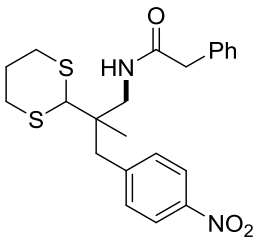
293p, 47%



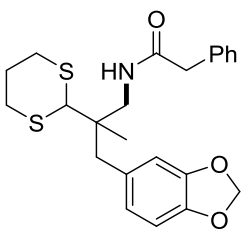
293q, 51%



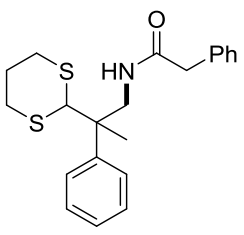
293r, 49%



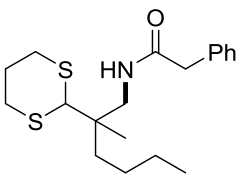
293s, 55%



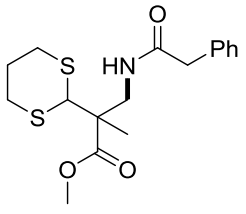
293t, 50%



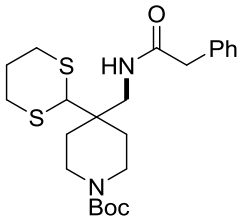
293u, 36%



293v, 56%



293w, 47%



293x, 53%

Scheme 54: Substrate scope with respect to dithiane starting material.

With benzyl dioxazolone **288a** as the amidating reagent, the scope with respect to the dithiane partner was also found to be broad. Pleasingly, phenyl bearing dithiane **293p** could be synthesised in 47% yield. *Para*-trifluoromethyl, trifluoromethoxy substitution on this phenyl ring was well tolerated, giving good yields of the amidated products (**293p**-**q**). The reaction was also tolerant of electron deficient *para*-nitro substituted dithiane **293s** as well as electron rich benzodioxole bearing dithiane **293t**. With these benzyl-substituted dithianes, a greater steric bulk is introduced around the reacting C-H bond, and so a generally lower yield was achieved when compared with pivaldehyde-derived dithiane. Direct phenyl substitution at the α-carbon centre could also be accommodated in the reaction, though a decrease in yield to 36% was observed due to further increased steric hinderance of the proximal aromatic ring. Extension of the alkyl chain to a 4-carbon subunit displayed a 56% yield for the corresponding amidodithiane product **293v**. Pleasingly, ester-bearing dithiane could be activated and a 47% yield of **293w** was isolated, displaying notable functional group tolerance for this methodology. Finally *N*-Boc piperidine derived dithiane could be transformed in 53% yield, delivering amidodithiane **293x**.

With the use of prochiral dithiane substrates, we were conscious that the chiral amino acid additive used in the reaction could lead to enantioenriched products. To verify this proposal, the enantiomers of **293p** were separated by chiral HPLC. The enantiomeric excess of the reaction was found to be 0% and the product was formed as totally racemic. To enable an enantioselective C-H activation, further studies into alternative additives and chiral ligands would be needed and investigations into this concept were beyond the scope and timeframes of this thesis.

5.6 Substrate Control Experiments

In order to further understand the capabilities and limitations of this methodology, a series of modified substrates **299** were synthesised and tested in the amidation reaction (figure 12).

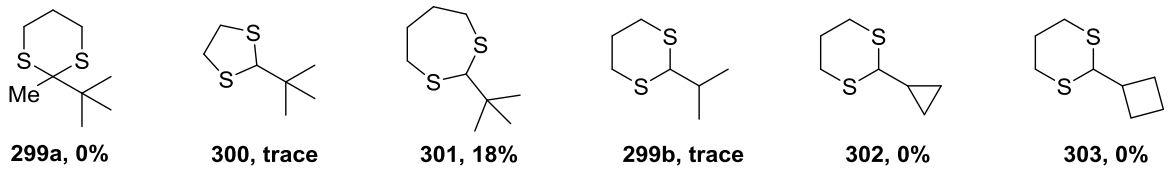
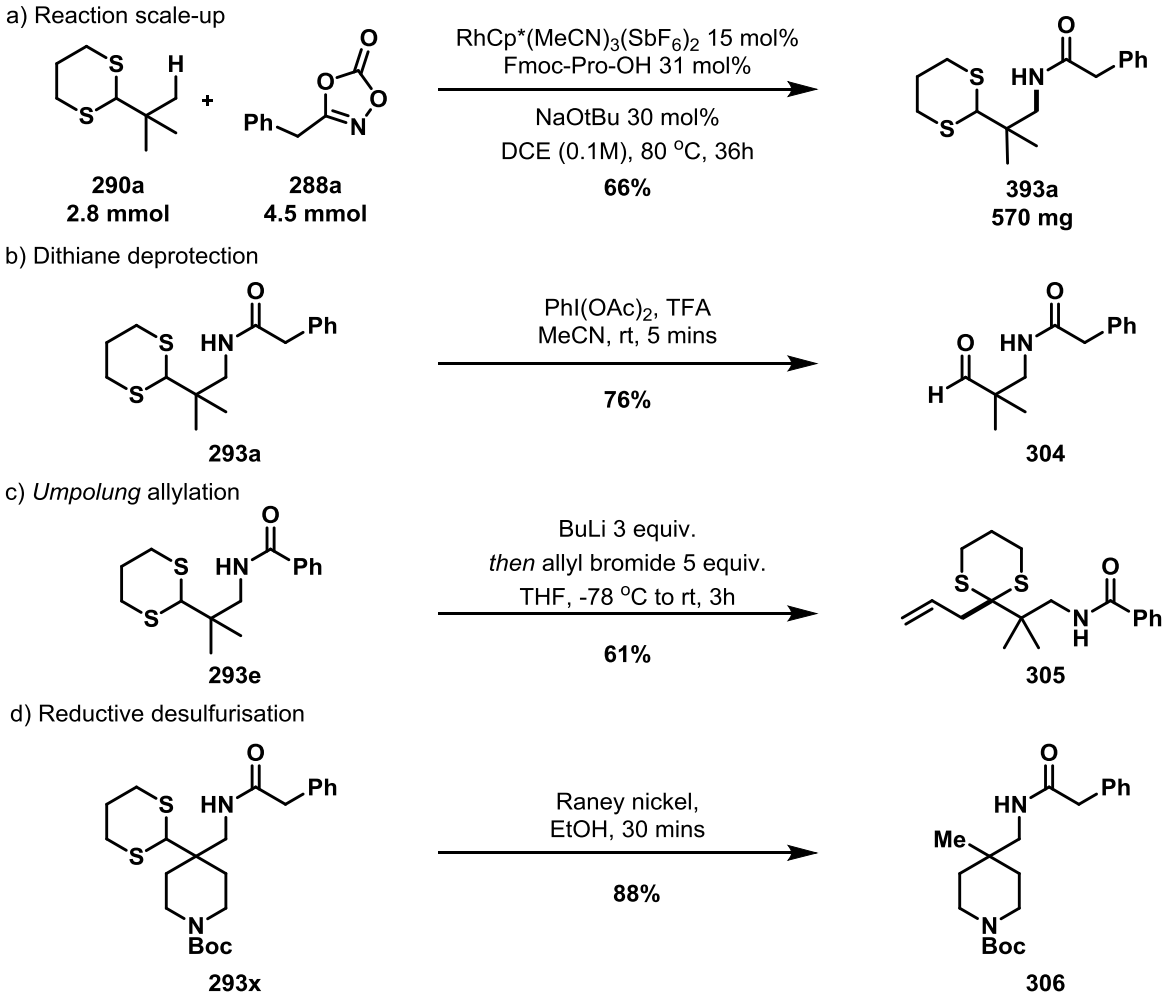


Figure 12: Control reactions using modified substrates.

Ketone derived dithiane **299a** was found to be completely unreactive in the reaction. From the substrate scope, we knew the reaction was strongly affected by steric bulk around the reaction centre, and so the additional steric clash of the extra methyl group appears to suppress reactivity. Dithiolane **300** was also unsuccessful and 7-membered ring thiepane **301** gave a low 18% yield for the corresponding amidated product. These two examples show the importance of geometry, and the unique reactivity of the 6 membered ring dithiane is likely due to it possessing the correct bond angles and geometry required for the cyclometallated intermediate. Isobutyraldehyde-derived dithiane **299b** was only reactive in trace amounts, despite possessing the 6 membered ring dithiane and two reactive methyl groups. In the ground state of this molecule, the acidic dithiane C-H and isopropyl C-H bond adopt an anti-conformation, thus placing the two methyl groups pointing away from the two sulfur atoms of the dithiane moiety. An additional kinetic barrier must be overcome in order to rotate the bond and this is postulated to be the reason for poor reactivity in this substrate. Finally, cyclopropyl and cyclobutyl bearing dithianes **302** and **303** were also found to be completely unreactive in this method. Despite possessing reactive, strained C-H bonds, this pair demonstrates that

our method is unable to transform methylene C-H bonds, and only methyl C-Hs are reactive.

5.7 Reaction Scale-up and Derivatisation



Scheme 55: a) 56 times scale-up reaction. b) Oxidative deprotection of dithiane. c) Corey-Seebach *umpolung* alkylation with allyl bromide. d) Reductive desulfurisation.

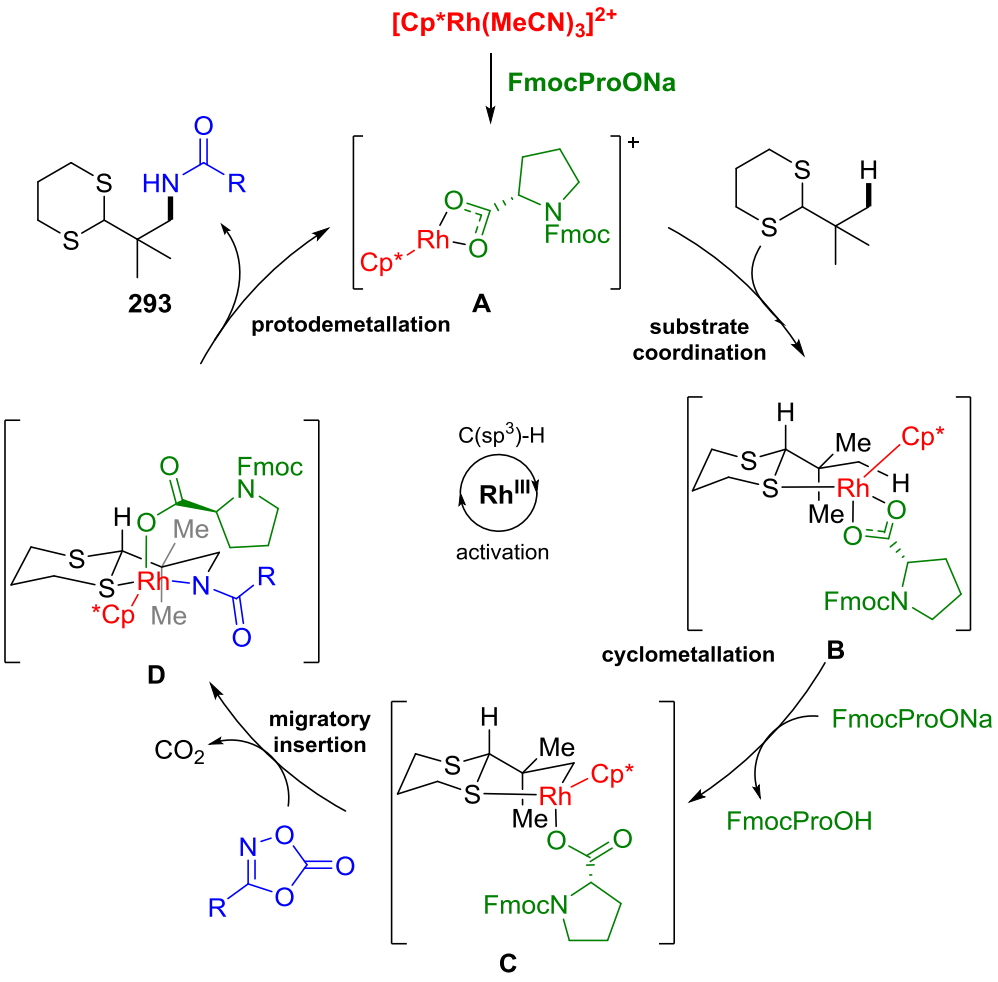
In order to investigate the practicality and efficiency of this transformation, a 56-times scale up reaction was performed using 500 mg of dithiane **290a** as the starting material, and pleasingly amidodithiane **293a** was delivered in 66% yield. Next, to demonstrate synthetic versatility and utility of the dithiane functional group as set out in the initial synthetic plan, diverse modifications were then performed.

Oxidative deprotection with $PhI(OAc)_2$ in acidic acetonitrile smoothly removed the dithiane protecting group and unmasked aldehyde **304** poised for further functionalisation (scheme 55b). The Corey-Seebach *umpolung* reaction was importantly demonstrated by alkylating amidodithiane **293e** with allyl bromide to give **305** in 61% yield. An excess of n-BuLi was required to account for the acidic secondary amide proton, and only a single allylated product was delivered. Our initial project proposal was to mediate challenging C-H functionalisation utilising a synthetically enabling and versatile directing group, and with successful synthesis of **305** this vision has been realised. Finally, reductive desulfurization of piperidine-derived dithiane **293x** with Raney nickel afforded piperidine **306** bearing a quaternary methyl group in excellent yield. This ability for dithianes to act as a latent methyl or methylene group allows our method to enable synthesis of highly functionalised amine building blocks containing a synthetically challenging quaternary methyl group. Decoration of a lead drug compound with methyl groups is one important strategy for improving potency and the colloquially given term 'magic methyl' effect highlights the importance for methods able to install such methyl groups.[181]

5.8 Proposed Mechanism

In line with previous studies performed in the group, a plausible reaction mechanism is suggested in scheme 56.[182] Initial dissociation of the three acetonitrile ligands in the Cp^*Rh^{III} precatalyst and complexation by the Fmoc-Pro-ONa additive gives intermediate **A**. Next, the dithiane substrate coordinates to occupy the empty site on the metal centre, leading to intermediate **B**. With the rhodium metal held near the reactive methyl C-H bond, cyclometallation via carboxylate mediated CMD next occurs leading to

cyclometallated intermediate **C**. From previous studies in the group on a Co^{III} system, an external equivalent of additive mediates this transformation, allowing the already coordinated Fmoc-prolinate to remain coordinated. Migratory insertion of the Rh-C bond, perhaps through initial coordination of the dioxazolone reagent next occurs, forming the key C-N bond and affording intermediate **D**. Finally, protodemetallation Fmoc-Pro-OH formed earlier in the catalytic cycle releases the amidodithiane product **293** and regenerates the Rh catalyst for further turnovers. In the case of this reaction, it is unlikely that a nitrene precursor is generated from the dioxazolone reagent due to incompatibility of the ensuing reactive intermediate with the Lewis basic sulfide groups on the dithiane.



Scheme 56: Postulated reaction mechanism.

5.9 Conclusions

In summary, a methodology introducing the easily installed/cleaved and synthetically versatile dithiane as a directing group for Rh^{III} catalysed C(sp^3)-H functionalisation has been realised. Utilising the uniquely reactive dioxazolone amidating reagents, a range of usefully protected 1,3-aminoaldehyde derivatives could be accessed in good yield. The reaction is tolerant of a wide range of dioxazolone reagents as well as dithiane partners, and diverse downstream functionalisations exploiting the dithiane functional group demonstrated practicality and usefulness of the method. This discovery has made advancements on classically used directing groups which are either structural (e.g. pyridyl, amide, heterocycle) or do not enable useful downstream functionalisations (e.g. oxime, hydrazone, imine).

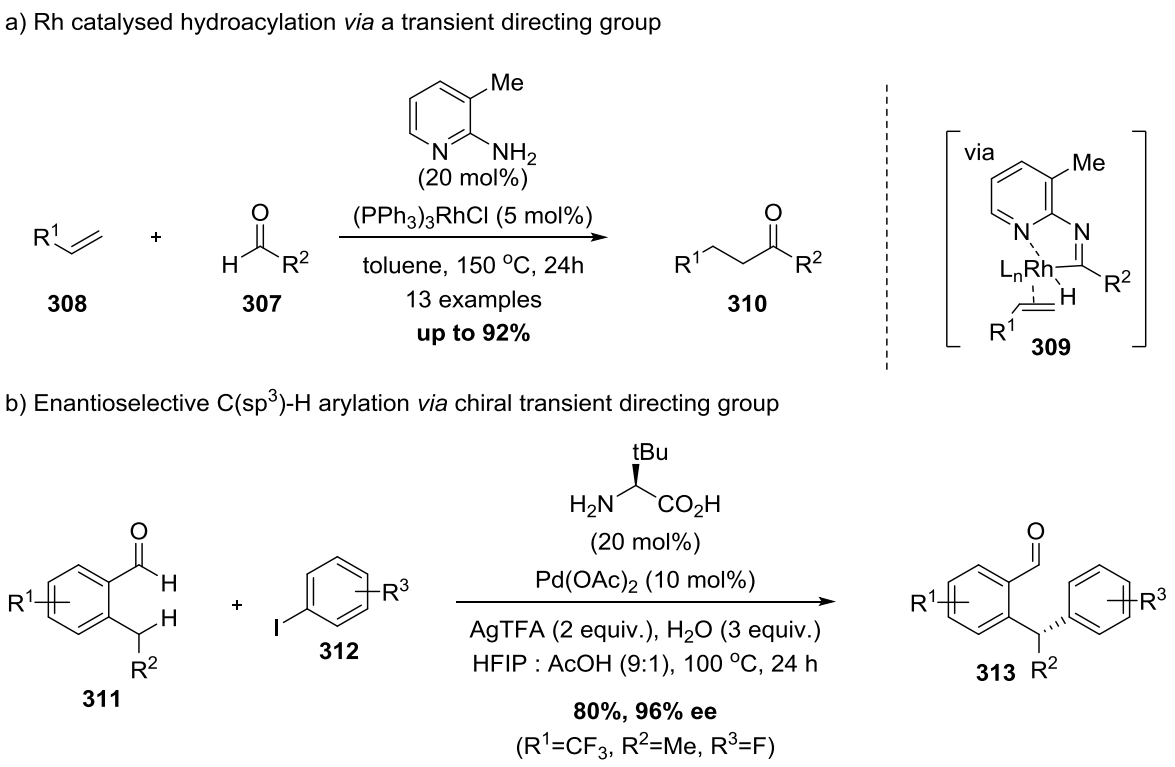
Chapter 6: Rh^{III} Catalysed Amidation of Unactivated C(sp^3)-H Bonds *via* a Transient Imine Directing Group

6.1 Introduction to Transient Directing Groups

Since the turn of the century, C-H activation remains one of the biggest paradigm shifts in chemistry.[183] By mitigating the need for prefunctionalisation at the reaction centre, huge improvements to atom, step and yield economy in synthesis can be achieved. Classically, although directing-free methodologies exist, the use of a suitable directing group is the best way to enable regioselective activation of C-H bonds, and much work has focussed on the identification of suitable functionalities which can be easily installed, cleaved and enable useful downstream functionalisation.[156,184,185] One limitation of this approach is the necessity for additional steps to both install the key directing group prior to C-H transformation and/or cleave/transform it afterward.[186] Of the different approaches to combat this problem, the concept of transient directing groups (TDG) provides one solution to the problem.

A transient directing group attaches reversibly to the substrate and so C-H functionalisation and directing group cleavage occurs in the same pot. Given that reversible attachment/cleavage can occur, catalytic use of the transient directing group is also possible when the rate is comparable with that of C-H functionalisation. This strategy was first demonstrated in Jun's 1997 seminal paper describing the hydroacylation of alkenes through aldehydic C-H activation using 2-amino-3-picoline to form a transient imine directing group (scheme 57a).[187] After reversible imine formation of picoline with aldehyde **307,** acyl C-H activation and binding of olefin **308** leads to rhodacycle intermediate **309**, poised to form the key intermolecular C-C bond. Hydroacylation and

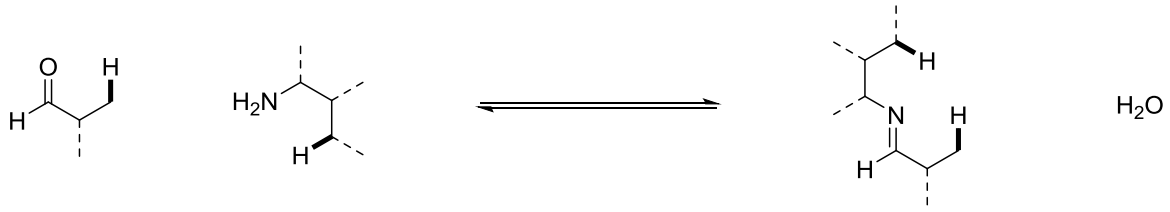
subsequent cleavage of the picoline directing group by hydrolysis then releases the ketone product **310**. The field was further advanced in 2016 with Yu's elegant use of an amino acid as a transient directing group for palladium catalysed enantioselective C(sp^3)-H arylation (scheme 57b).[188] By exploiting the nature of the covalently bound DG-substrate intermediate, Yu and co-workers utilised L-tert-leucine as a chiral additive to generate a chiral transient imine with benzylic aldehydes **311**. Subsequent diastereoselective C-H activation and arylation with **312** occurred with high selectivity, providing arylated products **313** in high yield and up to 96% ee. A wide range of benzaldehyde and aryliodide derivatives are demonstrated and functional groups such as esters, nitro groups and halides were well-tolerated. Since the publication of these two seminal papers, the field has seen rapid progress and multiple reviews and examples have been discovered in the past couple years.[189–192]



Scheme 57: Metal-catalysed methodologies enabled by a transient directing group.

6.2 Imines as Transient Directing Groups

Out of the various transient directing groups explored, imines have emerged as the most widely utilised and explored. Both aldehydes/ketones and amines are common, useful and attractive substrates for methods development and the reversible reaction of these functional groups to form imines has been a well-explored phenomenon in the field of organocatalysis.[193] The *in situ* formed imine intermediate is a much stronger Lewis base than the parent carbonyl group and able to coordinate metal centres and bring them in close proximity to reactive C-H bonds on both the aldehyde or the amine reaction partners, allowing this strategy to be applied to both aldehyde/ketone or amine substrates (scheme 58).



C-H bond activation possibilities on both aldehyde and amine substrates

Scheme 58: Equilibrium between aldehyde/amine and imine/water.

In order to have a successful reaction using this strategy, two things must be true of the catalytic system:

a) The metal catalyst employed must be tolerant of the primary amine component as well as generated water.
b) The electrophile employed in the reaction must be tolerant of the primary amine component.

Other considerations must also be taken when deciding if a catalytic directing group strategy can be employed:

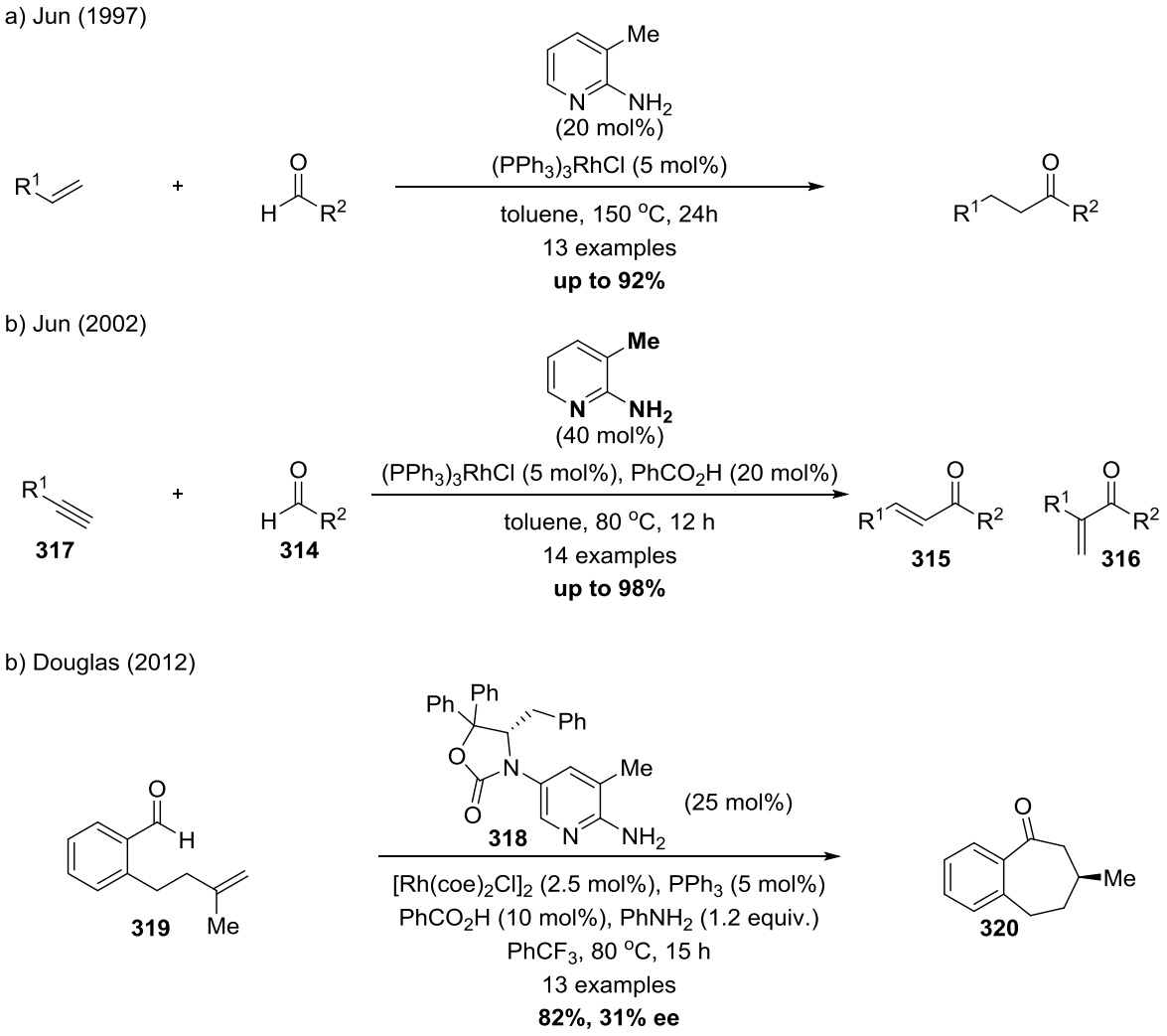
a) Water must be tolerated in the reaction conditions for reversible formation of the imine. If not, equal stoichiometry of amine and aldehyde is required.
b) Both the aldehyde/ketone and amine components must be tolerated in the reaction for *in situ* formation of the imine. If not, preformation of the imine is required.

Despite these complexities and the challenge of combining an organocatalytic cycle with metal catalysed C-H functionalisation, many systems for the activation of different aldehydes, ketones and amines have been developed. For the purposes of this thesis, focus will be placed upon reviewing the activation of aldehydes.

6.3 C-H Activation of Aldehydic C-H Bonds

Since Jun's seminal report describing the activation of aldehydic C-H bonds, many other Rh-catalysed hydroacylation protocols have been developed (scheme 59). Jun expanded the scope of his seminal paper, showing hydroacylation of alkynes is also possible using picoline as a transient imine directing group with aldehyde derivatives **314** (scheme 59a).[194] Benzoic acid was employed as an acidic additive used to facilitate smooth imine formation and hydrolysis. Substrate dependent formation of either linear enone **315** or branched enone **316** was observed, depending on the particular alkyne starting material **317** employed.

Intramolecular aldehydic functionalisation has also been demonstrated, leading to cyclic ketone products. Douglas demonstrated this concept in his Rh catalysed intramolecular hydroacylation of benzylic aldehydes, leading to cycloheptanone products in excellent yield.[195] One notable example is shown in scheme 59c, where a chiral picoline derivative **318** is used to generate a transient imine directing group with aldehyde **319**. Subsequent



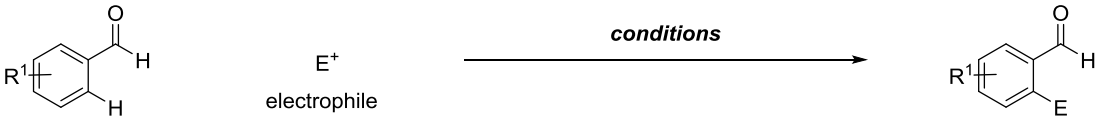
Scheme 59: Aldehydic C-H activation *via* transient imine directing group.

hydroacylation affords ketone **320** in good yield and modest ee. Importantly, 1.2 equivalents of aniline was required as an additive to protect any free aldehyde as the phenylimine, thus preventing the Rh catalysed decarbonylation side reaction.

6.4 C(sp^2)-H Functionalisation *via* a Transient Imine Directing Group

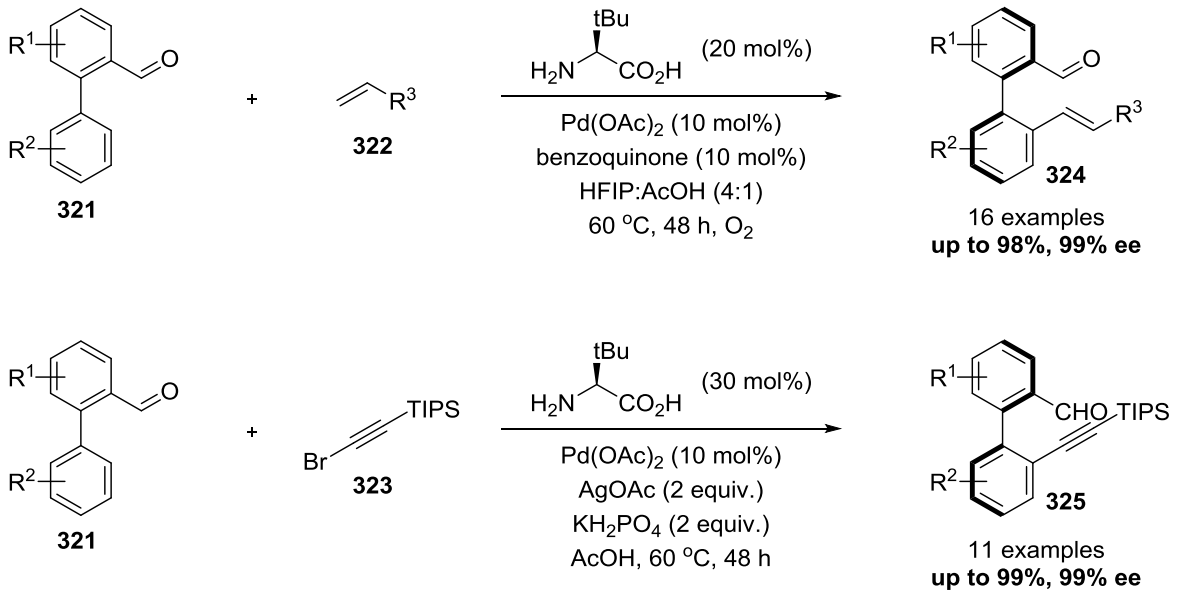
Aromatic aldehydes are important building blocks with the ability to diversify toward a wide range of different functional groups. The benzylic aldehyde carbonyl oxygen is very weakly coordinating and only a handful of methods exist using them as a directing group for *ortho* C-H functionalisation.[196–198] Conversion of aldehyde to the more strongly

coordinating imine functionality is a commonplace strategy, allowing *ortho* C-H functionalisation and outcompeting other more weakly coordinating functionalities. This strategy is exemplified by the breadth of work in Yu's 2017 paper, describing 4 separate methodologies utilising imine transient directing groups (scheme 60).[199] Extensive optimisation of reaction conditions for each transformation enables excellent yields for *ortho*-arylation, chlorination, bromination and amidation reactions. In each case, a different reaction condition and transient directing group is found to be optimal, highlighting the subtleties involved in this reaction type.



Product	Electrophile	TDG	Catalyst (x) mol%	Conditions
24 examples **up to 90%**	I–Ar	(50 mol%)	$Pd(OAc)_2$ (10)	AgTFA (1 equiv.) HFIP:TFA (9:1) 100 °C, 24 h
25 examples **up to 98%**	NCS	(50 mol%)	$Pd(OAc)_2$ (10)	AgTFA (10 mol%) TFA (10 equiv.) DCE, 60 °C, 24 h
24 examples **up to 96%**	NBS	(50 mol%)	$Pd(OAc)_2$ (10)	AgTFA (10 mol%) pTSA (1 equiv.) DCE:TFA (1:1) 90 °C, 24 h
18 examples **up to 93%**	TsN_3	(10 mol%)	$[Cp^*IrCl_2]_2$ (4)	$AgNTf_2$ (16 mol%) AgTFA (30 mol%) TFA (5 equiv.) DCE, 50 °C, 24 h

Scheme 60: Yu's diverse *ortho*-C-H functionalisation *via* a transient imine directing group.

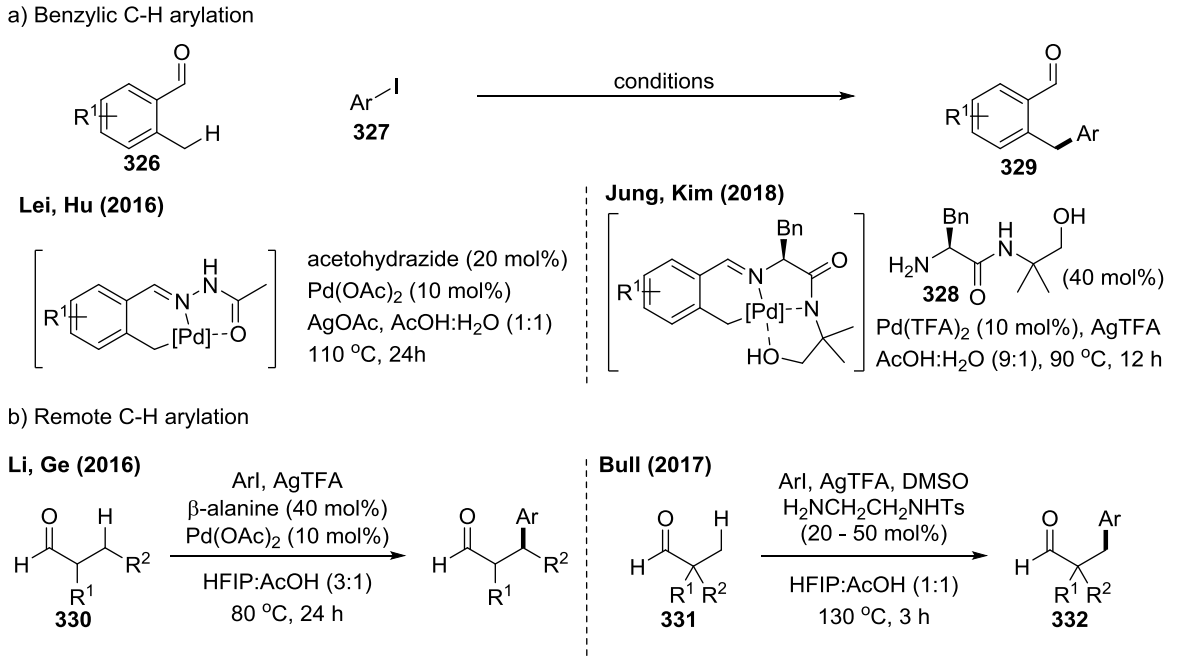


Scheme 61: Enantioselective C(sp^2)-H functionalisation *via* a transient imine directing group by dynamic kinetic resolution.

Shi and co-workers were able to apply the TDG strategy to enable enantioselective C(sp^2)-H functionalisation of biaryls **321** through dynamic kinetic resolution (scheme 61).[200,201] In two separate reports, L-*tert*-leucine is found to be the optimal amine component to form the transient imine, enabling the enantioselective oxidative C-H Heck reaction with electron deficient olefins **322** as well as C-H cross coupling with TIPS-bromoalkyne **323**, affording chiral atropisomers **324** and **325** respectively.

6.5 C(sp^3)-H Functionalisation *via* a Transient Imine Directing Group

In contrast to C(sp^2)-H functionalisation, transient directing group enabled C(sp^3)-H functionalisation is a much less realised area of study. Despite the difficulty of combining the already difficult challenge of C(sp^3)-H functionalisation with a second organocatalytic cycle, several advancements have been made in the past couple of years since the seminal report of Yu in 2016 (scheme 57b).



Scheme 62: C(sp^3)-H arylation *via* a transient imine directing group.

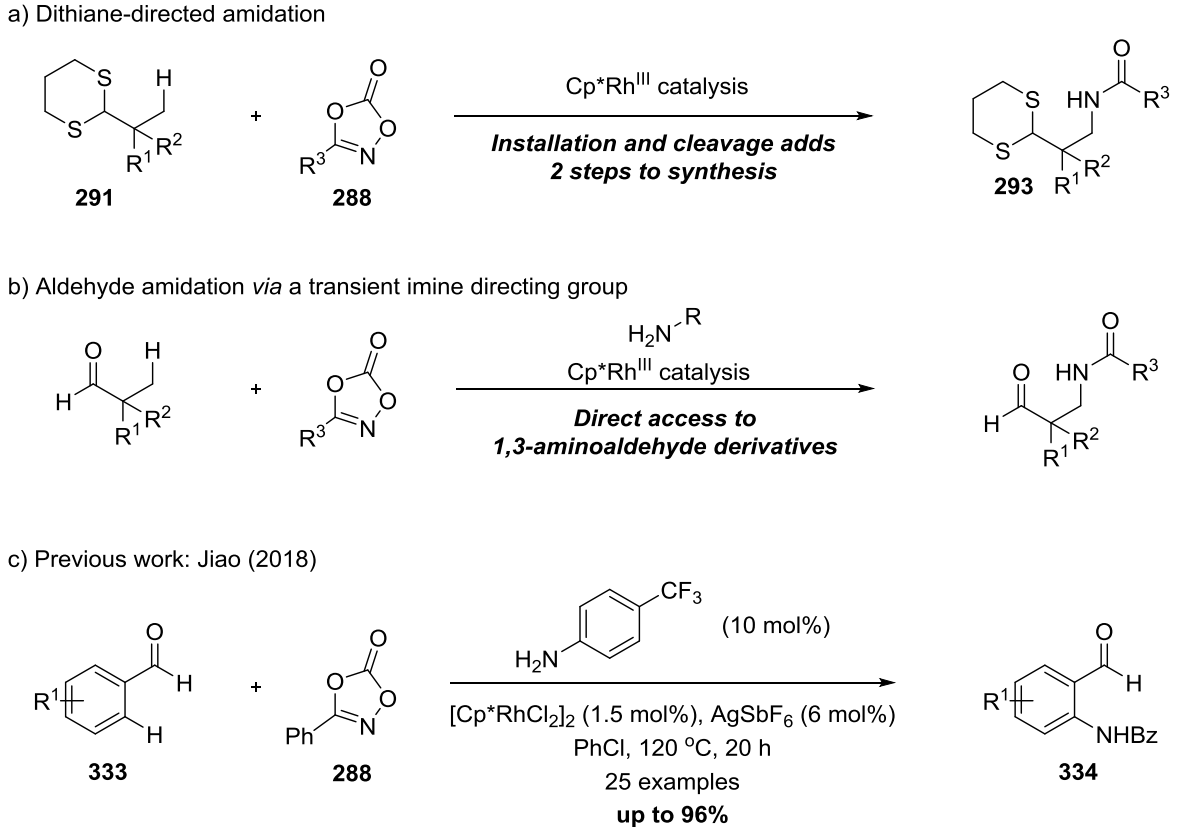
Following on from Yu's achievements in activating benzylic C(sp^3)-H bonds in aromatic aldehydes, Lei and Hu as well as Jung and Kim demonstrated acetohydrazolide and amino acids as competent transient imine directing group mediators for arylation of aromatic aldehydes **326** with aryl iodides **327** (scheme 62a).[202,203] With acetohydrazide, a bidentate hydrazone is formed with the ability to bind palladium at two points and direct it towards the reactive benzylic C-H bond. Jung and Kim employed a tridentate phenylalanine derivative **328** as a transient imine mediator. This directing group strongly coordinates palladium, enabling the subsequent C-H functionalisation reaction. With both these methodologies, excellent yields of the arylated product **329** could be achieved using 10 mol% loading of palladium acetate as the catalyst.

Transient imine directing groups have also been used to functionalise C(sp^3)-H bonds in remote, unactivated positions. The ability to install functionality at a remote C-H bond without the need for a suitable directing group is an extremely powerful concept to streamline chemical synthesis and enable new disconnections. This was first reduced to

practice by Li and Ge's elegant palladium catalysed methylene C-H arylation methodology (scheme 62b). β-Alanine was utilised to generate a transient bidentate imine, directing Pd towards the β-C-H bond in a range of linear aliphatic aldehydes **330**. This reaction type was further expanded with Bull's 2017 publication reporting arylation of unactivated methyl C(sp^3)-H bonds in α-tertiary aldehydes **331**. After screening a wide range of bidentate amines, tosyl-ethylenediamine was found to be the optimal mediator for the reaction, and a fast reaction time of 3 h was needed for full conversion of the starting material towards the arylated aldehyde products **332**.

6.6 Development of Rh^{III} Catalysed Amidation of unactivated C(sp^3)-H Bonds *via* a Transient Imine Directing Group

The successful development of the dithiane directed C(sp^3)-H methodology described previously (chapter 5) represents an advancement to the field of Rh^{III} C-H functionalisation due to the synthetic versatility of the dithiane functional group (scheme 63a). However, it possesses the same weakness as is present in all directing group mediated strategies: an addition step is required to both install and cleave the functional group. Due to this, direct access to unmasked 1,3-amidoaldehydes is still an unrealised synthetic challenge. Therefore, we decided to investigate if a transient imine directing group strategy could be used to enable this transformation (scheme 63b). Recently, Jiao and co-workers were able to combine transient imine directing group mediated C-H functionalisation with the reactivity of aromatic dioxazolone reagents to enable Cp*Rh^{III} catalysed *ortho*-C(sp^2)-H amidation of benzaldehyde derivatives **333**, leading to amidated amidoaldehyde products **334** (scheme 63c).[204] Excellent yields could be achieved using low rhodium loadings and only 10 mol% of an electron dificient aniline co-catalyst. However, the substrate scope was limited to only phenyldioxazolone derivatives.



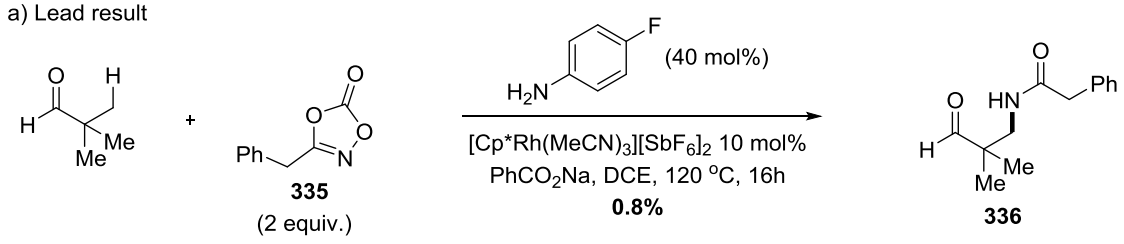
Scheme 63: a) Dithiane directed C(sp^3)-H amidation. b) Reaction concept: direct access to 1,3 aminoaldehyde derivatives. c) Previous work: *ortho* C(sp^2)-H amidation.

The report by Jiao provides a strong proof of concept and complementary transient imine directed functionalisation of C(sp^3)-H bonds would be a powerful method to access synthetically useful 1,3-amidoaldehyde derivatives directly without need for prefunctionalisation or downstream directing group cleavage.

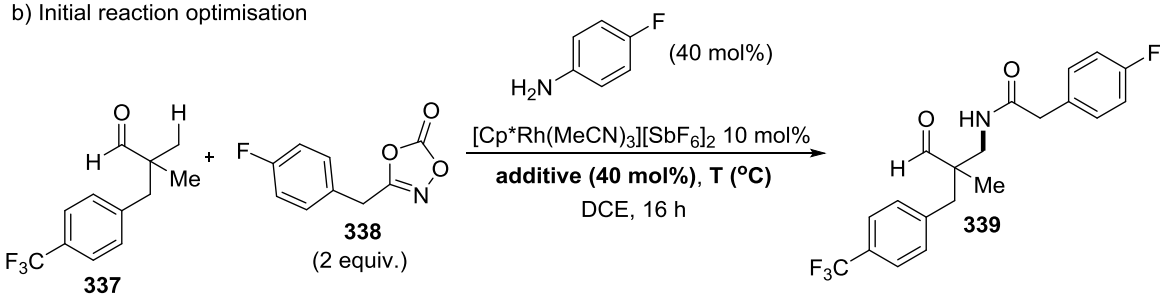
We began our studies using pivaldehyde and benzyldioxazolone **335** as model substrates (scheme 64a). Applying model conditions, pivaldehyde and benzyldioxazlone was treated with *p*-F-aniline (40 mol%) as an TDG mediator and sodium benzoate (40 mol%) as base additive in dichloroethane at 120 °C for 24 h. Pleasingly by analysis of the crude reaction NMR, the desired amidated product **336** could be identified, albeit in 0.8% (NMR yield). With this promising, yet humble lead result, optimisation studies began. As the reaction was performed far above the boiling point of pivaldehyde, it was exchanged with

aldehyde **337** to avoid loss due to vaporisation. Benzyl dioxazolone, which has a melting point around room temperature, was also exchanged for the solid crystalline *p*-F benzyldioxazolone **338** for ease of handling reasons. Initial screening of a range of carboxylate additive derivatives (table 12, entry 2 to 4) identified benzoic acid and adamantylcarboxylic acid both with an equal improvement from 1% to 8% yield (scheme 64b).

a) Lead result



b) Initial reaction optimisation



Entry	Additive	Temperature	NMR Yield (%)
1	$PhCO_2Na$	120	1
2	$PhCO_2H$	120	8
3	$AdCO_2H$	120	8
4	Fmoc-Pro-OH	120	2

Scheme 64: Reaction discovery and initial optimisation.

Despite only an 8% NMR yield for the amidated product, a 38% of the aldehyde starting material had been consumed. The crude NMR was far too messy to determine other species present in the reaction mixture. Postulating the product may still be trapped as the imine species, a post reaction work-up with 1M aqueous HCl was performed. Pleasingly when this was performed, a rise in NMR yield to 36% was observed. The near matching of conversion with yield indicated a clean reaction profile and selective formation of the desired mono-amidated product **339**.

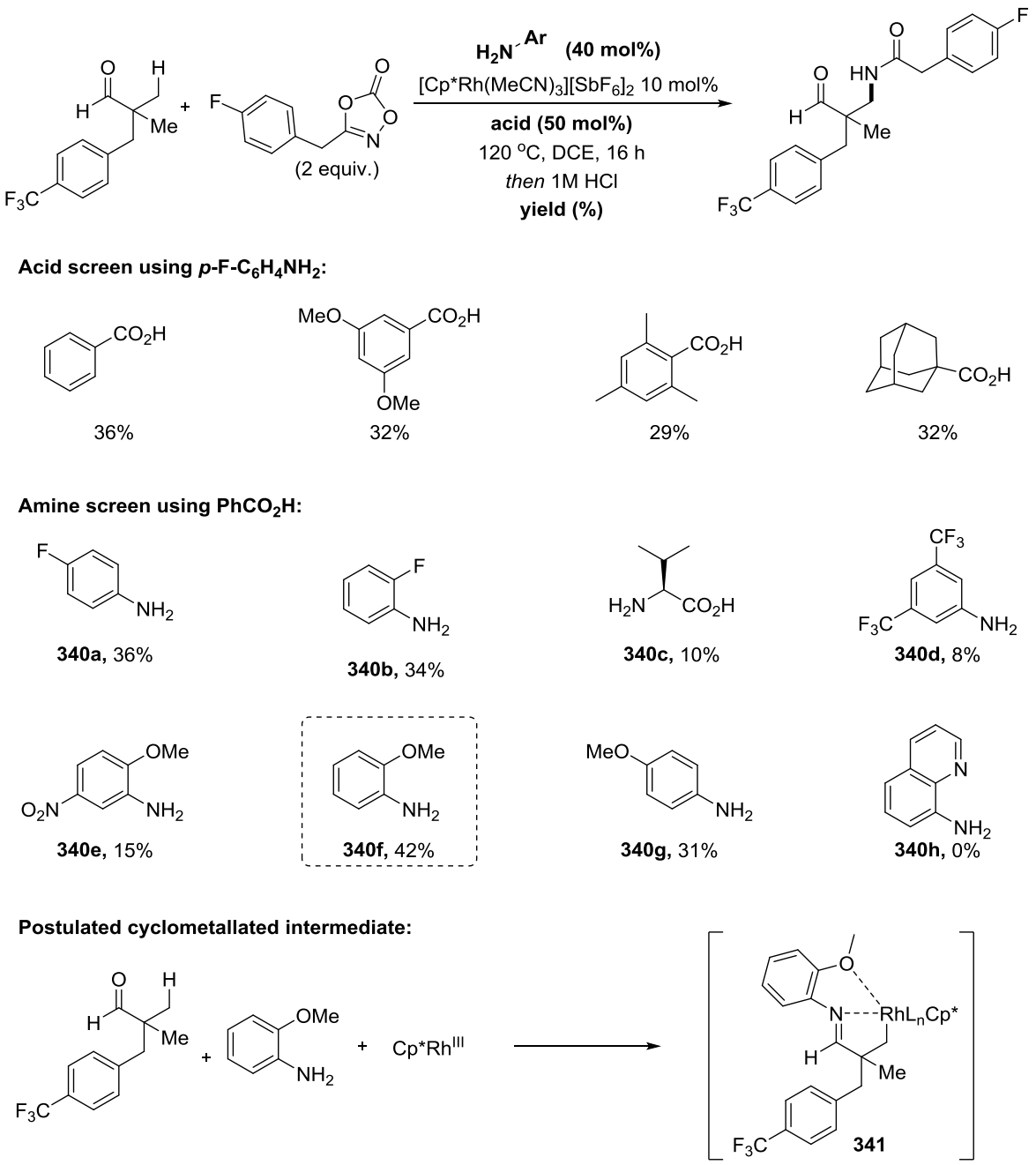


Figure 12: Screening of acid additive and amine transient DG mediator.

With parafluoroaniline as a model amine, 4 structurally different carboxylic acid additives were evaluated for performance in the reaction (figure 12). Similar yields were obtained with each of the acids, and benzoic acid was found to be best with an NMR yield of 36%. Taking this acid forward, a range of amines were screened. Fluorinated anilines **340a** and **340b** gave similar yields of 36 and 34% respectively. Valine was selected as a

representative amino acid additive but this performed poorly in the reaction. Strongly electron deficient anilines **340d** and **340e** also produced very low yields, likely due to difficulty in imine formation. Pleasingly, electron-rich anisidine derivatives **340f** and **340g** showed promising yields, with the former providing the highest yields out of all amines screened. 8-Aminoquinoline **340h** was totally unsuccessful, leading to no desired product formation. From these acid and amine screening studies, benzoic acid and *o*-anisidine were taken forward as optimal. We postulate the 1,2 aminoether functionality in *o*-anisidine enables bidentate coordination to Rh in the cyclometallated intermediate **341**, thus stabilising this intermediate and favouring the C-H activation step in the reaction.

The observed yield of product with optimised acid and amine additives is similar to the 40 mol% equivalents of amine in the reaction, indicating the aldehyde/imine catalytic cycle is not progressing efficiently. Given dioxazolone reagents are known to readily hydrolyse in the prescence of water, we believe under the harsh reaction conditions, hydrolysis of excess dioxazolone from water formed in the imine condensation removes this component and shuts down the aldehyde/amine to imine equilibrium. To combat this, an additional equivalent of dioxazolone was added to counter the loss from hydrolysis, and the equivalents of the amine partner were screened (figure 13). From the data, it can be seen two different correlations are present. From 10 to 100 mol% equivalents of additive, a positive correlation is observed and the optimal yield is obtained with 100 mol% of amine, indicating stoichiometric formation of imine is necessary. Interestingly at low amine equivalents, the NMR yield for the desired product is higher than the equivalents of amine present showing that the imine organocatalytic cycle is indeed in operation.

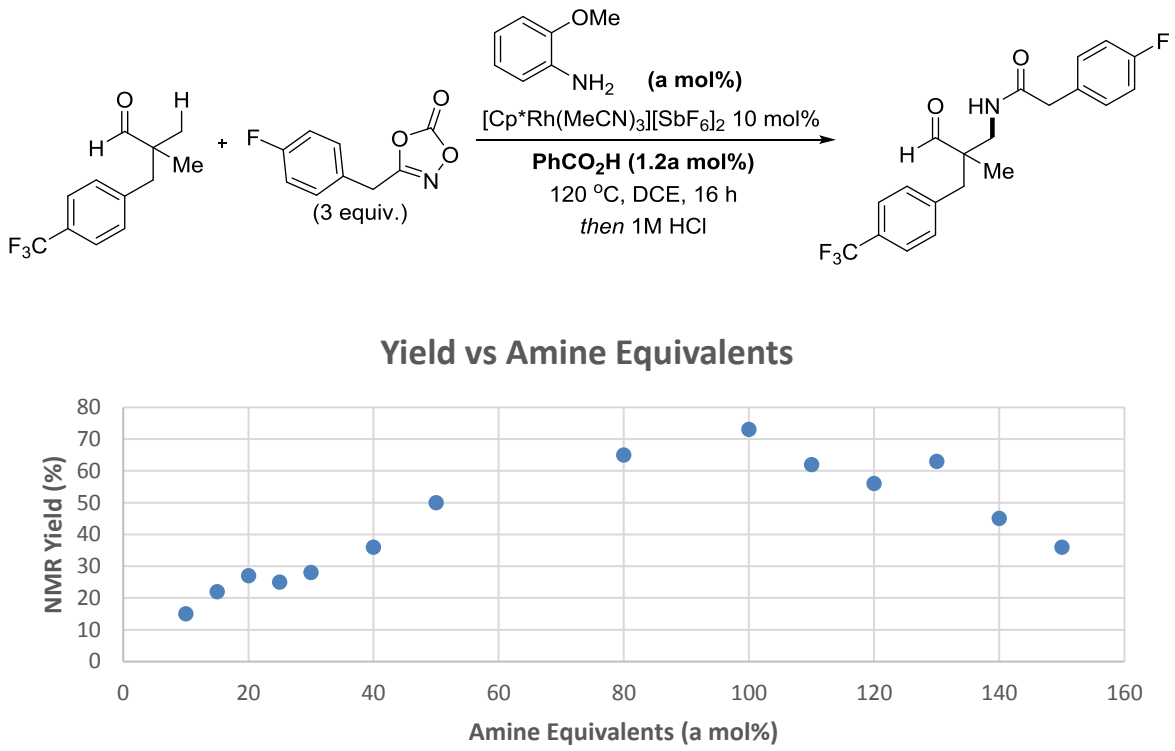
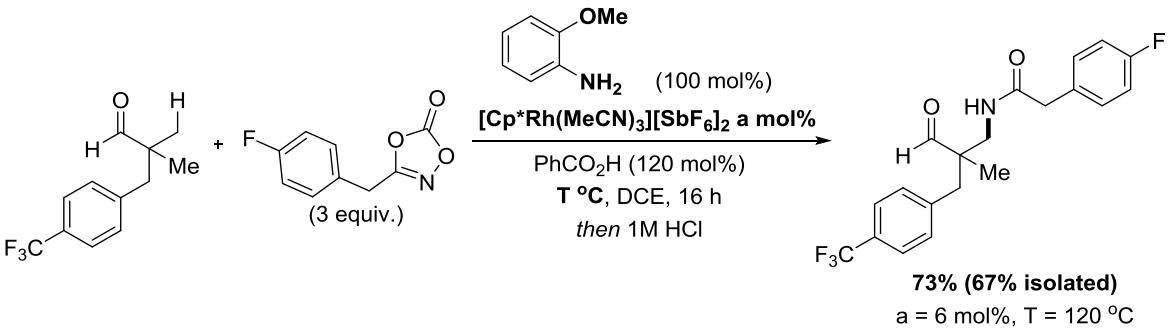


Figure 13: Optimisation of additive equivalents.

Above 100 mol%, a negative correlation is observed with increasing additive equivalents. With no aldehyde left to bind, the excess amine becomes a hinderance to the reaction. This could be due to its ability to bind to the rhodium catalyst and sequestering reactivity, or reaction with the excess electrophilic dioxazolone leading to deleterious side products. Accordingly, the best result from this study (100 mol% of amine additive) was taken forward as optimal.

Screening of temperature and catalyst loading were performed in an attempt to improve the yield (figure 14). Temperature variations were made, and optimal results were observed at 120 °C with an NMR yield of 75%. Taking this temperature forward, reactions were performed with a range of catalyst loadings and the results are presented in figure 14. A bell-shaped relationship was observed, with a maximum yield obtained at 6 mol% catalyst loading. Considering this data, the catalyst loading was reduced down from 10 to

6 mol%. With fully optimised conditions now in hand, a final experiment was performed, and a 73% NMR yield and 67% isolated yield was achieved.



Temperature screen with 10 mol% catalyst:

Entry	Temperature (°C)	NMR Yield (%)
1	80	trace
2	100	29
3	**120**	**75**
4	140	65

Catalyst loading screen at 120 °C:

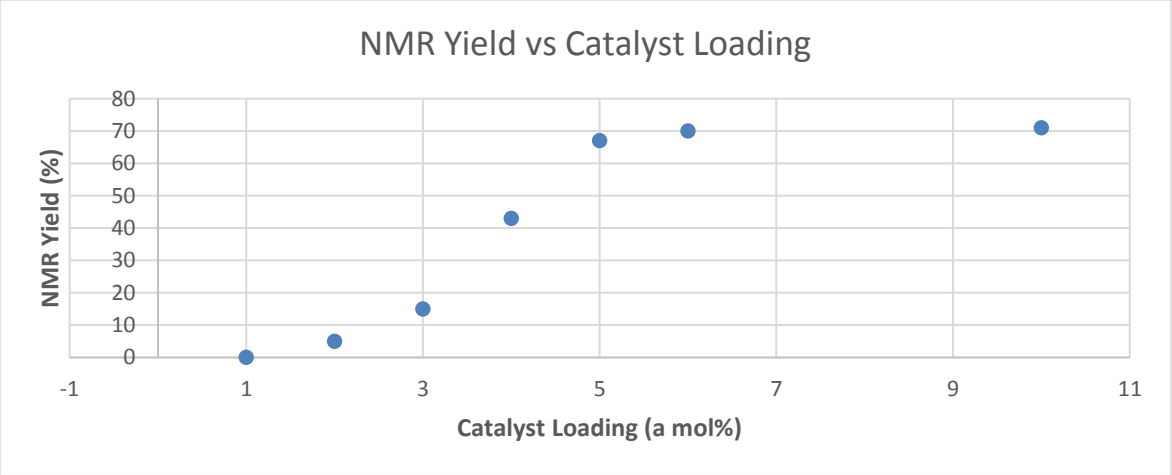


Figure 14: Optimisation of temperature and catalyst loading.

6.7 Conclusions and Future Work

A Cp*Rh^{III} catalysed C(sp^3)-H amidation of aliphatic aldehydes *via* a transient imine directing group has been developed, allowing direct access to unprotected 1,3-amidoaldehyde derivatives in good yield. This is a rare example of Rh^{III} catalysed functionalisation of unactivated C(sp^3)-H bonds and the first example of use of a transient

directing group within this field. Key features of the reaction include use of *o*-anisidine as the optimal amine additive and a low catalyst loading of 6 mol%.

Currently, the substrate scope for this reaction is being evaluated. However due to limitation of time, full investigation and characterisation of all the variables is yet to be completed. Initial results show the reaction is tolerant of a wide range of functionality on the aldehyde partner, with electron rich and electron poor arene, nitrile, halogen and sterically demanding functionality well-tolerated as well as highly congested α-quaternary substituted and aliphatic aldehydes also compatible. Various alkyl substitution on the dioxazolone amidating partner is also well-tolerated, however aromatic dioxazolones display poor yields.

Future work is focused on completing evaluation of the substrate scope and demonstrating applicability of the method with a scale-up reaction and downstream derivatisations.

References

[1] J. Kobayashi, T. Kubota, *Nat. Prod. Rep.* **2009**, 936–962.
[2] H. Wu, X. Zhang, L. Ding, S. Chen, J. Yang, X. Xu, *Planta Med.* **2013**, *79*, 1589–1598.
[3] S. Yagi, *Kyoto Igaku Zassi* **1909**, *6*, 208.
[4] H. Zhang, S. L. Shyaula, J.-Y. Li, J. Li, J.-M. Yue, *Org. Lett.* **2016**, 1205–1205.
[5] H. Zhang, S. L. Shyaula, J.-Y. Li, J. Li, J.-M. Yue, *J. Nat. Prod.* **2015**, *78*, 2761–2767.
[6] J. B. Xu, H. Zhang, L. S. Gan, Y. S. Han, M. A. Wainberg, J. M. Yue, *J. Am. Chem. Soc.* **2014**, *136*, 7631–7633.
[7] F.-P. Wang, X.-T. Liang, *Alkaloids. Chem. Biol.* **2002**, *59*, 1–280.
[8] E. C. Cherney, P. S. Baran, *Isr. J. Chem.* **2011**, *51*, 391–405.
[9] K. T. Suzuki, S. Okuda, H. Niwa, M. Toda, Y. Hirata, S. Yamamura, *Tetrahedron Lett.* **1973**, *14*, 799–802.
[10] H. Niwa, Y. Hirata, *Tetrahedron Lett.* **1973**, 2129–2132.
[11] C. H. Heathcock, *Proc. Natl. Acad. Sci.* **1996**, *93*, 14323–14327.
[12] C. H. Heathcock, S. Piettre, R. B. Ruggeri, J. A. Ragan, J. C. Kath, *J. Org. Chem.* **1992**, *57*, 2554–2566.
[13] H. Morita, J. Kobayashi, *Org. Lett.* **2003**, *5*, 2895–2898.
[14] H. Zhang, S. P. Yang, C. Q. Fan, J. Ding, J. M. Yue, *J. Nat. Prod.* **2006**, *69*, 553–557.
[15] Y. Zhang, Y. T. Di, Q. Zhang, S. Z. Mu, C. J. Tan, X. Fang, H. P. He, S. N. Li, X. J. Hao, *Org. Lett.* **2009**, *11*, 5414–5417.
[16] Z. Lu, Y. Li, J. Deng, A. Li, *Nat. Chem.* **2013**, *5*, 679–684.
[17] F. Sladojevich, I. N. Michaelides, B. Darses, J. W. Ward, D. J. Dixon, *Org. Lett.* **2011**, *13*, 5132–5135.
[18] Y. Ito, T. Hirao, T. Saegusa, *J. Org. Chem.* **1978**, *43*, 1011–1013.
[19] R. Yamada, Y. Adachi, S. Yokoshima, T. Fukuyama, *Angew. Chem. Int. Ed.* **2016**, *55*, 6067–6070.
[20] J. Li, W. Zhang, F. Zhang, Y. Chen, A. Li, *J. Am. Chem. Soc.* **2017**, *139*, 14893–14896.
[21] S.-P. Yang, H. Zhang, C.-R. Zhang, H.-D. Cheng, J.-M. Yue, *J. Nat. Prod.* **2006**, *69*, 79–82.
[22] X. Chen, H. J. Zhang, X. Yang, H. Lv, X. Shao, C. Tao, H. Wang, B. Cheng, Y. Li, J. Guo, J. Zhang, H. Zhai, *Angew. Chem. Int. Ed.* **2018**, *57*, 947–951.
[23] S. Baskaran, I. Islam, M. Raghavan, S. Chandrasekaran, *Chem. Lett.* **1987**, *16*, 1175–1178.
[24] Y. Chen, W. Zhang, L. Ren, J. Li, A. Li, *Angew. Chem. Int. Ed.* **2018**, *57*, 952–956.
[25] Y. Motoyama, M. Aoki, N. Takaoka, R. Aoto, H. Nagashima, *Chem. Commun.* **2009**, 1574–1576.
[26] Y. Nakayama, Y. Maeda, M. Kotatsu, R. Sekiya, M. Ichiki, T. Sato, N. Chida, *Chem. Eur. J.* **2016**, *22*, 3300–3303.
[27] A. D. Gammack Yamagata, D. J. Dixon, *Org. Lett.* **2017**, *19*, 1894–1897.
[28] H. Shi, I. N. Michaelides, B. Darses, P. Jakubec, Q. N. N. Nguyen, R. S. Paton, D. J. Dixon, *J. Am. Chem. Soc.* **2017**, *139*, 17755–17758.
[29] J. Feierfeil, A. Grossmann, T. Magauer, *Angew. Chem. Int. Ed.* **2015**, *54*, 11835–11838.
[30] F. Wang, M. F. Mao, G. Z. Wei, Y. Gao, F. C. Ren, J. K. Liu, *Phytochemistry* **2013**, *95*, 428–435.

[31] W. Zhang, M. Ding, J. Li, Z. Guo, M. Lu, Y. Chen, L. Liu, Y. H. Shen, A. Li, *J. Am. Chem. Soc.* **2018**, *140*, 4227–4231.
[32] B. Darses, I. N. Michaelides, F. Sladojevich, J. W. Ward, P. R. Rzepa, D. J. Dixon, *Org. Lett.* **2012**, *14*, 1684–1687.
[33] T. L. Hua, 'Application of Daphniyunnine D in preparation of medicines for treating chronic obstructive pulmonary disease', **2015**, CN105287544A
[34] A. J. M. Farley, C. Sandford, D. J. Dixon, *J. Am. Chem. Soc.* **2015**, *137*, 15992-15995.
[35] M. Formica, G. Sorin, A. J. M. Farley, J. Díaz, R. S. Paton, D. J. Dixon, *Chem. Sci.* **2018**, *9*, 6969–6974.
[36] A. J. M. Farley, P. Jakubec, A. M. Goldys, D. J. Dixon, *Tetrahedron* **2018**, *74*, 5206–5212.
[37] J. Yang, A. J. M. Farley, D. J. Dixon, *Chem. Sci.* **2016**, *8*, 606–610.
[38] M. G. Núñez, A. J. M. Farley, D. J. Dixon, *J. Am. Chem. Soc.* **2013**, *135*, 16348–16351.
[39] G. Prabhu, N. Narendra, Basavaprabhu, V. Panduranga, V. V. Sureshbabu, *RSC Adv.* **2015**, *5*, 48331–48362.
[40] G. A. Kraus, K. Frazier, *J. Org. Chem.* **1980**, *45*, 4262–4263.
[41] M. Zeng, S. K. Murphy, S. B. Herzon, *J. Am. Chem. Soc.* **2017**, *139*, 16377–16388.
[42] J. J. Kennedy-Smith, S. T. Staben, F. D. Toste, *J. Am. Chem. Soc.* **2004**, *126*, 4526–4527.
[43] B. K. Corkey, F. D. Toste, *J. Am. Chem. Soc.* **2005**, *127*, 17168–17169.
[44] T. Yang, A. Ferrali, F. Sladojevich, L. Campbell, D. J. Dixon, *J. Am. Chem. Soc.* **2009**, *131*, 9140–9141.
[45] R. Manzano, S. Datta, R. S. Paton, D. J. Dixon, *Angew. Chem. Int. Ed.* **2017**, *56*, 5834–5838.
[46] J. F. Brazeau, S. Zhang, I. Colomer, B. K. Corkey, F. D. Toste, *J. Am. Chem. Soc.* **2012**, *134*, 2742–2749.
[47] S. T. Staben, J. J. Kennedy-Smith, D. Huang, B. K. Corkey, R. L. LaLonde, F. D. Toste, *Angew. Chem. Int. Ed.* **2006**, *45*, 5991–5994.
[48] B. K. Corkey, F. D. Toste, *J. Am. Chem. Soc.* **2007**, *129*, 2764–2765.
[49] C. Nevado, D. J. Cardenas, A. M. Echavarren, *Chem. Eur. J.* **2003**, *9*, 2627–2635.
[50] J. Drouin, M. A. Boaventura, J. M. Conia, *J. Am. Chem. Soc.* **1985**, *107*, 1726–1729.
[51] C. H. Suresh, N. Koga, *Inorg. Chem.* **2002**, *41*, 1573–1578.
[52] P. Politzer, P. R. Laurence, K. Jayasuriya, *Environ. Health Perspect.* **1985**, *61*, 191–202.
[53] T. Posner, *Ber. Dtsch. Chem. Ges.* **1899**, *38*, 646–657.
[54] A. B. Lowe, *Polym. Chem.* **2010**, *1*, 17–36.
[55] C. E. Hoyle, C. N. Bowman, *Angew. Chem. Int. Ed.* **2010**, *49*, 1540–1573.
[56] C. Nilsson, N. Simpson, M. Malkoch, M. Johansson, E. Malmström, *J. Polym. Sci. Part A: Polym. Chem.* **2008**, *46*, 1339–1348.
[57] H. C. Kolb, M. G. Finn, K. B. Sharpless, *Angew. Chem. Int. Ed.* **2001**, *40*, 2004–2021.
[58] H. Bader, L. C. Cross, I. Heilbron, E. R. H. Jones, *J. Chem. Soc.* **1949**, 619–623.
[59] P. C. Montevecchi, M. L. Navacchia, *Tetrahedron Lett.* **1998**, *39*, 9077–9080.
[60] T. Taniguchi, T. Fujii, A. Idota, H. Ishibashi, *Org. Lett.* **2009**, *11*, 3298–3301.
[61] U. Wille, *Chem. Rev.* **2013**, *113*, 813–853.
[62] Y. Ichinose, K. Wakamatsu, K. Nozaki, J.-L. Birbaum, K. Oshima, K. Utimoto, *Chem. Lett.* **1987**, *16*, 1647–1650.
[63] M. Lachia, F. Dénès, F. Beaufils, P. Renaud, *Org. Lett.* **2005**, *7*, 4103–4106.

[64] M. Toyota, M. Yokota, M. Ihara, *J. Am. Chem. Soc.* **2001**, *123*, 1856–1861.
[65] P. Lang, A. Mayer, P. Jung, D. Tritsch, J.-F. Biellmann, A. Burger, *Tetrahedron Lett.* **2004**, *45*, 4013–4015.
[66] S. J. Gharpure, S. K. Porwal, *Tetrahedron Lett.* **2009**, *50*, 7162–7165.
[67] E. Bosch, M. D. Bachi, *J. Org. Chem.* **1993**, *58*, 5581–5582.
[68] J. Rentner, M. Kljajic, L. Offner, R. Breinbauer, *Tetrahedron* **2014**, *70*, 8983–9027.
[69] P. Fouilloux, *Appl. Catal.* **1983**, *8*, 1–42.
[70] L. F. Tietze, U. Hartfiel, T. Hübsch, E. Voß, K. Bogdanowicz-Szwed, J. Wichmann, *Liebigs Ann. der Chemie*. **1991**, 275–281.
[71] E. Lieber, F. L. Morritz, The Uses of Raney Nickel, *Advances in Catalysis,* **1953**, *5*, 417-455.
[72] J. Romo, M. Romero, C. Djerassi, G. Rosenkranz, *J. Am. Chem. Soc.* **1951**, *73*, 1528–1533.
[73] M. Hannoun, *An-Najah Univ. J. Res.* **2002**, *16*, 57.
[74] R. Crabtree, *Acc. Chem. Res.* **1979**, *12*, 331–337.
[75] R. R. Schrock, J. A. Osborn, *J. Am. Chem. Soc.* **1976**, *98*, 2134–2143.
[76] T. L. Church, P. G. Andersson, *Coord. Chem. Rev.* **2008**, *252*, 513–531.
[77] J. J. Verendel, O. Pàmies, M. Diéguez, P. G. Andersson, *Chem. Rev.* **2014**, *114*, 2130–2169.
[78] H. W. Thompson, R. E. Naipawer, *J. Am. Chem. Soc.* **1973**, *95*, 6379–6386.
[79] M. Saburi, L. Shao, T. Sakurai, Y. Uchida, *Tetrahedron Lett.* **1992**, *33*, 7877–7880.
[80] Y. Takemoto, S. Kuraoka, T. Ohra, Y. Yonetoku, C. Iwata, *Chem. Commun.* **1996**, 1655–1656.
[81] D. Wright, M. C. McMills, *Encycl. Reagents Org. Synth.* **2001**, DOI 10.1002/047084289X.rl075.
[82] J.-Q. Yu, H.-C. Wu, E. J. Corey, *Org. Lett.* **2005**, *7*, 1415–1417.
[83] J. Q. Yu, E. J. Corey, *J. Am. Chem. Soc.* **2003**, *125*, 3232–3233.
[84] D. Haas, J. M. Hammann, R. Greiner, P. Knochel, *ACS Catal.* **2016**, *6*, 1540–1552.
[85] K. Hornberger, M. Cheung, M. A. Pobanz, K. A. Emmitte, K. W. Kuntz, J. G. Badiang, '*Regioselective Process for Preparing Benzimidazole Thiophenes,* **2007**, WO2006US33793 20060828, US.
[86] A. J. Pearson, X. Wang, *J. Am. Chem. Soc.* **2003**, *125*, 13326–13327.
[87] H. Stetter, M. Schreckenberg, *Angew. Chem. Int. Ed. English* **1973**, *12*, 81.
[88] M. E. Webb, A. Marquet, R. R. Mendel, F. Rébeillé, A. G. Smith, *Nat. Prod. Rep.* **2007**, *24*, 988–1008.
[89] R. Breslow, *J. Am. Chem. Soc.* **1958**, *80*, 3719–3726.
[90] D. Enders, K. Breuer, J. Runsink, J. H. Teles, *Helv. Chim. Acta*. **1996**, *79*, 1899–1902.
[91] M. S. Kerr, J. Read de Alaniz, T. Rovis, *J. Am. Chem. Soc.* **2002**, *124*, 10298–10299.
[92] J. Pesch, K. Harms, T. Bach, *European J. Org. Chem.* ***2004***, 2025–2035.
[93] S. M. Mennen, J. T. Blank, M. B. Tran-Dubé, J. E. Imbriglio, S. J. Miller, *Chem. Commun.* **2005**, 195–197.
[94] D. A. DiRocco, K. M. Oberg, D. M. Dalton, T. Rovis, *J. Am. Chem. Soc.* **2009**, *131*, 10872–10874.
[95] B. M. Trost, C. D. Shuey, F. DiNinno, *J. Am. Chem. Soc.* **1979**, *101*, 1284–1285.
[96] N. Yamazaki, T. Ito, C. Kibayashi, *Org. Lett.* **2000**, *2*, 465–467.
[97] A. Volkov, F. Tinnis, T. Slagbrand, P. Trillo, H. Adolfsson, *Chem. Soc. Rev.* **2016**, *45*, 6685–6697.

[98] G. Barbe, A. B. Charette, *J. Am. Chem. Soc.* **2008**, *130*, 18–19.
[99] S. Raucher, P. Klein, *Tetrahedron Lett.* **1980**, *21*, 4061–4064.
[100] Y. Wang, Z. Zheng, L. Zhang, *Angew. Chem. Int. Ed.* **2014**, *53*, 9572–9576.
[101] R. C. Chadwick, V. Kardelis, P. Lim, A. Adronov, *J. Org. Chem.* **2014**, *79*, 7728–7733.
[102] S. Hanada, E. Tsutsumi, Y. Motoyama, H. Nagashima, *J. Am. Chem. Soc.* **2009**, *131*, 15032–15040.
[103] B. J. Simmons, M. Hoffmann, J. Hwang, M. K. Jackl, N. K. Garg, *Org. Lett.* **2017**, *19*, 1910–1913.
[104] L. G. Xie, D. J. Dixon, *Chem. Sci.* **2017**, *8*, 7492–7497.
[105] L.-G. Xie, D. J. Dixon, *Nat. Commun.* **2018**, *9*, 2841.
[106] Á. L. de Arriba, E. Lenci, M. Sonawane, O. Formery, D. J. Dixon, *Angew. Chem. Int. Ed.* **2017**, *56*, 3655–3659.
[107] Y. Nakayama, Y. Maeda, M. Kotatsu, R. Sekiya, M. Ichiki, T. Sato, N. Chida, *Chem. Eur. J.* **2016**, *22*, 3300–3303.
[108] H. Kobayashi, Y. Sasano, N. Kanoh, E. Kwon, Y. Iwabuchi, *Eur. J. Org. Chem.* **n.d.**, *2016*, 270–273.
[109] R. Giri, B.-F. Shi, K. M. Engle, N. Maugel, J.-Q. Yu, *Chem. Soc. Rev.* **2009**, *38*, 3242–3272.
[110] T. W. Lyons, M. S. Sanford, *Chem. Rev.* **2010**, *110*, 1147–1169.
[111] M. García-Melchor, A. A. C. Braga, A. Lledós, G. Ujaque, F. Maseras, *Acc. Chem. Res.* **2013**, *46*, 2626–2634.
[112] X. Chen, K. M. Engle, D.-H. Wang, J.-Q. Yu, *Angew. Chem. Int. Ed.* **2009**, *48*, 5094–5115.
[113] A. Chandy, A. Singh Thakur, R. Panik, P. Tiwari, *Med. Chem. Drug Discov.* **2013**, *2013*, 108–126.
[114] F. Ullmann, *Ber. Dtsch. Chem. Ges.* **1901**, *36*, 2382–2384.
[115] I. Goldberg, *Ber. Dtsch. Chem. Ges.* **1906** *39*, 1691–1692.
[116] D. M. T. Chan, K. L. Monaco, R.-P. Wang, M. P. Winters, *Tetrahedron Lett.* **1998**, *39*, 2933–2936.
[117] P. Y. S. Lam, C. G. Clark, S. Saubern, J. Adams, M. P. Winters, D. M. T. Chan, A. Combs, *Tetrahedron Lett.* **1998**, *39*, 2941–2944.
[118] M. Kosugi, M. Kameyama, T. Migita, *Chem. Lett.* **1983**, *12*, 927–928.
[119] A. S. Guram, S. L. Buchwald, *J. Am. Chem. Soc.* **1994**, *116*, 7901–7902.
[120] F. Paul, J. Patt, J. F. Hartwig, *J. Am. Chem. Soc.* **1994**, *116*, 5969–5970.
[121] P. Ruiz-Castillo, S. L. Buchwald, *Chem. Rev.* **2016**, *116*, 12564–12649.
[122] S. R. Neufeldt, M. S. Sanford, *Acc. Chem. Res.* **2012**, *45*, 936–946.
[123] R. Breslow, S. H. Gellman, *J. Chem. Soc., Chem. Commun.* **1982**, 1400–1401.
[124] R. Breslow, S. H. Gellman, *J. Am. Chem. Soc.* **1983**, *105*, 6728–6729.
[125] G. Besenyei, L. Párkányi, I. Foch, L. I. Simándi, *Angew. Chem. Int. Ed.* **2000**, *39*, 956–958.
[126] I. I. Moiseev, T. A. Stromnova, M. N. Vargaftik, S. T. Orlova, T. V Chernysheva, I. P. Stolarov, *Catal. Today* **1999**, *51*, 595–602.
[127] H.-Y. Thu, W.-Y. Yu, C.-M. Che, *J. Am. Chem. Soc.* **2006**, *128*, 9048–9049.
[128] D. Lee, Y. Kim, S. Chang, *J. Org. Chem.* **2013**, *78*, 11102–11109.
[129] K.-H. Ng, F.-N. Ng, W.-Y. Yu, *Chem. Commun.* **2012**, *48*, 11680–11682.
[130] G. Song, F. Wang, X. Li, *Chem. Soc. Rev.* **2012**, *41*, 3651–3678.
[131] J. Wencel-Delord, T. Dröge, F. Liu, F. Glorius, *Chem. Soc. Rev.* **2011**, *40*, 4740–4761.

[132] M. Zhang, Y. Zhang, X. Jie, H. Zhao, G. Li, W. Su, *Org. Chem. Front.* **2014**, *1*, 843–895.
[133] J. Wu, X. Cui, L. Chen, G. Jiang, Y. Wu, *J. Am. Chem. Soc.* **2009**, 13888–13889.
[134] Y. Tan, J. F. Hartwig, *J. Am. Chem. Soc.* **2010**, *132*, 3676–3677.
[135] P. M. Maitlis, *Acc. Chem. Res.* **1978**, *11*, 301–307.
[136] D. A. Colby, R. G. Bergman, J. A. Ellman, *Chem. Rev.* **2010**, *110*, 624–655.
[137] K.-H. Ng, Z. Zhou, W.-Y. Yu, *Org. Lett.* **2012**, *14*, 272–275.
[138] K.-H. Ng, Z. Zhou, W.-Y. Yu, *Chem. Commun.* **2013**, *49*, 7031–7033.
[139] C. Grohmann, H. Wang, F. Glorius, *Org. Lett.* **2012**, *14*, 656–659.
[140] B. Zhou, J. Du, Y. Yang, Y. Li, *Org. Lett.* **2013**, *15*, 2934–2937.
[141] J. Shi, G. Zhao, X. Wang, H. E. Xu, W. Yi, *Org. Biomol. Chem.* **2014**, *12*, 6831–6836.
[142] M. A. Ali, X. Yao, H. Sun, H. Lu, *Org. Lett.* **2015**, *17*, 1513–1516.
[143] S. Yu, B. Wan, X. Li, *Org. Lett.* **2013**, *15*, 3706–3709.
[144] Y. Park, K. T. Park, J. G. Kim, S. Chang, *J. Am. Chem. Soc.* **2015**, *137*, 4534–4542.
[145] J. Sauer, K. K. Mayer, *Tetrahedron Lett.* **1968**, *9*, 319–324.
[146] K. Shin, J. Ryu, S. Chang, *Org. Lett.* **2014**, *16*, 2022–2025.
[147] Y. Park, S. Jee, J. G. Kim, S. Chang, *Org. Process Res. Dev.* **2015**, *19*, 1024–1029.
[148] B. Jeon, U. Yeon, J. Y. Son, P. H. Lee, *Org. Lett.* **2016**, *18*, 4610–4613.
[149] G. L. Hoang, K. Søholm Halskov, J. A. Ellman, *J. Org. Chem.* **2018**, *83*, 9522–9529.
[150] K. M. Engle, T.-S. Mei, M. Wasa, J.-Q. Yu, *Acc. Chem. Res.* **2012**, *45*, 788–802.
[151] F. G. Bordwell, *Acc. Chem. Res.* **1988**, *21*, 456–463.
[152] R. W. Taft, F. G. Bordwell, *Acc. Chem. Res.* **1988**, *21*, 463-469.
[153] X. Tan, B. Liu, X. Li, B. Li, S. Xu, H. Song, B. Wang, *J. Am. Chem. Soc.* **2012**, *134*, 16163–16166.
[154] T. Cochet, V. Bellosta, D. Roche, J.-Y. Ortholand, A. Greiner, J. Cossy, *Chem. Commun.* **2012**, *48*, 10745–10747.
[155] B. Liu, T. Zhou, B. Li, S. Xu, H. Song, B. Wang, *Angew. Chem. Int. Ed.* **2014**, *53*, 4191–4195.
[156] G. Rouquet, N. Chatani, *Angew. Chem. Int. Ed.* **2013**, *52*, 11726–11743.
[157] X. Wang, D.-G. Yu, F. Glorius, *Angew. Chem. Int. Ed.* **2015**, *54*, 10280–10283.
[158] C. Yuan, G. Tu, Y. Zhao, *Org. Lett.* **2017**, *19*, 356–359.
[159] X. Huang, Y. Wang, J. Lan, J. You, *Angew. Chem. Int. Ed.* **2015**, *54*, 9404–9408.
[160] H. Wang, G. Tang, X. Li, *Angew. Chem. Int. Ed.* **2015**, *127*, 13241–13244.
[161] T. E. Burghardt, *Journal of Sulfur Chemistry,* **2005**, *26*, 411–427.
[162] A. B. Smith, C. M. Adams, *Acc. Chem. Res.* **2004**, *37*, 365–377.
[163] M. Yus, C. Nájera, F. Foubelo, *Tetrahedron* **2003**, *59*, 6147–6212.
[164] D. Seebach, E. J. Corey, *J. Org. Chem.* **1975**, *40*, 231–237.
[165] E. J. Corey, D. Seebach, *Angew. Chem. Int. Ed.* **1965**, *1*, 1075–1077.
[166] D. Seebach, *Angew. Chem. Int. Ed.* **1979**, *18*, 239–258.
[167] A. B. Smith, B. D. Dorsey, M. Visnick, T. Maeda, M. S. Malamas, *J. Am. Chem. Soc.* **1986**, *108*, 3110–3112.
[168] A. B. Smith, K. Chen, D. J. Robinson, L. M. Laakso, K. J. Hale, *Tetrahedron Lett.* **1994**, *35*, 4271–4274.
[169] A. B. Smith, S. M. Pitram, M. J. Fuertes, *Org. Lett.* **2003**, 783–786.
[170] S. A. Baker Dockrey, A. K. Makepeace, J. R. Schmink, *Org. Lett.* **2014**, *16*, 4730–4733.
[171] B. Yucel, P. J. Walsh, *Adv. Synth. Catal.* **2014**, *356*, 3659–3667.
[172] F. G. Bordwell, J. E. Bares, J. E. Bartmess, G. E. Drucker, J. Gerhold, G. J. McCollum, M. Van der Puy, N. R. Vanier, W. S. Matthews, *J. Org. Chem.* **1977**, *42*, 326–332.

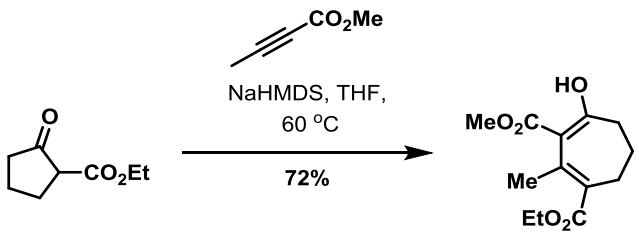
[173] W. Du, L. Tian, J. Lai, X. Huo, X. Xie, X. She, S. Tang, *Org. Lett.* **2014**, *16*, 2470–2473.
[174] A. Kondoh, M. Oishi, T. Takeda, M. Terada, *Angew. Chem. Int. Ed.* **2015**, *54*, 15836–15839.
[175] Y. Unoh, K. Hirano, T. Satoh, M. Miura, *Org. Lett.* **2015**, *17*, 704–707.
[176] J. Sherwood, *Angew. Chem. Int. Ed.* **2018**, 14286–14290.
[177] K. Hong, H. Park, J. Q. Yu, *ACS Catal.* **2017**, *7*, 6938–6941.
[178] G.-J. Cheng, Y.-F. Yang, P. Liu, P. Chen, T.-Y. Sun, G. Li, X. Zhang, K. N. Houk, J.-Q. Yu, Y.-D. Wu, *J. Am. Chem. Soc.* **2014**, *136*, 894–897.
[179] K. S. L. Chan, H.-Y. Fu, J.-Q. Yu, *J. Am. Chem. Soc.* **2015**, *137*, 2042–2046.
[180] R. D. Taylor, M. MacCoss, A. D. G. Lawson, *J. Med. Chem.* **2014**, *57*, 5845–5859.
[181] H. Schönherr, T. Cernak, *Angew. Chem. Int. Ed.* **2013**, *52*, 12256–12267.
[182] P. W. Tan, A. M. Mak, M. B. Sullivan, D. J. Dixon, J. Seayad, *Angew. Chem. Int. Ed.* **2017**, *56*, 16550–16554.
[183] K. Godula, D. Sames, *Science.* **2006**, *312*, 67–72.
[184] O. Daugulis, J. Roane, L. D. Tran, *Acc. Chem. Res.* **2015**, *48*, 1053–1064.
[185] Y. Xu, G. Dong, *Chem. Sci.* **2018**, *9*, 1424–1432.
[186] J. Cornella, M. Righi, I. Larrosa, *Angew. Chem. Int. Ed.* **2011**, *50*, 9429–9432.
[187] C.-H. Jun, H. Lee, J.-B. Hong, *J. Org. Chem.* **1997**, *62*, 1200–1201.
[188] F.-L. Zhang, K. Hong, T.-J. Li, H. Park, J.-Q. Yu, *Science.* **2016**, *351*, 252–256.
[189] J. Lv, Q. Zhang, M. Cai, Y. Han, S. Luo, *Chem. – An Asian J.* **2018**, *13*, 740–753.
[190] P. Gandeepan, L. Ackermann, *Chem* **2018**, *4*, 199–222.
[191] Q. Zhao, T. Poisson, X. Pannecoucke, T. Besset, *Synthesis.* **2017**, *49*, 4808–4826.
[192] H. Sun, N. Guimond, Y. Huang, *Org. Biomol. Chem.* **2016**, *14*, 8389–8397.
[193] D. W. C. MacMillan, *Nature* **2008**, *455*, 304.
[194] C.-H. Jun, H. Lee, J.-B. Hong, B.-I. Kwon, *Angew. Chem. Int. Ed.* **2002**, *41*, 2146–2147.
[195] E. V Beletskiy, C. Sudheer, C. J. Douglas, *J. Org. Chem.* **2012**, *77*, 5884–5893.
[196] R. Santhoshkumar, S. Mannathan, C.-H. Cheng, *J. Am. Chem. Soc.* **2015**, *137*, 16116–16120.
[197] K. Padala, M. Jeganmohan, *Org. Lett.* **2012**, *14*, 1134–1137.
[198] F. Yang, K. Rauch, K. Kettelhoit, L. Ackermann, *Angew. Chem. Int. Ed.* **2014**, *53*, 11285–11288.
[199] X.-H. Liu, H. Park, J.-H. Hu, Y. Hu, Q.-L. Zhang, B.-L. Wang, B. Sun, K.-S. Yeung, F.-L. Zhang, J.-Q. Yu, *J. Am. Chem. Soc.* **2017**, *139*, 888–896.
[200] Q.-J. Yao, S. Zhang, B.-B. Zhan, B.-F. Shi, *Angew. Chem. Int. Ed.* **2017**, *56*, 6617–6621.
[201] G. Liao, Q.-J. Yao, Z.-Z. Zhang, Y.-J. Wu, D.-Y. Huang, B.-F. Shi, *Angew. Chem. Int. Ed.* **2018**, *57*, 3661–3665.
[202] F. Ma, M. Lei, L. Hu, *Org. Lett.* **2016**, *18*, 2708–2711.
[203] H. Park, K. Yoo, B. Jung, M. Kim, *Tetrahedron* **2018**, *74*, 2048–2055.
[204] X. Wang, S. Song, N. Jiao, *Chin. J. Chem.* **2018**, *36*, 213–216.

Experimental

General Methods and Materials

Reactions were carried out under a nitrogen atmosphere in oven-dried glassware at room temperature (rt = 20 - 25 ^{o}C) unless stated otherwise. Standard inert atmosphere techniques were used in handling all air and moisture sensitive reagents. Thin-layer chromatography (TLC) was performed using Merck aluminium backed sheets coated with Merck Kieselgel 60 F254 (230-400 mesh) fluorescent treated silica, which were visualised under UV light (λ_{max}= 254 or 365 nm). Flash column chromatography was performed using Merck Kieselgel (230-400 mesh). All ^{1}H and ^{13}C NMR spectra were recorded using a Bruker 500 MHz and Bruker 400 MHz spectrometers and are quoted in ppm for measurement against a tetramethylsilane (TMS) or residual solvent peak internal standard. Coupling constants (J) are reported in hertz (Hz), and rounded to the nearest 0.5Hz. Two-dimensional spectroscopy (COSY, HSQC and HMBC) was used to assist in the assignment and the data is not reported. IR spectra were recorded on a Bruker Tensor 27 FT-IR spectrometer deposited as a thin film. Melting points were recorded using a Leica Galen III hot-stage microscope apparatus and are reported uncorrected in degrees Celsius (^{o}C). Low resolution mass spectra were recorded on a Waters LCT premier XE Micromass spectrometer (ESI). High resolution mass spectra (ESI) were recorded on a Bruker MicroTof mass spectrometer. Optical rotations were recorded using a Perkin Elmer 341 polarimeter; $[\alpha]_D^T$ values are reported in 10^{-1} deg·cm^2·g^{-1}; concentrations (c) are quoted in g/100 mL; D refers to the D-line of sodium (589 nm); temperatures (T) are given in degrees Celsius (°C). (+) and (–) compound number prefixes indicate the sign of the optical rotation. The enantiomeric excesses were determined by HPLC analysis on an

Agilent 1200 Series instrument or by GC analysis on an Agilent 7820A instrument employing a chiral stationary phase column specified in the individual experiment and by comparing the samples with the appropriate racemic mixtures. Commercial grade reagents and solvents were used without further purification. Anhydrous toluene, tetrahydrofuran and dichloromethane were obtained by filtration through activated alumina (powder ~150 mesh, pore size 58Å, basic, Sigma-Aldrich) columns. Other solvents were used directly as received from commercial suppliers. Procedures and characterisation for compounds **85, 86**, **86a** and **82** were developed by Iacovos Neal Michaelides and included for completeness in the supporting information.



Compound 85

To a suspension of NaH (60% dispersion in mineral oil, 27.0g, 675 mmol) in anhydrous THF (1 L) at reflux under a nitrogen atmosphere was added ethyl 2-oxocyclopentanecarboxylate (104 mL, 702 mmol) dropwise. After stirring for 10 minutes, a clear yellow solution was formed, to which methyl 2-butylnoate (50.0 mL, 500 mmol) was added dropwise. The reaction mixture was allowed to stir at reflux for 3h before being cooled to rt and quenched with aqueous HCl (1 M, 800 mL). The reaction was extracted with ethyl acetate (3 x 800 mL), the combined organic layers were dried over sodium sulfate and concentrated in vacuo. The crude product was purified by flash column chromatography (PE:EtOAc [97:3]) to provide **85** as a white solid (91.4g, 72% yield).[1]

mp 44-48 °C

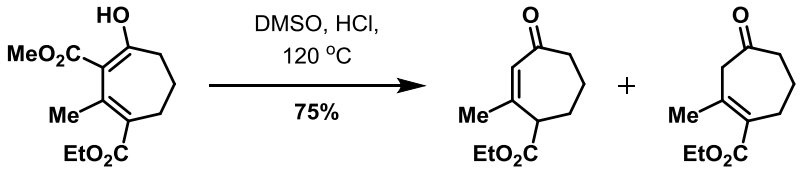
IR (film)/cm^{-1} $\boldsymbol{\nu_{max}}$ 2930, 2865, 1710, 1645, 1587, 1241.

^{1}H NMR ($CDCl_3$, 500 MHz) δ_H 12.85 (s, 1H), 4.20 (q, 2H, J = 7.0 Hz), 3.77 (s, 3H), 2.21-2.36 (br s, 4H), 2.21-2.15 (m, 2H), 2.14 (s, 3H), 1.30 (t, 3H, J = 7.0 Hz)

^{13}C NMR ($CDCl_3$, 125 MHz) δ_C 178.7, 171.6, 168.6, 143.6, 129.2, 103.8, 60.1, 51.5, 32.8, 31.2, 27.3, 20.8, 14.3.

HRMS (ES+) exact mass calculated for $[M+Na]^+$ ($C_{13}H_{18}NaO_5^+$) requires **m/z** 277.1046, found **m/z** 277.1043.

[1] Data agrees with literature values; Dixon *et al.*, *Org. Lett.*, **2011**, *13*, 664-667



Compound 86.

To a mixture of **85** (97.0 g, 381 mmol) and LiCl (80.8 g, 1.91 mol) in DMSO (1.45 L) at rt under a nitrogen atmosphere, was added aqueous HCl (1 M, 150 mL). The reaction was heated to 120 °C for 5 hours. The reaction was cooled to rt and diluted to half its original concentration with diethyl ether. The reaction mixture was washed with brine three times and the aqueous layers back-extracted with diethyl ether. The combined organic layers were dried over sodium sulfate and concentrated *in vacuo*. The crude product was purified by flash column chromatography with PE:EtOAc [85:15] as the eleuent to provide **30** as an inseparate isomeric mixture **(86a: 86b**, 1:0.22) as a colourless oil (56.3g, 75% yield). For ease of interpretation, the integrations below are indicated as if each isomer was isolated in 100% purity.[2]

IR (film)/cm^{-1} ν_{max} 2980, 2939, 2871, 1730, 1709, 1665.

NMR data for **86a**:

^{1}H NMR ($CDCl_3$, 500 MHz) δ_H 5.95 (s, 1H), 4.20-4.09 (m, 2H), 3.40 (dd, 1H, J = 7.0, 4.0 Hz), 2.63-2.50 (m, 1H), 2.44 (app dt, 1H, J = 15.5, 6.0 Hz), 2.22 (app ddt, 1H, J = 14.0, 7.0, 5.5 Hz), 2.01–1.88 (m, 4H), 1.88-1.79 (m, 1H), 1.79-1.69 (m, 1H), 1.23 (t, 3H, J = 7.0 Hz).

^{13}C NMR ($CDCl_3$, 125 MHz) δ_C 202.5, 171.8, 151.7, 131.4, 61.1, 50.5, 42.1, 28.3, 26.3, 19.4, 13.9.

NMR data for **86b**:

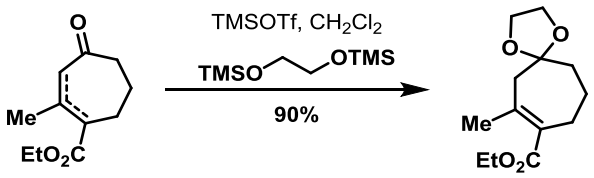
^{1}H NMR ($CDCl_3$, 500 MHz) δ_H 4.20-4.09 (m, 2H), 3.21 (s, 2H), 2.63-2.50 (m, 4H), 2.05 (s, 3H), 2.01-1.88 (m, 2H), 1.28-1.20 (t, 3H, J = 7.0 Hz).

^{13}C NMR ($CDCl_3$, 125 MHz) δ_C 206.6, 168.6, 140.9, 129.7, 60.3, 51.4, 43.5, 28.1, 25.4, 23.0, 14.1.

HRMS (ES+) exact mass calculated for $[M+Na]^+$ ($C_{11}H_{16}NaO_3^+$) requires **m/z** 219.0992, found **m/z** 219.0991.

---

[2] Data agrees with literature values; Dixon *et al.*, *Org. Lett.*, **2011**, *13*, 664-667



Compound 86a.

To a solution of **86** (45.0 g, 229 mmol) in freshly distilled dichloromethane (2.0 L) under a nitrogen atmosphere at rt, was added 2,2,7,7-tetramethyl-3,6-dioxa-2,7-disilaoctane (225 mL, 918 mmol) followed by TMSOTf (1.7 mL, 9.39 mmol) dropwise. The mixture gradually changed from yellow to dark red. After 14 h, the reaction mixture was quenched with a saturate aqueous solution of $NaHCO_3$ and extracted with dichloromethane (3 x 600 mL). The combined organic layers were dried over sodium sulfate and concentrated *in vacuo*. The concentrate was dissolved in the minimal amount of pentane and cooled to -20 ^oC. Upon crystallisation, the crystals were filtered off and washed with cold pentane. This process was repeated 8 times to provide **86a** as transparent pink crystals (49.5 g, 90%).

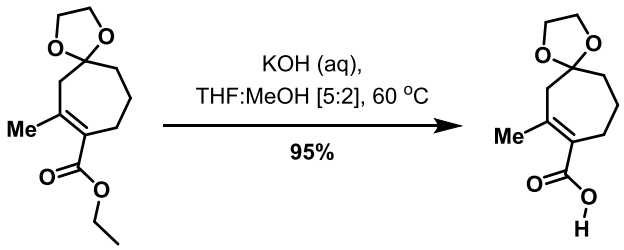
mp 35-37 ^oC

IR (film)/cm^{-1} $\boldsymbol{\nu_{max}}$ 2938, 1707, 1641.

^{1}H NMR ($CDCl_3$, 500 MHz) δ_H 4.18 (q, 2H, J = 7.0 Hz), 4.00-3.90 (m, 4H), 2.58 (s, 2H), 2.47-2.41 (m, 2H), 2.08 (s, 3H), 1.93-1.84 (m, 2H), 1.71-1.61 (m, 2H), 1.29 (s, 3H).

^{13}C NMR ($CDCl_3$, 125 MHz) δ_C 169.4, 144.2, 130.6, 107.1, 64.6, 60.2, 46.0, 40.7, 28.7, 24.5, 23.5, 14.3.

HRMS (ES+) exact mass calculated for $[M+Na]^+$ ($C_{13}H_{20}NaO_4^+$) requires **m/z** 263.1254, found **m/z** 263.1254.



Compound 82

To a solution of **86a** (20.0 g, 83.2 mmol) in MeOH (60 mL) and THF (150 mL) at rt, was added aqueous KOH (2 M, 150 mL). The reaction mixture was heated to 60 °C for 24 h and then cooled to rt, quenched with aqueous HCl (2 M, 150 mL) and extracted with ethyl acetate (3 x 200 mL). The combined organic layers were dried over sodium sulfate and concentrated *in vacuo*. The crude product was purified by flash column chromatography with PE:EtOAc:AcOH [88:10:2] as the eluent to give **82** as a white solid (16.8 g, 95%).

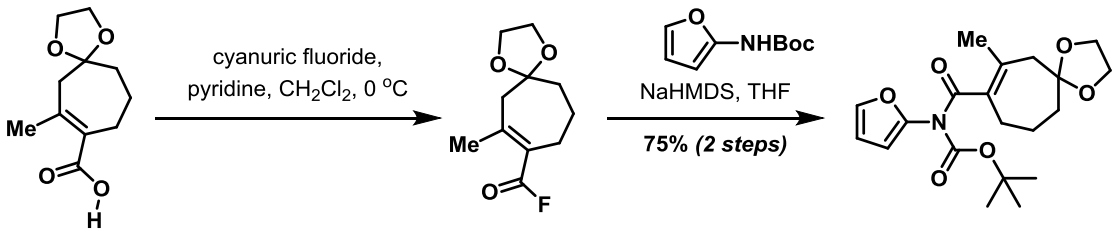
mp 82-84 °C

IR (film)/cm^{-1} ν_{max} 3444, 2939, 1676.

^{1}H NMR ($CDCl_3$, 500 MHz) δ_H 12.10 (br s, 1H), 4.01-3.91 (m, 4H), 2.64 (s, 2H), 2.54-2.49 (m, 2H), 2.19 (s, 3H), 1.93-1.87 (m, 2H), 1.70-1.62 (m, 2H).

^{13}C NMR ($CDCl_3$, 125 MHz) δ_C 174.5, 149.2, 129.6, 107.0, 64.6 (2C), 46.9, 40.7, 28.2, 25.1, 23.3.

HRMS (ES+) exact mass calculated for $[M+Na]^+$ ($C_{11}H_{16}NaO_4^+$) requires **m/z** 235.0941, found **m/z** 235.0943.



Compound 93

To a solution of acid **82** (4.10 g, 19.33 mmol) in dichloromethane (41 mL) held at 0 °C was added pyridine (1.72 mL, 21.26 mmol) followed by dropwise addition of cyanuric fluoride (1.66 mL, 19.3 mmol). The reaction was allowed to warm to room temperature and stirred for 30 mins. The crude reaction mixture was purified directly by flash column chromatography with PE:EtOAc [0.15:0.85] as the eluent to give the acid fluoride **94** as a colourless oil (assumed quantitative in next step).

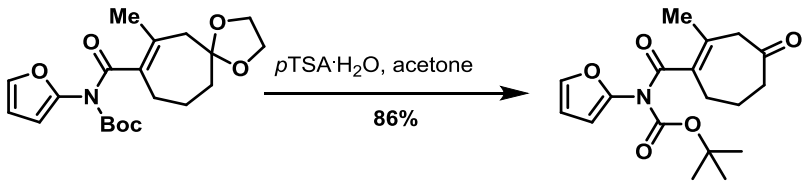
To a solution of *N*-Boc-2-aminofuran (3.90g, 21.26 mmol) in THF (20 mL) was added NaHMDS (1M in THF, 21.26 mL, 21.26 mmol) and the reaction stirred for 15 minutes. This amidofuran anion solution was added to a solution of acid fluoride (assumed quantitative from previous step) in THF (20 mL). After stirring for 1h, the reaction was quenched with saturated ammonium chloride (20 mL) and diluted with water (20 mL). The reaction was extracted with EtOAc (3 x 100 mL) and the combined organic layers washed with brine, dried over sodium sulfate and concentrated *in vacuo*. The crude product was purified by flash column chromatography with PE:EtOAc [0.85:0.15] as the eluent to give **93** as an orange oil (5.45g, 14.44 mmol, 75%).

IR (film)/cm^{-1} ν_{max} 2980, 2940, 2886, 1746, 1698.

^{1}H NMR ($CDCl_3$, 500 MHz) δ_H 7.31 (dd, 1H, J = 2.0, 1.0 Hz), 6.40 (dd, 1H, J = 3.0, 2.0 Hz), 6.16 (dd, 1H, J = 3.0, 1.0 Hz), 3.95-3.83 (m 4H), 2.45 (s, 2H), 2.32-2.29 (m, 2H), 1.90 (s, 3H), 1.85-1.81 (m, 2H), 1.65-1.59 (m, 2H), 1.46-1.43 (m, 9H).

^{13}C NMR ($CDCl_3$, 125 MHz) δ_C 172.2, 151.2, 143.8, 140.5, 136.2, 133.8, 111.2, 107.3, 105.9, 83.6, 64.4, 44.5, 30.0, 27.7, 23.7, 22.9.

HRMS (ES^+) exact mass calculated for $[M+Na]^+$ ($C_{20}H_{27}NO_6{}^{23}Na^+$) requires **m/z** 400.1731, found **m/z** 400.1725.



Compound 87

To a solution of **93** (5.80g, 15.4 mmol) in anhydrous acetone (153 mL) was added para-toluene sulfonic acid monohydrate (397 mg, 2.3 mmol, 0.15 eq.). The reaction mixture was stirred for 5 days until complete consumption of the starting material (analysed by ^{1}H NMR). The reaction was quenched with saturated sodium bicarbonate (150 mL), extracted with ethyl acetate (3 x 200 mL). The combined organic layers were washed with brine, dried over sodium sulfate and concentrated *in vacuo*. The crude product was purified by flash column chromatography with PE:EtOAc [8:2] as the eluant to give **87** as a pale yellow solid. (4.40g, 13.2 mmol, 86% yield.).

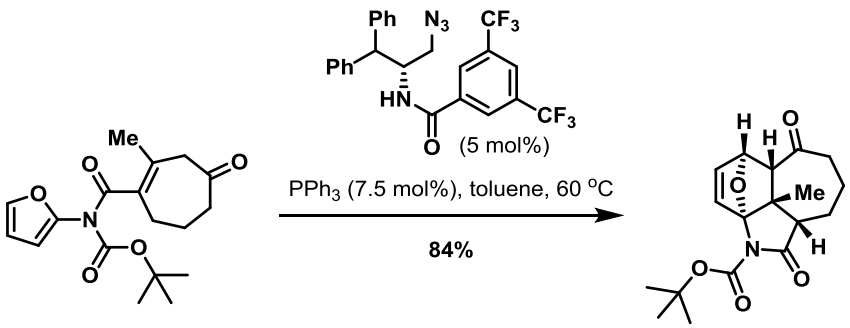
mp 44-47 ^{o}C

IR (film)/cm^{-1} ν_{max} 2981, 2939, 1748, 1706, 1609.

^{1}H NMR ($CDCl_3$, 500 MHz) δ_H 7.32 (dd, 1H, J = 2.0, 1.0 Hz), 6.42 (dd, 1H, J = 3.5, 2.0 Hz), 6.18 (dd, 1H, J = 3.5, 1.0 Hz), 3.18 (s, 2H), 2.55-2.48 (m, 4H), 2.01-1.94 (m, 2H), 1.90 (s, 3H), 1.45-1.41 (s, 9H).

^{13}C NMR ($CDCl_3$, 125 MHz) δ_C 207.3, 172.0, 150.8, 143.4, 140.7, 133.0, 130.6, 111.3, 105.9, 84.0, 49.4, 43.0, 29.9, 27.7, 23.7, 22.7.

HRMS (ES^{+}) exact mass calculated for $[M+Na]^{+}$ ($C_{18}H_{23}NO_5{}^{23}Na^{+}$) requires m/z 356.1468, found **m/z** 356.1467.



Compound 88

An oven dried round-bottom flask was charged **87** (4.0 g, 12.00 mmol), azide **96** (296 mg, 0.60 mmol) and triphenylphosphine (236 mg, 0.90 mmol). The flask was purged with argon followed by addition of anhydrous toluene (200 mL) and the reaction was heated to 60 °C for 24 hours. The reaction was concentrated to approximately 5 mL remaining solvent *in vacuo*, and the crude product was purified by flash column chromatography with PE:EtOAc [0.65:0.35] as the eluent to give **88** as an off white solid foam (3.35 g, 84%, 92:8 dr, 90% ee major diastereomer).

HPLC (Chiralpak AD, hexane:isopropanol [95:5], 1.0 mL/min, λ=220 nm) t_R= 26.7 min (major), 37.3 min (minor).

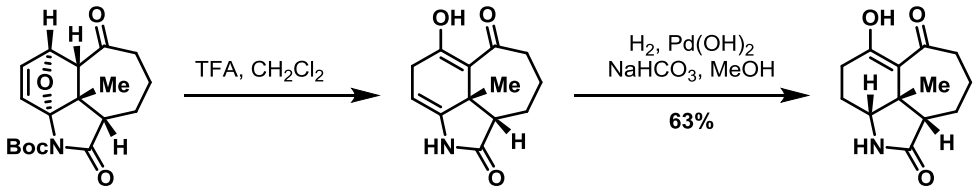
mp 137-140 °C.

IR (film)/cm^{-1} ν_{max} 2980 (C-H), 2872 (C-H), 1791 (C=O), 1766 (C=O), 1705 (C=O)

^{1}H NMR ($CDCl_3$, 500 MHz) δ_H 6.55 (d, 1H, H^{11}, J = 6.0 Hz), 6.47 (dd, 1H, H^{12}, J = 6.0, 2.0 Hz), 5.44 (br d, 1H, H^{13}, J = 2.0 Hz), 2.62-2.42 (m, 3H, $H^{3, 6}$), 2.27 (s, 1H, H^1), 2.08-1.94 (m, 2H, $H^{4a, 5a}$), 1.92-1.78 (m, 2H, $H^{4b, 5b}$), 1.52 (s, 9H, H^{16}), 1.29 (s, 3H, H^8).

^{13}C NMR ($CDCl_3$, 125 MHz) δ_C 207.9 (C^2), 176.8 (C^9), 149.0 (C^{14}), 134.4 (C^{11}), 134.1 (C^{12}), 104.0 (C^{10}), 84.3 (C^{15}), 76.5 (C^{13}), 64.9 (C^1), 54.6 (C^6), 45.4 (C^7), 39.5 (C^3), 27.9 ($C^{8, 16}$), 27.8 (C^5), 24.5 (C^4).

HRMS (ES^+) exact mass calculated for $[M+Na]^+$ ($C_{18}H_{23}NO_5{}^{23}Na^+$) requires **m/z** 356.1468, found **m/z** 356.1465.



Compound 104

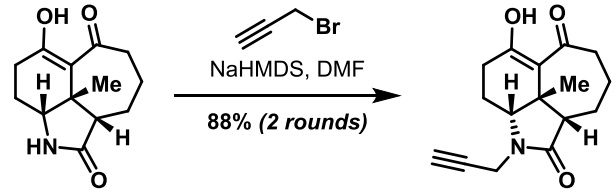
To a solution of **88** (2.0g, 6.00 mmol) in dichloromethane (100 mL) with light protection was added trifluoroacetic acid (4.59 mL, 60 mmol) and the reaction stirred for 5 hours. Next, toluene (20 mL) was added, and the reaction concentrated *in vacuo*, first removing the dichloromethane, then TFA and finally the toluene. The crude enamide was redissolved in methanol (100 mL) followed by addition of sodium hydrogencarbonate (approx. 100mg) and palladium hydroxide (2g, 20% on carbon, nominally 50% water). The atmosphere was replaced by hydrogen (quad-skinned balloon pressure) and the reaction was stirred vigorously overnight. The reaction was filtered through celite, washing through with methanol, and concentrated *in vacuo*. The crude product was purified twice by flash column chromatography with acetone:EtOAc [2:8] and then MeOH:CH_2Cl_2 [3:97] as the eluents to give **104** as a white solid (895 g, 3.80 mmol, 63%).

IR (film)/cm^{-1} $\boldsymbol{\nu_{max}}$ 3220, 2950, 2866, 1691, 1593, 1452.

^{1}H NMR ($CDCl_3$, 500 MHz) δ_H 6.80 (br s, 1H), 3.40 (dd, 1H, J = 11.0, 4.0 Hz), 2.68 (app dt, 1H, J = 13.5, 10.0 Hz), 2.46-2.39 (m, 2H), 2.30 (ddd, 1H, J = 17.5, 12.5, 4.5 Hz), 2.22-2.15 (m, 2H), 2.03 (app dq, 1H, J = 13.0, 4.5 Hz), 1.86-1.78 (m, 2H), 1.63-1.54 (m, 1H), 1.51-1.41 (m, 4H).

^{13}C NMR ($CDCl_3$, 125 MHz) δ_C 199.2, 185.7, 178.5, 111.2, 62.2, 52.1, 42.3, 37.0, 31.5, 29.6, 28.5, 26.3, 22.1.

HRMS (ES^+) exact mass calculated for $[M+Na]^+$ ($C_{13}H_{17}NO_3{}^{23}Na^+$) requires **m/z** 258.1101, found **m/z** 258.1099.



Compound 105

To a solution of **104** (880 mg, 3.74 mmol) in anhydrous DMF (44 mL) at 0 °C was added NaHMDS (1M in THF, 7.86 mL, 7.86 mmol) dropwise. After 15 minutes, propargyl bromide (80% w/w in toluene, 1.0 mL, 9.36 mmol) was added in one portion, and the reaction stirred for a further 15 minutes. The reaction was quenched with 1M HCl (100 mL) and extracted with EtOAc (3 x 100 mL). The combined organic layers were washed with 5% aqueous LiCl, dried over sodium sulfate and concentrated *in vacuo*. The crude product was purified by flash column chromatography with PE:EtOAc [6:4] as the eluent to give **105** as an off white solid (640 mg , 2.36 mmol, 63%), followed by acetone:EtOAc [2:8] as the eluent to give the starting material **104** (240 mg, 1.02 mmol, 27%). The starting material was re-subjected to the same reaction conditions to yield further product (210 mg, 0.77 mmol, 75%). Combined yield of **105** (850 mg, 3.11 mmol, 83%).

A sample of enantioenriched material was recrystallised to enantiopurity from dichloromethane/hexane. The first two crops of crystals were collected (178 mg, 65% ee). The mother liquor was concentrated *in vacuo* to give upgraded **105** (580 mg, >99% ee). **HPLC** (Chiralpak IB, hexane:isopropanol [95:5], 1.0 mL/min, λ=280 nm) t_R= 36.0 min (major), 40.3 min (minor).

mp enantiopure: 139-143 °C.

IR (film)/cm^{-1} ν_{max} 3259, 2980, 2889, 1673, 1586, 1451.

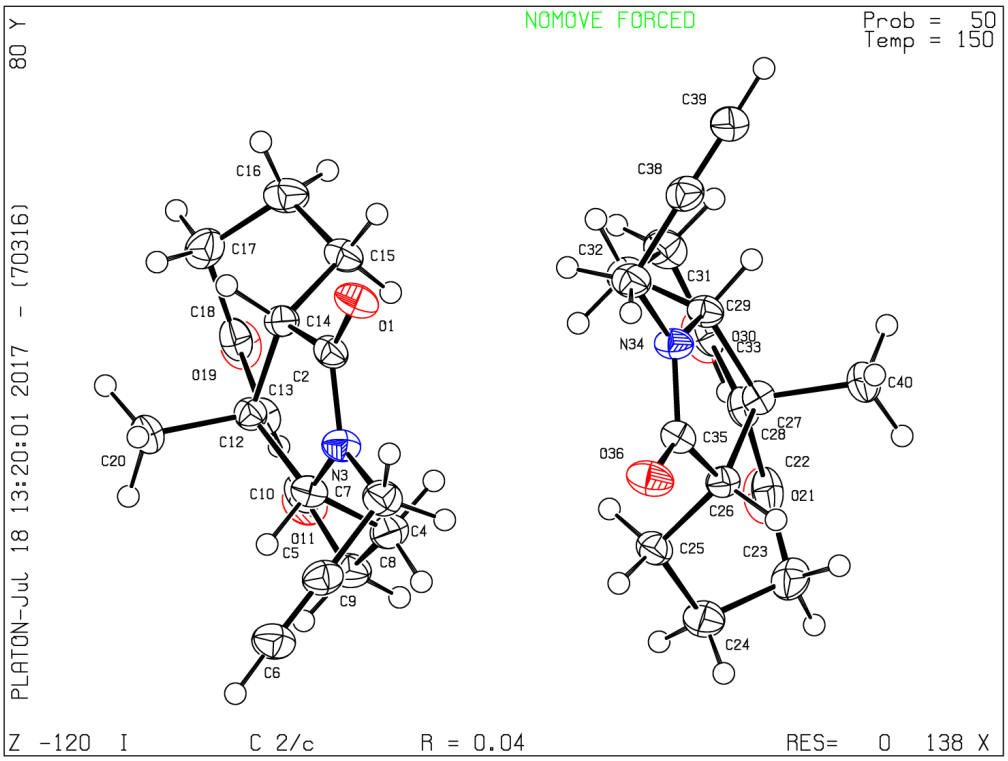
^{1}H NMR ($CDCl_3$, 400 MHz) δ_H 4.61 (dd, 1H, J = 17.7, 2.6 Hz), 3.74 (dd, 1H, J = 17.7, 2.6 Hz), 3.50 (dd, J = 11.8, 4.3 Hz), 2.65 (m, 1H), 2.49 – 2.29 (m, 3H), 2.29 – 2.21 (m, 3H), 2.17 (dddd, 1H, J = 14.1, 5.9, 3.9, 2.0 Hz), 1.81 (m, 2H), 1.50 (dddd, 1H, J = 14.1, 12.2, 10.8, 7.9 Hz), 1.40 (s, 3H), 1.29 (m, 1H).

^{13}C NMR ($CDCl_3$, 100 MHz, δ_C 199.1, 185.8, 174.4, 111.3, 77.3, 72.6, 65.7, 52.6, 40.0, 36.8, 31.7, 30.4, 29.6, 26.5, 25.7, 22.1.

HRMS (ES^+) exact mass calculated for $[M+Na]^+$ ($C_{16}H_{19}O_3N^{23}Na^+$) requires 296.1257, found **m/z** 296.1258.

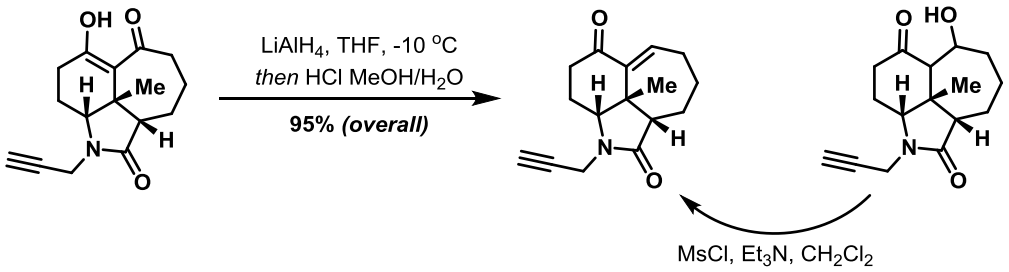
Crystallographic data for compound 105

Crystal data	
Chemical formula	$C_{18.29}H_{21.71}N_{1.14}O_{3.43}$
M_r	312.38
Crystal system, space group	Monoclinic, *C*2/*c*
Temperature (K)	150
a, *b*, *c* (Å)	31.6613 (3), 8.1740 (1), 22.2379 (2)
β (°)	107.4753 (5)
V (Å^3)	5489.54 (10)
Z	14
Radiation type	Mo *K*α
μ (mm^{-1})	0.09
Crystal size (mm)	0.30 × 0.20 × 0.20
Data collection	
Diffractometer	Nonius KappaCCD
Absorption correction	Multi-scan *DENZO*/*SCALEPACK* (Otwinowski & Minor, 1997)
T_{min}, T_{max}	0.77, 0.98
No. of measured, independent and observed [$I > 2.0\sigma(I)$] reflections	58584, 6260, 4980
R_{int}	0.020
$(\sin\theta/\lambda)_{max}$ (Å^{-1})	0.650
Refinement	
$R[F^2 > 2\sigma(F^2)]$, $wR(F^2)$, S	0.039, 0.100, 1.02
No. of reflections	6259
No. of parameters	369
No. of restraints	4
H-atom treatment	H atoms treated by a mixture of independent and constrained refinement
$\Delta\rho_{max}$, $\Delta\rho_{min}$ (e Å^{-3})	0.33, −0.29



O1—C2	1.2289 (15)	O21—C22	1.2765 (15)
C2—N3	1.3474 (16)	C22—C23	1.492 (2)
C2—C14	1.5128 (17)	C22—C28	1.4291 (18)
N3—C4	1.4604 (16)	C23—C24	1.538 (2)
N3—C7	1.4537 (15)	C24—C25	1.5355 (18)
C4—C5	1.4695 (18)	C25—C26	1.5328 (16)
C5—C6	1.1794 (19)	C26—C27	1.5622 (16)
C7—C8	1.5183 (17)	C26—C35	1.5182 (16)
C7—C13	1.5653 (17)	C27—C28	1.5284 (16)
C8—C9	1.5220 (19)	C27—C33	1.5646 (16)
C9—C10	1.4927 (19)	C27—C40	1.5427 (16)
C10—O11	1.3129 (15)	C28—C29	1.3879 (18)
C10—C12	1.3871 (18)	C29—O30	1.3150 (15)
C12—C13	1.5288 (16)	C29—C31	1.490 (2)
C12—C18	1.4304 (18)	C31—C32	1.5189 (19)
C13—C14	1.5647 (16)	C32—C33	1.5156 (17)
C13—C20	1.5418 (16)	C33—N34	1.4528 (15)
C14—C15	1.5344 (16)	N34—C35	1.3431 (15)
C15—C16	1.5272 (18)	N34—C37	1.4632 (15)
C16—C17	1.535 (2)	C35—O36	1.2276 (14)
C17—C18	1.496 (2)	C37—C38	1.4640 (18)
C18—O19	1.2772 (15)	C38—C39	1.1838 (19)
O1—C2—N3	124.95 (11)	O21—C22—C23	117.34 (12)

O1—C2—C14	126.01 (11)	O21—C22—C28	121.13 (13)
N3—C2—C14	109.04 (10)	C23—C22—C28	121.34 (11)
C2—N3—C4	122.75 (10)	C22—C23—C24	111.33 (11)
C2—N3—C7	115.19 (10)	C23—C24—C25	113.79 (11)
C4—N3—C7	122.05 (10)	C24—C25—C26	112.54 (10)
N3—C4—C5	110.65 (11)	C25—C26—C27	115.84 (10)
C4—C5—C6	177.90 (14)	C25—C26—C35	110.91 (10)
N3—C7—C8	112.55 (10)	C27—C26—C35	104.76 (9)
N3—C7—C13	103.83 (9)	C26—C27—C28	115.24 (10)
C8—C7—C13	115.05 (10)	C26—C27—C33	103.78 (9)
C7—C8—C9	108.35 (11)	C28—C27—C33	111.70 (10)
C8—C9—C10	109.52 (11)	C26—C27—C40	109.15 (10)
C9—C10—O11	114.95 (11)	C28—C27—C40	109.62 (9)
C9—C10—C12	122.07 (11)	C33—C27—C40	106.92 (10)
O11—C10—C12	122.87 (12)	C27—C28—C22	121.29 (11)
C10—C12—C13	121.31 (11)	C27—C28—C29	121.33 (11)
C10—C12—C18	117.45 (11)	C22—C28—C29	117.37 (11)
C13—C12—C18	121.21 (11)	C28—C29—O30	122.48 (13)
C12—C13—C7	111.97 (10)	C28—C29—C31	122.35 (11)
C12—C13—C14	114.97 (10)	O30—C29—C31	115.09 (12)
C7—C13—C14	103.83 (9)	C29—C31—C32	109.40 (11)
C12—C13—C20	109.56 (10)	C31—C32—C33	108.11 (11)
C7—C13—C20	106.32 (10)	C32—C33—C27	115.35 (10)
C14—C13—C20	109.75 (10)	C32—C33—N34	112.47 (10)
C13—C14—C2	104.98 (9)	C27—C33—N34	103.75 (9)
C13—C14—C15	116.25 (10)	C33—N34—C35	115.16 (10)
C2—C14—C15	111.31 (10)	C33—N34—C37	122.05 (10)
C14—C15—C16	111.92 (11)	C35—N34—C37	122.48 (10)
C15—C16—C17	113.44 (11)	C26—C35—N34	109.01 (10)
C16—C17—C18	111.66 (11)	C26—C35—O36	125.84 (11)
C17—C18—C12	121.35 (11)	N34—C35—O36	125.15 (11)
C17—C18—O19	117.47 (12)	N34—C37—C38	110.68 (10)
C12—C18—O19	121.11 (12)	C37—C38—C39	177.64 (14)



Compound 108

To a solution of **105** (550 mg, 2.01 mmol) in anhydrous THF (55 mL) at -10 °C (acetone/ice bath) was added $LiAlH_4$ (1M in THF, 4.02 mL, 4.02 mmol) dropwise (vigorous gas evolution observed). The reaction was stirred for 15 minutes and carefully quenched with dropwise addition of MeOH (20 mL) followed by aqueous 1M HCl (40 mL). The reaction was warmed to rt and stirred for 1 hour, before being extracted with DCM (3 x 40 mL). The combined organic layers were dried over sodium sulfate and concentrated *in vacuo*. The crude product was purified by flash column chromatography with PE:EtOAc [6:4] as the eluant to give **108** as a white solid (443 mg) then PE:EtOAc [2:8] to give **110** as a crude yellow oil (75 mg, 0.27 mmol).

110 was redissolved in CH_2Cl_2 (3 mL) followed by addition of Et_3N (0.078 mL, 0.56 mmol) and MsCl (0.042 mL, 0.54 mmol) in sequence. The reaction was stirred for 5 hours, and quenched with addition of 1M HCl (5 mL). The reaction was extracted with CH_2Cl_2 (3 x 5 mL) and the combined organic layers dried over sodium sulfate and concentrated *in vacuo*. The crude product was purified by flash column chromatography with PE:EtOAc [6:4] as the eluent to give **108** as a white solid (49 mg). Combined total yield: (492 mg, 1.91 mmol, 95%).

$[\alpha]_D^{25}$ = -25.4 (*c* 1.0, $CHCl_3$)

mp: 91-94 °C.

IR (film)/cm^{-1} ν_{max} 2981 (C-H), 2361 (C≡C), 1675 (C=O), 1604 (C=O), 1443 (C=C).

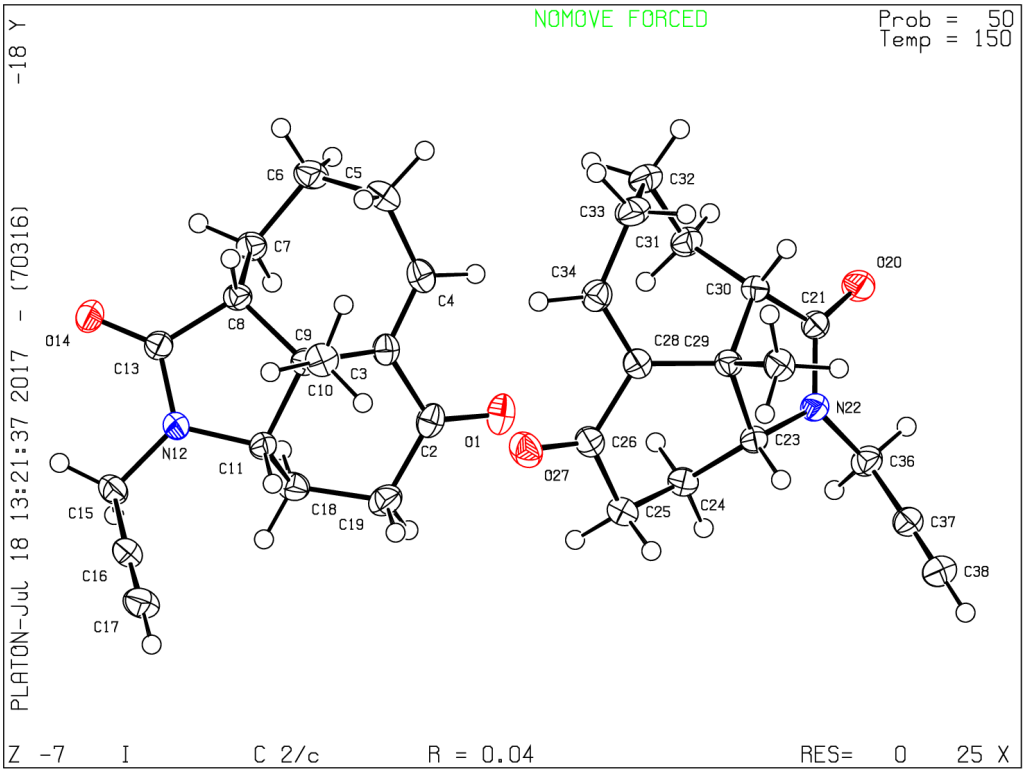
^{1}H NMR ($CDCl_3$, 400 MHz) δ_H 6.88 (dd, 1H, J = 8.6, 7.6 Hz), 4.60 (dd, 1H, J = 17.7, 2.6 Hz), 3.76 (dd, 1H, J = 17.7, 2.5 Hz), 3.48 (dd, 1H, J = 12.0, 3.8 Hz), 2.54 (dt, 1H, J = 18.4, 3.3, 2.5 Hz), 2.38-2.19 (m, 6H), 2.11 (ddt, 1H), 1.85-1.46 (, 5H), 1.32 (s, 3H).

^{13}C NMR ($CDCl_3$ 100 MHz) δ_C 200.3, 175.1, 141.9, 139.8, 100.0, 72.6, 65.3, 51.7, 43.0, 35.3, 30.3, 29.1, 27.2, 25.4, 24.1, 22.2.

HRMS (ES^+) exact mass calculated for $[M+Na]^+$ ($C_{16}H_{19}O_2N^{23}Na$) requires 280.1308, found **m/z** 280.1308.

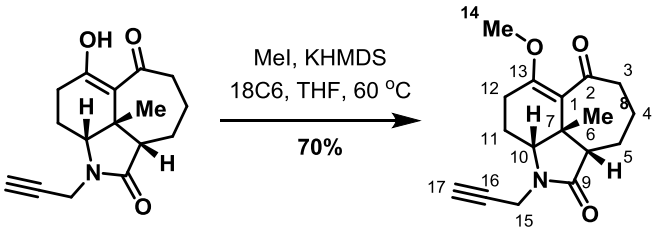
Crystallographic data for compound 108

Crystal data	
Chemical formula	$C_{17.07}H_{20.27}N_{1.07}O_{2.13}$
M_r	274.49
Crystal system, space group	Monoclinic, *C*2/*c*
Temperature (K)	150
a, *b*, *c* (Å)	30.6579 (4), 8.2851 (1), 21.8388 (3)
β (°)	104.9073 (5)
V (Å^3)	5360.44 (12)
Z	15
Radiation type	Mo *K*α
μ (mm^{-1})	0.08
Crystal size (mm)	0.30 × 0.25 × 0.20
Data collection	
Diffractometer	Nonius KappaCCD
Absorption correction	Multi-scan *DENZO*/*SCALEPACK* (Otwinowski & Minor, 1997)
T_{min}, T_{max}	0.87, 0.98
No. of measured, independent and observed [$I > 2.0\sigma(I)$] reflections	36191, 6124, 5005
R_{int}	0.021
$(\sin\theta/\lambda)_{max}$ (Å^{-1})	0.650
Refinement	
$R[F^2 > 2\sigma(F^2)]$, $wR(F^2)$, S	0.041, 0.104, 1.01
No. of reflections	6124
No. of parameters	343
H-atom treatment	H-atom parameters constrained
$\Delta\rho_{max}$, $\Delta\rho_{min}$ (e Å^{-3})	0.31, −0.28



O1—C2	1.2237 (15)	O20—C21	1.2290 (14)
C2—C3	1.4940 (17)	C21—N22	1.3479 (15)
C2—C19	1.5014 (18)	C21—C30	1.5165 (16)
C3—C4	1.3411 (17)	N22—C23	1.4530 (15)
C3—C9	1.5298 (15)	N22—C36	1.4609 (15)
C4—C5	1.4954 (18)	C23—C24	1.5201 (16)
C5—C6	1.5396 (18)	C23—C29	1.5592 (16)
C6—C7	1.5332 (17)	C24—C25	1.5200 (17)
C7—C8	1.5339 (16)	C25—C26	1.5144 (18)
C8—C9	1.5638 (16)	C26—O27	1.2219 (15)
C8—C13	1.5168 (16)	C26—C28	1.4952 (16)
C9—C10	1.5394 (16)	C28—C29	1.5283 (16)
C9—C11	1.5655 (16)	C28—C34	1.3410 (17)
C11—N12	1.4532 (14)	C29—C30	1.5659 (16)
C11—C18	1.5181 (17)	C29—C35	1.5391 (16)
N12—C13	1.3455 (15)	C30—C31	1.5391 (16)
N12—C15	1.4625 (15)	C31—C32	1.5327 (18)
C13—O14	1.2272 (14)	C32—C33	1.5385 (19)
C15—C16	1.4639 (17)	C33—C34	1.4957 (18)
C16—C17	1.1874 (19)	C36—C37	1.4651 (18)
C18—C19	1.5218 (17)	C37—C38	1.1890 (19)
O1—C2—C3	121.84 (12)	O20—C21—N22	125.29 (11)
O1—C2—C19	120.43 (11)	O20—C21—C30	125.77 (11)

C3—C2—C19	117.71 (10)	N22—C21—C30	108.94 (10)
C2—C3—C4	116.31 (11)	C21—N22—C23	114.91 (10)
C2—C3—C9	121.02 (10)	C21—N22—C36	123.02 (10)
C4—C3—C9	122.67 (11)	C23—N22—C36	121.94 (10)
C3—C4—C5	125.04 (11)	N22—C23—C24	112.75 (10)
C4—C5—C6	110.62 (10)	N22—C23—C29	103.71 (9)
C5—C6—C7	113.35 (10)	C24—C23—C29	114.29 (9)
C6—C7—C8	112.71 (10)	C23—C24—C25	108.39 (10)
C7—C8—C9	116.65 (9)	C24—C25—C26	112.05 (10)
C7—C8—C13	110.36 (10)	C25—C26—O27	120.53 (11)
C9—C8—C13	104.88 (9)	C25—C26—C28	117.64 (10)
C3—C9—C8	114.07 (9)	O27—C26—C28	121.83 (11)
C3—C9—C10	108.52 (9)	C26—C28—C29	120.36 (10)
C8—C9—C10	109.49 (9)	C26—C28—C34	116.71 (11)
C3—C9—C11	112.98 (9)	C29—C28—C34	122.93 (11)
C8—C9—C11	103.89 (9)	C28—C29—C23	112.65 (9)
C10—C9—C11	107.65 (9)	C28—C29—C30	114.20 (9)
C9—C11—N12	103.69 (9)	C23—C29—C30	103.73 (9)
C9—C11—C18	114.49 (9)	C28—C29—C35	108.78 (9)
N12—C11—C18	112.81 (10)	C23—C29—C35	107.35 (9)
C11—N12—C13	115.24 (10)	C30—C29—C35	109.86 (9)
C11—N12—C15	121.79 (10)	C21—C30—C29	104.61 (9)
C13—N12—C15	122.79 (10)	C21—C30—C31	110.85 (10)
C8—C13—N12	108.98 (10)	C29—C30—C31	116.55 (9)
C8—C13—O14	125.69 (11)	C30—C31—C32	111.90 (11)
N12—C13—O14	125.33 (11)	C31—C32—C33	112.46 (10)
N12—C15—C16	110.80 (10)	C32—C33—C34	111.46 (11)
C15—C16—C17	178.19 (13)	C33—C34—C28	124.46 (11)
C11—C18—C19	108.23 (10)	N22—C36—C37	110.80 (10)
C18—C19—C2	111.22 (10)	C36—C37—C38	178.19 (14)



Compound 106

To a solution of **105** (75 mg, 0.274 mmol) in anhydrous tetrahydrofuran (7.5 mL) was added 18-crown-6 (29 mg, 0.110 mmol, 0.4 eq.). Next KHMDS (0.5M in toluene, 659 µL, 0.329 mmol, 1.2 eq.) was added dropwise, and the resultant slurry stirred for 15 minutes, followed by addition of methyl iodide (51 µL, 0.823 mmol, 3 eq.). The reaction mixture was heated to 60 °C for 4 hours until complete consumption of the staring material. The reaction mixture was diluted with water (15 mL) and extracted with ethyl acetate (3 x 15 mL). The combined organic layers were washed with brine, dried over anhydrous sodium sulfate and concentrated *in vacuo*. The crude product was purified by flash column chromatography with a gradient of 30:70 to 40:60 ethyl acetate/pet. ether as the eluant to give **106** as an orange crystalline solid. (55.3 mg, 0.192 mmol, 70% yield).

mp 118 - 122 °C.

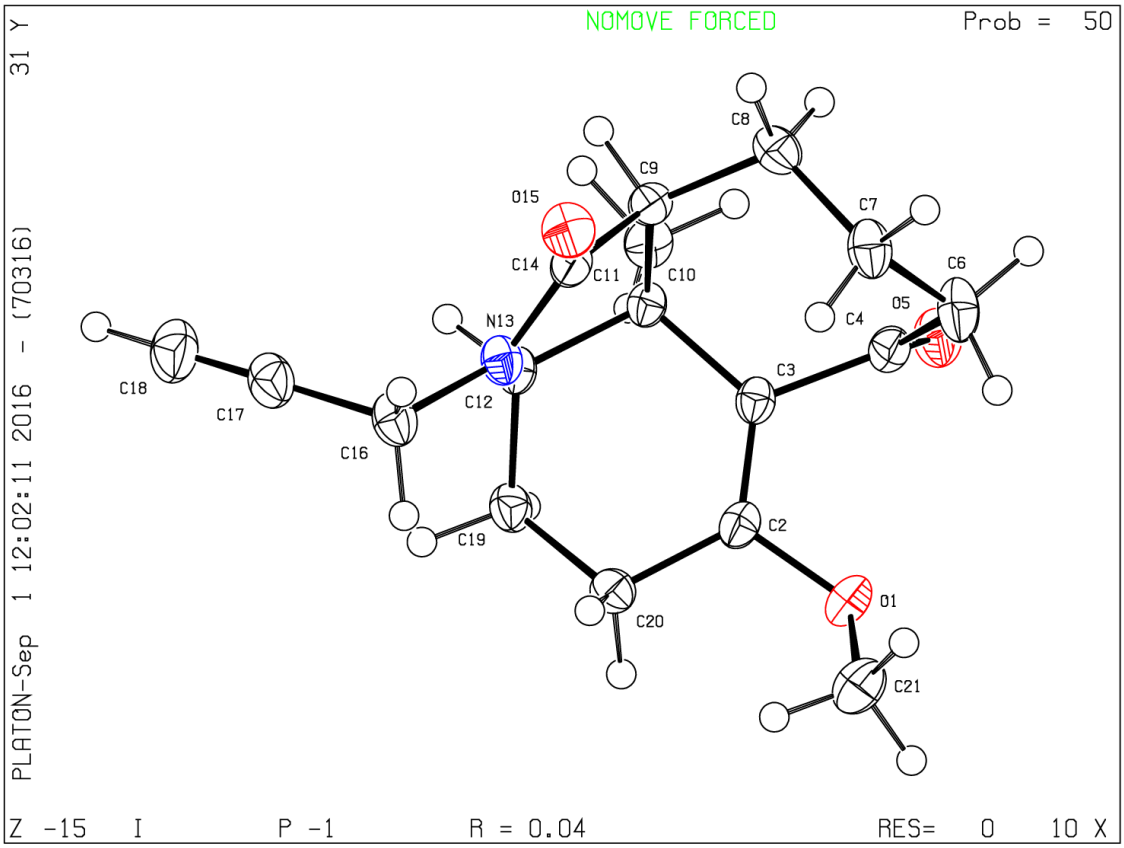
IR (powder)/cm^{-1} ν_{max} 2957 (C-H), 1681 (C=O), 1433 (C=C).

^{1}H NMR ($CDCl_3$, 400 MHz) δ_H 4.68 (dd, 1H, H^{15a}, J = 17.6, 2.6 Hz), 3.66 (dd, 1H, H^{15b}, J = 17.6, 2.4 Hz), 3.53 (dd, 1H, H^{10}, J = 5.3, 2.9 Hz), 3.49 (s, 3H, H^{14}), 2.60 (dtd, 1H, H^{3a}, J = 15.9, 5.4, 1.2 Hz), 2.43-2.33 (m, 2H, $H^{3b, 6}$), 2.29-2.19 (m, 2H, $H^{5a, 17}$), 2.18-2.01 (m, 3H, $H^{11a, 12}$), 1.95 (dddd, 1H, H^{11b}, J = 14.2, 9.9, 5.6, 2.9 Hz), 1.75-1.68 (m, 2H, H^4), 1.58 (m, 1H, H^{5b}), 1.27 (s, 3H, H^8).

^{13}C NMR ($CDCl_3$, 100 MHz, δ_C 210.3 (C^2), 175.2 (C^9), 150.1 (C^1), 121.1 (C^{13}), 77.2 (C^{18}), 72.4 (C^{17}), 60.6 (C^{10}), 55.7 (C^{14}), 54.5 (C^6), 44.5 (C^3), 40.6 (C^7), 20.1 (C^{15}), 25.9 (C^8), 25.1 (C^5), 21.9 (C^{11}), 20.8 (C^4), 19.3 (C^{12}).

HRMS (ES^+) exact mass calculated for $[M+H]^+$ ($C_{17}H_{22}O_3N^+$) requires 288.1594, found **m/z** 288.1593.

Crystallographic data for compound 106

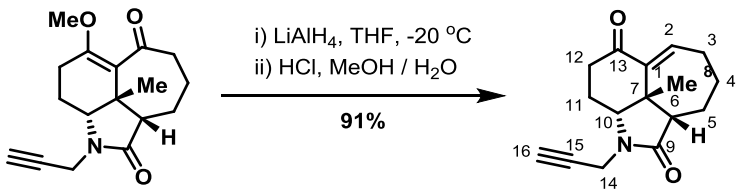


Crystal data	
Chemical formula	$C_{17}H_{21}NO_3$
M_r	287.36
Crystal system, space group	Triclinic, *P*1
Temperature (K)	150
a, *b*, *c* (Å)	8.3621 (2), 8.7019 (2), 11.4231 (3)
α, β, γ (°)	81.9776 (13), 75.6891 (12), 66.5459 (12)
V (Å³)	738.08 (2)
Z	2
Radiation type	Mo *K*α
μ (mm⁻¹)	0.09
Crystal size (mm)	0.3×0.2×0.4
Data collection	
Diffractometer	Nonius KappaCCD
Absorption correction	Multi-scan *DENZO*/*SCALEPACK* (Otwinowski & Minor, 1997)
T_{min}, T_{max}	1.00, 1.00
No. of measured, independent and observed [$I > 2.0\sigma(I)$] reflections	5727, 3345, 2834
R_{int}	0.017
$(\sin \theta/\lambda)_{max}$ (Å⁻¹)	0.650

Refinement	
$R[F^2 > 2\sigma(F^2)]$, $wR(F^2)$, S	0.038, 0.092, 0.96
No. of reflections	3345
No. of parameters	190
H-atom treatment	H-atom parameters constrained
$\Delta\rho_{max}$, $\Delta\rho_{min}$ (e Å^{-3})	0.32, −0.21

Selected geometric parameters (Å, º).

O1—C2	1.3876 (13)	C9—C14	1.5193 (16)
O1—C21	1.4285 (15)	C10—C11	1.5339 (15)
C2—C3	1.3289 (16)	C10—C12	1.5467 (15)
C2—C20	1.4998 (15)	C12—N13	1.4691 (14)
C3—C4	1.5096 (15)	C12—C19	1.5201 (15)
C3—C10	1.5222 (14)	N13—C14	1.3542 (15)
C4—O5	1.2141 (14)	N13—C16	1.4567 (14)
C4—C6	1.5036 (16)	C14—O15	1.2299 (13)
C6—C7	1.5293 (17)	C16—C17	1.4751 (17)
C7—C8	1.5311 (17)	C17—C18	1.1861 (19)
C8—C9	1.5316 (16)	C19—C20	1.5239 (15)
C9—C10	1.5537 (15)		
C2—O1—C21	115.62 (9)	C3—C10—C11	110.03 (9)
O1—C2—C3	117.32 (10)	C9—C10—C12	101.53 (8)
O1—C2—C20	117.63 (10)	C3—C10—C12	110.57 (9)
C3—C2—C20	124.74 (10)	C11—C10—C12	110.47 (9)
C2—C3—C4	118.84 (10)	C10—C12—N13	103.18 (8)
C2—C3—C10	124.37 (10)	C10—C12—C19	113.78 (9)
C4—C3—C10	116.77 (9)	N13—C12—C19	112.71 (9)
C3—C4—O5	121.50 (10)	C12—N13—C14	112.93 (9)
C3—C4—C6	116.64 (10)	C12—N13—C16	121.87 (9)
O5—C4—C6	121.84 (11)	C14—N13—C16	122.52 (9)
C4—C6—C7	112.83 (10)	C9—C14—N13	108.07 (9)
C6—C7—C8	114.00 (10)	C9—C14—O15	126.37 (10)
C7—C8—C9	115.28 (10)	N13—C14—O15	125.55 (11)
C8—C9—C10	121.12 (9)	N13—C16—C17	111.66 (10)
C8—C9—C14	112.41 (9)	C16—C17—C18	176.40 (13)
C10—C9—C14	104.17 (9)	C12—C19—C20	111.74 (9)
C9—C10—C3	111.66 (8)	C19—C20—C2	109.57 (9)
C9—C10—C11	112.32 (9)		



Compound 108

To a solution of **106** (20 mg, 0.070 mmol) in anhydrous tetrahydrofuran (2 mL) at -20 °C was added lithium aluminium hydride (1M solution in THF, 0.070 mL, 0.070 mmol, 1.0 eq.) and the reaction stirred for 30 mins. Next, the reaction was quenched with careful dropwise addition of methanol (1 mL) followed by aqueous HCl (1M, 2 mL). The reaction was warmed to room temperature and stirred for a further 30 mins before addition of a solution of Rochelle's salt (10 mL, aqueous 20% w/w.) and saturated $NaHCO_3$ (5 mL). The reaction was stirred for 30 mins and extracted with ethyl acetate (3 x 5 mL). The combined organic layers were washed with brine, dried over anhydrous sodium sulfate and concentrated *in vacuo*. The crude product was purified by flash column chromatography with 1:1 ethyl acetate: pet. ether as the eluent to give **108** as a pale yellow crystalline solid (16.3 mg, 0.0633 mmol, 91%).

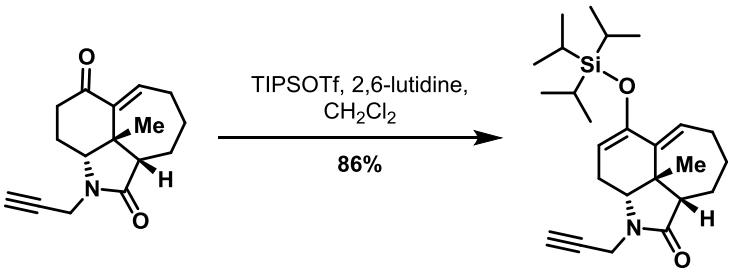
mp 128 – 130 °C.

IR 2981 (C-H), 2361 (C≡C), 1675 (C=O), 1604 (C=O), 1443 (C=C).

^{1}H NMR ($CDCl_3$, 400 MHz) δ_H 6.88 (dd, 1H, H^2, J = 8.6, 7.6 Hz), 4.60 (dd, 1H, H^{14a}, J = 17.7, 2.6 Hz), 3.76 (dd, 1H, H^{14b}, J = 17.7, 2.5 Hz), 3.48 (dd, 1H, H^{10}, J = 12.0, 3.8 Hz), 2.54 (dt, 1H, H^{3a}, J = 18.4, 3.3, 2.5 Hz), 2.38-2.19 (m, 6H, $H^{3b, 6, 11a, 12, 16}$), 2.11 (ddt, 1H, H^{5a}), 1.85-1.46 (, 5H, $H^{4, 5b, 11b}$), 1.32 (s, 3H, H^8).

^{13}C NMR ($CDCl_3$ 100 MHz) δ_C 200.3 (C^{13}), 175.1 (C^9), 141.9 (C^1), 139.8 (C^2), 100.0 (C^{15}), 72.6 (C^{16}), 65.3 (C^{10}), 51.7 (C^6), 43.0 (C^7), 35.3 (C^3), 30.3 (C^{14}), 29.1 (C^8), 27.2 (C^5), 25.4 (C^{11}), 24.1 (C^{12}), 22.2 (C^4).

HRMS (ES^+) exact mass calculated for $[M+Na]^+$ ($C_{16}H_{19}O_2N^{23}Na$) requires 280.1308, found **m/z** 280.1308.



Compound 123

To a solution of **108** (420 mg, 1.63 mmol) in CH_2Cl_2 (40 mL) was added 2,6-lutidine (0.473 mL, 4.08 mmol) and TIPSOTf (0.877 mL, 3.26 mmol) sequentially and the reaction was left to stir overnight at rt. The reaction mixture was washed with saturated copper sulfate (3 x 10 mL), washed with brine, dried over sodium sulfate and concentrated *in vacuo*. The crude product was purified by flash column chromatography eluting first with PE:Et_2O [9:1] to remove silyl impurities, then PE:Et_2O [8:2] to give **123** as an off-white crystalline solid (580 mg, 1.40 mmol, 86%).

$[\alpha]_D^{25}$ = -1.1 (*c* 1.0, $CHCl_3$)

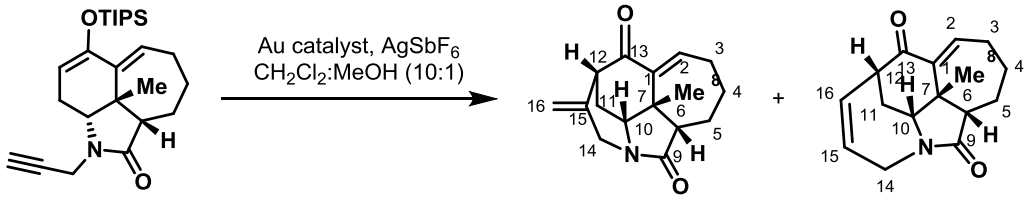
mp: 96-99 ^oC

IR (film)/cm^{-1} ν_{max} 3329, 2940, 2865, 2114, 1699, 1448.

^{1}H NMR ($CDCl_3$, 400 MHz) δ_H 6.33 (dd, 1H, J = 8.9, 5.8 Hz), 4.80 (app t, J = 4.7 Hz), 4.59 (dd, 1H, J = 17.6, 2.6 Hz), 3.50 (dd, 1H, J = 17.6, 2.5 Hz), 3.37 (app t, 1H, J = 5.3 Hz), 2.54 (dt, 1H, J = 16.8, 4.7 Hz), 2.34-2.16 (m, 5H), 1.96 (m, 2H), 1.70 (m, 1H), 1.50 (m, 1H), 1.34 (s, 3H), 1.18 (3H, m), 1.10 (app dd, 12H, J = 7.3, 4.3 Hz).

^{13}C NMR ($CDCl_3$ 100 MHz) δ_C 175.9, 150.5, 135.9, 126.4, 97.9, 77.9, 71.7, 62.4, 52.5, 45.7, 29.4, 26.3, 26.1, 24.8, 23.9, 22.0, 18.1, 12.8.

HRMS (ES^+) exact mass calculated for $[M+H]^+$ ($C_{25}H_{40}O_2N^{28}Si$) requires 414.2823, found **m/z** 414.2817.



Compound 124 and 125

To a solution of **123** (5 mg) in a 10:1 mixture of dichloromethane:methanol (0.5 mL) was added the relevant gold catalyst (20 mol%) followed by silver hexafluoroantimonate (20 mol%). The reaction was monitored by TLC and purified directly by flash column chromatography.

Characterisation for product 124.

^{1}H NMR ($CDCl_3$, 400 MHz) δ_H 7.31 (dd, 1H, H^2, J = 9.6, 4.8 Hz), 4.99 (dt, 1H, H^{16a}, J = 2.4, 1.1 Hz), 4.88 (dt, 1H, H^{16b}, J = 2.3, 1.0 Hz), 4.47 (dd, 1H, H^{14a}, J = 16.0, 0.9 Hz), 3.58-3.49 (m, 2H, $H^{10, 14b}$), 3.32 (dt, 1H, H^{12}, J = 3.6, 1.9 Hz), 2.50 (t, 1H, H^6, J = 5.0 Hz), 2.40 (m, 1H, H^{3a}), 2.18 (m, 4H, $H^{4a, 5a, 11}$), 1.85 (dddd, 1H, H^{2b}, J = 14.9, 12.0, 5.7, 3.0 Hz), 1.63 (app ddq, 1H, H^{4b}, J = 13.1, 6.5, 3.2 Hz), 1.48-1.39 (m, 1H, H^{5b}), 1.31 (s, 3H, H^8).

^{13}C NMR ($CDCl_3$ 100 MHz) δ_C 195.7 (C^{13}), ,175.1 (C^9), 149.4 (C^{16}), 139.5 (C^1), 136.8 (C^{15}), 112.2 (C^2), 58.2 (C^{10}), 51.4 (C^7), 51.0 (C^6), 46.5 (C^{12}), 39.7 (C^{14}), 27.4 (C^3), 24.6 (C^4), 19.9 (C^8), 19.3 (C^5), 18.7 (C^{11}).

HRMS (ES^+) exact mass calculated for $[M+Na]^+$ ($C_{16}H_{19}O_2N^{23}Na$) requires **m/z** 280.1308, found **m/z** 280.1308.

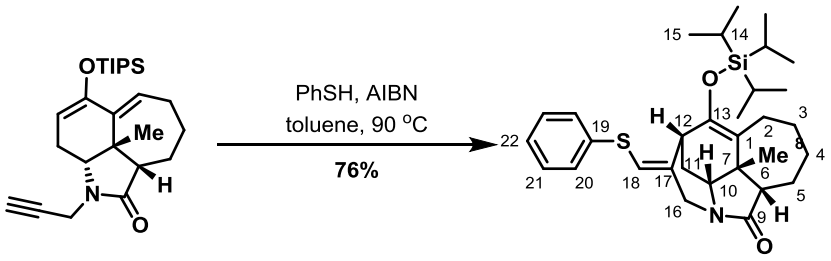
Characterisation for isomer 125.

mp 147 – 152 ^{o}C.

^{1}H NMR ($CDCl_3$, 400 MHz) δ_H 7.27 (ddd, 1H, H^2, J = 9.3, 4.0, 0.7 Hz), 5.79 (app ddt, 1H, H^{16}, J = 10.7, 8.3, 1.7, 1.4 Hz), (ddd, 1H, H^{15}, J = 10.8, 8.3, 2.9 Hz), 4.52 (dd, 1H, H^{14a}, J = 17.6, 6.8 Hz), 3.46 (m, 2H, $H^{10, 14b}$), 3.22 (ddd, 1H, H^{12}, J = 8.0, 4.8, 3.2 Hz), 2.35 (m, 5H, $H^{3a, 4a, 5a, 11}$), 2.08-1.96 (m, 1H, H^{5b}), 1.90 (dddd, 1H, H^{3b}, J = 14.7, 10.6, 6.0, 2.4 Hz). 1.69 (dtdd, 1H, H^{4b}, J = 15.1, 7.5, 4.6, 2.6 Hz), 1.56-1.43 (m, 1H, H^{5b}), 1.35 (s, 3H, H^8).

^{13}C NMR ($CDCl_3$ 100 MHz) δ_C 195.4 (C^{13}), 173.2 (C^9), 147.6 (C^{16}), 136.1 (C^1), 129.1 (C^{15}), 128.8 (C^2), 60.1 (C^{10}), 51.1 (C^6), 48.2 (C^7), 44.5 (C^{12}), 36.9 (C^{14}), 27.8 (C^3), 24.5 (C^4), 23.5 (C^8), 20.8 (C^5), 19.7 (C^{11}).

HRMS (ES^+) exact mass calculated for $[M+Na]^+$ ($C_{16}H_{19}O_2N^{23}Na$) requires **m/z** 280.1308, found **m/z** 280.1308.



Compound 137

To a solution of **123** (185mg, 0.447 mmol) in anhydrous toluene (75 mL) was added AIBN (22mg, 0.134 mmol, 0.3 eq.). The reaction was degassed under vacuum and the atmosphere replaced with nitrogen; this operation was repeated three times. Next, thiophenol (182 µL, 1.789 mmol, 4 eq.) was added and the reaction heated to 90 °C for 3 hours. The reaction was diluted with saturated sodium bicarbonate (100 mL) and extracted with ethyl acetate (3 x 100 mL). The combined organic layers were washed with brine, dried over anhydrous sodium sulfate and concentrated *in vacuo*. The crude product was purified by flash column chromatography with a gradient of 10:90 to 15:85 ethyl acetate/petrol ether as the eluent to give **137** as a white solid. (177 mg, 0.338 mmol 76%).

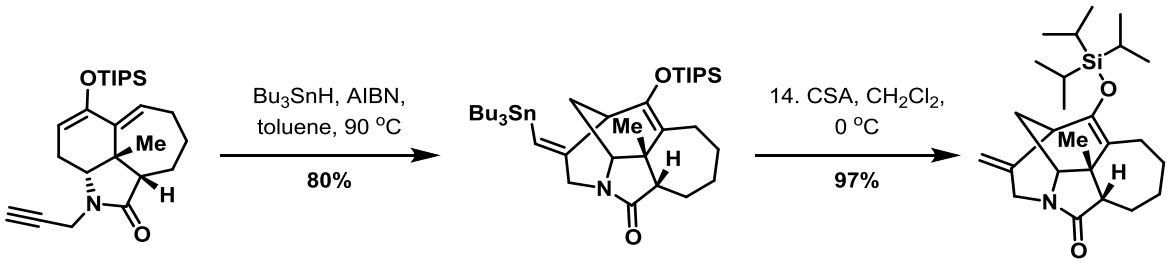
mp 128-135 °C.

IR 2944 (C-H), 2866 (C-H), 1698 (C=O), 1462 (C=C).

^{1}H NMR ($CDCl_3$, 400 MHz) δ_H 7.32 (m, 2H, H^{20}), 7.26 (m, 2H, H^{21}), 7.19 (m, 1H, H^{22}), 6.08 (br s, 1H, H^{18}), 4.97 (dd, 1H, H^{16a}, J = 17.0, 1.6 Hz), 3.60 (dt, 1H, H^{10} , J = 5.1, 1.3 Hz), 3.45 (ddd, 1H, H^{16b}, J = 17.0, 2.6, 1.2 Hz), 2.94 (t, 1H, H^{12}, J = 3.2 Hz), 2.53 (ddd, 1H, H^{2a}, J = 13.8, 6.7, 2.5 Hz), 2.48 (t, 1H, H^{6}, J = 3.9 Hz), 2.13 (m, 1H, H^{5a}), 2.03 (ddd, 1H, H^{11a}, J = 13.4, 5.0, 2.4 Hz), 1.89 (ddd, 1H, H^{11b}, J = 13.4, 5.0, 2.4 Hz), 1.81 (m, 1H, H^{2b}), 1.86-1.76 (m, 3H, $H^{3a, 4a, 5b}$), 1.51-1.35 (m, 2H, $H^{3b, 4b}$), 1.23 (3H, s, H^{8}), 1.14 (m, 3H, H^{14}), 1.06 (m, 18H, H^{15}).

^{13}C NMR ($CDCl_3$ 100 MHz) δ_C 177.4 (C^{9}), 147.6 (C^{19}), 139.3 (C^{17}), 135.9 (C^{13}), 129.3 (C^{20}), 128.9 (C^{21}), 126.4 (C^{22}), 117.4 (C^{18}), 115.6 (C^{1}), 59.1 (C^{10}), 52.2 (C^{6}), 49.5 (C^{7}), 41.6 (C^{12}), 38.7 (C^{16}), 24.1 (C^{11}), 23.6 (C^{3}) ,23.2 (C^{2}), 22.0 (C^{5}), 21.3 (C^{8}), 20.8 (C^{4}), 18.13 (C^{15a}), 18.22 (C^{15b}), 14.1 (C^{14}).

HRMS (ES^+) exact mass calculated for $[M+H]^+$ ($C_{31}H_{46}O_2N^{32}S^{28}Si$) requires **m/z** 524.3013, found **m/z** 524.3008.



Compound 145

A solution of tributyltin hydride (0.754 mL, 2.80 mmol) and AIBN (92 mg, 0.561 mmol) in toluene (5.8 mL) was added dropwise over 2 hours to a solution of **123** (580 mg, 1.40 mmol) in toluene (58 mL) at 90 °C. Upon completion of addition, the reaction was cooled to room temperature, and partially concentrated *in vacuo*. The crude reaction was purified directly by flash column chromatography with PE:EtOAc [85:15] as the eluent to give **147** as a colourless oil (790 mg, 1.12 mmol, 80%). This was taken on directly to the next step.

147 (600 mg, 0.85 mmol) was dissolved in dichloromethane (30 mL) and cooled to 0 °C. CSA (208 mg, 0.894 mmol) was added in one portion and the reaction allowed to stir for 30 minutes. The reaction mixture was directly purified by flash column chromatography with PE:EtOAc [8:2] as the eluent to give **145** as a white solid (342 mg, 0.823 mmol, 97%).

$[\alpha]_D^{25}$ = -169.3 (*c* 0.5, $CHCl_3$)

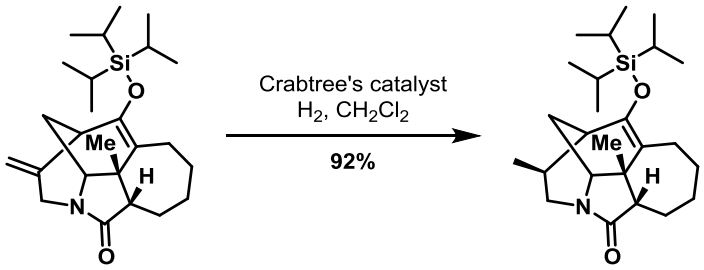
mp 98 - 99 °C.

IR (film)/cm^{-1} ν_{max} 2980, 2867, 1690, 1639, 1461.

^{1}H NMR ($CDCl_3$, 400 MHz) δ_H 4.92 (dd, 1H, J = 2.5, 1.2 Hz), 4.84 (dd, 1H, J = 2.5, 0.9 Hz), 4.53 (d, 1H, J = 16.1 Hz), 3.61-3.51 (m, 2H), 2.87 (t, 1H), 2.50 (ddd, 1H, J = 13.7, 6.8, 2.3 Hz), 2.45 (t, 1H, J = 3.9 Hz), 2.10 (m, 1H), 2.02 (ddd, 1H, J = 13.4, 4.9, 2.6 Hz), 1.85-1.72 (m, 2H), 1.72-1.49 (m, 3H), 1.46-1.30 (m, 2H), 1.22 (s, 3H), 1.16 (m, 3H), 1.12-1.08 (m, 18H).

^{13}C NMR ($CDCl_3$ 100 MHz) δ_C 176.5, 147.5, 143.0, 113.5, 108.9, 57.9, 51.2, 48.2, 39.9, 39.5, 22.6, 22.5, 22.0, 20.9, 20.5, 19.8, 17.1, 12.9.

HRMS (ES^+) exact mass calculated for $[M+Na]^+$ ($C_{25}H_{41}O_2N^{23}Na^{28}Si$) requires **m/z** 438.2799, found **m/z** 438.2797.



Compound 156

An oven dried round-bottom flask was charged with **145** (300 mg, 0.722 mmol) and Crabtree's catalyst (116 mg, 0.144 mmol). Dichloromethane was added (30 mL) and the atmosphere replaced with H_2/Ar [33:66] (single-skinned balloon pressure); a gradual colour change from deep orange to pale yellow was observed. The reaction was left to stir for 1 hour then directly purified by flash column chromatography with PE:EtOAc [8:2] as the eluent to give **156** as a white solid (278 mg, 0.665 mmol, 92%, >20:1 dr).

$[\alpha]_D^{25}$ = -1264 (*c* 0.5, $CHCl_3$)

mp 79-81 ^oC

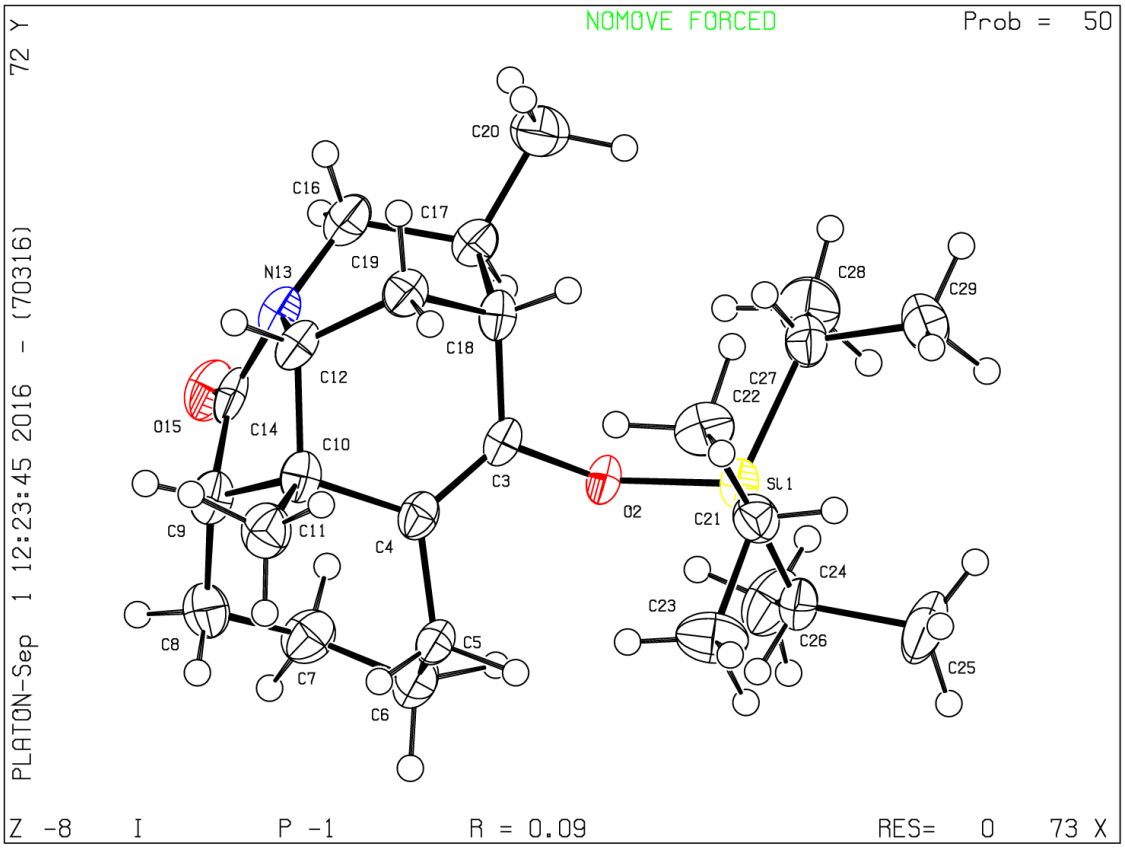
IR (film)/cm^{-1} ν_{max} 2884, 1685, 1650, 1460.

^{1}H NMR ($CDCl_3$, 400 MHz) δ_H 4.07 (dd, 1H, J = 13.6, 8.1 Hz), 3.48 (dt, 1H, J = 5.0, 1.2 Hz), 2.52 (ddd, 1H, J = 13.3, 6.8, 2.3 Hz), 2.43 (t, 1H, J = 3.8 Hz), 2.36 (ddd, 1H, J = 13.5, 10.3, 1.0 Hz), 2.18-2.05 (m, 2H), 1.93 (ddd, 1H, J = 13.5, 5.0, 2.5 Hz), 1.84 (t, 1H, J = 2.9 Hz), 1.78 (m, 1H), 1.68 (m, 1H), 1.64-1.48 (m, 3H), 1.46 (m, 1H), 1.35 (m, 1H), 1.19 (s, 3H), 1.11 (m, 1H), 1.07 (m, 18H), 0.93 (d, 3H, J = 6.8 Hz).

^{13}C NMR ($CDCl_3$ 100 MHz) δ_C 175.6, 149.6, 112.7, 58.3, 51.2, 48.0, 40.1, 38.7, 32.0, 22.4, 21.6, 20.9, 20.3, 19.8, 19.3, 18.2, 17.1, 17.0, 12.8.

HRMS (ES^+) exact mass calculated for $[M+Na]^+$ ($C_{25}H_{43}O_2N^{23}Na^{28}Si$) requires **m/z** 440.2955, found **m/z** 440.2955.

Crystallographic data for compound 156

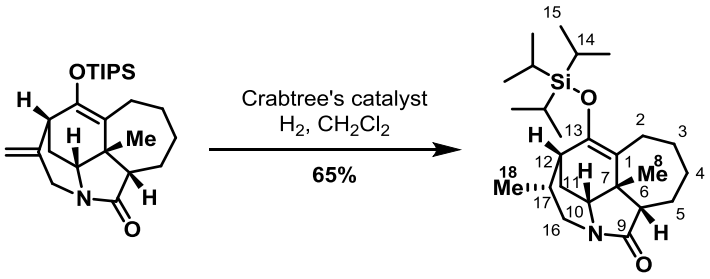


Crystal data	
Chemical formula	$C_{25}H_{43}NO_2Si$
M_r	417.71
Crystal system, space group	Triclinic, *P*1
Temperature (K)	150
a, *b*, *c* (Å)	7.5178 (8), 11.6743 (11), 14.3982 (16)
α, β, γ (°)	106.666 (4), 96.161 (5), 92.491 (5)
V (Å³)	1199.92 (13)
Z	2
Radiation type	Mo *K*α
μ (mm⁻¹)	0.12
Crystal size (mm)	0.2×0.1×0.1
Data collection	
Diffractometer	Nonius KappaCCD
Absorption correction	Multi-scan *DENZO*/*SCALEPACK* (Otwinowski & Minor, 1997)
T_{min}, T_{max}	1.00, 1.00
No. of measured, independent and observed [$I > 2.0\sigma(I)$] reflections	7345, 4310, 2233
R_{int}	0.146
$(\sin\theta/\lambda)_{max}$ (Å⁻¹)	0.605
Refinement	

$R[F^2 > 2\sigma(F^2)]$, $wR(F^2)$, S	0.089, 0.186, 0.96
No. of reflections	4306
No. of parameters	263
H-atom treatment	H-atom parameters constrained
$\Delta\rho_{max}$, $\Delta\rho_{min}$ (e Å^{-3})	1.07, −1.19

Selected geometric parameters (Å, º)

Si1—O2	1.657 (3)	C10—C12	1.544 (6)
Si1—C21	1.879 (5)	C12—N13	1.467 (6)
Si1—C24	1.869 (5)	C12—C19	1.501 (6)
Si1—C27	1.878 (5)	N13—C14	1.343 (6)
O2—C3	1.395 (5)	N13—C16	1.457 (6)
C3—C4	1.330 (6)	C14—O15	1.228 (5)
C3—C18	1.503 (6)	C16—C17	1.532 (6)
C4—C5	1.513 (6)	C17—C18	1.557 (6)
C4—C10	1.523 (6)	C17—C20	1.513 (6)
C5—C6	1.531 (6)	C18—C19	1.518 (6)
C6—C7	1.514 (7)	C21—C22	1.536 (6)
C7—C8	1.538 (6)	C21—C23	1.535 (7)
C8—C9	1.521 (6)	C24—C25	1.520 (6)
C9—C10	1.551 (6)	C24—C26	1.530 (7)
C9—C14	1.531 (7)	C27—C28	1.537 (7)
C10—C11	1.541 (6)	C27—C29	1.543 (7)
O2—Si1—C21	112.28 (19)	C10—C12—N13	102.2 (3)
O2—Si1—C24	102.97 (19)	C10—C12—C19	113.8 (4)
C21—Si1—C24	108.6 (2)	N13—C12—C19	110.3 (4)
O2—Si1—C27	108.98 (19)	C12—N13—C14	113.0 (4)
C21—Si1—C27	109.3 (2)	C12—N13—C16	119.3 (4)
C24—Si1—C27	114.6 (2)	C14—N13—C16	123.7 (4)
Si1—O2—C3	134.8 (3)	C9—C14—N13	107.4 (4)
O2—C3—C4	119.6 (4)	C9—C14—O15	126.7 (5)
O2—C3—C18	114.7 (4)	N13—C14—O15	125.8 (5)
C4—C3—C18	125.6 (4)	N13—C16—C17	110.9 (4)
C3—C4—C5	120.9 (4)	C16—C17—C18	111.1 (4)
C3—C4—C10	121.9 (4)	C16—C17—C20	110.0 (4)
C5—C4—C10	117.2 (4)	C18—C17—C20	112.5 (4)
C4—C5—C6	114.7 (4)	C17—C18—C3	114.1 (4)
C5—C6—C7	115.6 (4)	C17—C18—C19	110.0 (4)
C6—C7—C8	117.1 (4)	C3—C18—C19	108.3 (4)
C7—C8—C9	115.7 (4)	C18—C19—C12	107.1 (4)
C8—C9—C10	121.2 (4)	Si1—C21—C22	114.0 (3)
C8—C9—C14	112.9 (4)	Si1—C21—C23	113.7 (3)
C10—C9—C14	102.3 (4)	C22—C21—C23	109.6 (4)
C9—C10—C4	110.6 (4)	Si1—C24—C25	114.7 (3)
C9—C10—C11	112.8 (4)	Si1—C24—C26	116.0 (3)
C4—C10—C11	112.0 (4)	C25—C24—C26	110.5 (4)
C9—C10—C12	100.3 (4)	Si1—C27—C28	114.3 (3)
C4—C10—C12	109.8 (4)	Si1—C27—C29	114.6 (4)
C11—C10—C12	110.8 (4)	C28—C27—C29	110.0 (4)



Compound 146

To a flask charged with Crabtree's catalyst (1.94 mg, 0.00241 mmol, 0.1 eq.) under vacuum was added a solution of **145** (10 mg, 0.0241 mmol) in anhydrous dichloromethane (1 mL) followed by immediate atmosphere replacement with hydrogen (quad-skinned balloon pressure). The reaction was stirred for 30 mins, and the crude reaction mixture was directly purified by flash column chromatography to give **146** as colourless crystalline solid (6.5 mg, 0.0156 mmol, 65%).

mp 143-148 ^{o}C.

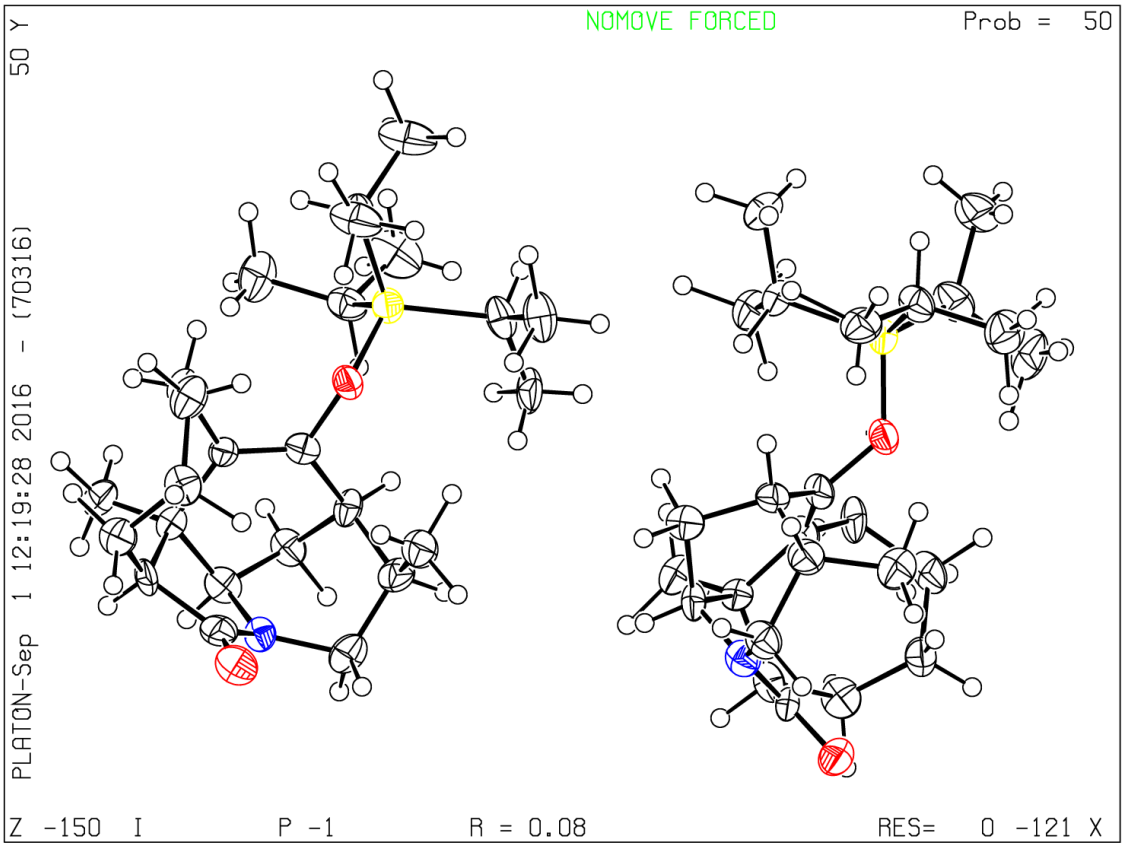
IR 2980 (C-H), 1889 (C-H), 1678 (C=O), 1462 (C=C).

^{1}H NMR ($CDCl_3$, 400 MHz) δ_H 3.57 (d, 1H, H^{16a}, J = 13.6 Hz), 3.49 (dt, 1H, H^{10}, J = 5.0, 1.3 Hz), 3.02 (dd, 1H, H^{16b}, J = 13.6, 6.6 Hz), 2.54 (ddd, 1H, H^{2a}, J = 13.2, 6.7, 2.0 Hz), 2.42 (t, 1H, H^{6}, J = 3.8 Hz), 2.33 (dd, 1H, H^{12}, J = 7.3, 3.5 Hz), 2.17-2.07 (m, 2H, $H^{5a, 17}$), 1.96 (ddd, 1H, H^{11a}, J = 13.4, 4.9, 2.6 Hz), 1.84-1.72 (m, 1H, H^{2b}), 1.71-1.61 (m, 3H, $H^{3a, 4a, 11b}$), 1.59-1.31 (m, 3H, $H^{3b, 4b, 5b}$), 1.18 (s, 3H, H^{8}), 1.16-1.06 (m, 21H, $H^{14, 15}$), 1.05 (d, 3H, H^{18}, J = 3.4 Hz).

^{13}C NMR ($CDCl_3$ 100 MHz) δ_C 177.3 (C^{9}), 148.1 (C^{1}), 117.0 (C^{13}), 59.4 (C^{10}), 51.9 (C^{6}), 48.4 (C^{7}), 41.3 (C^{16}), 36.5 (C^{12}), 33.6 (C^{17}), 23.9 (C^{3}), 23.7 (C^{11}), 22.6 (C^{2}), 21.8 (C^{8}), 21.6 (C^{5}), 21.1 (C^{4}), 18.2 (C^{15a}), 18.1 (C^{15b}), 13.4 (C^{14}).

HRMS (ES^{+}) exact mass calculated for $[M+Na]^{+}$ ($C_{25}H_{43}O_2N^{23}Na^{28}Si$) requires **m/z** 440.2955, found **m/z** 440.2941.

Crystallographic data for compound 146



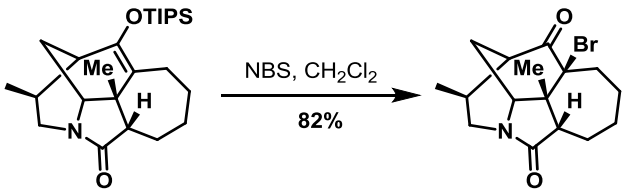
Crystal data	
Chemical formula	$C_{25}H_{43}NO_2Si$
M_r	417.71
Crystal system, space group	Triclinic, *P*1
Temperature (K)	150
a, *b*, *c* (Å)	8.7028 (8), 14.3272 (16), 19.691 (2)
α, β, γ (°)	82.854 (5), 90.019 (4), 90.004 (4)
V (Å³)	2436.1 (3)
Z	4
Radiation type	Mo *K*α
μ (mm^{-1})	0.12
Crystal size (mm)	0.2×0.1×0.1
Data collection	
Diffractometer	Nonius KappaCCD
Absorption correction	Multi-scan *DENZO*/*SCALEPACK* (Otwinowski & Minor, 1997)
T_{min}, T_{max}	1.00, 1.00
No. of measured, independent and observed [$I > 2.0\sigma(I)$] reflections	6128, 3970, 2538

R_{int}	0.097
θ_{max} (°)	19.6
$(\sin \theta/\lambda)_{max}$ (Å^{-1})	0.472
Refinement	
$R[F^2 > 2\sigma(F^2)]$, $wR(F^2)$, S	0.084, 0.207, 1.06
No. of reflections	3970
No. of parameters	779
H-atom treatment	H atoms treated by a mixture of independent and constrained refinement
	Method = Modified Sheldrick $w = 1/[\sigma^2(F^2) + (0.0P)^2 + 17.51P]$, where $P = (\max(F_o^2,0) + 2F_c^2)/3$
$(\Delta/\sigma)_{max}$	3.504
$\Delta\rho_{max}$, $\Delta\rho_{min}$ (e Å^{-3})	0.92, −0.82

Selected geometric parameters (Å, º)

Si1—O2	1.662 (7)	Si30—O31	1.657 (7)
Si1—C21	1.882 (11)	Si30—C50	1.865 (10)
Si1—C24	1.872 (11)	Si30—C53	1.899 (10)
Si1—C27	1.862 (11)	Si30—C56	1.882 (11)
O2—C3	1.407 (11)	O31—C32	1.400 (12)
C3—C4	1.345 (13)	C32—C33	1.311 (12)
C3—C18	1.490 (13)	C32—C47	1.517 (14)
C4—C5	1.511 (14)	C33—C34	1.516 (14)
C4—C10	1.521 (14)	C33—C39	1.512 (14)
C5—C6	1.551 (16)	C34—C35	1.523 (15)
C6—C7	1.526 (16)	C35—C36	1.521 (16)
C7—C8	1.542 (15)	C36—C37	1.546 (15)
C8—C9	1.529 (14)	C37—C38	1.533 (14)
C9—C10	1.562 (15)	C38—C39	1.546 (13)
C9—C14	1.505 (15)	C38—C43	1.528 (14)
C10—C11	1.506 (15)	C39—C40	1.543 (14)
C10—C12	1.542 (14)	C39—C41	1.543 (14)
C12—N13	1.454 (12)	C41—N42	1.455 (13)
C12—C19	1.523 (15)	C41—C48	1.519 (14)
N13—C14	1.352 (13)	N42—C43	1.341 (12)
N13—C16	1.491 (13)	N42—C45	1.453 (13)
C14—O15	1.227 (12)	C43—O44	1.246 (11)
C16—C17	1.531 (15)	C45—C46	1.548 (15)
C17—C18	1.588 (14)	C46—C47	1.575 (14)
C17—C20	1.509 (15)	C46—C49	1.516 (16)
C18—C19	1.514 (14)	C47—C48	1.548 (15)
C21—C22	1.534 (15)	C50—C51	1.563 (15)
C21—C23	1.544 (15)	C50—C52	1.510 (16)
C24—C25	1.539 (17)	C53—C54	1.535 (16)
C24—C26	1.554 (16)	C53—C55	1.534 (16)
C27—C28	1.574 (16)	C56—C57	1.540 (17)
C27—C29	1.488 (15)	C56—C58	1.535 (16)
O2—Si1—C21	109.1 (4)	O31—Si30—C50	109.4 (4)
O2—Si1—C24	109.6 (4)	O31—Si30—C53	109.5 (4)
C21—Si1—C24	109.8 (5)	C50—Si30—C53	109.4 (5)
O2—Si1—C27	105.3 (4)	O31—Si30—C56	105.7 (4)

C21—Si1—C27	111.4 (5)	C50—Si30—C56	112.2 (5)
C24—Si1—C27	111.5 (5)	C53—Si30—C56	110.5 (5)
Si1—O2—C3	129.7 (6)	Si30—O31—C32	130.1 (6)
O2—C3—C4	118.3 (8)	O31—C32—C33	121.2 (8)
O2—C3—C18	115.6 (8)	O31—C32—C47	113.5 (8)
C4—C3—C18	126.0 (9)	C33—C32—C47	125.3 (9)
C3—C4—C5	122.1 (9)	C32—C33—C34	120.2 (9)
C3—C4—C10	121.5 (9)	C32—C33—C39	123.2 (9)
C5—C4—C10	116.4 (9)	C34—C33—C39	116.6 (9)
C4—C5—C6	114.5 (10)	C33—C34—C35	113.6 (10)
C5—C6—C7	113.3 (10)	C34—C35—C36	115.8 (9)
C6—C7—C8	116.0 (10)	C35—C36—C37	112.0 (10)
C7—C8—C9	114.7 (9)	C36—C37—C38	114.6 (9)
C8—C9—C10	119.2 (9)	C37—C38—C39	119.4 (9)
C8—C9—C14	112.4 (10)	C37—C38—C43	112.1 (9)
C10—C9—C14	103.3 (9)	C39—C38—C43	101.4 (8)
C4—C10—C9	112.5 (8)	C38—C39—C33	112.8 (8)
C4—C10—C11	112.3 (9)	C38—C39—C40	110.5 (8)
C9—C10—C11	112.1 (9)	C33—C39—C40	112.0 (8)
C4—C10—C12	110.0 (8)	C38—C39—C41	100.3 (8)
C9—C10—C12	99.2 (8)	C33—C39—C41	109.9 (8)
C11—C10—C12	109.9 (9)	C40—C39—C41	110.9 (8)
C10—C12—N13	104.3 (8)	C39—C41—N42	104.3 (8)
C10—C12—C19	114.3 (9)	C39—C41—C48	114.6 (9)
N13—C12—C19	109.7 (9)	N42—C41—C48	110.2 (9)
C12—N13—C14	111.9 (8)	C41—N42—C43	110.7 (8)
C12—N13—C16	119.5 (9)	C41—N42—C45	119.3 (9)
C14—N13—C16	123.4 (9)	C43—N42—C45	125.0 (9)
C9—C14—N13	108.1 (10)	C38—C43—N42	109.7 (9)
C9—C14—O15	125.6 (11)	C38—C43—O44	126.2 (10)
N13—C14—O15	126.3 (10)	N42—C43—O44	124.1 (10)
N13—C16—C17	109.4 (8)	N42—C45—C46	110.0 (9)
C16—C17—C18	110.8 (9)	C45—C46—C47	110.9 (9)
C16—C17—C20	109.4 (10)	C45—C46—C49	109.5 (10)
C18—C17—C20	113.6 (9)	C47—C46—C49	112.2 (9)
C17—C18—C3	115.6 (8)	C32—C47—C46	117.2 (9)
C17—C18—C19	110.1 (9)	C32—C47—C48	107.1 (8)
C3—C18—C19	107.5 (8)	C46—C47—C48	108.9 (9)
C12—C19—C18	106.5 (8)	C47—C48—C41	105.4 (9)
Si1—C21—C22	113.7 (8)	Si30—C50—C51	112.8 (7)
Si1—C21—C23	113.3 (7)	Si30—C50—C52	116.0 (8)
C22—C21—C23	111.0 (10)	C51—C50—C52	109.3 (10)
Si1—C24—C25	115.7 (9)	Si30—C53—C54	113.6 (8)
Si1—C24—C26	112.8 (8)	Si30—C53—C55	112.3 (7)
C25—C24—C26	108.6 (11)	C54—C53—C55	112.2 (10)
Si1—C27—C28	111.4 (8)	Si30—C56—C57	112.9 (9)
Si1—C27—C29	117.2 (9)	Si30—C56—C58	114.7 (8)
C28—C27—C29	110.3 (10)	C57—C56—C58	110.3 (11)



Compound 158

To a solution of **156** (280 mg, 0.670 mmol) in dichloromethane (20 mL) was added *N*-bromosuccinimide (125 mg, 0.704 mmol). The reaction was stirred for 5 minutes, before being directly purified by flash column chromatography with PE:EtOAc [1:1] as the eluent to give **158** as a white solid (227 mg, 17.3% w/w succinimide, 0.552 mmol, 82%). [3]

$[\alpha]_D^{25}$ = -396 (*c* 0.2, $CHCl_3$)

mp 97-102 °C.

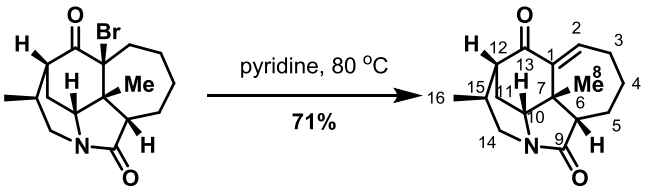
IR (film)/cm^{-1} ν_{max} 2980, 1662, 1687.

^{1}H NMR ($CDCl_3$, 400 MHz) δ_H 4.06 (dd, 1H, J = 13.6, 9.2 Hz), 3.52 (app d, 1H, J = 6.1 Hz), 2.97 (m, 1H), 2.82 (ddd, 1H, J = 14.7, 4.8, 1.4 Hz), 2.67 (ddd, 1H, J = 14.8, 10.2, 1.3 Hz), 2.61 (ddd, 1H, J = 7.0, 3.3, 1.3 Hz), 2.46 (app dq, 1H, J = 4.7, 1.1 Hz), 2.21 (ddd, 1H, J = 13.7, 9.3, 1.3 Hz), 2.12-1.90 (m, 4H), 1.88-1.72 (m, 2H), 1.61 (s, 3H), 1.49 (app dddd, 1H, J = 15.0, 12.9, 7.4, 3.0 Hz), 1.27 (m, 1H), 1.08 (d, 3H, J = 7.0 Hz).

^{13}C NMR ($CDCl_3$ 100 MHz) δ_C 203.2, 173.4, 61.1, 52.2, 51.6, 44.0, 41.9, 39.9, 38.3, 36.3, 25.6, 21.9, 20.6, 18.5, 18.0, 17.5.

HRMS (ES^+) exact mass calculated for $[M+Na]^+$ ($C_{16}H_{22}O_2N^{79}Br^{23}Na$) requires **m/z** 362.0726, found **m/z** 362.0726.

[3] Sample contaminated with succinimide which was difficult to remove by flash column chromatography. Characterised and carried through to next step as the mixture.



Compound 159

A solution of **156** (12mg, 0.0353 mmol) in pyridine (1.2 mL) was heated to 80 °C overnight. The reaction was diluted with ethyl acetate (5 mL) and washed with saturated copper sulfate (3 x 5mL), brine, dried over anhydrous sodium sulfate and concentrated *in vacuo*. The crude product was purified by flash column chromatography with a gradient of 50:50 to 65:35 ethyl acetate/petrol ether as the eluent to give **159** as a pale yellow solid (6.5 mg, 0.0251 mmol, 71%).

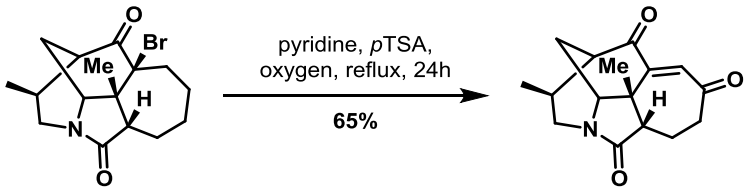
mp 121 – 126 °C.

IR 2980 (C-H), 2888 (C-H), 1680 (C=O), 1600 (C=O), 1461 (C=C).

^{1}H NMR ($CDCl_3$, 400 MHz) δ_H 7.36 (ddd, 1H, H^2, J = 9.6 4.8, 0.5 Hz), 4.02 (dd, 1H, H^{14a}, J = 13.7, 7.8 Hz), 3.49 (app dq, 1H, H^{10}, J = 4.9, 1.1 Hz), 2.51 (t, 1H, H^6, J = 5.5 Hz), 2.46 (m, 2H, $H^{3a, 14b}$), 2.31 (ddt, 1H, H^{3a}, J = 3.8, 2.5, 1.4 Hz), 2.29-2.22 (m, 1H, H^{3b}), 2.21-2.15 (m, 2H, $H^{4a, 11a}$), 2.08 (m, 1H, H^{15}), 2.00 (ddt, 1H, H^{11b}, J = 14.8, 3.8, 0.9 Hz), 1.91 (dddd, 1H, H^{4b}, J = 14.7, 11,6, 5.9, 2.9 Hz), 1.70 (ddq, 1H, H^{5a}, J = 13.7, 6.8, 3.4 Hz), 1.53 (m, 1H, H^{5b}), 1.35 (s, 3H, H^8), 1.03 (d, 3H, H^{16}, J = 6.9 Hz).

^{13}C NMR ($CDCl_3$ 100 MHz) δ_C 200.8 (C^{13}), 175.5 (C^9), 149.9 (C^2), 138.1 (C^1), 59.5 (C^{10}), 51.9 (C^6), 51.8 (C^7), 46.5 (C^{12}), 40.6 (C^{14}), 35.3 (C^{15}), 28.3 (C^3), 25.5 (C^4), 20.7 (C^5), 19.8 (C^8), 19.8 (C^{16}), 17.9 (C^{11}).

HRMS (ES^+) exact mass calculated for $[M+Na]^+$ ($C_{16}H_{21}O_2N^{23}Na$) requires **m/z** 282.1476, found **m/z** 282.1465.



Compound 62

To a solution of **158** from the previous step (145 mg, 83% mass purity, 0.353 mmol) in pyridine (15 mL) was added *p*TSA monohydrate (400 mg, 2.10 mmol) and the atmosphere replaced with oxygen. The reaction was vigorously refluxed for 24h and cooled to rt. The reaction mixture was diluted 1M HCl (50 mL) and extracted with dichloromethane (3 x 50 mL). The combined organic layers were washed with 1M HCl (50 mL), dried over sodium sulfate and concentrated *in vacuo*. The crude product was purified by flash column chromatography with PE:EtOAc [1:9] as the eluent to give **62** as a white solid (62.2 mg, 0.228 mmol, 65%). The enantiomeric excess was measured to be >99% ee.

$[\alpha]_D^{25}$ = -22.0 (*c* 0.2, $CHCl_3$)

HPLC (Chiralpak AD-H, hexane:isopropanol [80:20], 1.0 mL/min, λ=220 nm) t_R= 20.9 min (minor), 22.9 min (major).

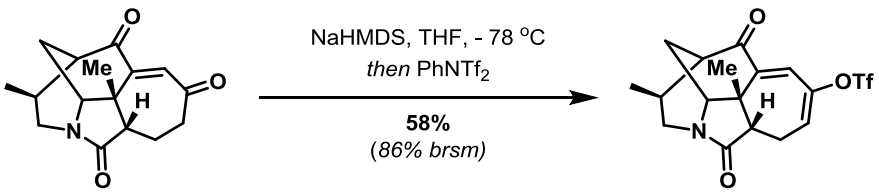
mp 177-180 °C.

IR (film)/cm^{-1} $\boldsymbol{\nu_{max}}$ 2947 (C-H), 1681 (C=O), 1593 (C=C).

^{1}H NMR ($CDCl_3$, 400 MHz) δ_H 6.97 (s, 1H), 4.06 (dd, 1H, J = 13.5, 8.0 Hz), 3.65 (d, 1H, J = 5.6 Hz), 2.75 (dd, 1H, J = 10.8, 7.4 Hz), 2.70-2.56 (m, 2H), 2.49 (dd, 1H, J = 13.5, 10.3 Hz), 2.41-2.29 (m, 3H), 2.25 (ddd, 1H, J = 14.9, 5.9, 2.1 Hz), 2.08 (dd, 1H, J = 14.9, 4.1 Hz), 1.87 (dddd, J = 18.9, 15.3, 10.7, 4.1 Hz). 1.44 (s, 3H), 1.10 (d, 3H, J = 6.8 Hz).

^{13}C NMR ($CDCl_3$ 100 MHz) δ_C 207.1, 199.9, 175.1, 142.9, 139.2, 58.1, 50.4, 45.9, 41.1, 37.7, 37.6, 29.9, 25.8, 21.7, 19.8, 17.7.

HRMS (ES^+) exact mass calculated for $[M+H]^+$ ($C_{16}H_{20}O_3N$) requires **m/z** 274.14377, found **m/z** 274.14371.



Compound 167

To a solution of **62** (35 mg, 0.128 mmol) in anhydrous THF (3 mL) cooled at -78 °C was added NaHMDS (1M in THF, 0.154 mL, 0.154 mmol) dropwise; a colour change to deep red was observed. The reaction was stirred for 5 minutes and a solution of $PhNTf_2$ (114 mg, 0.320 mmol) in THF (0.5 mL) was added dropwise at – 78°C. After stirring for 30 minutes, the reaction was quenched by addition of saturated ammonium chloride (1 mL) and warmed to room temperature. The reaction was diluted with water (4 mL) and extracted with dichloromethane (3 x 5 mL). The combined organic layers were washed with brine, dried over sodium sulfate and concentrated *in vacuo*. The crude product was purified by flash column chromatography with PE:EtOAc [3:7] as the eluent to give **167** as a white solid (30.3 mg, 0075 mmol, 58%) then EtOAc as the eluent to give starting material **62** as an off white solid (9.9 mg, 0.036 mmol, 28%).

$[\alpha]_{D}^{25}$ = -173.0 (*c* 0.1, $CHCl_3$)

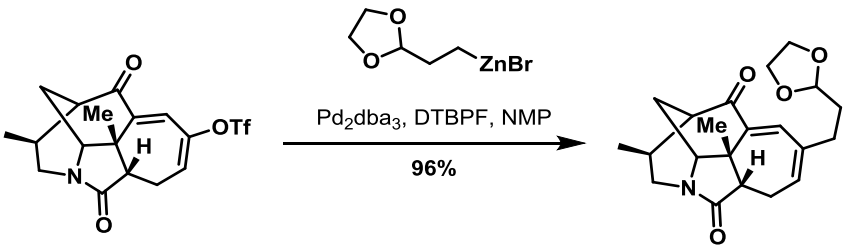
mp 115-119 °C.

IR (film)/cm^{-1} ν_{max} 2980 (C-H), 1736 (C=O), 1698 (C=O).

^{1}H NMR ($CDCl_3$, 500 MHz) δ_H 7.11 (s, 1H), 6.43 (ddd, 1H, J = 8.2, 4.8, 1.3 Hz), 4.08 (dd, 1H, J = 13.6 8.1 Hz), 3.55 (dd, 1H, J = 5.8, 1.1 Hz), 3.14 (ddd, 1H, J = 9.6, 8.7, 1.0 Hz), 2.66-2.47 (m, 3H), 2.43-2.33 (m, 2H), 2.24 (ddd, 1H, J = 14.8, 5.7, 2.1 Hz), 2.10 (ddt ,1H, J = 14.6, 4.0. 0.8 Hz), 1.48 (s, 3H), 1.11 (d, 3H, J = 6.9 Hz).

^{13}C NMR ($CDCl_3$ 125 MHz) δ_C 199.2, 174.4, 146.3, 143.9, 135.5, 129.1, 120.0, 61.8, 58.8, 51.5, 46.1, 41.3, 37.9, 23.4, 19.9, 19.6, 18.0.

HRMS (ES^+) exact mass calculated for $[M+H]^+$ ($C_{17}H_{19}O_5NF_3{}^{32}S$) requires **m/z** 406.09305, found **m/z** 406.09305.



Compound 170

A flask was charged with **167** (11 mg, 0.0271 mmol), Pd_2dba_3 (3.7 mg, 0.00407 mmol), DTBPF (3.9 mg, 0.00814 mmol) and NMP (1 mL). The atmosphere was replaced with argon and the red solution stirred for 10 minutes. Organozinc reagent **166** (1 M in THF, 0.081 mL, 0.081 mmol) was added dropwise and the reaction stirred for 30 minutes. The reaction was diluted with ammonium chloride (3 mL), and extracted with EtOAc (3 x 5 mL). The combined organic layers were washed with water (3 x 5 mL), dried over sodium sulfate and concentrated *in vacuo*. The crude product was purified by flash column chromatography with PE:EtOAc [3:7] as the eluent to give **170** as a colourless oil (9.3 mg, 0.0260 mmol, 96%).

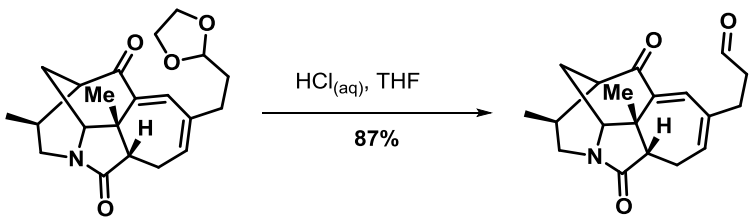
$[\alpha]_D^{25}$ = -302 (*c* 0.1, $CHCl_3$)

IR (film)/cm^{-1} ν_{max} 2954 (C-H), 1717 (C=O), 1697 (C=O).

^{1}H NMR ($CDCl_3$, 400 MHz) δ_H 7.26 (s, 1H), 6.12 (ddd, 1H, J = 8.2, 5.0, 1.4 Hz), 4.87 (t, 1H, J = 4.6 Hz), 4.07 (q, 1H, J = 6.4 Hz), 3.99 – 3.79 (m, 4H), 3.48 (d, 1H, J = 5.9 Hz), 3.05 (dd, 1H, J = 11.3, 8.4 Hz), 2.53-2.21 (m, 7H), 2.17 (ddd, 1H, J = 14.6, 5.8, 2.1 Hz), 1.99 (dd, 1H, J = 14.6, 4.0 Hz), 1.79 (m, 2H), 1.39 (s, 3H), 1.08 (d, 3H, J = 6.5 Hz).

^{13}C NMR ($CDCl_3$ 100 MHz) δ_C 200.8, 175.7, 145.4, 141.9, 140.8, 131.0, 104.0, 65.1, 63.3, 58.7, 49.8, 46.1, 41.5, 38.3, 32.9, 30.5, 26.1, 21.0, 20.1, 18.1.

HRMS (ES^+) exact mass calculated for $[M+Na]^+$ ($C_{21}H_{27}O_4N^{23}Na$) requires **m/z** 380.18323, found **m/z** 380.18323.



Compound 171

To a solution of **170** (8.0 mg, 0.0224 mmol) in THF (0.5 mL) was added aqueous HCl (1M, 0.5 mL) and the reaction left to stir for 5 hours. The reaction was diluted with water (5 mL) and extracted with DCM (3 x 5 mL). The combined organic layers were dried over sodium sulfate and concentrated *in vacuo*. The crude product was purified by flash column chromatography with PE:EtOAc [2:8] as the eluent to give **171** as an off white solid (6.1 mg, 0.0195 mmol, 87%).

$[\boldsymbol{\alpha}]_{\boldsymbol{D}}^{\mathbf{25}}$ = -666 (*c* 0.1, $CHCl_3$)

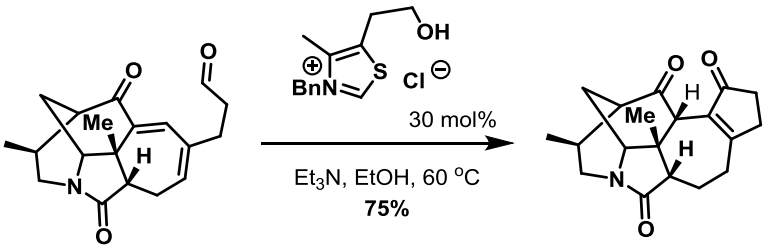
mp 79 - 83 ^{o}C.

IR (film)/cm^{-1} $\boldsymbol{\nu_{max}}$ 2953 (C-H), 1718 (C=O), 1685 (C=O), 1672 (C=O).

^{1}H NMR ($CDCl_3$, 400 MHz) δ_H 9.79 (t, 1H, J = 1.3 Hz), 7.20 (s, 1H), 6.12 (ddt, 1H, J = 8.0, 5.1, 1.4 Hz), 4.07 (dd, 1H, J = 12.7, 7.2 Hz), 3.49 (dd, 1H, J = 5.7, 1.2 Hz), 3.05 (ddd, 1H, J = 11.3, 8.4, 1.0 Hz), 2.66-2.56 (m, 2H), 2.53-2.46 (m, 3H), 2.46-2.22 (m, 4H), 2.18 (ddd, 1H, J = 14.6, 5.8, 2.1 Hz), 1.99 (ddt, 1H, J = 14.8, 4.3, 0.8 Hz), 1.37 (s, 3H), 1.09 (d, 3H, J = 6.6 Hz).

^{13}C NMR ($CDCl_3$ 100 MHz) δ_C 201.3, 200.8, 175.5, 144.5, 141.3, 140.4, 131.8, 63.2, 58.6, 49.9, 46.1, 42.4, 41.5, 38.3, 28.3, 26.1, 20.8, 20.1, 18.1.

HRMS (ES^+) exact mass calculated for $[M+Na]^+$ ($C_{19}H_{23}O_3N^{23}Na$) requires **m/z** 336.15701, found **m/z** 336.15701.



Compound 191

To a solution of **171** (13 mg, 0.0415 mmol) and thiazolium catalyst **190** (5.6 mg, 0.0207 mmol) in EtOH (2.6 mL) was added triethylamine (0.058 mL, 0.415 mmol) and the reaction heated at 60 °C for 6 hours. The reaction was quenched with addition of aqueous HCl (1M, 5 mL) and extracted with dichloromethane (3 x 5mL). The combined organic layers were dried over sodium sulfate and concentrated *in vacuo*. The crude product was purified by flash column chromatography with PE:EtOAc [1:9] as the eluent to give **191** as an off white solid (9.7 mg, 0.0310 mmol, 75%).

$[\alpha]_{D}^{25}$ = -69.8 (*c* 0.1, $CHCl_3$)

mp decomposition at 240 °C

IR (film)/cm^{-1} ν_{max} 2925 (C-H), 1735 (C=O), 1685 (C=O), 1653 (C=O).

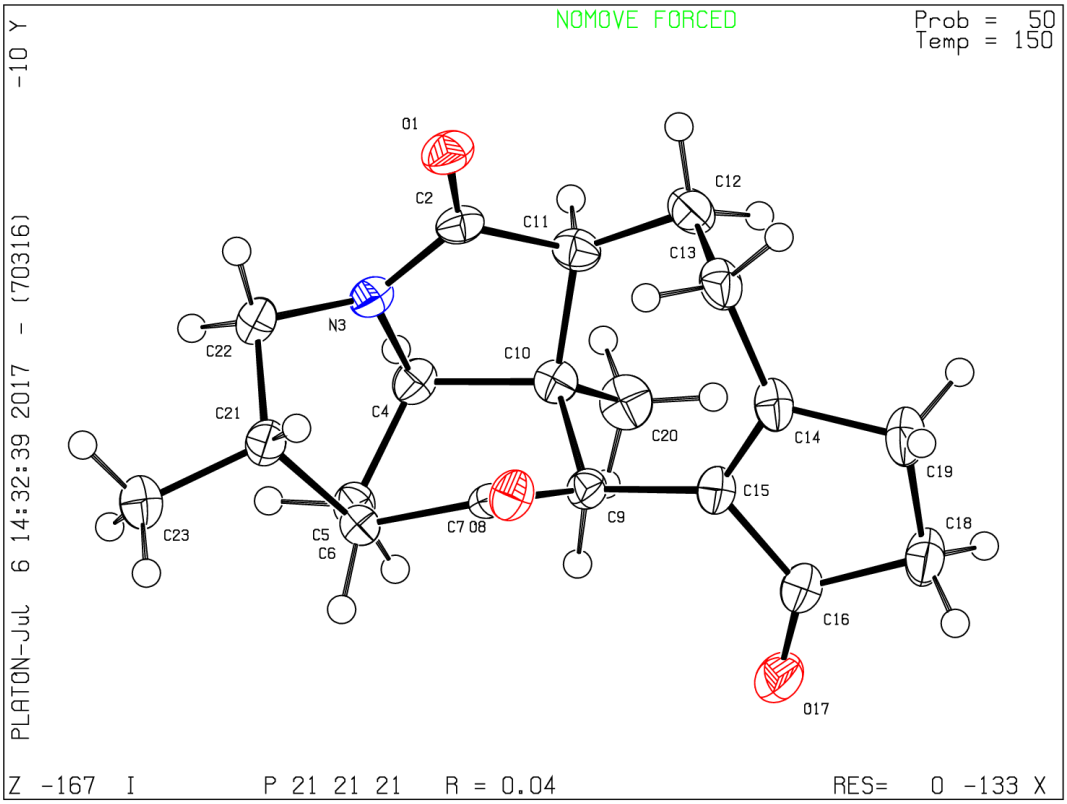
^{1}H NMR ($CDCl_3$, 400 MHz) δ_H 4.07 (dd, 1H, J = 13.6, 9.0 Hz), 3.73-3.68 (m, 2H), 310-2.92 (m, 1H), 2.80-2.74 (m, 1H), 2.74-2.58 (m, 2H), 2.54 (t, 1H, J = 4.4 Hz), 2.46-2.35 (m, 3H), 2.28-2.19 (m, 2H), 2.20-2.10 (m, 2H), 2.03 (m, 1H), 1.65-1.59 (m, 1H), 1.24 (s, 3H), 1.02 (d, 3H, J – 7.0 Hz).

^{13}C NMR ($CDCl_3$ 100 MHz) δ_C 208.7, 208.5, 182.1, 173.4, 134.2, 61.9, 51.7, 50.3, 49.1, 46.3, 40.6, 36.2, 34.6, 31.9, 28.2, 23.7, 20.9, 19.6, 17.8.

HRMS (ES^+) exact mass calculated for $[M+H]^+$ ($C_{19}H_{24}O_3N$) requires **m/z** 314.17507, found **m/z** 314.17505.

Crystallographic data for compound 191

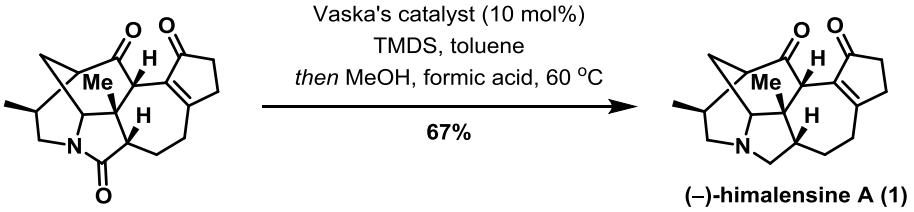
Crystal data	
Chemical formula	$C_{19}H_{23.00}NO_3$
M_r	313.40
Crystal system, space group	Orthorhombic, $P2_12_12_1$
Temperature (K)	150
a, b, c (Å)	11.3931 (2), 11.4712 (2), 11.9193 (2)
V (Å^3)	1557.76 (5)
Z	4
Radiation type	Cu $K\alpha$
μ (mm^{-1})	0.72
Crystal size (mm)	0.20 × 0.20 × 0.10
Data collection	
Diffractometer	Unknown
Absorption correction	Multi-scan *DENZO*/*SCALEPACK* (Otwinowski & Minor, 1997)
T_{min}, T_{max}	0.70, 0.93
No. of measured, independent and observed [$I > 2.0\sigma(I)$] reflections	10974, 3218, 3156
R_{int}	0.032
$(\sin\theta/\lambda)_{max}$ (Å^{-1})	0.630
Refinement	
$R[F^2 > 2\sigma(F^2)]$, $wR(F^2)$, S	0.038, 0.106, 1.01
No. of reflections	3218
No. of parameters	209
H-atom treatment	H-atom parameters constrained
$\Delta\rho_{max}$, $\Delta\rho_{min}$ (e Å^{-3})	0.20, −0.23
Absolute structure	Flack (1983), 1360 Friedel-pairs
Absolute structure parameter	0.02 (17)



Selected geometric parameters (Å, º)

O1—C2	1.2210 (19)	C10—C11	1.5620 (18)
C2—N3	1.3497 (19)	C10—C20	1.5275 (19)
C2—C11	1.522 (2)	C11—C12	1.530 (2)
N3—C4	1.4700 (18)	C12—C13	1.530 (2)
N3—C22	1.4523 (18)	C13—C14	1.492 (2)
C4—C5	1.5245 (19)	C14—C15	1.339 (2)
C4—C10	1.5567 (18)	C14—C19	1.5069 (19)
C5—C6	1.536 (2)	C15—C16	1.4647 (19)
C6—C7	1.5268 (18)	C16—O17	1.2228 (19)
C6—C21	1.5448 (19)	C16—C18	1.518 (2)
C7—O8	1.2093 (17)	C18—C19	1.530 (2)
C7—C9	1.5297 (18)	C21—C22	1.5420 (19)
C9—C10	1.5678 (18)	C21—C23	1.517 (2)
C9—C15	1.4988 (17)		
O1—C2—N3	125.83 (14)	C9—C10—C20	108.48 (11)
O1—C2—C11	126.80 (14)	C11—C10—C20	111.59 (11)
N3—C2—C11	107.37 (12)	C2—C11—C10	103.37 (11)
C2—N3—C4	113.88 (11)	C2—C11—C12	112.33 (12)
C2—N3—C22	123.47 (12)	C10—C11—C12	123.62 (12)
C4—N3—C22	119.65 (11)	C11—C12—C13	115.86 (12)

N3—C4—C5	107.57 (11)	C12—C13—C14	109.49 (12)
N3—C4—C10	103.08 (11)	C13—C14—C15	124.92 (13)
C5—C4—C10	114.03 (11)	C13—C14—C19	122.05 (13)
C4—C5—C6	105.79 (11)	C15—C14—C19	112.70 (13)
C5—C6—C7	110.15 (11)	C9—C15—C14	127.92 (13)
C5—C6—C21	110.18 (11)	C9—C15—C16	121.84 (12)
C7—C6—C21	111.03 (11)	C14—C15—C16	110.12 (12)
C6—C7—O8	121.77 (12)	C15—C16—O17	126.58 (14)
C6—C7—C9	114.93 (11)	C15—C16—C18	107.66 (12)
O8—C7—C9	123.26 (12)	O17—C16—C18	125.74 (13)
C7—C9—C10	111.15 (10)	C16—C18—C19	105.41 (12)
C7—C9—C15	115.23 (11)	C18—C19—C14	104.03 (13)
C10—C9—C15	114.59 (11)	C6—C21—C22	108.71 (11)
C4—C10—C9	107.35 (11)	C6—C21—C23	112.91 (12)
C4—C10—C11	100.87 (11)	C22—C21—C23	110.90 (12)
C9—C10—C11	115.73 (11)	C21—C22—N3	109.13 (11)
C4—C10—C20	112.68 (12)		



Himlensine A (1).

To a solution of **191** (4.2 mg, 0.0134 mmol) and Vaska's catalyst (1.1 mg, 0.00134 mmol) in anhydrous toluene (0.42 mL) was added TMDS (6 drops, ~0.0025 mL, 0.144 mmol) dropwise and the reaction mixture was analysed by TLC for disappearance of the starting material after addition of each drop. After complete conversion of the starting material, formic acid (2 mL) was added to form a biphasic mixture. MeOH was then added dropwise until the reaction mixture became one phase, and the reaction heated at 60 °C for 10 hours. The reaction mixture was added dropwise to saturated aqueous potassium carbonate (10 mL) and extracted with dichloromethane (3 x 10 mL). The combined organic layers were dried over sodium sulfate and concentrated *in vacuo*. The crude product was purified by flash column chromatography with $CHCl_3$:MeOH:Et_3N [96:2:2] as the eluent[4] to give himalensine A (**1**) as an off white amorphous solid (2.7 mg, 0.00912 mmol, 67%). A small amount of material was repurified by HPLC, (20%–80% MeCN-H2O in 10 min with 0.2% $HNMe_2$).

$[\alpha]_D^{25}$ = -74.0 (*c* 0.12, MeOH) *(Literature value: -44.0* (*c* 0.10, MeOH*[4]*

IR (film)/cm^{-1} ν_{max}**:** 2955, 2923, 1696, 1653, 1456

HRMS (ES^+) exact mass calculated for $[M+H]^+$ ($C_{19}H_{26}O_2N$) requires **m/z** 300.19581, found **m/z** 300.19583.

We observed the NMR signals of the isolated material to drift depending upon purification method and solvent, and time after purification. We found the ^1H signals were shifted downfield and filtering the sample through potassium carbonate or washing with an aqueous saturated potassium carbonate solution returned the signals back upfield. We postulate that this shift upfield is due to protonation of the product from

[4] Silica TLC plates prewashed with Et_3N used for TLC analysis of himalensine A. Natural product readily protonates on untreated silica.

residual acid in the chloroform/silica and when washed with saturated potassium carbonate solution, the full free-base form of the natural product is observed. The ^{1}H signals in the fully free-base form is further upfield than reported in literature, however we were able to obtain a ^{1}H and ^{13}C spectra of our synthetic sample which was in excellent agreement with the literature report. Re-purification of this same sample by HPLC with 0.2% dimethylamine in the eluent also upshifted the signals to the freebase form. This data suggests the reported spectrum of isolated natural product is of a partially protonated form of himalensine A.

Matched sample:

^{1}H NMR ($CDCl_3$, 400 MHz) δ_H 3.64 (s, 1H), 3.50 (brs, 1H), 2.90 (t, 1H, J = 8 Hz), 2.81 (dd, 1H, J = 13.6, 7.2 Hz), 2.80 – 2.57 (m, 5H), 2.55 (dd, 1H, J = 14.1, 10.1 Hz), 2.49 (m, 1H), 2.43 (ddd, 1H, J = 18.8, 6.4, 2.8 Hz), 2.30 (dt, 1H, J = 11.8, 5.8 Hz), 2.22 (m, 1H), 2.13 (dd, 1H, J = 14.8, 4.3 Hz), 2.07 (ddd, 1H, J = 14.8, 4.9, 1.8 Hz), 2.04 (brs, 1H), 1.80 (m, 2H), 1.12 (s, 3H), 0.98 (d, 3H, 6.7 Hz).

^{13}C NMR ($CDCl_3$ 100 MHz) δ_C 214.4, 208.7, 179.9, 135.9, 65.1, 54.9, 51.7, 49.6, 48.9, 48.3, 46.1, 34.6, 32.0, 31.8, 28.1, 26.3, 22.9, 20.3, 19.1.

HPLC re-purified sample:

^{1}H NMR ($CDCl_3$, 700 MHz) δ_H 3.63 (s, 1H), 3.46 (d, 1H, J = 5.2 Hz), 2.87 (dd, 1H, J = 9.0, 6.7 Hz), 2.84 – 2.73 (m, 3H), 2.70 (dddd, 1H, J = 18.8, 6.9, 2.6, 1.2 Hz), 2.68 – 2.55 (m, 2H), 2.52 (dd, 1H, J = 14.1, 9.1 Hz), 2.48 (m, 1H), 2.42 (ddd, 1H, J = 18.8, 6.7, 2.6 Hz), 22.29 – 2.20 (m, 2H), 2.11 (dd, 1H, J = 14.7, 4.4 Hz), 2.06 (ddd, 1H, J = 14.7, 5.0, 1.8 Hz), 2.02 (app dp, 1H, J = 4.2, 1.2 Hz), 1.81 – 1.78 (m, 2H), 1.11 (s, 3H), 0.97 (d, 3H, J = 6.8 Hz).

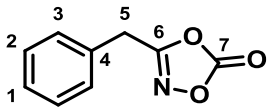
^{13}C NMR ($CDCl_3$, 175 MHz) δ_C 214.6, 208.8, 179.9, 136.0, 65.0, 54.9, 51.7, 49.7, 49.0, 48.3, 46.2, 34.6, 32.0, 31.9, 28.2, 26.3, 23.0, 20.4, 19.1.

General Procedure A: Synthesis of Dioxazolones from Acid Chlorides

A flask was charged with hydroxylamine hydrochloride (1 equivalent), potassium carbonate (1 equivalent) and solvent (diethyl ether/water; 7.5:1). The reaction was cooled to 0 ^{o}C with vigorous stirring before addition of acid chloride (1 equivalent) dropwise. The reaction was stirred overnight, diluted with water and extracted with ethyl acetate. The combined organic layers were washed with brine, dried over anhydrous sodium sulfate and concentrated *in vacuo*. The crude hydroxamic acid product was purified by trituration with pentane/diethyl ether if necessary.

To a slurry of hydroxamic acid (1 equivalent) in dichloromethane was added carbonyl diimidazole (CDI, 1.5 equivalents). The reaction was stirred for 30 minutes, diluted with 1M aqueous HCl and extracted with dichloromethane. The combined organic layers were dried over sodium sulfate and concentrated *in vacuo* to give dioxazolone **288**. Purification by dissolving in toluene and filtration was performed in necessary.

Compound 288a

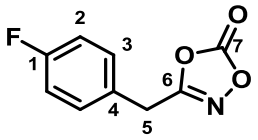


^{1}H NMR ($CDCl_3$, 400 MHz) δ_H 7.42 – 7.33 (m, 3H, $H^{1, 2}$), 7.32 – 7.28 (m, 2H, H^3), 3.93 (s, 2H, H^5)

^{13}C NMR ($CDCl_3$, 100 MHz) δ_C 165.4 (C^6), 154.1 (C^7), 130.6 (C^4), 129.4 (C^3), 129.1 (C^2), 128.6 (C^1), 31.4 (C^5).

Data matches previous literature report. V. Bizet, L. Buglioni, C. Bolm, *Angew. Chem. Int. Ed.***2014**, *53*, 5639.

Compound 288b



mp 39-40 °C

IR (film)/cm^{-1} ν_{max} 2917 (C-H), 2849 (C-H), 1861 (C=O), 1828 (C=N).

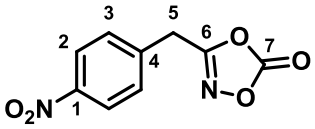
^{1}H NMR ($CDCl_3$, 400 MHz) δ_H 7.33 – 7.23 (m, 2H, H^2), 7.11 – 7.05 (m, 2H, H^3), 3.91 (s, 2H, H^5).

^{13}C NMR ($CDCl_3$, 100 MHz) δ_C 165.3 (C^7), 162.9 (d, J = 248 Hz, C^1), 153.9 (C^6), 130.9 (d, J = 8.3 Hz, C^3), 126.2 (d, J = 3.5 Hz, C^4), 116.3 (d, J = 21.9 Hz, C^2), 30.6 (C^5).

^{19}F NMR ($CDCl_3$, 400 MHz) δ_F -113.1.

HRMS (EI^+) exact mass calculated for [M]+ ($C_9H_6FNO_3$) requires m/z 195.0326, found m/z 195.0330.

Compound 288c



mp 89-94 °C.

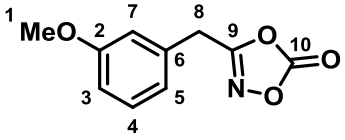
IR (film)/cm^{-1} ν_{max} 2981 (C-H stretch), 1866 (C=O stretch), 1837 (C=N stretch), 1520 (N-O stretch).

^{1}H NMR ($CDCl_3$, 400 MHz) δ_H 8.27 (d, *J* = 8.7 Hz, 1H, H^2), 7.53 – 7.49 (m, 2H, H^3), 4.07 (s, 2H, H^5).

^{13}C NMR ($CDCl_3$, 100 MHz) δ_C 164.2 (C^6), 153.5 (C^7), 148.2 (C^1), 137.5 (C^4), 130.3 (C^2), 124.6 (C^3), 31.1 (C^5).

HRMS (EI^+) exact mass calculated for [M+Na]+ ($C_9H_6N_2O_5$) requires m/z 222.0271, found m/z 222.0278.

Compound 288d



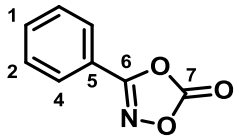
IR (film)/cm^{-1} ν_{max} 2972 (C-H stretch), 1860 (C=O stretch), 1828 (C=N stretch), 1600 (C=C stretch).

^{1}H NMR ($CDCl_3$, 400 MHz) δ_H 7.30 (dd, *J* = 8.3, 7.6 Hz, 1H, H^4), 6.92 – 6.84 (m, 1H, $H^{3,5}$), 6.82 (t, *J* = 2.1 Hz, 1H, H^7), 3.90 (s, 2H, H^8), 3.82 (s, 3H, H^1).

^{13}C NMR ($CDCl_3$, 100 MHz) δ_C 165.4 (C^9), 160.3 (C^{10}), 154.0 (C^2), 131.9 (C^6), 130.5 (C^4), 121.3 (C^5), 115.0 (C^7), 113.9 (C^3), 55.5 (C^1), 31.4 (C^8).

HRMS (EI^+) exact mass calculated for [M]+ ($C_{10}H_9NO_4$) requires m/z 207.0526, found m/z 207.0531.

Compound 288e

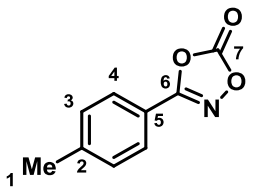


^{1}H NMR ($CDCl_3$, 400 MHz) δ_H 7.90 – 7.83 (m, 2H, H^4), 7.69 – 7.61 (m, 1H, H^1), 7.59 – 7.50 (m, 1H, H^2).

^{13}C NMR ($CDCl_3$, 100 MHz) δ_C 163.7 (C^6), 154.0 (C^7), 133.9 (C^1), 129.5 (C^4), 126.8 (C^2), 120.3 (C^5).

Matches literature report: Bolm *et al. Angew. Chem. Int. Ed.* **2014**, *53*, 5639 –5642

Compound 288f

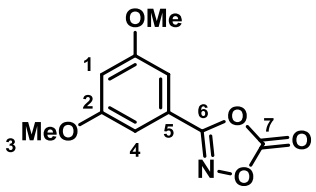


^{1}H NMR ($CDCl_3$, 400 MHz) δ_H 7.77 – 7.70 (m, 2H, H^4), 7.34 (d, *J* = 8.1 Hz, 2H, H^3), 2.45 (s, 3H, H^1).

^{13}C NMR ($CDCl_3$, 100 MHz) δ_C δ 163.8 (C^6), 154.1 (C^7), 145.0 (C^2), 130.2(C^3), 126.7(C^4), 117.4 (C^5), 21.9 (C^1).

Matches literature report: Bolm *et al. Angew. Chem. Int. Ed.* **2014**, *53*, 5639 –5642.

Compound 288g



mp 89-92 °C.

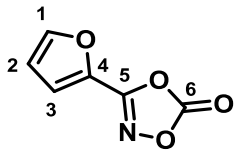
IR (film)/cm^{-1} ν_{max} 2981 (C-H stretch), 1824 (C=O stretch), 1585 (C=C stretch).

^{1}H NMR ($CDCl_3$, 400 MHz) δ_H 6.96 (d, *J* = 2.3 Hz, 2H, H^4), 6.69 (t, *J* = 2.3 Hz, 1H, H^1), 3.84 (s, 6H, H^3).

^{13}C NMR ($CDCl_3$, 100 MHz) δ_C 163.7 (C^6), 161.5 (C^7), 153.9 (C^2), 121.7 (C^5), 106.3 (C^1), 104.5 (C^4), 55.9 (C^3).

HRMS (EI^+) exact mass calculated for [M]+ ($C_{10}H_9NO_5$) requires m/z 223.0475, found m/z 223.0481.

Compound 288h

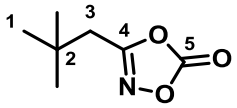


^{1}H NMR ($CDCl_3$, 400 MHz) δ_H 7.72 (dd, *J* = 1.8, 0.8 Hz, 1H, H^3), 7.19 (dd, *J* = 3.6, 0.8 Hz, 1H, H^1), 6.66 (dd, *J* = 3.6, 1.8 Hz, 1H, H^2).

^{13}C NMR ($CDCl_3$, 100 MHz) δ_C 156.7 (C^5), 153.2 (C^6), 147.9 (C^3), 135.2 (C^4), 117.9 (C^1), 112.7 (C^2).

Matches literature report: Bolm *et al. Angew. Chem. Int. Ed.* **2014**, *53*, 5639 –5642.

Compound 288i

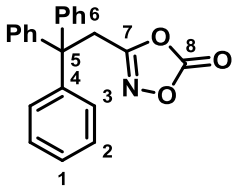


IR (film)/cm^{-1} ν_{max} 2964 (C-H stretch), 1878 (C=O stretch), 1832 (C=N stretch), 1630 (N-O) stretch.

^{1}H NMR ($CDCl_3$, 400 MHz) δ_H 2.50 (s, 2H, H^3), 1.07 (s, 9H, H^1).

^{13}C NMR ($CDCl_3$, 100 MHz) δ_C 165.7 (C^4), 154.4 (C^5), 38.5 (C^3), 31.4 (C^2), 29.5 (C^1).

Compound 288j



mp 98-101 ^oC

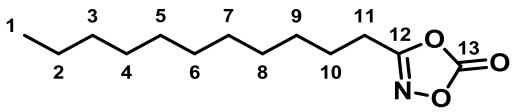
IR (film)/cm^{-1} ν_{max} 1867 (C=O stretch), 1828 (C=N stretch), 1627 (C=C stretch).

^{1}H NMR ($CDCl_3$, 400 MHz) δ_H 7.38 – 7.15 (m, 15H, $H^{1, 2, 3, 4}$), 3.97 (s, 2H, H^6).

^{13}C NMR ($CDCl_3$, 100 MHz) δ_C 165.0 (C^7), 153.8 (C^8), 144.8 (C^4), 128.9 (C^3), 128.5 (C^2), 127.2 (C^1), 56.3 (C^5), 37.1 (C^6).

HRMS (EI^+) exact mass calculated for [M]+ ($C_{22}H_{17}NO_3$) requires m/z 343.1203, found m/z 343.1209.

Compound 288k

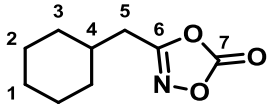


IR (film)/cm^{-1} ν_{max} 2924 (C-H stretch), 1869 (C=O stretch), 1829 (C=N stretch), 1637 (N-O stretch).

^{1}H NMR ($CDCl_3$, 400 MHz) δ_H 2.64 – 2.58 (m, 2H, H^{11}), 1.79 – 1.66 (m, 2H, H^{10}), 1.46 – 1.22 (m, 16H, $H^{2, 3, 4, 5, 6, 7, 8, 9}$), 0.93 – 0.83 (m, 3H, H^1).

^{13}C NMR ($CDCl_3$, 100 MHz) δ_C 166.9 (C^{12}), 154.4 (C^{13}), 32.0 ($C^{2/3/4/5/6/7/8/9}$), 29.7 ($C^{2/3/4/5/6/7/8/9}$), 29.7 ($C^{2/3/4/5/6/7/8/9}$), 29.6 ($C^{2/3/4/5/6/7/8/9}$), 29.4 ($C^{2/3/4/5/6/7/8/9}$), 29.1 ($C^{2/3/4/5/6/7/8/9}$), 28.8 ($C^{2/3/4/5/6/7/8/9}$), 24.9 (C^{11}), 24.7 (C^{10}), 22.8 ($C^{2/3/4/5/6/7/8/9}$), 14.2 (C^{1}).

Compound 288l

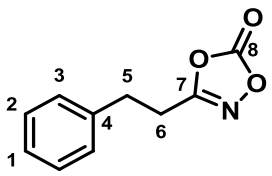


IR (film)/cm^{-1} ν_{max} 2926 (C-H stretch), 1859 (C=O stretch), 1826 (C=N stretch), 1633 (N-O stretch).

^{1}H NMR ($CDCl_3$, 400 MHz) δ_H 2.50 (d, *J* = 6.7 Hz, 2H, H^5), 1.83 – 1.64 (m, 6H, $H^{4, 1a, 2a, 3a}$), 1.36 – 1.10 (m, 3H, $H^{2b, 3b}$), 1.05 (qd, *J* = 11.3, 10.1, 5.6 Hz, 1H, H^{1b}).

^{13}C NMR ($CDCl_3$, 100 MHz) δ_C 166.1 (C^6), 154.4 (C^7), 34.7 (C^4), 32.8 (C^3), 32.2 (C^5), 25.9 (C^1), 25.8 (C^2).

Compound 288m



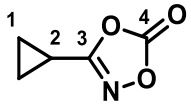
IR (film)/cm^{-1} ν_{max} 2981 (C-H stretch), 1867 (C=O stretch), 1827 (C=N stretch).

^{1}H NMR ($CDCl_3$, 400 MHz) δ_H 7.38 – 7.32 (m, 2H, H^2), 7.31 – 7.25 (m, 1H, H^1), 7.24 – 7.20 (m, 2H, H^3), 3.09 – 3.02 (m, 2H, H^6), 2.98 – 2.92 (m, 2H, H^5)

^{13}C NMR ($CDCl_3$, 100 MHz) δ_C 166.0 (C^7), 154.1 (C^8), 138.1 (C^4), 129.0 (C^2), 128.3 (C^3), 127.3 (C^1), 30.6 (C^6), 26.8 (C^5).

HRMS (EI^+) exact mass calculated for [M]+ ($C_{10}H_9NO_3$) requires m/z 191.0577, found m/z 191.0578.

Compound 288n



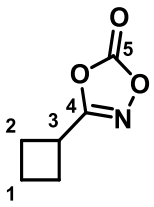
IR (film)/cm^{-1} ν_{max} 2917 (C-H stretch), 1881 (C=O stretch), 1827 (C=N stretch), 1630 (N-O stretch).

^{1}H NMR ($CDCl_3$, 400 MHz) δ_H 1.90 (tt, *J* = 8.3, 5.1 Hz, 1H, H^2), 1.22 – 1.12 (m, 4H, H^1)

^{13}C NMR ($CDCl_3$, 100 MHz) δ_C 168.0 (C^3), 154.1 (C^4), 7.4 (C^1), 5.5 (C^2).

HRMS (EI^+) exact mass calculated for [M]+ ($C_5H_5NO_3$) requires m/z 127.0264, found m/z 127.0264.

Compound 288o



IR (film)/cm^{-1} ν_{max} 2954 (C-H stretch), 1871 (C=O stretch), 1827 (C=N stretch), 1626 (N-O stretch).

^{1}H NMR ($CDCl_3$, 400 MHz) δ_H 3.47 (pd, *J* = 8.4, 1.1 Hz, 1H, H^3), 2.43 – 2.35 (m, 4H, H^2), 2.21 – 2.00 (m, 2H, H^1)

^{13}C NMR ($CDCl_3$, 100 MHz) δ_C 168.4 (C^4), 154.5 (C^5), 29.5 (C^3), 25.2 (C^2), 19.0 (C^1).

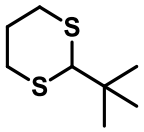
HRMS (EI^+) exact mass calculated for [M]+ ($C_6H_7NO_3$) requires m/z 141.0420, found m/z 141.0419.

General Procedure B: Synthesis of Dithianes

To a solution of aldehyde (1 equivalent) in dichloromethane cooled to 0 ^oC, was added potassium tert-butoxide (1.3 equivalents), followed by dropwise addition of electrophile (2 equivalents). The reaction was warmed to room temperature and stirred overnight, followed by addition of 1M HCl. The reaction was extracted with dichloromethane, dried over anhydrous sodium sulfate and concentrated in vacuo. The crude product was purified by flash column chromatography to α-methylated aldehyde.

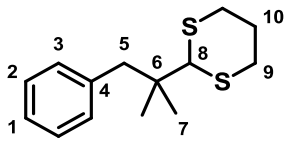
To a solution of α-methylated aldehyde in toluene, was pTSA.H2O (0.05 equivalents) and propane dithiol (1.3 equivalents) sequentially. The reaction was purged with nitrogen and heated to 80 °C until full consumption of the aldehyde. The reaction was diluted with diethyl ether and washed twice with 1M aqueous KOH. The organic layers were dried over anhydrous sodium sulfate and concentrated in vacuo. The crude product was purified by flash column chromatography to give desired dithiane **290**.

Compound 290a



Prepared according to an analogous procedure to General Procedure B. To a solution of trimethylacetaldehyde (3 mL, 27.62 mmol) in toluene (50 mL) was added para-toluenesulfonic acid monohydrate (263 mg, 0.05 eq.), followed by 1,3-propanedithiol (3.61 mL, 1.3 eq.). The reaction was purged with nitrogen and heated to 80 °C overnight. The reaction mixture was diluted with diethyl ether (100 mL) and washed three times with 1M aqueous KOH. The organic layers were washed with brine, dried over anhydrous sodium sulfate and concentrated in vacuo. The crude oil was seeded with a crystal of product, and the crystals were collected and washed with ice methanol to give **290a** as a clear crystalline solid, 4.70g, 96%.

Compound 290b



Clear crystalline solid, 23%.

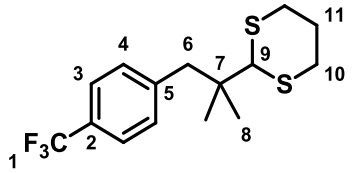
mp 36-40 °C.

IR (film)/cm^{-1} ν_{max} 2964 (C-H stretch), 1493 (C-S stretch), 1422 (C=C stretch).

^{1}H NMR ($CDCl_3$, 400 MHz) δ_H 7.31 – 7.23 (m, 5H, $H^{1,2,3}$), 3.93 (s, 1H, H^8), 2.96 – 2.82 (m, 4H, H^9), 2.81 (s, 2H, H^5), 2.08 (dtt, *J* = 13.6, 3.8, 2.8 Hz, 1H, H^{10a}), 1.84 (dtt, *J* = 14.0, 11.2, 4.6 Hz, 1H, H^{10b}), 1.09 (s, 6H, H^7).

^{13}C NMR ($CDCl_3$, 100 MHz) δ_C 138.4 (C^4), 130.8 (C^3), 128.0 (C^2), 126.3 (C^1), 60.4 (C^8), 45.7 (C^5), 39.6 (C^6), 31.5 (C^9), 26.3 (C^{10}), 25.5 (C^7).

Compound 290c



Clear crystalline solid, 19%.

mp 58-59 °C.

IR (film)/cm^{-1} ν_{max} 2964 (C-H stretch), 2935 (C-H stretch), 2899 (C-H stretch), 1324.

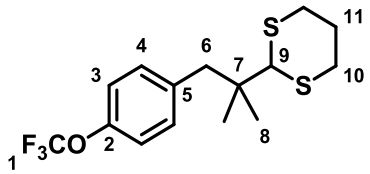
^{1}H NMR ($CDCl_3$, 400 MHz) δ_H 7.54 (d, *J* = 8.0 Hz, 2H, H^3), 7.40 – 7.37 (m, 2H, H^4), 3.88 (s, 1H, H^9), 2.95 – 2.82 (m, 6H, $H^{6, 10}$), 2.09 (dtt, *J* = 13.7, 3.9, 2.8 Hz, 1H, H^{11a}), 1.84 (dtt, *J* = 14.0, 11.6, 4.1 Hz, 1H, H^{11b}), 1.09 (s, 6H, H^8).

^{13}C NMR ($CDCl_3$, 100 MHz) δ_C 142.6 (C^5), 131.0 (C^4), 128.9 (C^2), 125.9 (C^1), 124.9 (C^3), 60.1 (C^9), 45.5 (C^{10}), 39.7 (C^7), 31.4 (C^6), 26.2 (C^{11}), 25.5 (C^8).

^{19}F NMR ($CDCl_3$, 400 MHz) δ_F -62.34.

HRMS ($APCI^+$) exact mass calculated for [M+H]+ ($C_{15}H_{20}F_3{}^{32}S_2$) requires m/z 321.0953, found m/z 321.0957.

Compound 290d



Oil, 17%.

IR (film)/cm^{-1} ν_{max} 2968 (C-H stretch), 2899 (C-H stretch), 1508 (C-S stretch).

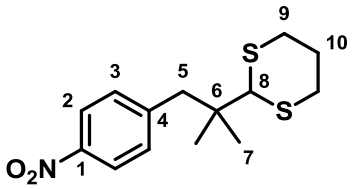
^{1}H NMR ($CDCl_3$, 400 MHz) δ_H 7.30 – 7.27 (m, 2H, H^4), 7.12 (dq, *J* = 7.6, 1.0 Hz, 2H, H^3), 3.88 (s, 1H, H^9), 2.94 – 2.81 (m, 4H, H^{10}), 2.81 (s, 2H, H^6), 2.09 (dtt, *J* = 13.6, 3.9, 2.8 Hz, 1H, H^{11a}), 1.83 (dtt, *J* = 14.0, 11.4, 4.4 Hz, 1H, H^{11b}), 1.08 (s, 6H, H^8).

^{13}C NMR ($CDCl_3$, 100 MHz) δ_C 148.00 (q, *J* = 2.0 Hz, C^2), 137.09 (C^5), 132.0 (C^4), 120.7 (q, J = 257 Hz, C^1), 120.4 (C^3), 60.1 (C^9), 45.0 (C^6), 39.6 (C^7), 31.4 (C^{10}), 26.2 (C^{11}), 25.5 (C^8).

^{19}F NMR ($CDCl_3$, 400 MHz) δ_F -57.82.

HRMS ($APCI^+$) exact mass calculated for [M+H]+ ($C_{15}H_{20}OF_3{}^{32}S_2$) requires m/z 337.0902, found m/z 337.0906.

Compound 290e



Off-white solid, 15%.

mp 73-77 °C.

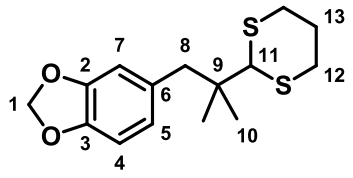
IR (film)/cm^{-1} ν_{max} 2963 (C-H stretch), 2931 (C-H stretch), 1517 (C-S stretch), 1345 (N-O stretch).

^{1}H NMR ($CDCl_3$, 400 MHz) δ_H 8.17 – 8.12 (m, 2H, H^2), 7.46 – 7.42 (m, 2H, H^3), 3.84 (s, 1H, H^8), 2.95 – 2.81 (m, 6H, $H^{5, 9}$), 2.10 (dtt, *J* = 13.7, 4.0, 2.7 Hz, 1H, H^{10a}), 1.83 (dtt, *J* = 14.0, 11.9, 3.8 Hz, 1H, H^{10b}), 1.10 (s, 6H, H^7).

^{13}C NMR ($CDCl_3$, 100 MHz) δ_C 146.9 (C^1), 146.4 (C^4), 131.5 (C^3), 123.2 (C^2), 60.0 (C^8), 45.5 (C^5), 39.9 (C^9), 31.4 (C^6), 26.1 (C^{10}), 25.6 (C^7).

HRMS ($APCI^+$) exact mass calculated for [M+H]+ ($C_{14}H_{20}O_2N^{32}S_2$) requires m/z 298.0930, found m/z 298.0934.

Compound 290f



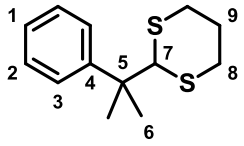
Oil, 21%.

IR (film)/cm^{-1} ν_{max} 2961 (C-H stretch), 2895 (C-H stretch), 1501 (C-S stretch), 1488 (C=C stretch).

^{1}H NMR ($CDCl_3$, 400 MHz) δ_H 6.80 – 6.77 (m, 1H, H^7), 6.76 – 6.68 (m, 2H, $H^{4, 5}$), 5.93 (s, 2H, H^1), 3.91 (s, 1H, H^{11}), 2.93 – 2.81 (m, 4H, H^{12}), 2.72 (s, 2H, H^8), 2.14 – 2.02 (m, 1H, H^{13a}), 1.82 (dtt, *J* = 14.0, 10.9, 4.8 Hz, 1H, H^{13b}), 1.07 (s, 6H, H^{10}).

^{13}C NMR ($CDCl_3$, 100 MHz) δ_C 147.3 (C^2), 146.1 (C^3), 132.0 (C^6), 123.7 (C^5), 111.1 (C^7), 107.8 (C^4), 100.9 (C^1), 60.2 (C^{11}), 45.4 (C^8), 39.6 (C^9), 31.4 (C^{12}), 26.2 (C^{13}), 25.5 (C^{10}).

Compound 290g



Oil, 52%.

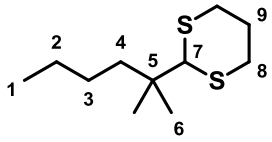
IR (film)/cm^{-1} ν_{max} 2971 (C-H stretch), 2893 (C-H stretch), 1496 (C-S stretch).

^{1}H NMR ($CDCl_3$, 400 MHz) δ_H 7.46 – 7.38 (m, 2H, H^3), 7.35 (ddd, *J* = 7.8, 6.8, 1.2 Hz, 2H, H^2), 7.30 – 7.21 (m, 1H, H^1), 4.38 (s, 1H, H^7), 2.91 – 2.77 (m, 4H, H^8), 2.08 – 1.9f7 (m, 1H, H^{9a}), 1.87 – 1.63 (m, 1H, H^{9b}), 1.55 (s, 6H, H^6).

^{13}C NMR ($CDCl_3$, 100 MHz) δ_C 146.7 (C^4), 128.2 (C^2), 126.7 (C^3), 126.3 (C^1), 61.9 (C^7), 42.8 (C^5), 31.6 (C^8), 26.4 (C^9), 26.0 (C^6).

HRMS (ES^+) exact mass calculated for [M+H]+ ($C_{13}H_{19}{}^{32}S_2$) requires m/z 239.0923, found m/z 239.0925.

Compound 290h



Oil, 27%.

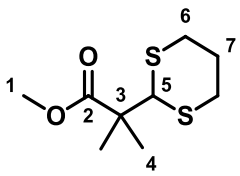
IR (film)/cm^{-1} ν_{max} 2966 (C-H stretch), 1422.

^{1}H NMR ($CDCl_3$, 400 MHz) δ_H 4.02 (s, 1H, H^7), 2.94 – 2.81 (m, 4H, H^8), 2.11 – 2.00 (m, 1H, H^{9a}), 1.89 – 1.73 (m, 1H, H^{9b}), 1.48 – 1.40 (m, 2H, H^4), 1.36 – 1.20 (m, 4H, $H^{2, 3}$), 1.07 (s, 6H, H^6), 0.91 (t, *J* = 6.9 Hz, 3H, H^1).

^{13}C NMR ($CDCl_3$, 100 MHz) δ_C 61.2 (C^7), 40.3 (C^4), 38.3 (C^5), 31.6 (C^8), 26.4 (C^9), 26.1 (C^3), 25.6 (C^6), 23.5 (C^2), 14.3 (C^1).

HRMS (ES^+) exact mass calculated for [M+Na]+ ($C_{19}H_{30}ON^{32}S_2$) requires m/z 352.1763, found m/z 352.1757.

Compound 290i



Oil, 95% (from aldehyde).

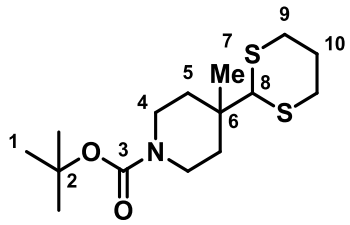
IR (film)/cm^{-1} ν_{max} 2981 (C-H stretch), 2948 (C-H stretch), 1731 (C=O stretch), 1464 (C-S stretch).

^{1}H NMR ($CDCl_3$, 400 MHz) δ_H 4.44 (s, 1H, H^5), 3.71 (s, 3H, H^1), 2.98 – 2.82 (m, 4H, H^6), 2.09 (dtt, *J* = 14.0, 4.2, 2.7 Hz, 1H, H^{7a}), 1.83 (dtt, *J* = 14.0, 11.7, 3.8 Hz, 1H, H^{7b}), 1.34 (s, 6H, H^4)

^{13}C NMR ($CDCl_3$, 100 MHz) δ_C 175.9 (C^2), 57.7 (C^5), 52.4 (C^1), 47.9 (C^3), 31.4 (C^6), 26.1 (C^7), 22.8 (C^4).

HRMS (ES^+) exact mass calculated for [M+Na]+ ($C_9H_{16}O_2{}^{23}Na^{32}S_2$) requires m/z 243.0484, found m/z 243.0484.

Compound 290j



White solid, 47%.

mp 59-61 ^oC.

IR (film)/cm^{-1} ν_{max} 2966 (C-H stretch), 1688 (C=O stretch), 1453 (C-S stretch).

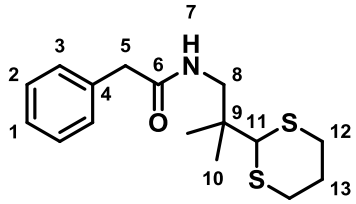
^{1}H NMR ($CDCl_3$, 400 MHz) δ_H 4.10 (s, 1H, H^8), 3.66 – 3.56 (m, 2H, H^{4a}), 3.17 (ddd, *J* = 13.5, 9.5, 3.6 Hz, 2H, H^{4b}), 2.92 – 2.83 (m, 4H, H^9), 2.13 – 2.05 (m, 1H, H^{10a}), 1.88 – 1.76 (m, 1H, H^{10b}), 1.71 (ddd, *J* = 13.8, 9.5, 4.3 Hz, 2H, H^{5a}), 1.55 – 1.48 (m, 2H, H^{5b}), 1.45 (s, 9H, H^1), 1.14 (s, 3H, H^7)

^{13}C NMR ($CDCl_3$, 100 MHz) δ_C 155.1 (C^3), 79.5 (C^2), 60.4 (C^8), 39.7 (C^4), 36.8 (C^6), 35.4 (C^5), 31.4 (C^9), 28.6 (C^7), 26.4 (C^{10}), 20.7 (C^1).

General Procedure C: Synthesis of Amidated dithianes 293.

A 14 mL oven dried vial is charged with dithiane (0.05 mmol, 1 equivalent), $[Cp^*Rh(MeCN)_3][(SbF_6)_2]$ (0.15 equivalents), Fmoc-Pro-OH (0.31 equivalents), NaOtBu (0.30 equivalents) and dioxazolone (2 equivalents). The vial is sealed, dichloroethane (0.5 mL, 0.1 M) was added, and the atmosphere replaced with nitrogen. The reaction was left to stir for 36 hours, and the crude product was purified directly by flash column chromatography to give amidodithianes **293**.

Compound 293a



Off-white solid, 71%.

mp 111-113 °C.

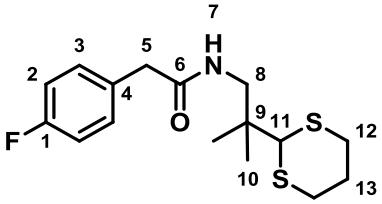
IR (film)/cm^{-1} ν_{max} 3305 (N-H stretch), 2929 (C-H stretch), 1647 (C=O stretch), 1527.

^{1}H NMR ($CDCl_3$, 400 MHz) δ_H 7.41 – 7.35 (m, 2H, H^2), 7.33 – 7.28 (m, 3H, $H^{1,3}$), 5.80 (br s, 1H, H^7), 3.65 (s, 1H, H^{11}), 3.62 (s, 2H, H^5), 3.26 (d, *J* = 6.6 Hz, 2H, H^8), 2.76 (dt, *J* = 14.5, 3.7 Hz, 2H, H^{12a}), 2.64 (ddd, *J* = 14.5, 12.5, 2.5 Hz, 2H, H^{12b}), 2.01 (dtt, *J* = 13.6, 4.2, 2.5 Hz, 1H, H^{13a}), 1.70 (dtt, *J* = 13.9, 12.4, 3.3 Hz, 1H, H^{13b}), 1.00 (s, 6H, H^{10}).

^{13}C NMR ($CDCl_3$, 100 MHz) δ_C 171.3 (C^6), 135.4 (C^4), 129.8 (C^3), 129.2 (C^2), 127.4 (C^1), 58.7 (C^{11}), 47.5 (C^8), 44.3 (C^5), 40.1 (C^9), 31.4 (C^{12}), 26.0 (C^{13}), 23.9 (C^{10}).

HRMS (ES^+) exact mass calculated for [M+Na]+ ($C_{16}H_{23}ON^{23}Na^{32}S_2$) requires m/z 332.1113, found m/z 332.1109.

Compound 293b



Off-white solid, 74%.

mp 104-105 °C.

IR (film)/cm^{-1} ν_{max} 3307 (N-H stretch), 2971 (C-H stretch), 1648 (C=O stretch), 1508 (C=C stretch).

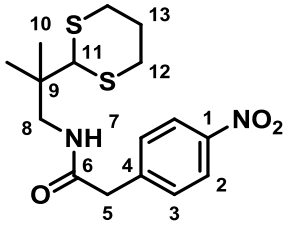
^{1}H NMR ($CDCl_3$, 500 MHz) δ_H 7.30 – 7.25 (m, 2H, H^2), 7.09 – 7.04 (m, 2H, H^3), 5.84 (s, 1H, H^7), 3.74 (s, 1H, H^{11}), 3.58 (s, 2H, H^5), 3.27 (d, *J* = 6.6 Hz, 2H, H^8), 2.85 – 2.77 (m, 2H, H^{12a}), 2.70 (ddd, *J* = 14.6, 12.4, 2.4 Hz, 2H, H^{12b}), 2.05 (dtt, *J* = 13.6, 4.1, 2.5 Hz, 1H, H^{13a}), 1.72 (dtt, *J* = 14.1, 12.5, 3.3 Hz, 1H, H^{13b}), 1.02 (s, 6H, H^{10})

^{13}C NMR ($CDCl_3$, 125 MHz) δ_C 170.90 (C^6), 162.27 (d, *J* = 246.0 Hz, C^1), 131.38 (d, *J* = 7.9 Hz, C^3) 131.11 (d, *J* = 3.3 Hz, C^4), 116.01 (d, *J* = 21.4 Hz, C^2) , 58.9 (C^{11}), 47.5 (C^8), 43.4 (C^5), 40.1 (C^9), 31.5 (C^{12}), 26.0 (C^{13}), 24.2 (C^{10}).

^{19}F NMR ($CDCl_3$, 400 MHz) δ_F -115.3.

HRMS (ES^+) exact mass calculated for [M+H]+ ($C_{16}H_{23}ONF^{32}S_2$) requires m/z 328.1200, found m/z 328.1201.

Compound 293c



Yellow solid, 40%.

mp 96-101 °C.

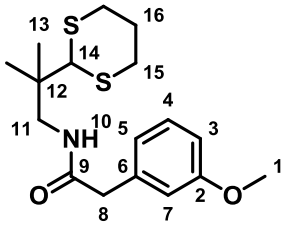
IR (film)/cm^{-1} ν_{max} 3291 (N-H stretch), 3081 (C-H stretch), 1650 (C=O stretch), 1519 (N-O stretch).

^{1}H NMR ($CDCl_3$, 500 MHz) δ_H 8.23 – 8.20 (m, 2H, H^2), 7.52 – 7.48 (m, 2H, H^3), 6.01 (s, 1H, H^7), 3.88 (s, 1H, H^{11}), 3.68 (s, 2H, H^5), 3.31 (d, *J* = 6.5 Hz, 2H, H^8), 2.88 – 2.71 (m, 4H, H^{12}), 2.10 – 2.04 (m, 1H, H^{13a}), 1.72 (dtt, *J* = 14.1, 12.2, 3.7 Hz, 1H, H^{13b}), 1.05 (s, 6H, H^{10})

^{13}C NMR ($CDCl_3$, 125 MHz) δ_C 169.3 (C^6), 147.4 (C^1), 142.7 (C^4), 130.6 (C^3), 124.1 (C^2), 59.1 (C^{11}), 47.7 (C^8), 43.8 (C^5), 40.1 (C^9), 31.6 (C^{12}), 26.0 (C^{13}), 24.5 (C^{10}).

HRMS (ES^+) exact mass calculated for [M+Na]+ ($C_{16}H_{22}O_3N_2{}^{23}Na^{32}S_2$) requires m/z 377.0964, found m/z 377.0964.

Compound 293d



Off-white solid, 67%.

mp 96-99 °C.

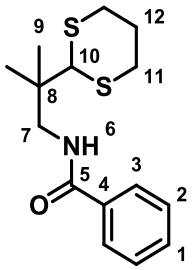
IR (film)/cm^{-1} ν_{max} 3304 (N-H stretch), 2980 (C-H stretch), 1649 (N-H stretch), 1532 (C=C stretch).

^{1}H NMR ($CDCl_3$, 500 MHz) δ_H 7.30 (td, *J* = 7.5, 1.0 Hz, 1H, H^4), 6.90 – 6.82 (m, 3H, $H^{3,5,7}$), 5.84 (s, 1H, H^{10}), 3.81 (s, 3H, H^1), 3.66 (s, 1H, H^{14}), 3.59 (s, 2H, H^8), 3.26 (d, *J* = 6.6 Hz, 2H, H^{11}), 2.77 (dt, *J* = 14.2, 3.7 Hz, 2H, H^{15a}), 2.66 (ddd, *J* = 14.4, 12.4, 2.5 Hz, 2H, H^{15b}), 2.02 (dtt, *J* = 13.6, 4.2, 2.5 Hz, 1H, H^{16a}), 1.71 (dtt, *J* = 14.2, 12.5, 3.4 Hz, 1H, H^{16b}), 1.01 (s, 6H, H^{13}).

^{13}C NMR ($CDCl_3$, 100 MHz) δ_C 171.0 (C^9), 160.3 (C^2), 136.9 (C^6), 130.3 (C^4), 122.1 (C^3), 115.1 (C^7), 113.2 (C^5), 58.7 (C^{14}), 55.4 (C^1), 47.4 (C^{11}), 44.4 (C^8), 40.2 (C^{12}), 31.4 (C^{15}), 26.1 (C^{16}), 24.0 (C^{13}).

HRMS (ES^+) exact mass calculated for [M+Na]+ ($C_{17}H_{25}O_2N^{23}Na^{32}S_2$) requires m/z 362.1219, found m/z 362.1213.

Compound 293e



White solid, 49%.

mp 89-92 °C.

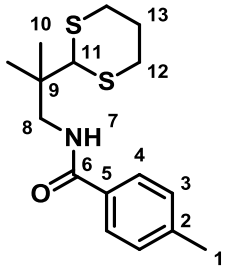
IR (film)/cm^{-1} ν_{max} 3328 (N-H stretch), 2971 (C-H stretch), 1643 (C=O stretch), 1537 (C=C stretch).

^{1}H NMR ($CDCl_3$, 400 MHz) 7.86 – 7.81 (m, 1H, H^3), 7.53 – 7.48 (m, 1H, H^1), 7.48 – 7.42 (m, 2H, H^2), 6.75 (s, 1H, H^6), 4.12 (s, 1H, H^{10}), 3.56 (d, *J* = 6.6 Hz, 2H, H^7), 3.05 – 2.86 (m, 4H, H^{11}), 2.17 – 2.09 (m, 1H, H^{12a}), 1.94 – 1.80 (m, 1H, H^{12b}), 1.18 (s, 6H, H^9).

^{13}C NMR ($CDCl_3$, 100 MHz) δ_C 167.6 (C^5), 134.9 (C^4), 131.5 (C^1), 128.7 (C^3), 127.1 (C^2), 59.5 (C^{10}), 47.9 (C^7), 40.4 (C^8), 31.7 (C^{11}), 26.2 (C^{12}), 24.6 (C^9).

HRMS (ES^+) exact mass calculated for [M+Na]+ ($C_{15}H_{21}ON^{23}Na^{32}S_2$) requires m/z 318.0957, found m/z 318.0958.

Compound 293f



White solid, 41%.

mp 167-168 ^{o}C.

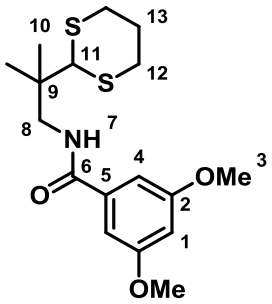
IR (film)/cm^{-1} ν_{max} 3348 (N-H stretch), 2980 (C-H stretch), 1642 (C=O stretch), 1503 (C=C stretch).

^{1}H NMR ($CDCl_3$, 500 MHz) δ_H 7.72 (d, *J* = 8.2 Hz, 2H, H^4), 7.25 (m, 2H, H^3), 6.69 (s, 1H, H^7), 4.11 (s, 1H, H^{11}), 3.55 (d, *J* = 6.6 Hz, 2H, H^8), 2.97 – 2.85 (m, 4H, H^{12}), 2.40 (s, 3H, H^1), 2.13 (app dq, *J* = 14.0, 3.2 Hz, 1H, H^{13a}), 1.91 – 1.81 (m, 1H, H^{13b}), 1.17 (s, 6H).

^{13}C NMR ($CDCl_3$, 125 MHz) δ_C 167.5 (C^6), 141.9 (C^2), 132.0 (C^5), 129.4 (C^3), 127.1 (C^4), 59.5 (C^{11}), 47.8 (C^8), 40.4 (C^9), 31.7 (C^{12}), 26.2 (C^{13}), 24.5 (C^{10}), 21.6 (C^1).

HRMS (ES^+) exact mass calculated for [M+Na]+ ($C_{16}H_{23}ON^{23}Na^{32}S_2$) requires m/z 332.1113, found m/z 332.1112.

Compound 293g



White solid, 55%.

mp 103-108 °C.

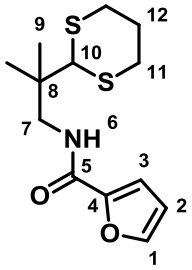
IR (film)/cm^{-1} ν_{max} 3332 (N-H stretch), 2933 (C-H stretch), 1649 (C=O stretch), 1593 (C=C stretch).

^{1}H NMR ($CDCl_3$, 400 MHz) δ_H 6.97 (d, *J* = 2.3 Hz, 2H, H^4), 6.67 (t, *J* = 6.9 Hz, 1H, H^7), 6.58 (t, *J* = 2.3 Hz, 1H, H^1), 4.11 (s, 1H, H^{11}), 3.83 (s, 6H, H^3), 3.53 (d, *J* = 6.6 Hz, 2H, H^8), 2.99 – 2.88 (m, 4H, H^{12}), 2.16 – 2.08 (m, 1H, H^{13a}), 1.93 – 1.77 (m, 1H, H^{13b}), 1.17 (s, 6H, H^{10}).

^{13}C NMR ($CDCl_3$, 100 MHz) δ_C 167.3 (C^6), 161.0 (C^2), 137.2 (C^5), 105.1 (C^4), 103.6 (C^1), 59.4 (C^{11}), 55.7 (C^3), 47.9 (C^8), 40.4 (C^9), 31.7 (C^{12}), 26.2 (C^{13}), 24.5 (C^{10}).

HRMS (ES^+) exact mass calculated for [M+H]+ ($C_{17}H_{26}O_3N^{32}S_2$) requires m/z 356.1349, found m/z 356.1343.

Compound 293h



Pale yellow solid, 46%.

mp 137-139 °C.

IR (film)/cm^{-1} ν_{max} 3267 (N-H stretch), 2827 (C-H stretch), 1653 (C=O stretch), 1524 (C=C stretch).

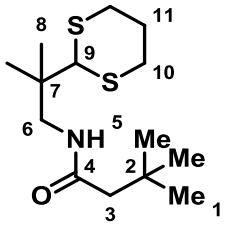
^{1}H NMR ($CDCl_3$, 400 MHz) δ_H 7.48 – 7.44 (m, 1H, H^3), 7.11 (d, *J* = 3.5 Hz, 1H, H^1), 6.77 (s, 1H, H^6), 6.50 (dd, *J* = 3.5, 1.8 Hz, 1H, H^2), 4.11 (s, 1H, H^{10}), 3.51 (d, *J* = 6.8 Hz, 2H, H^7), 2.98

– 2.88 (m, 4H, H^{11}), 2.12 (dp, *J* = 13.6, 3.3 Hz, 1H, H^{12a}), 1.86 (dtt, *J* = 15.6, 8.8, 6.9 Hz, 1H, H^{12b}), 1.15 (s, 6H, H^{9}).

^{13}C NMR ($CDCl_3$, 100 MHz) δ_C 158.7 (C^5), 148.3 (C^4), 144.0 (C^3), 114.4 (C^1), 112.3 (C^2), 59.0 (C^{10}), 47.0 (C^7), 40.4 (C^8), 31.6 (C^{11}), 26.2 (C^{12}), 24.1 (C^9).

HRMS (ES^+) exact mass calculated for [M+Na]+ ($C_{13}H_{19}O_2N^{23}Na^{32}S_2$) requires m/z 308.0749, found m/z 308.0748.

Compound 293i



Off-white solid, 54%.

mp 136-139 °C.

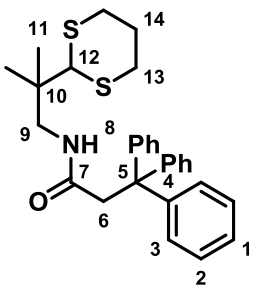
IR (film)/cm^{-1} ν_{max} 3309 (N-H stretch), 2962 (C-H stretch), 1645 (C=O stretch), 1556 (C=C stretch).

^{1}H NMR ($CDCl_3$, 400 MHz) δ_H 5.81 (s, 1H, H^5), 4.03 (s, 1H, H^9), 3.33 (d, *J* = 6.7 Hz, 2H, H^6), 2.95 – 2.81 (m, 4H, H^{10}), 2.15 – 2.03 (m, 3H, $H^{3, 11a}$), 1.89 – 1.77 (m, 1H, H^{11b}), 1.10 (s, 6H, H^8), 1.06 (s, 9H, H^1).

^{13}C NMR ($CDCl_3$, 100 MHz) δ_C 171.9 (C^4), 59.3 (C^9), 51.2 (C^3), 47.4 (C^6), 40.0 (C^7), 31.7 (C^{10}), 31.0 (C^2), 30.1 (C^1), 26.2 (C^{11}), 24.3 (C^8).

HRMS (ES^+) exact mass calculated for [M+H]+ ($C_{14}H_{28}ON^{32}S_2$) requires m/z 290.1607, found m/z 290.1607.

Compound 293j



Off-white solid, 61%.

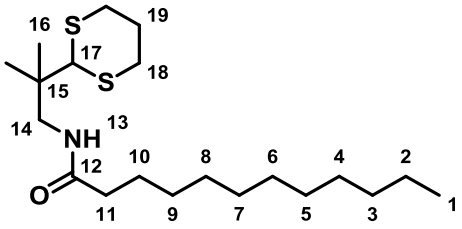
IR (film)/cm^{-1} ν_{max} 3337 (N-H stretch), 2964 (C-H stretch), 1653 (C=O stretch), 1522 (C=C stretch).

^{1}H NMR ($CDCl_3$, 400 MHz) δ_H 7.33 – 7.20 (m, 15H, $H^{1,2,3,4}$), 5.27 (t, *J* = 5.9 Hz, 1H, H^8), 3.65 (s, 2H, H^6), 3.59 (s, 1H, H^{12}), 3.04 (d, *J* = 6.4 Hz, 2H, H^9), 2.86 – 2.68 (m, 4H, H^{13}), 2.08 – 2.00 (m, 1H, H^{14a}), 1.75 (dtt, *J* = 13.9, 12.0, 3.6 Hz, 1H, H^{14b}), 0.83 (s, 6H, H^{11}).

^{13}C NMR ($CDCl_3$, 100 MHz) δ_C 170.8 (C^7), 146.5 (C^4), 129.4 (C^3), 128.3 (C^2), 126.7 (C^1), 58.1 (C^{12}), 56.1 (C^5), 49.1 (C^6), 47.7 (C^9), 39.6 (C^{10}), 31.2 (C^{13}), 26.1 (C^{14}), 23.6 (C^{11}).

HRMS (ES^+) exact mass calculated for [M+H]+ ($C_{29}H_{34}ON^{32}S_2$) requires m/z 476.2087, found m/z 476.2075.

Compound 293k



Off-white solid, 62%.

mp 64-66 °C.

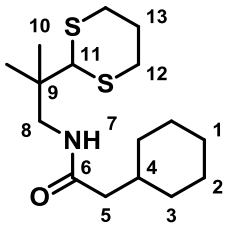
IR (film)/cm^{-1} ν_{max} 3279 (N-H stretch), 2924 (C-H stretch), 1649 (C=O stretch), 1559 C=C stretch).

^{1}H NMR ($CDCl_3$, 400 MHz) δ_H 5.89 (s, 1H, H^{13}), 4.03 (s, 1H, H^{17}), 3.34 (d, *J* = 6.6 Hz, 2H, H^{14}), 3.00 – 2.84 (m, 4H, H^{18}), 2.23 – 2.18 (m, 2H, H^{11}), 2.15 – 2.07 (m, 1H, H^{19a}), 1.91 – 1.77 (m, 1H, H^{19b}), 1.64 (p, *J* = 7.4 Hz, 2H, H^{10}), 1.36 – 1.22 (m, 16H, $H^{2,3,4,5,6,7,8,9}$), 1.10 (s, 6H, H^{16}), 0.91 – 0.85 (m, 3H, H^1).

^{13}C NMR ($CDCl_3$, 100 MHz) δ_C 173.3 (C^{12}), 59.3 (C^{17}), 47.3 (C^{14}), 40.1 (C^{15}), 37.3 (C^{11}), 32.1 (C^3), 31.7 (C^{18}), 29.8 ($C^{4/5/6/7/8/9}$), 29.8 ($C^{4/5/6/7/8/9}$), 29.8 ($C^{4/5/6/7/8/9}$), 29.7 ($C^{4/5/6/7/8/9}$), 29.5 ($C^{4/5/6/7/8/9}$), 29.5 ($C^{4/5/6/7/8/9}$), 26.2 (C^{19}), 26.0 (C^{10}), 24.3 (C^{16}), 22.8 ($C^{4/5/6/7/8/9}$), 14.3 (C^1).

HRMS (ES^+) exact mass calculated for [M+H]+ ($C_{20}H_{40}ON^{32}S_2$) requires m/z 374.2546, found m/z 374.2540.

Compound 293l



Off-white solid, 69%.

mp 98-99 °C.

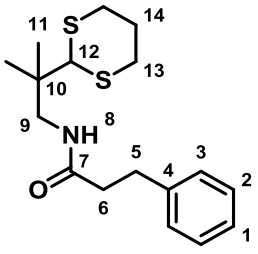
IR (film)/cm^{-1} ν_{max} 3304 (N-H stretch), 2922 (C-H stretch), 1642 (C=O stretch), 1546 (C=C stretch).

^{1}H NMR ($CDCl_3$, 400 MHz) δ_H 5.88 (s, 1H, H^{7}), 4.02 (s, 1H, H^{11}), 3.33 (d, *J* = 6.7 Hz, 2H, H^{8}), 2.94 – 2.83 (m, 4H, H^{12}), 2.15 – 2.04 (m, 3H, $H^{5, 13a}$), 1.89 – 1.60 (m, 8H, H, $H^{1a, 2a, 3a, 4, 13b}$), 1.28 (qt, *J* = 13.3, 3.4 Hz, 2H, H^{3b}), 1.20 – 1.10 (m, 1H, H^{1b}), 1.09 (s, 6H, H^{10}), 1.02 – 0.90 (m, 2H, H^{2b})

^{13}C NMR ($CDCl_3$, 100 MHz) δ_C 172.6 (C^{6}), 59.3 (C^{11}), 47.3 (C^{8}), 45.4 (C^{5}), 40.0 (C^{9}), 35.4 (C^{4}), 33.3 (C^{2}), 31.7 (C^{12}), 26.4 (C^{1}), 26.2 (C^{3}), 26.2 (C^{13}), 24.3 (C^{10}).

HRMS (ES^{+}) exact mass calculated for [M+Na]+ ($C_{16}H_{29}ON^{23}Na^{32}S_2$) requires m/z 338.1583, found m/z 338.1578.

Compound 293m



Off-white solid, 58%.

mp 96-97 °C.

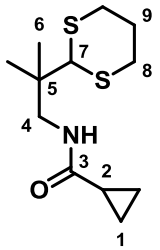
IR (film)/cm^{-1} ν_{max} 3308 (N-H stretch), 2929 (C-H stretch), 1647 (C=O stretch), 1545 (C=C stretch).

^{1}H NMR ($CDCl_3$, 400 MHz) δ_H 7.33 – 7.18 (m, 5H, $H^{1,2,3}$), 5.79 (br s, 1H, H^{8}), 3.82 (s, 1H, H^{12}), 3.29 (d, *J* = 6.7 Hz, 2H, H^{9}), 2.99 (t, *J* = 7.6 Hz, 2H, H^{6}), 2.89 – 2.77 (m, 4H, H^{13}), 2.53 (t, *J* = 7.6 Hz, 2H, H^{5}), 2.12 – 2.04 (m, 1H, H^{14a}), 1.85 – 1.73 (m, 1H, H^{14b}), 1.02 (s, 6H, H^{11}).

^{13}C NMR ($CDCl_3$, 100 MHz) δ_C 172.2 (C^{7}), 141.0 (C^{4}), 128.7 (C^{2}), 128.5 (C^{3}), 126.4 (C^{1}), 58.8 (C^{12}), 47.4 (C^{9}), 40.0 (C^{10}), 38.8 (C^{5}), 31.8 (C^{6}), 31.5 (C^{13}), 26.1 (C^{14}), 24.1 (C^{11}).

HRMS (ES^+) exact mass calculated for [M+Na]+ ($C_{17}H_{25}ON^{23}Na^{32}S_2$) requires m/z 346.1270, found m/z 346.1267.

Compound 293n



Clear oil, 45%.

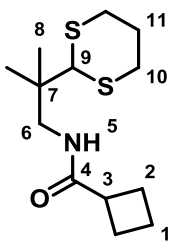
IR (film)/cm^{-1} ν_{max} 3365 (N-H stretch), 2927 (C-H stretch), 1629 (C=O stretch), 1459 (C-S stretch).

^{1}H NMR (MeOH-d_4, 500 MHz) δ_H 4.24 (s, 1H, H^{7}), 3.01 (ddd, *J* = 14.8, 12.5, 2.5 Hz, 2H, H^{8a}), 2.89 (ddd, *J* = 14.6, 4.2, 3.2 Hz, 2H, H^{8b}), 2.11 (dtd, *J* = 13.6, 4.3, 2.1 Hz, 1H, H^{9a}), 1.78 (dtt, *J* = 13.9, 12.5, 3.2 Hz, 1H, H^{9b}), 1.70 (tt, *J* = 7.9, 4.6 Hz, 1H, H^{2}), 1.07 (s, 6H, H^{6}), 0.89 – 0.84 (m, 2H, H^{1a}), 0.80 – 0.75 (m, 2H, H^{1b}).

^{13}C NMR (MeOH-d_4, 500 MHz) δ_C 177.8 (C^{3}), 60.6 (C^{7}), 41.8 (C^{5}), 33.0 (C^{8}), 28.2 (C^{9}), 24.6 (C^{6}), 15.6 (C^{2}), 8.1 (C^{1}).

HRMS (ES^+) exact mass calculated for [M+Na]+ ($C_{12}H_{21}ON^{23}Na^{32}S_2$) requires m/z 282.0957, found m/z 282.0957.

Compound 293o



Pale brown solid, 52%.

mp 89-93 °C.

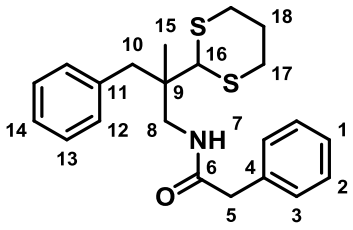
IR (film)/cm^{-1} ν_{max} 3303 (N-H stretch), 2971 (C-H stretch), 1646 (C=O stretch), 1543 (C-S stretch).

^{1}H NMR ($CDCl_3$, 400 MHz) δ_H 5.82 (s, 1H, H^5), 4.02 (s, 1H, H^9), 3.33 (d, *J* = 6.7 Hz, 2H, H^6), 3.03 (pd, *J* = 8.6, 1.0 Hz, 1H, H^3), 2.94 – 2.83 (m, 4H, H^{10}), 2.34 – 2.24 (m, 2H, H^{2a}), 2.22 – 2.07 (m, 3H, $H^{2b, 11a}$), 2.02 – 1.76 (m, 3H, $H^{1, 11b}$), 1.09 (s, 6H, H^8).

^{13}C NMR ($CDCl_3$, 400 MHz) δ_C 175.2 (C^4), 59.4 (C^9), 47.2 (C^6), 40.4 (C^3), 40.2 (C^7), 31.7 (C^{10}), 26.2 (C^{11}), 25.6 (C^2), 24.3 (C^8), 18.4 (C^1).

HRMS (ES^+) exact mass calculated for [M+Na]+ ($C_{13}H_{23}ON^{23}Na^{32}S_2$) requires m/z 296.1113, found m/z 296.1113.

Compound 293p



Off-white solid, 47%.

mp 146-148 °C.

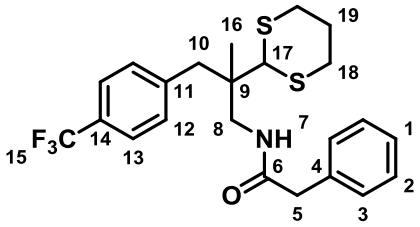
IR (film)/cm^{-1} ν_{max} 3313 (N-H stretch), 2927 (C-H stretch), 1647 (C=O stretch), 1529 (C-S stretch), 1495 (C=C stretch).

^{1}H NMR ($CDCl_3$, 400 MHz) δ_H 7.39 – 7.34 (m, 2H, $H^{2/13}$), 7.32 – 7.21 (m, 8H, $H^{1, 2/13, 3, 12, 14}$), 5.92 (s, 1H, H^7), 3.74 (s, 1H, H^{16}), 3.58 (s, 2H, H^5), 3.40 – 3.27 (m, 2H, H^8), 2.85 (d, *J* = 13.5 Hz, 1H, H^{10a}), 2.78 (dtdd, *J* = 11.8, 4.8, 3.8, 2.0 Hz, 2H, H^{17a}), 2.71 – 2.60 (m, 3H, $H^{10b, 17b}$), 2.07 – 1.99 (m, 1H, H^{18a}), 1.72 (dtt, *J* = 13.9, 12.4, 3.3 Hz, 1H, H^{18b}), 0.95 – 0.92 (s, 3H, H^{15}).

^{13}C NMR ($CDCl_3$, 100 MHz) δ_C 171.0 (C^6), 137.2 (C^4), 135.3 (C^{11}), 130.8 (C^3), 129.9 (C^{12}), 129.1 (C^2), 128.2 (C^{13}), 127.4 (C^1), 126.7 (C^{14}), 57.6 (C^{16}), 45.9 (C^8), 44.3 (C^5), 43.3 (C^9), 42.0 (C^{10}), 31.6 (C^{17a}), 31.4 (C^{17b}), 26.0 (C^{18}), 21.6 (C^{15}).

HRMS (ES^+) exact mass calculated for [M+H]+ ($C_{22}H_{28}ON^{32}S_2$) requires m/z 386.1607, found m/z 386.1614.

Compound 293q



Oil, 51%.

IR (film)/cm^{-1} ν_{max} 3304 (N-H stretch), 2971 (C-H stretch), 1647 (C=O stretch), 1540 (C-S stretch).

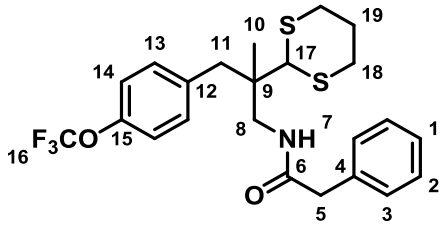
^{1}H NMR ($CDCl_3$, 500 MHz) δ_H 7.52 (d, *J* = 8.0 Hz, 2H, H^{13}), 7.44 – 7.34 (m, 4H, $H^{3, 12}$), 7.33 – 7.25 (m, 3H, $H^{1, 2}$), 5.97 (t, *J* = 6.6 Hz, 1H, H^{7}), 3.66 (s, 1H, H^{17}), 3.60 (s, 2H, H^{5}), 3.40 (dd, *J* = 14.2, 6.6 Hz, 1H, H^{8a}), 3.25 (dd, *J* = 14.2, 6.6 Hz, 1H, H^{8b}), 2.92 (d, *J* = 13.4 Hz, 1H, H^{10a}), 2.79 (dt, *J* = 14.4, 3.6 Hz, 2H, H^{18a}), 2.74 – 2.57 (m, 3H, $H^{10b, 18b}$), 2.04 (dtt, *J* = 10.7, 4.2, 2.2 Hz, 1H, H^{19a}), 1.79 – 1.65 (m, 1H, H^{19b}), 0.91 (s, 3H, H^{16}).

^{13}C NMR ($CDCl_3$, 100 MHz) δ_C 171.2 (C^{6}), 141.4 (C^{11}), 135.2 (C^{4}), 131.1 (C^{3}), 129.9 (C^{2}), 129.2 (C^{12}), 129.0 (q, *J* = 32.3 Hz, C^{13}), 127.4 (C^{1}), 125.07 (q, *J* = 3.8 Hz, H^{13}), 123.3 (d, *J* = 272.8 Hz, H^{15}), 57.4 (C^{17}), 45.6 (C^{8}), 44.3 (C^{5}), 43.4 (C^{9}), 41.5 (C^{10}), 31.6 (C^{18a}), 31.4 (C^{18b}), 25.9 (C^{19}), 21.6 (C^{16}).

^{19}F NMR ($CDCl_3$, 400 MHz) δ_F -62.40.

HRMS (ES^+) exact mass calculated for [M+Na]+ ($C_{23}H_{26}F_3N^{32}S_2Na$) requires m/z 476.2087, found m/z 476.2075.

Compound 293r



Oil, 49%.

IR (film)/cm^{-1} ν_{max} 3308 (N-H stretch), 2931 (C-H stretch), 1647 (C=O stretch), 1509 (C=C stretch).

^{1}H NMR ($CDCl_3$, 400 MHz) δ_H 7.41 – 7.24 (m, 7H, $H^{1,2,3,13}$), 7.11 (dt, *J* = 7.6, 1.1 Hz, 2H, H^{14}), 5.96 (t, *J* = 6.6 Hz, 1H, H^{7}), 3.68 (s, 1H, H^{17}), 3.60 (s, 1H, H^{11a}), 2.82 – 2.76 (m, 2H, H^{18a}),

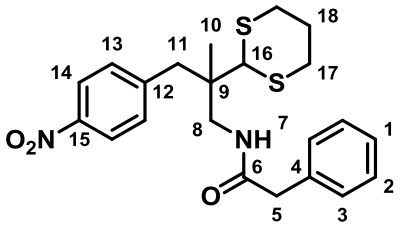
2.71 – 2.57 (m, 3H, $H^{11b, 18b}$), 2.09 – 1.99 (m, 1H, H^{19a}), 1.72 (dtt, *J* = 13.9, 12.4, 3.2 Hz, 1H, H^{19b}), 0.91 (s, 3H, H^{10}).

^{13}C NMR ($CDCl_3$, 100 MHz) δ_C 171.1 (C^6), 148.2 (C^{15}), 135.9 (C^4), 135.2 (C^3), 132.1 (C^2), 129.9 (C^{13}), 129.2 (C^{16}), 128.8 (C^{12}), 127.4 (C^1), 120.6 (C^{14}), 57.4 (C^{17}), 45.7 (C^8), 44.3 (C^5), 43.3 (C^9), 41.0 (C^{11}), 31.6 (C^{18a}), 31.4 (C^{18b}), 26.0 (C^{19}), 21.6 (C^{10}).

^{19}F NMR ($CDCl_3$, 400 MHz) δ_F -57.79.

HRMS (ES^+) exact mass calculated for [M+H]+ ($C_{23}H_{27}ONF_3{}^{32}S_2$) requires m/z 454.1481, found m/z 454.1475.

Compound 293s



Cream solid, 55%.

mp 97-98 °C

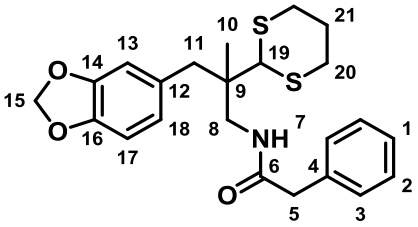
IR (film)/cm^{-1} ν_{max} 3305 (N-H stretch), 2969 (C-H stretch), 1648 (C=O stretch), 1520 (C-S stretch), 1454 (N-O stretch).

^{1}H NMR ($CDCl_3$, 400 MHz) δ_H 8.13 (d, *J* = 8.7 Hz, 2H, H^{14}), 7.47 (d, *J* = 8.7 Hz, 2H, H^{13}), 7.44 – 7.28 (m, 5H, $H^{1, 2, 3}$), 5.97 (s, 1H, H^7), 3.64 (s, 1H, H^{16}), 3.62 (s, 2H, H^5), 3.44 (dd, *J* = 14.2, 6.9 Hz, 1H, H^{8a}), 3.22 (dd, *J* = 14.3, 6.4 Hz, 1H, H^{8b}), 2.99 (d, *J* = 13.3 Hz, 1H, H^{11a}), 2.80 (dt, *J* = 14.3, 3.7 Hz, 2H, H^{17a}), 2.73 – 2.57 (m, 3H, H^{17b}), 2.12 – 2.00 (m, 1H, H^{18a}), 1.81 – 1.66 (m, 1H, H^{18b}), 0.91 (s, 3H, H^{10}).

^{13}C NMR ($CDCl_3$, 100 MHz) δ_C 171.3 (C^6), 147.0 (C^{15}), 145.2 (C^{12}), 135.1 (C^4), 131.7 (C^{13}), 129.9 (C^2), 129.3 (C^3), , 127.5 (C^1), 123.3 (C^{14}), 57.5 (C^{16}), 45.5 (C^8), 44.3 (C^5), 43.6 (C^9), 41.3 (C^{11}), 31.6 (C^{17a}), 31.4 (C^{17b}), 25.9 (C^{18}), 21.6 (C^{10}).

HRMS (ES^+) exact mass calculated for [M+Na]+ ($C_{22}H_{26}O_3N_2{}^{23}Na^{32}S_2$) requires m/z 453.1277, found m/z 453.1268.

Compound 293t



Oil, 50%.

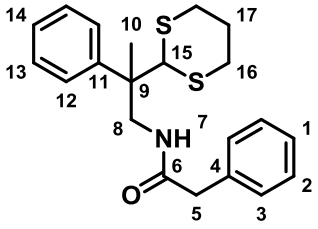
IR (film)/cm^{-1} ν_{max} 3309 (N-H stretch), 2929 (C-H stretch), 1648 (C=O stretch), 1528 (C-S stretch).

^{1}H NMR ($CDCl_3$, 400 MHz) 7.43 – 7.34 (m, 2H, H^{2}), 7.32 – 7.27 (m, 3H, $H^{1, 3}$), 6.75 (d, *J* = 1.6 Hz, 1H, H^{13}), 6.71 (d, *J* = 7.9 Hz, 1H, H^{18}), 6.67 (dd, *J* = 8.0, 1.6 Hz, 1H, H^{17}), 5.96 – 5.90 (m, 3H, $H^{7, 15}$), 3.72 (s, 1H, H^{19}), 3.59 (s, 2H, H^{5}), 3.31 (d, *J* = 6.5 Hz, 2H, H^{8}), 2.85 – 2.71 (m, 3H, $H^{11a, 20a}$), 2.65 (dddd, *J* = 13.9, 12.4, 2.6, 1.1 Hz, 2H, H^{20b}), 2.53 (d, *J* = 13.7 Hz, 1H, H^{11b}), 2.07 – 1.98 (m, 1H, H^{21a}), 1.71 (dtt, *J* = 13.7, 12.4, 3.3 Hz, 1H, H^{21b}), 0.92 (s, 3H, H^{10}).

^{13}C NMR ($CDCl_3$, 100 MHz) δ_C 171.0 (C^{6}), 147.5 (C^{14}), 146.4 (C^{16}), 135.3 (C^{4}), 130.7 (C^{12}), 129.9 (C^{1}), 129.1 (C^{2}), 127.4 (C^{3}), 123.8 (C^{18}), 111.1 (C^{13}), 108.1 (C^{17}), 101.0 (C^{15}), 57.6 (C^{19}), 45.9 (C^{8}), 44.4 (C^{5}), 43.4 (C^{9}), 41.7 (C^{11}), 31.6 (C^{20a}), 31.4 (C^{20b}), 26.0 (C^{21}), 21.6 (C^{10}).

HRMS (ES^{+}) exact mass calculated for [M+Na]+ ($C_{23}H_{27}O_3N^{23}Na^{32}S_2$) requires m/z 452.1325, found m/z 452.1324.

Compound 293u



Oil, 36%.

IR (film)/cm^{-1} ν_{max} 3308 (N-H stretch), 2980 (C-H stretch), 1649 (C=O stretch), 1529 (C-S stretch).

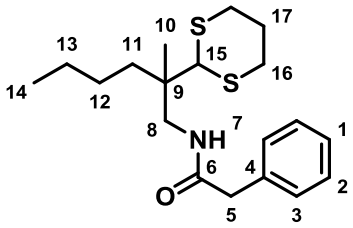
^{1}H NMR ($CDCl_3$, 500 MHz) δ_H 7.31 – 7.19 (m, 8H, $H^{1, 2, 3, 13, 14}$), 7.08 – 7.00 (m, 2H, H^{12}), 5.29 (s, 1H, H^{7}), 4.26 (s, 1H, H^{15}), 3.87 (dd, *J* = 13.8, 7.1 Hz, 1H, H^{8a}), 3.55 (dd, *J* = 13.8, 5.1 Hz, 1H, H^{8b}), 3.49 (d, *J* = 16.0 Hz, 1H, H^{5a}), 3.45 (d, *J* = 16.1 Hz, 1H, H^{5b}), 2.86 – 2.77 (m, 2H,

H^{16a}), 2.74 – 2.65 (m, 2H, H^{16b}), 2.08 – 1.95 (m, 1H, H^{17a}), 1.74 (ddtd, *J* = 15.6, 9.5, 7.9, 6.3 Hz, 1H, H^{17b}), 1.43 (s, 3H, H^{10}).

^{13}C NMR ($CDCl_3$, 126 MHz) δ_C 170.8 (C^6), 142.0 (C^{11}), 134.7 (C^4), 129.4 (C^3), 129.0 (C^2), 128.5 (C^{13}), 127.2 (C^1), 127.2 (C^{14}), 126.5 (C^{12}), 59.2 (C^{15}), 47.8 (C^8), 46.8 (C^9), 44.0 ($C5^j$), 31.7 (C^{16a}), 31.4 (C^{16b}), 25.9 (C^{17}), 20.3 (C^{10}).

HRMS (ES^+) exact mass calculated for [M+H]+ ($C_{21}H_{26}ON^{32}S_2$) requires m/z 372.1450, found m/z 372.1448.

Compound 293v



Oil, 56%.

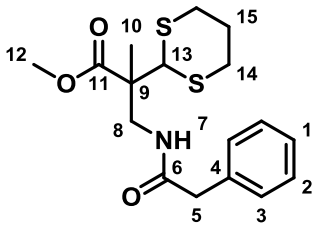
IR (film)/cm^{-1} ν_{max} 3309 (N-H stretch), 2931 (C-H stretch), 1648 (C=O stretch), 1544 (C-S stretch).

^{1}H NMR ($CDCl_3$, 400 MHz) 7.41 – 7.35 (m, 2H, H^2), 7.32 – 7.27 (m, 3H, $H^{1,3}$), 5.88 (s, 1H, H^{15}), 3.74 (s, 1H, H^{15}), 3.60 (s, 2H, H^5), 3.36 – 3.22 (m, 2H, H^8), 2.82 – 2.72 (m, 2H, H^{16a}), 2.71 – 2.59 (m, 2H, H^{16b}), 2.02 (dtt, *J* = 13.5, 4.1, 2.5 Hz, 1H, H^{17a}), 1.70 (dtt, *J* = 14.0, 12.3, 3.4 Hz, 1H, H^{17b}), 1.53 – 1.37 (m, 1H, H^{11a}), 1.34 – 1.15 (m, 5H, $H^{11b,12,13}$), 0.96 (s, 3H, H^{10}), 0.93 – 0.84 (m, 3H, H^{14}).

^{13}C NMR ($CDCl_3$, 100 MHz) δ_C 171.0 (C^6), 135.5 (C^4), 129.9 (C^2), 129.2 (C^3), 127.4 (C^1), 58.6 (C^{15}), 45.6 (C^8), 44.4 (C^5), 42.3 (C^9), 36.2 (C^{11}), 31.6 (C^{16a}), 31.6 (C^{16b}), 26.2 (C^{17}), 25.7 (C^{12}), 23.5 (C^{13}), 21.5 (C^{10}), 14.2 (C^{14}).

HRMS (ES^+) exact mass calculated for [M+H]+ ($C_{19}H_{30}ON^{32}S_2$) requires m/z 352.1763, found m/z 352.1757.

Compound 293w



Oil, 47%.

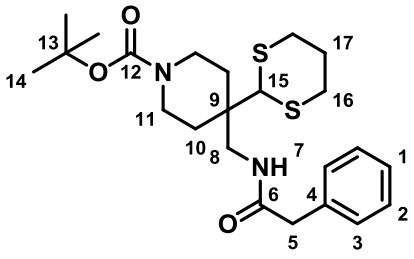
IR (film)/cm^{-1} ν_{max} 3308 (N-H stretch), 2940 (C-H stretch), 1732 (C=O ester stretch), 1654 (C=O amide stretch), 1546 (C-S stretch).

^{1}H NMR ($CDCl_3$, 400 MHz) δ_H 7.40 – 7.27 (m, 5H, H^{1,2,3}), 5.87 (s, 1H, H^{7}), 4.29 (s, 1H, H^{13}), 3.70 (dd, *J* = 14.1, 7.3 Hz, 1H, H^{8a}), 3.63 (s, 3H, H^{12}), 3.57 (d, *J* = 1.7 Hz, 2H, H^{5}), 3.42 (dd, *J* = 14.0, 5.7 Hz, 1H, H^{8b}), 2.90 – 2.68 (m, 4H, H^{14}), 2.11 – 2.01 (m, 1H, H^{15a}), 1.85 – 1.71 (m, 1H, H^{15b}), 1.24 (s, 3H, H^{10}).

^{13}C NMR ($CDCl_3$, 100 MHz) δ_C 174.0 (C^{11}), 171.0 (C^{6}), 135.2 (C^{4}), 129.7 (C^{2}), 129.2 (C^{3}), 127.5 (C^{1}), 54.8 (C^{13}), 52.6 (C^{12}), 51.8 (C^{9}), 44.2 (C^{5}), 44.1 (C^{8}), 31.6 (C^{14a}), 31.4 (C^{14b}), 26.0 (C^{15}), 18.2 (C^{10}).

HRMS (ES^{+}) exact mass calculated for [M+Na]+ ($C_{17}H_{23}O_3N^{23}Na^{32}S_2$) requires m/z 376.1012, found m/z 376.1006.

Compound 293x



Clear crystalline solid, 53%.

mp 24-25 ^{o}C.

IR (film)/cm^{-1} ν_{max} 3291 (N-H stretch), 2980 (C-H stretch), 1685 (C=O carbamate stretch), 1652 (C=O amide stretch), 1525 (C-S stretch).

^{1}H NMR ($CDCl_3$, 500 MHz) 7.39 – 7.35 (m, 2H, H^{2}), 7.32 – 7.27 (m, 3H, H^{1,3}), 6.08 (t, *J* = 6.7 Hz, 1H, H^{7}), 3.90 (s, 1H, H^{15}), 3.60 (s, 2H, H^{5}), 3.59 – 3.23 (m, 6H, H^{8,11}), 2.77 (dt, *J* = 14.1,

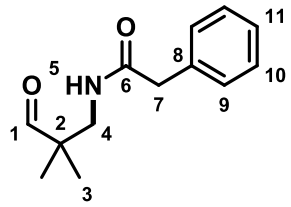
3.7 Hz, 2H, H^{16a}), 2.67 (t, *J* = 13.2 Hz, 2H, H^{16b}), 2.04 (dtt, *J* = 13.5, 4.1, 2.5 Hz, 1H, H^{17a}), 1.79 – 1.61 (m, 3H, $H^{10a, 17b}$), 1.44 (s, 11H, $H^{10b, 14}$).

^{13}C NMR ($CDCl_3$, 125 MHz) δ_C 171.2 (C^6), 155.0 (C^{12}), 135.2 (C^4), 129.9 (C^3), 129.1 (C^2), 127.4 (C^1), 79.6 (C^{13}), 57.4 (C^{15}), 44.2 (C^5), 42.4 (C^8), 41.0 (C^9), 40.0 (C^{11a}), 39.1 (C^{11b}), 31.6 (C^{16}), 31.3 (C^{10}), 28.6 (C^{14}), 26.2 (C^{17}).

HRMS (ES^+) exact mass calculated for [M+Na]+ ($C_{23}H_{34}O_3N_2{}^{23}Na^{32}S_2$) requires m/z 473.1903, found m/z 473.1898.

Product Derivatisation

Compound 304



To a solution of **293a** (30.9 mg, 0.1 mmol) in MeCN (3 mL) was added TFA (77 µL, 1 mmol) followed by $PhI(OAc)_2$ (97 mg, 0.3 mmol). The reaction was stirred for 10 minutes or until full disappearance of the starting material by TLC. The reaction mixture was diluted with water, extracted with diethyl ether and the combined organic layers dried over magnesium sulfate and concentrated *in vacuo*. The crude product was purified by flash column chromatography to give **304** as an oil (16.8 mg, 0.077 mmol, 77%).

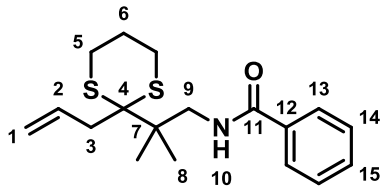
IR (film)/cm^{-1} ν_{max} 3301 (N-H stretch), 2980 (C-H stretch), 2929 (C-H stretch), 1723 (C=O aldehyde stretch), 1651 (C=O amide stretch), 1544 (C-S stretch).

^{1}H NMR ($CDCl_3$, 400 MHz) δ_H 9.36 (s, 1H, H^1), 7.36 (ddt, *J* = 8.1, 6.6, 1.1 Hz, 2H, H^{10}), 7.32 – 7.27 (m, 1H, H^{11}), 7.25 – 7.20 (m, 2H, H^9), 5.73 (s, 1H, H^5), 3.55 (s, 2H, H^7), 3.32 (d, *J* = 6.5 Hz, 2H, H^4), 1.01 (s, 6H, H^3).

^{13}C NMR ($CDCl_3$, 100 MHz) δ_C 205.3 (C^1), 171.2 (C^6), 134.9 (C^8), 129.5 (C^{10}), 129.2 (C^9), 127.6 (C^{11}), 47.6 (C^2), 44.4 (C^4), 44.0 (C^7), 19.7 (C^3).

HRMS (ES^+) exact mass calculated for [M+H]+ ($C_{13}H_{18}O_2N$) requires m/z 220.1332, found m/z 220.1335.

Compound 305



A solution of **293e** (20 mg, 0.068 mmol) in tetrahydrofuran (3 mL) cooled to -78 ^{o}C was added n-BuLi (0.13 mL, 1.6M in hexane, 0.20 mmol). The reaction was stirred for 15 minutes, before addition of allyl bromide (29 µL, 0.34 mmol). The reaction was warmed slowly to room temperature and stirred for a further 3 hours. The reaction was diluted with saturated ammonium chloride and extracted with ethyl acetate. The combined organic layers were washed with brine, dried over sodium sulfate and concentrated *in vacuo*. The crude product was purified by flash column chromatography to give **305** as an oil (14 mg, 61%).

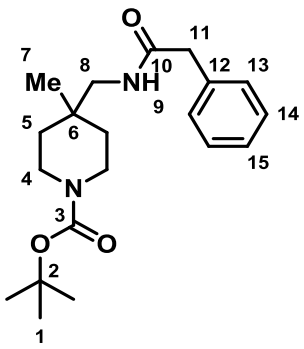
IR (film)/cm^{-1} ν_{max} 3324 (N-H stretch), 2973 (C-H stretch), 2933 (C-H stretch), 1645 (C=O stretch), 1537 (C=C stretch).

^{1}H NMR ($CDCl_3$, 500 MHz) δ_H 7.86 (d, *J* = 7.3 Hz, 2H, H^{13}), 7.53 – 7.36 (m, 3H, $H^{14, 15}$), 7.30 (s, 1H, H^{10}), 6.13 (ddt, *J* = 17.0, 10.2, 6.8 Hz, 1H, H^{2}), 5.20 (dt, *J* = 17.1, 1.9 Hz, 1H, H^{1a}), 5.12 (dd, *J* = 10.2, 1.8 Hz, 1H, H^{1b}), 3.73 (d, *J* = 6.1 Hz, 2H, H^{9}), 3.11 – 2.99 (m, 4H, $H^{3, 5a}$), 2.76 (dt, *J* = 14.5, 4.2 Hz, 2H, H^{5b}), 2.10 (dp, *J* = 12.0, 3.9 Hz, 1H, H^{6a}), 1.92 – 1.78 (m, 1H, H^{6b}), 1.22 (s, 6H, H^{8}).

^{13}C NMR ($CDCl_3$, 100 MHz) δ_C 167.4 (C^{11}), 136.5 (C^{2}), 135.1 (C^{12}), 131.4 (C^{15}), 128.7 (C^{14}), 127.1 (C^{13}), 116.8 (C^{1}), 60.9 (C^{4}), 48.6 (C^{9}), 44.7 (C^{7}), 41.3 (C^{3}), 26.7 (C^{5}), 24.9 (C^{6}), 22.8 (C^{8}).

HRMS (ES^{+}) exact mass calculated for [M+H]+ ($C_{18}H_{26}ON^{32}S_2$) requires m/z 336.1450, found m/z 336.1450.

Compound 306



To a solution of **293x** (30 mg, 0.067 mmol) in ethanol (3 mL) was added Raney nickel (100 mg) and the reaction slurry stirred for 5 hours. The reaction was filtered through a pad of celite, taking care not to let the Raney nickel dry out. The filtrate was concentrated and the crude product was purified by flash column chromatography to give **306** as a clear oil (20.3 mg, 88%).

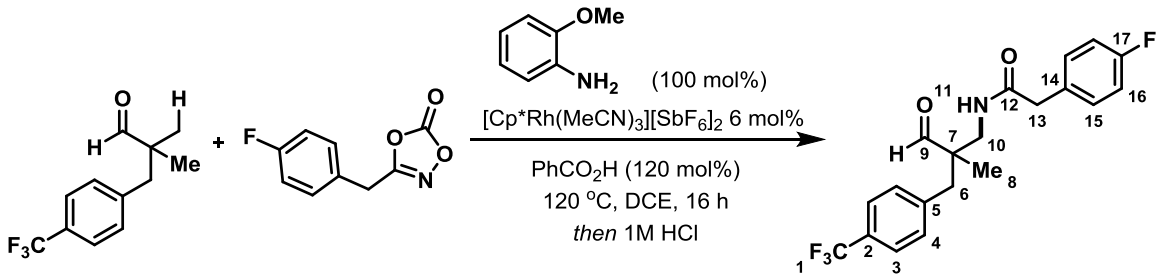
IR (film)/cm^{-1} ν_{max} 3305 (N-H stretch), 2931 (C-H stretch), 2926 (C-H stretch), 1691 (C=O carbamate stretch), 1652 (C=O amide stretch), 1552 (C=C stretch).

^{1}H NMR ($CDCl_3$, 500 MHz) δ_H 7.31 (t, *J* = 7.4 Hz, 2H, H^{12}), 7.31 (t, *J* = 7.4 Hz, 1H, H^{15}), 7.28 – 7.24 (m, 2H, H^{14}), 5.35 (s, 1H, H^{9}), 3.69 – 3.50 (m, 4H, $H^{11, 4a}$), 3.13 (ddd, *J* = 13.5, 9.3, 3.7 Hz, 2H, H^{4b}), 1.44 (s, 9H, H^{1}), 1.30 – 1.22 (m, 2H, H^{5a}), 1.16 (dt, *J* = 13.8, 4.0 Hz, 2H, H^{5b}), 0.80 (s, 3H, H^{7}).

^{13}C NMR ($CDCl_3$, 126 MHz) δ_C 171.3 (C^{10}), 155.0 (C^{3}), 135.0 (C^{12}), 129.6 (C^{13}), 129.3 (C^{14}), 127.7 (C^{15}), 79.5 (C^{2}), 48.7 (C^{4}), 44.1 (C^{8}), 34.4 (C^{5}), 33.4 (C^{6}), 28.6 (C^{1}), 22.0 (C^{7}).

HRMS (ES^+) exact mass calculated for [M+H]+ ($C_{20}H_{31}O_3N_2$) requires m/z 347.2329, found m/z 347.2326.

Compound 339



An oven-dried flask was charged with *o*-anisidine (12.3 mg, 0.10 mmol), benzoic acid (14.7 mg, 0.12 mmol) and $[Cp^*Rh(MeCN)_3][SbF_6]_2$ (5.0 mg, 0.006 mmol) followed by a solution of aldehyde **337** (23.2 mg, 0.10 mmol) and dioxazolone **338** (58.5 mg, 0.30 mmol) in dichloroethane (1 mL). The flask was purged with argon, sealed and heated to 120 °C for 16 hours. The reaction was cooled to room temperature and diluted with aqueous 1M HCl (1 mL). The mixture was stirred for 30 mins, diluted with 1M HCl (3 mL) and extracted with dichloromethane (3 x 5 mL). The combined organic layers were washed with saturated sodium carbonate solution, dried over anhydrous sodium sulfate and concentrated *in vacuo*. The crude product was purified by flash column chromatography with pentane:ether (3:7) as the eluant to give **339** as an amorphous solid (25.6 mg, 0.067 mmol, 67%).

IR (film)/cm^{-1} ν_{max} 3311 (N-H stretch), 2980 (C-H stretch), 2926 (C-H stretch), 1691 (C=O stretch aldehyde), 1659 (C=O stretch amide).

^{1}H NMR ($CDCl_3$, 400 MHz) δ_H 9.48 (s, 1H, H^9), 7.23 – 7.16 (m, 2H, H^{16}), 7.13 – 7.00 (m, 6H, $H^{3, 4, 15}$), 5.72 (s, 1H, H^{11}), 3.49 (s, 2H, H^{13}), 3.34 (dd, *J* = 6.4, 1.9 Hz, 2H, H^{10}), 2.78 (d, *J* = 13.9 Hz, 1H, H^{6a}), 2.74 (d, *J* = 14.1 Hz, 1H, H^{6b}), 1.00 (s, 3H, H^8).

^{13}C NMR ($CDCl_3$, 126 MHz) δ_C 205.1 (C^9), 171.1 (C^{12}), 162.3 (d, J = 246 Hz, C^{17}), 134.2 (C^5), 131.6 (C^4), 131.0 (d, J = 8.0 Hz, C^{16}), 130.5 (q, J = 3.5 Hz, C^2), 121.1 (C^3), 120.6 (q, J = 257 Hz, C^1), 116.2 (C^{15}), 116.0 (C^{16}), 51.5 (C^7), 43.1 (2C, $C^{10, 13}$), 39.4 (C^6), 17.5 (C^8).

HRMS (ES^+) exact mass calculated for [M+H]+ ($C_{20}H_{20}O_3NF_4$) requires m/z 398.1374, found m/z 398.1372.